

NCHRP

Research Report 1100

National
Cooperative
Highway
Research Program

MASH TL-3 Deflection Reduction for 31-Inch Guardrail

A GUIDE



NATIONAL
ACADEMIES *Sciences
Engineering
Medicine*

TRB TRANSPORTATION RESEARCH BOARD

TRANSPORTATION RESEARCH BOARD 2024 EXECUTIVE COMMITTEE*

OFFICERS

CHAIR: **Carol A. Lewis**, Professor, Transportation Studies, Texas Southern University, Houston

VICE CHAIR: **Leslie S. Richards**, General Manager, Southeastern Pennsylvania Transportation Authority (SEPTA), Philadelphia

EXECUTIVE DIRECTOR: **Victoria Sheehan**, Transportation Research Board, Washington, DC

MEMBERS

Michael F. Ableson, CEO, Arrival Automotive–North America, Detroit, MI

James F. Albaugh, President and CEO, The Boeing Company (retired), Scottsdale, AZ

Carlos M. Braceras, Executive Director, Utah Department of Transportation, Salt Lake City

Douglas C. Ceva, Vice President, Customer Lead Solutions, Prologis, Inc., Jupiter, FL

Nancy Daubenberger, Commissioner of Transportation, Minnesota Department of Transportation, St. Paul

Marie Therese Dominguez, Commissioner, New York State Department of Transportation, Albany

Chris T. Hendrickson, Hamerschlag University Professor of Engineering Emeritus, Carnegie Mellon University, Pittsburgh, PA

Randell Iwasaki, President and CEO, Iwasaki Consulting Services, Walnut Creek, CA

Ashby Johnson, Executive Director, Capital Area Metropolitan Planning Organization (CAMPO), Austin, TX

Joel M. Jundt, Secretary of Transportation, South Dakota Department of Transportation, Pierre

Hani S. Mahmassani, W.A. Patterson Distinguished Chair in Transportation; Director, Transportation Center, Northwestern University, Evanston, IL

Scott C. Marler, Director, Iowa Department of Transportation, Ames

Ricardo Martinez, Adjunct Professor of Emergency Medicine, Emory University School of Medicine, Decatur, GA

Michael R. McClellan, Vice President, Strategic Planning, Norfolk Southern Corporation, Norfolk, VA

Russell McMurry, Commissioner, Georgia Department of Transportation, Atlanta

Craig E. Philip, Research Professor and Director, VECTOR, Department of Civil and Environmental Engineering, Vanderbilt University, Nashville, TN

Steward T.A. Pickett, Distinguished Senior Scientist, Cary Institute of Ecosystem Studies, Millbrook, NY

Susan A. Shaheen, Professor and Co-director, Transportation Sustainability Research Center, University of California, Berkeley

EX OFFICIO MEMBERS

Michael R. Berube, Deputy Assistant Secretary for Sustainable Transportation, U.S. Department of Energy, Washington, DC

Shailen Bhatt, Administrator, Federal Highway Administration, U.S. Department of Transportation, Washington, DC

Amit Bose, Administrator, Federal Railroad Administration, Washington, DC

Tristan Brown, Deputy Administrator, Pipeline and Hazardous Materials Safety Administration, U.S. Department of Transportation, Washington, DC

Ann Carlson, Acting Administrator, National Highway Traffic Safety Administration, Washington, DC

Steven Cliff, Executive Officer, California Air Resources Board, Sacramento, CA

Nuria I. Fernandez, Administrator, Federal Transit Administration, Washington, DC

LeRoy Gishi, Chief, Division of Transportation, Bureau of Indian Affairs, U.S. Department of the Interior, Germantown, MD

William H. Graham, Jr. (Major General, U.S. Army), Deputy Commanding General for Civil and Emergency Operations, U.S. Army Corps of Engineers, Washington, DC

John T. Gray II, Senior Vice President, Policy and Economics, Association of American Railroads, Washington, DC

Robert C. Hampshire, Deputy Assistant Secretary for Research and Technology, U.S. Department of Transportation, Washington, DC

Eleftheria Kontou, Assistant Professor, University of Illinois at Urbana–Champaign, Urbana, and Chair, TRB Young Members Coordinating Council

Sue Lawless, Acting Deputy Administrator, Federal Motor Carrier Safety Administration, Washington, DC

Karl Simon, Director, Transportation and Climate Division, U.S. Environmental Protection Agency, Washington, DC

Paul P. Skoutelas, President and CEO, American Public Transportation Association, Washington, DC

Polly Trottenberg, Deputy Secretary of Transportation and Acting Administrator, Federal Aviation Administration, U.S. Department of Transportation, Washington, DC

Jim Tymon, Executive Director, American Association of State Highway and Transportation Officials, Washington, DC

* Membership as of February 2024.

NCHRP RESEARCH REPORT 1100

MASH TL-3 Deflection Reduction for 31-Inch Guardrail

A GUIDE

James Kovar
Roger Bligh
Sofokli Cakalli
William Schroeder
Daniel Curran
Alondra Loza
Maysam Kiani
Sana Moran
Heath Buttery
Sumedh Khair

TEXAS A&M TRANSPORTATION INSTITUTE
THE TEXAS A&M UNIVERSITY SYSTEM
College Station, TX

Subscriber Categories

Design • Operations and Traffic Management • Safety and Human Factors

Research sponsored by the American Association of State Highway and Transportation Officials
in cooperation with the Federal Highway Administration

NATIONAL COOPERATIVE HIGHWAY RESEARCH PROGRAM

Systematic, well-designed, and implementable research is the most effective way to solve many problems facing state departments of transportation (DOTs) administrators and engineers. Often, highway problems are of local or regional interest and can best be studied by state DOTs individually or in cooperation with their state universities and others. However, the accelerating growth of highway transportation results in increasingly complex problems of wide interest to highway authorities. These problems are best studied through a coordinated program of cooperative research.

Recognizing this need, the leadership of the American Association of State Highway and Transportation Officials (AASHTO) in 1962 initiated an objective national highway research program using modern scientific techniques—the National Cooperative Highway Research Program (NCHRP). NCHRP is supported on a continuing basis by funds from participating member states of AASHTO and receives the full cooperation and support of the Federal Highway Administration (FHWA), United States Department of Transportation, under Agreement No. 693JJ31950003.

The Transportation Research Board (TRB) of the National Academies of Sciences, Engineering, and Medicine was requested by AASHTO to administer the research program because of TRB's recognized objectivity and understanding of modern research practices. TRB is uniquely suited for this purpose for many reasons: TRB maintains an extensive committee structure from which authorities on any highway transportation subject may be drawn; TRB possesses avenues of communications and cooperation with federal, state, and local governmental agencies, universities, and industry; TRB's relationship to the National Academies is an insurance of objectivity; and TRB maintains a full-time staff of specialists in highway transportation matters to bring the findings of research directly to those in a position to use them.

The program is developed on the basis of research needs identified by chief administrators and other staff of the highway and transportation departments, by committees of AASHTO, and by the FHWA. Topics of the highest merit are selected by the AASHTO Special Committee on Research and Innovation (R&I), and each year R&I's recommendations are proposed to the AASHTO Board of Directors and the National Academies. Research projects to address these topics are defined by NCHRP, and qualified research agencies are selected from submitted proposals. Administration and surveillance of research contracts are the responsibilities of the National Academies and TRB.

The needs for highway research are many, and NCHRP can make significant contributions to solving highway transportation problems of mutual concern to many responsible groups. The program, however, is intended to complement, rather than to substitute for or duplicate, other highway research programs.

NCHRP RESEARCH REPORT 1100

Project 22-38

ISSN 2572-3766 (Print)

ISSN 2572-3774 (Online)

ISBN 978-0-309-70953-8

Library of Congress Control Number 2024932852

© 2024 by the National Academy of Sciences. National Academies of Sciences, Engineering, and Medicine and the graphical logo are trademarks of the National Academy of Sciences. All rights reserved.

COPYRIGHT INFORMATION

Authors herein are responsible for the authenticity of their materials and for obtaining written permissions from publishers or persons who own the copyright to any previously published or copyrighted material used herein.

Cooperative Research Programs (CRP) grants permission to reproduce material in this publication for classroom and not-for-profit purposes. Permission is given with the understanding that none of the material will be used to imply TRB, AASHTO, APTA, FAA, FHWA, FTA, GHSA, or NHTSA endorsement of a particular product, method, or practice. It is expected that those reproducing the material in this document for educational and not-for-profit uses will give appropriate acknowledgment of the source of any reprinted or reproduced material. For other uses of the material, request permission from CRP.

Cover photo credit: Courtesy of Texas A&M Transportation Institute

NOTICE

The research report was reviewed by the technical panel and accepted for publication according to procedures established and overseen by the Transportation Research Board and approved by the National Academies of Sciences, Engineering, and Medicine.

The opinions and conclusions expressed or implied in this report are those of the researchers who performed the research and are not necessarily those of the Transportation Research Board; the National Academies of Sciences, Engineering, and Medicine; the FHWA; or the program sponsors.

The Transportation Research Board does not develop, issue, or publish standards or specifications. The Transportation Research Board manages applied research projects which provide the scientific foundation that may be used by Transportation Research Board sponsors, industry associations, or other organizations as the basis for revised practices, procedures, or specifications.

The Transportation Research Board; the National Academies of Sciences, Engineering, and Medicine; and the sponsors of the National Cooperative Highway Research Program do not endorse products or manufacturers. Trade or manufacturers' names or logos appear herein solely because they are considered essential to the object of the report.

Published research reports of the

NATIONAL COOPERATIVE HIGHWAY RESEARCH PROGRAM

are available from

Transportation Research Board
Business Office
500 Fifth Street, NW
Washington, DC 20001

and can be ordered through the Internet by going to

<https://www.mytrb.org/MyTRB/Store/default.aspx>

Printed in the United States of America

NATIONAL ACADEMIES

*Sciences
Engineering
Medicine*

The **National Academy of Sciences** was established in 1863 by an Act of Congress, signed by President Lincoln, as a private, non-governmental institution to advise the nation on issues related to science and technology. Members are elected by their peers for outstanding contributions to research. Dr. Marcia McNutt is president.

The **National Academy of Engineering** was established in 1964 under the charter of the National Academy of Sciences to bring the practices of engineering to advising the nation. Members are elected by their peers for extraordinary contributions to engineering. Dr. John L. Anderson is president.

The **National Academy of Medicine** (formerly the Institute of Medicine) was established in 1970 under the charter of the National Academy of Sciences to advise the nation on medical and health issues. Members are elected by their peers for distinguished contributions to medicine and health. Dr. Victor J. Dzau is president.

The three Academies work together as the **National Academies of Sciences, Engineering, and Medicine** to provide independent, objective analysis and advice to the nation and conduct other activities to solve complex problems and inform public policy decisions. The National Academies also encourage education and research, recognize outstanding contributions to knowledge, and increase public understanding in matters of science, engineering, and medicine.

Learn more about the National Academies of Sciences, Engineering, and Medicine at www.nationalacademies.org.

The **Transportation Research Board** is one of seven major program divisions of the National Academies of Sciences, Engineering, and Medicine. The mission of the Transportation Research Board is to mobilize expertise, experience, and knowledge to anticipate and solve complex transportation-related challenges. The Board's varied activities annually engage about 8,500 engineers, scientists, and other transportation researchers and practitioners from the public and private sectors and academia, all of whom contribute their expertise in the public interest. The program is supported by state transportation departments, federal agencies including the component administrations of the U.S. Department of Transportation, and other organizations and individuals interested in the development of transportation.

Learn more about the Transportation Research Board at www.TRB.org.

COOPERATIVE RESEARCH PROGRAMS

CRP STAFF FOR NCHRP RESEARCH REPORT 1100

Waseem Dekelbab, *Deputy Director, Cooperative Research Programs, and Manager, National Cooperative Highway Research Program*

David M. Jared, *Senior Program Officer*

Mazen Alsharif, *Senior Program Assistant*

Natalie Barnes, *Director of Publications*

Heather DiAngelis, *Associate Director of Publications*

NCHRP PROJECT 22-38 PANEL

Field of Design—Area of Vehicle Barrier Systems

Kenneth Mora, *Texas Department of Transportation, Austin, TX (Chair)*

Robert W. Bielenberg, *University of Nebraska–Lincoln, Lincoln, NE*

Tracy Borchardt, *AECOM, Spotsylvania, VA*

Lyman L. Hale, *New York State Department of Transportation, Gansevoort, NY*

Randy Hiatt, *California Department of Transportation, Sacramento, CA*

Eric C. Lohrey, *ECL Engineering, PLLC, Warrensburg, NY*

Charles F. McDevitt, *McDevitt Consulting, Matthews, NC*

Alex Hamel Price, *Virginia Department of Transportation, Salem, VA*

Tom Rhoads, *Iowa Department of Transportation, Decorah, IA*

Aimee H. Zhang, *FHWA Liaison*

Kelly K. Hardy, *AASHTO Liaison*

AUTHOR ACKNOWLEDGMENTS

The research reported herein was performed under NCHRP Project 22-38 by the Texas A&M Transportation Institute, a member of The Texas A&M University System. The authors acknowledge and appreciate the computational support provided by the Texas A&M High Performance Research Computing (HPRC) (<http://hprc.tamu.edu/>).



FOREWORD

By David M. Jared

Staff Officer

Transportation Research Board

NCHRP Research Report 1100: MASH TL-3 Deflection Reduction for 31-Inch Guardrail: A Guide presents the use of stiffening mechanisms to reduce the deflection for 31-inch guardrail installations while maintaining system integrity and safety performance. The Guide reflects test conditions specified in the *Manual for Assessing Safety Hardware* (MASH) and is based on computer simulations and full-scale crash testing. The Guide should be of interest to state departments of transportation and other agencies considering the implementation of the stiffening mechanisms evaluated in this research.

Roadside obstacles are often too close to the roadway to permit the installation of common guardrail designs. When this occurs, the protective capability of a guardrail system is desired but without large deflections from vehicle impacts. To achieve this, guardrail systems are often modified with a combination of tighter post spacing, nesting of rails, and other guardrail stiffening mechanisms to reduce deflections. Considerable research has been completed on these topics, and the AASHTO *Roadside Design Guide* (RDG) provides guidelines on this topic. However, much of the available research is based on test conditions specified in *NCHRP Report 350: Recommended Procedures for the Safety Performance Evaluation of Highway Features*. Hence, a guide was needed on the use of stiffening mechanisms to locally reduce the deflection for 31-inch guardrail installations while maintaining system integrity and safety performance. This guide would reflect test conditions specified in MASH rather than *NCHRP Report 350*.

Under NCHRP Project 22-38, “Development of MASH TL-3 Deflection Reduction Guidance for 31-Inch Guardrail,” the Texas A&M University Transportation Institute was asked to develop a guide for the practical and cost-effective use of stiffening mechanisms to locally reduce the deflection for MASH TL-3-compliant 31-inch Midwest Guardrail System (MGS) installations or equivalent guardrail, including any needed transition from the standard system to the stiffened system while maintaining integrity and safety performance. The research team developed recommendations for selecting stiffening mechanisms to further investigate with computer simulation. This simulation effort estimated dynamic deflections and crash-worthiness for 26 stiffening mechanisms with a variety of evaluation conditions. From this effort, the research team provided recommendations for selecting stiffening mechanisms to further evaluate through full-scale crash testing, which involved four MASH crash tests: 3-10, 3-11, 3-20, and 3-21. All four crash tests showed the stiffening mechanism and appropriate transition successfully met MASH evaluation criteria. The research team also provided guidelines for implementing this stiffening mechanism on the roadside. Finally, an updated table summarizing guardrail deflections from recent crash tests and computer simulations

from this project was developed. This table is presented for consideration as a possible addition to future editions of the RDG.

Two deliverables associated with the Guide are not included herein, but are available on the National Academies Press website (nap.nationalacademies.org) by searching for *NCHRP Research Report 1100: MASH TL-3 Deflection Reduction for 31-Inch Guardrail: A Guide*. The deliverables are as follows:

- Slide presentation summarizing the project and including videos of crash testing.
- Slide presentation without the crash testing videos.



CONTENTS

1	Summary
3	Chapter 1 Introduction
4	Chapter 2 Literature Review and State Survey
4	Overview
4	Midwest Guardrail System
4	Guardrail Deflections
5	Development and Implementation of the Simplified MGS Stiffness Transition
6	Post Spacing
11	Fill Condition
12	Post Length and Embedment Depth
15	Nested and 10-Gauge Rail
17	Blockout Depth
19	Backup Rails
19	AASHTO RDG Guardrail Stiffening Guidelines
19	State Survey
51	Literature Review and State Survey Conclusions
53	Chapter 3 Computer Simulation and Modeling
53	Baseline Model and Validation
60	Stiffening Mechanism Investigation
69	Rub Rail
90	Backup Rail
139	Combination Rails
171	Summary and Conclusions
177	Chapter 4 System Details
177	Test Article and Installation Details for Stiffened MGS
177	Test Article and Installation Details for Stiffened MGS Transition
177	Design Modifications During Tests
183	Material Specifications
183	Soil Conditions
185	Chapter 5 Test Requirements and Evaluation Criteria
185	Crash Test Performed/Matrix
185	Evaluation Criteria
187	Chapter 6 Test Conditions
187	Test Facility
187	Vehicle Tow and Guidance System
187	Data Acquisition Systems

190	Chapter 7 MASH Test 3-10 (Crash Test No. 612941-02-2)
190	Test Designation and Actual Impact Conditions
190	Weather Conditions
190	Test Vehicle
193	Test Description
193	Damage to Test Installation
194	Damage to Test Vehicle
194	Occupant Risk Factors
194	Test Summary
199	Chapter 8 MASH Test 3-11 (Crash Test No. 612941-02-1)
199	Test Designation and Actual Impact Conditions
199	Weather Conditions
199	Test Vehicle
202	Test Description
202	Damage to Test Installation
203	Damage to Test Vehicle
203	Occupant Risk Factors
203	Test Summary
208	Chapter 9 MASH Test 3-21 (Crash Test No. 612941-02-3)
208	Test Designation and Actual Impact Conditions
208	Weather Conditions
208	Test Vehicle
211	Test Description
211	Damage to Test Installation
212	Damage to Test Vehicle
212	Occupant Risk Factors
212	Test Summary
217	Chapter 10 MASH Test 3-20 (Crash Test 612941-02-4)
217	Test Designation and Actual Impact Conditions
217	Weather Conditions
217	Test Vehicle
220	Test Description
220	Damage to Test Installation
221	Damage to Test Vehicle
221	Occupant Risk Factors
221	Test Summary
226	Chapter 11 Conclusions, Findings, and Suggested Research
226	Assessment of Test Results
226	Summary of Research Effort
226	Findings and Implementation
234	References
237	Acronyms

238	Appendix A	Details for the Stiffened MGS and Transition
269	Appendix B	Supporting Certification Documents
273	Appendix C	MASH Test 3-10 (Crash Test No. 612941-02-2)
283	Appendix D	MASH Test 3-11 (Crash Test No. 612941-02-1)
293	Appendix E	MASH Test 3-21 (Crash Test No. 612941-02-3)
303	Appendix F	MASH Test 3-20 (Crash Test No. 612941-02-4)

MASH TL-3 Deflection Reduction for 31-Inch Guardrail: A Guide

Obstacles to errant motorists, such as trees, overhead gantry supports, and luminaire poles, are often found on the roadside. Engineers design barriers to protect motorists from collisions with these roadside obstacles. Rigid barriers, such as concrete parapets, provide maximum protection against these obstacles but also produce the largest deceleration risk to the vehicle occupants during an impact. Conversely, guardrail systems allow much larger deflections into the roadside but also produce a much smaller deceleration risk to the vehicle occupants. Therefore, engineers implement guardrail systems when the roadside obstacles allow for larger deflections. This determination is primarily focused on the obstacle's setback distance away from the roadway.

In field applications, roadside obstacles are often too close to the roadway to permit the installation of common guardrail designs. When this occurs, engineers desire the protective capability of a guardrail system but without the large deflections. To achieve this, guardrail systems are often modified with a combination of tighter post spacing, nesting of rails, and other guardrail stiffening mechanisms to reduce deflections. Fortunately, much research has been completed on these topics, and the American Association of State Highway and Transportation Officials (AASHTO) *Roadside Design Guide* (RDG) provides guidelines on this topic (1). However, much of the available research and literature is based on conditions specified in *NCHRP Report 350: Recommended Procedures for the Safety Performance Evaluation of Highway Features* (2). The objective of this project was to develop guidelines for the use of stiffening mechanisms to locally reduce the deflection for 31-inch guardrail installations while maintaining system integrity and safety performance. These guidelines would reflect test conditions specified in the *AASHTO Manual for Assessing Safety Hardware* (MASH) rather than *NCHRP Report 350* (3, 2).

The research effort began in Phase I with a literature review to identify previous research and testing related to guardrail stiffening mechanisms. In parallel with this review, a survey targeting state departments of transportation (DOTs) was developed and distributed. This survey identified mechanisms that states are currently using for stiffening the Midwest Guardrail System (MGS). At the end of Phase I, the research team developed recommendations for selecting stiffening mechanisms to further investigate with computer simulation. Subsequently, stiffening mechanisms were prioritized for further investigation.

During Phase II, the research team completed over 100 finite element analyses (FEA) evaluating both the deflection-reduction capability of the stiffening mechanism and the crashworthiness of the system. The research team evaluated each stiffening mechanism with computer simulations of MASH Test 3-11, and the selected stiffening mechanisms were evaluated with computer simulations of MASH Test 3-10. Furthermore, transitions were developed for selected stiffening mechanisms and evaluated with computer simulations of MASH Tests 3-21 and 3-20.

The deflection-reducing capability of those crashworthy stiffening mechanisms proved to be wide-ranging. Some of the stiffening mechanisms exhibited limited reductions in deflection for the additional cost beyond a standard MGS. On the other hand, several of the stiffening mechanisms exhibited a high level of deflection reduction, usually accompanied by a larger cost increase.

Subsequently, stiffening mechanisms were prioritized, and a testing plan was selected. The combination of half-post spacing (37.5 inches) and an HSS8×8× $\frac{3}{16}$ blackout replacement tube was chosen for full-scale MASH crash testing.

Phase III involved the full-scale MASH crash testing and evaluation. This involved four MASH crash tests: 3-11, 3-10, 3-21, and 3-20. The stiffened MGS with the half-post spacing (37.5 inches) and an HSS8×8× $\frac{3}{16}$ blackout replacement tube successfully met MASH evaluation criteria for both tests 3-11 and 3-10. The transition from full-post spacing MGS to this stiffened system also successfully met MASH evaluation criteria for both Tests 3-21 and 3-20. Therefore, this system is suitable for implementation on the roadside. The research team reviewed installation damage and high-speed video to determine recommended installation lengths of the stiffened MGS. A minimum of 37.5 ft of the stiffened MGS with half-post spacing and HSS8×8× $\frac{3}{16}$ blackout replacement tube is recommended to be installed. The roadside obstacle is recommended to be placed near the center of this stiffened section. This placement considers the primary direction of traffic and conditions where the shielded obstacle is within the clear zone of opposing traffic. The working width was 28.8 inches, measured from the pre-impact traffic face of the rail to the furthest extent of the pickup truck's side mirror, and the height of the working width was 64.8 inches above grade. On both the upstream and downstream sides of the stiffened MGS, the research team recommends transitioning to standard MGS using the transition evaluated in Chapter 9 and Chapter 10. The research team also recommends terminating the total system with a MASH-compliant terminal or downstream anchor terminal as appropriate.

The simulations predicted values for occupant impact velocity (OIV), ridedown acceleration (RDA), working width, and dynamic deflection correlated well with the physical crash testing results. In particular, the difference between the physical crash test and the computer simulation dynamic deflections was 3.7%. Furthermore, an overlay comparison of the simulations and physical crash tests shows a positive qualitative comparison. These successful quantitative and qualitative comparisons provided the research team with confidence in the predictive capability of the computer simulations. Consequently, the research team believes the computer simulation values are reasonable estimates for the dynamic deflections of the various barrier systems evaluated in this project. Based on this conclusion, the research team compiled the deflections of previous crash tests and the computer simulations from this project to create a new table that could be considered for addition to future editions of the RDG.

Introduction

Obstacles to errant motorists, such as trees, overhead gantry supports, and luminaire poles, are often found on the roadside. Engineers design barriers to protect motorists from collisions with these roadside obstacles. Rigid barriers, such as concrete parapets, provide maximum protection against these obstacles but also produce the largest deceleration risk to the vehicle occupants during an impact. Conversely, guardrail systems allow much larger deflections into the roadside but also produce a much smaller deceleration risk to the vehicle occupants. Therefore, engineers implement guardrail systems when the roadside obstacles allow for larger deflections. This determination is primarily focused on the obstacle's setback distance away from the roadway.

In field applications, roadside obstacles are often too close to the roadway to permit the installation of common guardrail designs. When this occurs, engineers desire the protective capability of a guardrail system but without the large deflections. To achieve this, guardrail systems are often modified with a combination of tighter post spacing, nesting of rails, and other guardrail stiffening mechanisms to reduce deflections. Fortunately, much research has been completed on these topics, and the American Association of State Highway and Transportation Officials (AASHTO) *Roadside Design Guide* (RDG) provides guidelines on this topic (1). However, much of the available research and literature is based on conditions specified in *NCHRP Report 350: Recommended Procedures for the Safety Performance Evaluation of Highway Features* (2). The objective of this project was to develop guidelines for use of stiffening mechanisms to locally reduce the deflection for 31-inch guardrail installations while maintaining system integrity and safety performance. These guidelines would reflect test conditions specified in the AASHTO *Manual for Assessing Safety Hardware* (MASH) rather than *NCHRP Report 350* (3, 2).

Phase I of this project included a literature review of the previous research and a survey of state departments of transportation (DOTs). Both efforts collected available information regarding various guardrail stiffening mechanisms. In particular, the research team investigated the stiffening mechanisms' effects on the Midwest Guardrail System's (MGS) deflections.

During Phase II, the research team completed over 100 finite element analyses (FEA) evaluating both the deflection-reduction capability of the stiffening mechanism in question and the crash-worthiness of the system. The research team evaluated each stiffening mechanism with computer simulations of MASH Test 3-11, and the selected stiffening mechanisms were evaluated with computer simulations of MASH Test 3-10. Furthermore, transitions were developed for selected stiffening mechanisms and evaluated with computer simulations of MASH Test 3-21 and 3-20.

Finally, the research team evaluated prioritized designs through full-scale crash testing. The purpose of the tests reported herein was to assess the performance of a stiffened MGS according to the safety performance evaluation guidelines included in the second edition of MASH. The crash tests were performed in accordance with MASH Test Level 3 (TL-3), specifically Tests 3-11, 3-10, 3-21, and 3-20.



CHAPTER 2

Literature Review and State Survey

Overview

This chapter documents the literature review and state survey performed in Phase I of this project. The research team reviewed relevant research regarding stiffening guardrail systems. The six stiffening mechanisms evaluated in this literature review include post spacing, fill condition behind the barrier, post length and embedment depth, nested rails, thicker rails, and blockout depth.

Midwest Guardrail System

In 2004, a new strong-post W-beam guardrail system, the Midwest Guardrail System (MGS), was developed and evaluated at the Midwest Roadside Safety Facility (MwRSF). The system was specifically designed to better accommodate vehicles with the higher center of gravity found on today's roadways. The MGS consists of standard W-beam guardrail and standard W6×9 or W6×8.5 steel posts with the general dimensions shown in Figure 2.1. Additional design variations of the MGS include a guardrail design with a 6-inch curb and stiffened versions with half and quarter-post spacings (4). Full-scale crash tests have verified the satisfactory performance of these systems according to the *NCHRP Report 350* (2).

Guardrail Deflections

“Dynamic deflection” can be defined as the maximum displacement of the barrier during the impact event. “Working width” can be defined as the “distance between the traffic face of the test article before impact and the maximum lateral position of any major part of the system or vehicle after impact” (1). Dynamic deflection considers only the barrier, while the working width includes consideration of the vehicle as well. Furthermore, the working width is typically reported with the height above grade at which the maximum intrusion of the system or vehicle occurs.

When it is essential to shield motorists from a roadside hazard close to the edge of the travelway, it may be necessary to stiffen the standard guardrail system to limit the dynamic deflection and working width. This is accomplished through a variety of stiffening mechanisms that have been developed over the years, including reducing post spacing, nesting rail elements, and increasing embedment depth. These mechanisms and others are discussed later in this report.

In 2015, researchers at MwRSF studied the dynamic deflection and working width of the MGS for MASH impact conditions using LS-DYNA computer simulations. They modeled a 175-ft-long MGS and calibrated the model against previously completed crash tests. Impact simulations

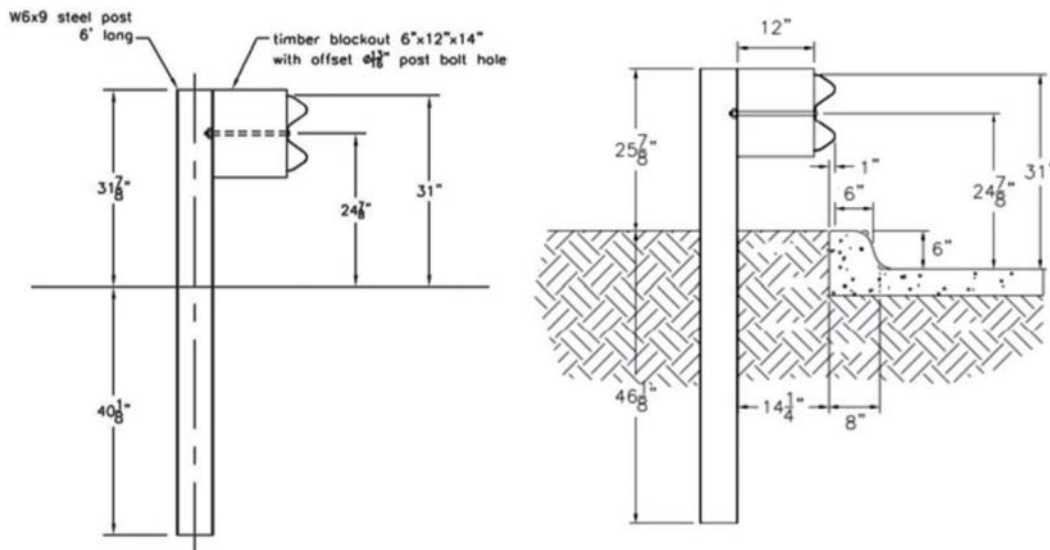


Figure 2.1. MGS variations (4).

Table 2.1. Recommended working width envelopes for guardrail (5).

Design Speed mph (km/h)	Minimum Working Width Envelope by Guardrail Configuration in. (mm)			
	Level Terrain with Blockouts	6 in. (152 mm) Behind Curb with Blockouts	Level Terrain without Blockouts	6 in. (152 mm) Behind Curb without Blockouts
31 (50)	37.6 (955)	30.5 (775)	25.9 (657)	Recommend Testing
44 (70)	49.3 (1,251)	40.9 (1,038)	34.3 (869)	Recommend Testing
62 (100)	60.2 (1,530) (simulation) 60.3 (1,532) ^[11] (full-scale)	49.6 (1,250) (simulation)	48.6 (1,232) (simulation) 49.6 (1,260) ^[15] (full-scale)	Recommend Testing

NOTE: [11] and [15] are references in the original document: [11] *Investigating the Use of Small-Diameter Softwood as Guardrail Posts (Dynamic Test Results)* is reference #25 in this report. [15] *Development of the Midwest Guardrail System (MGS) for Standard Reduced Post Spacing and in Combination with Curbs* is reference #4 in this report.

were then performed to quantify dynamic deflection and working width of the guardrail for MASH TL-1 (31-mph design speed), TL-2 (44-mph design speed), and TL-3 (62-mph design speed) impact conditions on level ground and in combination with a 6-inch-tall AASHTO Type B curb. The recommended working width for these MGS configurations is shown in Table 2.1 as a function of design impact speed (5).

Development and Implementation of the Simplified MGS Stiffness Transition

MwRSF researchers have developed a simplified version of the original MGS stiffness transition by utilizing two common sizes of steel posts (6). MASH Test 3-21 (Test No. MWTSP-2) and MASH Test 3-20 (Test No. MWTSP-3) were successfully performed on the simplified steel-post MGS stiffness transition system at the upstream transition (transition from standard post spacing to half-post spacing). Researchers determined from a detailed BARRIER VII analysis

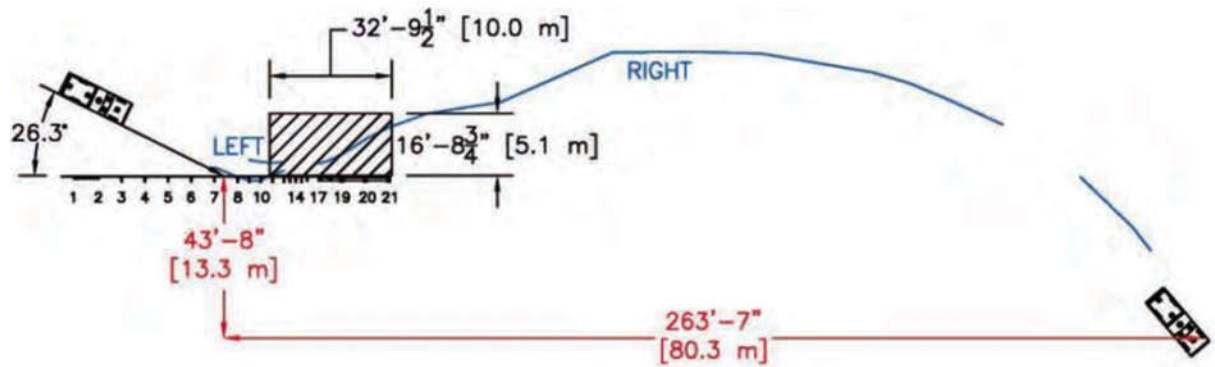


Figure 2.2. Test impact drawing for Test No. MWTSP-2 (6).

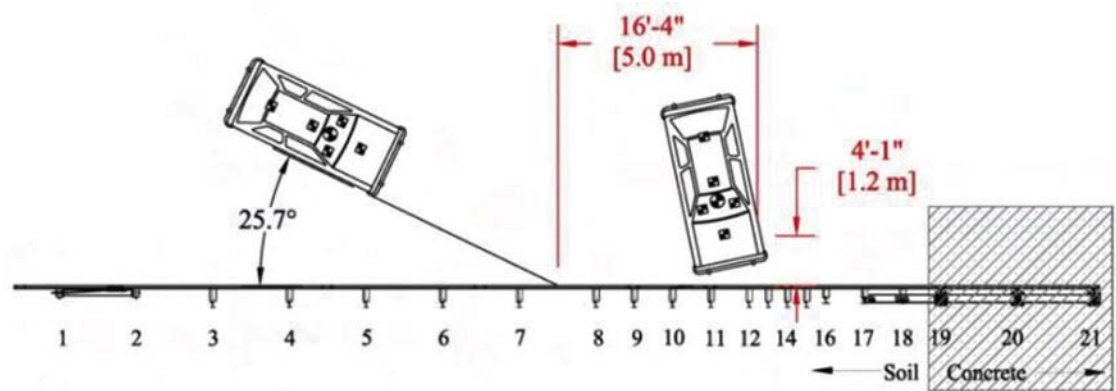


Figure 2.3. Test impact drawing for Test No. MWTSP-3 (6).

that the critical impact point (CIP) was the transition from standard post spacing to half-post spacing. Figure 2.2 and Figure 2.3 show the test impact drawings for Test Nos. MWTSP-2 and MWTSP-3, respectively.

The maximum dynamic deflection of the simplified steel-post MGS stiffness transition was 32.8 inches for MASH Test 3-21 and 18.5 inches for MASH Test 3-20. The simplified steel-post MGS stiffness transition satisfied all MASH TL-3 criteria.

Post Spacing

MGS with Reduced Post Spacing

A variation of the MGS with reduced post spacing was crash tested in accordance with *NCHRP Report 350* (2). The MGS with reduced post spacing was similar to the standard MGS but included additional posts. Full-post spacing is 75 inches, making half-post spacing 37.5 inches and quarter-post spacing 18 3/4 inches. Half-post spacing and quarter-post spacing were used to stiffen the original system.

The maximum dynamic deflection of the MGS with standard post spacing was 43 inches for *NCHRP Report 350* Test 3-11 and 17.5 inches for *NCHRP Report 350* Test 3-10 (2). The maximum dynamic deflection of the MGS with quarter-post spacing was approximately 2.5 times less than the dynamic deflection of the standard MGS.



Figure 2.4. Deflection during the quarter-post spacing MGS System Test 3-11 (7).

Testing MGSs with Reduced Post Spacing for MASH Compliance (7)

Texas A&M Transportation Institute (TTI) researchers completed a research project for the Roadside Safety Pooled Fund titled, “Testing of Midwest Guardrail Systems with Reduced Post Spacing for MASH Compliance.” The objective of the project was to test and evaluate the MGS with half-post and quarter-post spacings in accordance with MASH criteria. Furthermore, the research team investigated methods to safely transition the stiffness between various post spacings (7).

TTI researchers first evaluated a quarter-post spacing system (18.75 inches) with MASH Tests 3-11 and 3-10. The quarter-post spacing system successfully passed both MASH tests. The maximum dynamic deflection during MASH Test 3-11 was 19.5 inches, and the working width was 37.1 inches at a height of 27.9 inches above grade. Figure 2.4 shows the deflection of the system during impact (7).

TTI researchers also tested a transition between quarter- (18.75-inch) and full- (75-inch) post spacing following MASH Test 3-21 impact conditions. Figure 2.5 shows the transition design evaluated in this test. This transition used single W-beam rail elements and did not incorporate any nested rail sections. In this test, the pickup truck ruptured the rail and penetrated beyond the barrier. Figure 2.6 shows the rail rupturing and the test vehicle penetrating behind the guardrail system. TTI researchers attributed the failure to rail pocketing caused by the short transition in stiffness. Figure 2.7 shows the pocketing of the system (7).

The research team subsequently extended the transition and evaluated it through computer simulation. This extended transition can be seen in Figure 2.8. The results of the computer

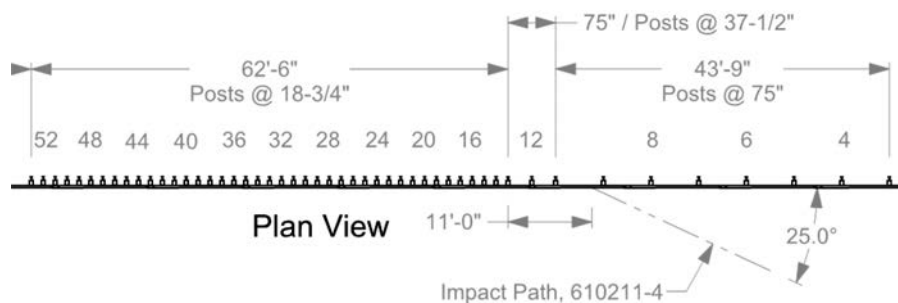


Figure 2.5. Plan view of MASH Test 3-21 on quarter- to full-post spacing transition (7).



Figure 2.6. MASH Test 3-21 on quarter- to full-post spacing transition rail rupture (7).



Figure 2.7. MASH Test 3-21 on quarter- to full-post spacing transition rail pocketing (7).

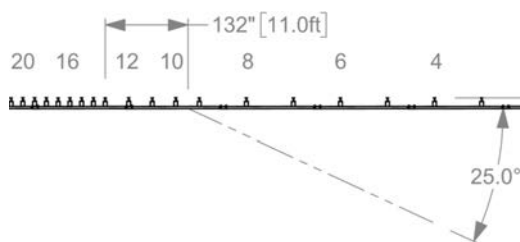


Figure 2.8. Plan view of MASH Test 3-21 with a longer quarter- to full-post spacing transition (7).

simulations showed the extension of the transition would likely improve its crashworthiness. Therefore, the research team performed MASH Test 3-21 on the extended transition. The system successfully contained and redirected the impacting test vehicle and was deemed crashworthy (7).

TTI researchers also tested a half-post spacing (37.5 inches) under this project. In this test, the pickup truck ruptured the rail and penetrated beyond the barrier. Figure 2.9 shows the rail rupturing and the test vehicle penetrating behind the guardrail system. The researchers attributed the rail rupture to an interaction between the lower edge of the W-beam guardrail and the timber blockout. Consequently, the researchers evaluated the replacement of the standard 14-inch-height blockout with a shortened 10-inch-height blockout. This would minimize any



Figure 2.9. MASH Test 3-11 on half-post spacing rail rupture (7).

interaction between the blockout and the bottom edge of the W-beam guardrail. Figure 2.10 shows a comparison of the two heights (7).

The research team subsequently evaluated the revised system with shortened blockouts through computer simulation. The results of the computer simulations showed the shortened blockout minimized the interaction between the bottom edge of the W-beam guardrail and the blockout. Therefore, the research team performed MASH Test 3-11 on this revised design. The system successfully contained and redirected the impacting test vehicle and was deemed crashworthy.

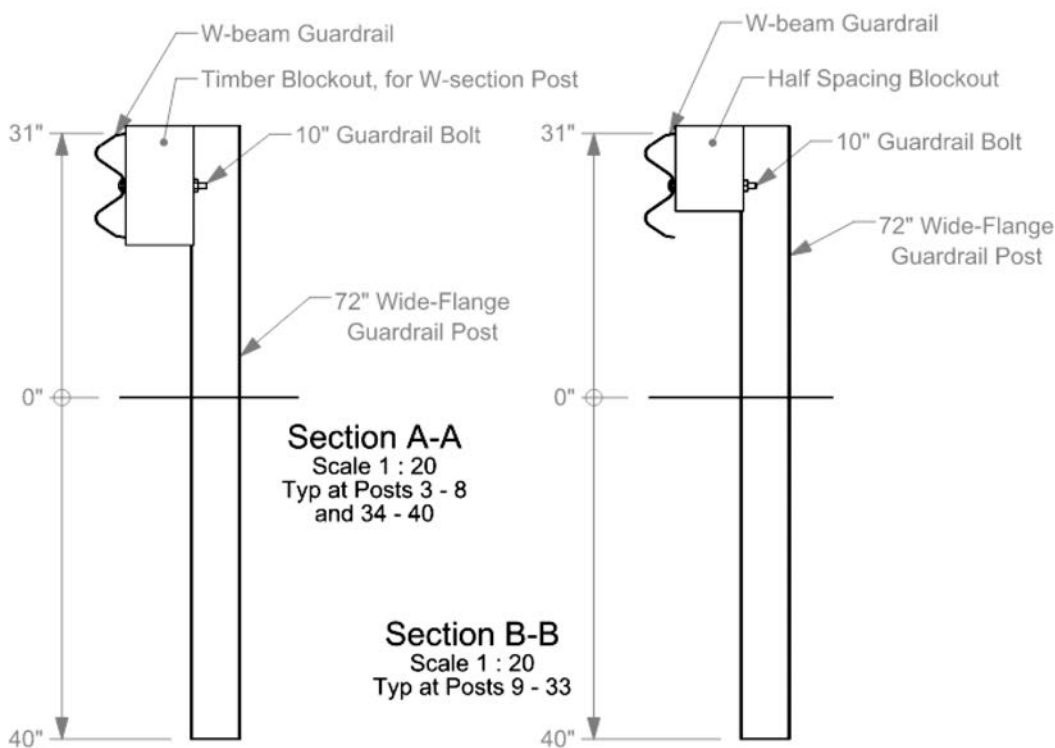


Figure 2.10. Comparison of standard blockout height and shortened blockout height (7). Typ = Typical.

The maximum dynamic deflection during MASH Test 3-11 was 25.6 inches, and the working width was 43.1 inches at a height of 10.1 inches above grade (7).

Barrier Deflection Characteristics of 31-Inch W-beam Guardrail Systems

TTI researchers conducted a research study to provide updated maximum deflection values for various configurations of 31-inch W-beam guardrail systems under MASH impact conditions. Computer simulations and the results from previous crash tests were used to determine maximum deflections for 31-inch W-beam guardrail systems with standard W6×8.5 strong posts with varying post spacing (full-post spacing, half-post spacing, and quarter-post spacing) and both single and nested guardrail elements (8).

After summarizing available crash-test data, simulations were performed on additional 31-inch guardrail systems to broaden the range of system configurations for which deflection data is available. The simulations were performed using BARRIER VII, a two-dimensional FEA program. This analysis package has been used historically on many projects to predict deflection of barrier systems. Since BARRIER VII is not capable of predicting snagging potential arising from vehicle wheel/suspension interacting with the posts, this research study was only able to address the deflection potential of 31-inch W-beam guardrail systems.

TTI researchers performed BARRIER VII simulations under MASH Test 3-11 impact conditions to determine the maximum deflections for the single W-beam guardrail system at full-post, half-post, and quarter-post spacing. The objective was to study the difference in the deflection characteristics of the guardrail when the system was stiffened by decreasing the post spacing. The results of the BARRIER VII simulation study for the single W-beam guardrail system are summarized in Table 2.2.

The results obtained from the simulation effort were used to predict the deflection characteristics of specific guardrail configurations. The resulting data were then combined with crash-test data to update the AASHTO RDG barrier deflection guidelines (1). The information gathered from this research study provides updated deflection values for various configurations of 31-inch W-beam guardrail under MASH impact conditions.

Assessment of Guardrail-Strengthening Techniques

Rosson et al. (10) investigated guardrail-strengthening techniques by full-scale crash testing according to Service Level 2 conditions of *NCHRP Report 230* (9) and by BARRIER VII computer simulations. Kansas DOT's standard W-beam guardrail with W6×8.5 steel posts was strengthened by nesting the W-beam and reducing the post spacing. Four rail variations of design, including combinations of post spacing and nesting, were computer simulated and crash tested. The

Table 2.2. Results for single W-beam guardrail system (8).

Strong-Post W-Beam Guardrail	
Post Spacing	Maximum Barrier Deflection (inches)
Full	48
Half	29
Quarter	18

guardrail designated KSWB-1 (full-post spacing with single W-beam) formed the basis for comparison with the other three guardrail installations. Reduced post spacing showed significant reductions in deflection.

Fill Condition

In the early 1990s, researchers at ENSCO Inc. conducted a crash test on a standard G4(1S) W-beam rail installed on a 2:1 downslope. The maximum permanent rail deflection was 43 inches, and the test article failed due to vehicle rollover (11).

In 2013, TTI researchers developed a MASH TL-3-compliant guardrail for placement on 2H:1V slopes (12). This system was developed for road conditions where terrain topology limits the available flat area required for typical guardrail performance. After an extensive simulation effort using LS-DYNA and various modifications, TTI researchers developed a guardrail system with 8-foot-long, W6×9 steel posts spaced 75 inches on center. In addition, the design included a 12-gauge W-beam rail element mounted at a rail height of 31 inches and aligned with the breakpoint of a 2H:1V slope. Figure 2.11 illustrates the cross section of the crash-tested system.

MASH Tests 3-11 and 3-10 were conducted on the system. In both tests, the guardrail contained and redirected the vehicles with maximum dynamic deflections of 4.3 ft and 2.7 ft, respectively. The guardrail on the slope performed acceptably according to the specifications for MASH TL-3 longitudinal barriers. Figure 2.12 shows the installation after MASH Test 3-11 (12).

In 2010, researchers at MwRSF developed a stiffened version of the MGS to be used adjacent to steep roadside slopes (13). The design consisted of 9-ft-long posts with 75-inch spacing. They conducted dynamic surrogate vehicle testing of W6×9 steel posts placed at the breakpoint of a 2H:1V fill slope to evaluate the post-soil behavior for various embedment depths. After the dynamic surrogate vehicle testing, the MGS with a 31-inch top-mounting height was successfully crash tested according to MASH Test 3-11 (Figure 2.13). The MGS installed adjacent to a 2H:1V fill slope exhibited a working width of 64.2 inches. Thus, the MwRSF researchers recommended a minimum lateral distance of 66 inches between the front face of any fixed object and the front face of the MGS adjacent to a 2:1 fill slope. The maximum lateral permanent and dynamic deflections were 42 inches and 57.6 inches, respectively.

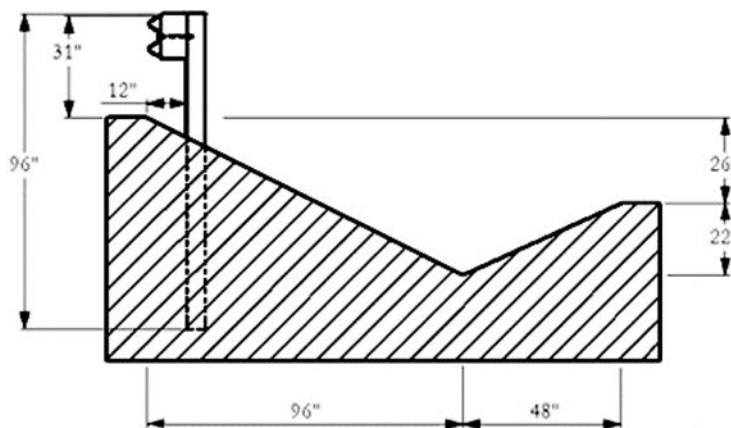


Figure 2.11. Cross section of 31-inch system (12).



Figure 2.12. *Top photo shows the traffic side of the installation; bottom photo shows the field side of the installation.*

Researchers at MwRSF crash tested the MGS with 72-inch-long W6×8.5 steel posts with 12-inch blockouts and 12-gauge guardrail sections at the breakpoint of a 2H:1V slope (Figure 2.14). The design successfully met the safety performance criteria for MASH Test 3-11. The maximum lateral permanent and dynamic deflections were 46 inches and 72.9 inches, respectively (14).

Post Length and Embedment Depth

Round Wood Post Project

In 2017, TTI evaluated Texas DOT's (TxDOT) round wood post guardrail system for MASH compliance. This system consisted of 7.25-inch-diameter round wood guardrail posts embedded 40 inches below grade. During the test, multiple posts fractured, which allowed the test vehicle to override the system (15). TTI researchers determined the post fracture attributed to the test failure and therefore began to modify the system to improve crashworthy performance.

In the subsequent project, TTI researchers evaluated the effects of post embedment depth on the crashworthy performance of the system. In particular, the researchers were evaluating the relationship between the embedment depth and the ability of the post to move through the soil. If the posts could move more freely through the soil, the load on the posts would be decreased and therefore the posts would maintain integrity and not fracture. To test this hypothesis, TTI performed a series of component pendulum tests before full-scale MASH testing. Figure 2.15

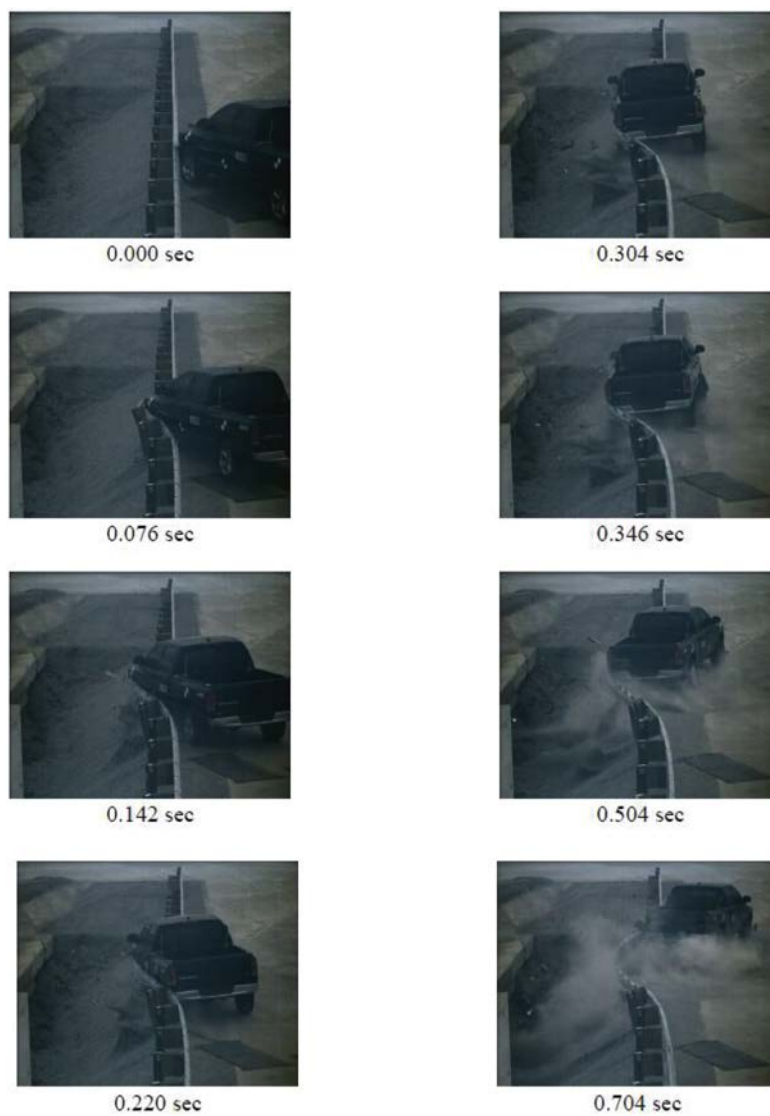


Figure 2.13. Sequential photographs, Test No. MGS221-2 (13).



Figure 2.14. Impact location, Test No. MGSS-1 (14).



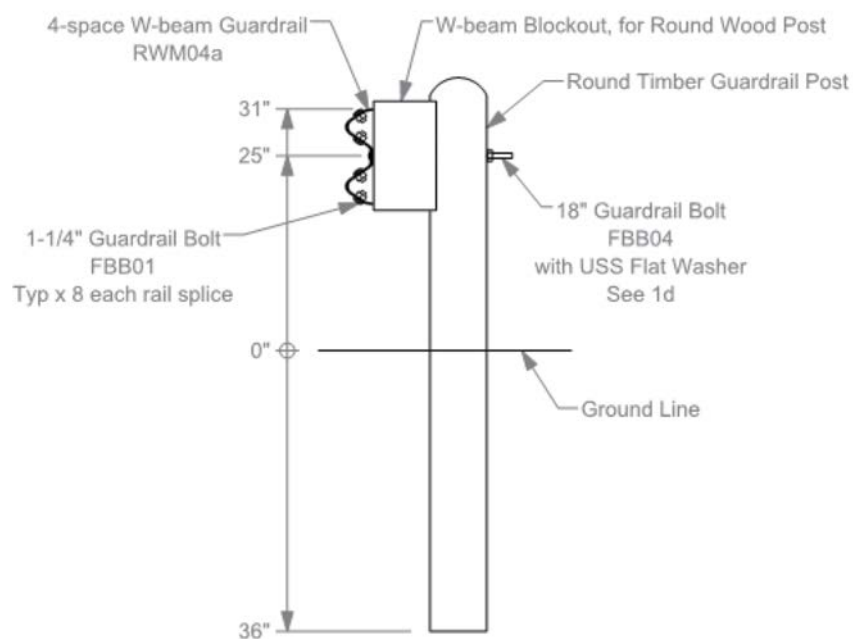
Figure 2.15. Component pendulum testing on round wood guardrail posts.

shows one of these tests. The results allowed TTI researchers to conclude that an embedment depth of 36 inches would decrease the load on the posts and improve crashworthy performance.

TTI then completed MASH Test 3-11 on the round wood post guardrail system with 36 inches of embedment instead of the prior 40 inches. Note: Notations, such as FBB01, are related specifically to the TTI project.

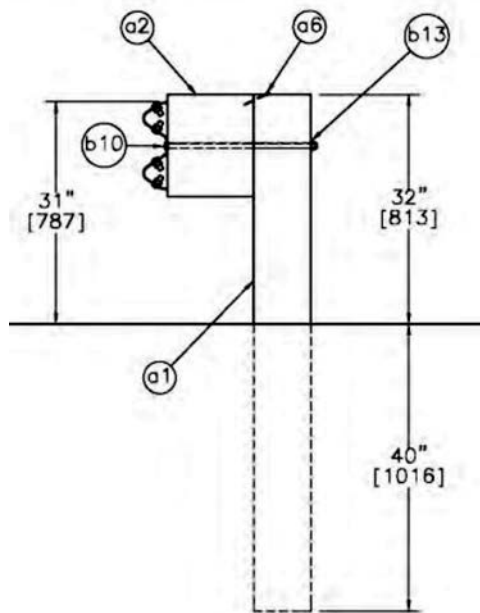
Figure 2.16 shows a section view of the round wood post guardrail system with a 36-inch embedment.

This system successfully passed MASH Test 3-11, and the TTI researchers evaluated the system as suitable for implementation on the roadside. The maximum dynamic deflection was 44.1 inches, and the working width was 62.2 inches at a height of 57.4 inches above grade.



NOTE: Notations, such as FBB01, are related specifically to the TTI project.

Figure 2.16. Section view of TxDOT round wood post guardrail system (16).



NOTE: Notations, such as "a1," are related to the MwRSF project.

Figure 2.17. Section view of MGS with WP posts (17).

Evaluation of the MGS with White Pine Wood Posts

MwRSF evaluated the white pine (WP) wood post MGS system according to MASH TL-3 criteria (17). The MGS utilizes 6-inch-wide \times 8-inch-deep \times 72-inch-long posts with approximately 4 inches less embedment than other W-beam systems. This decrease in post embedment results in lower forces imparted on the posts, indicating that the use of a lower capacity post with the MGS may be a possibility. In addition, the lower strength WP posts would allow the posts to fracture at lower loads than typical southern yellow pine posts and reduce the potential for significant wheel snag on the posts. Figure 2.17 shows a section view of the MGS with WP posts.

MASH Test 3-11 was successfully performed on the MGS with WP posts (17). The MGS with WP posts successfully contained and redirected the 2270P vehicle. The maximum dynamic deflection was 46.3 inches, the permanent deformation was 33.75 inches, and the working width was 58.4 inches. Figure 2.18 shows a picture of the MGS with WP posts test installation after the MASH Test 3-11.

Nested and 10-Gauge Rail

Nesting W-beam guardrail sections involves placing one piece of W-beam guardrail in front of another, effectively doubling the thickness of the cross section. This is a common practice for many DOTs, but industry members disagree on its effectiveness in reducing deflections. Some believe it significantly aids in reducing deflections, while others say this effect is minimal and does not outweigh installation difficulties. Due to the geometry of the W-beam section, nesting rail elements obscure the bolt holes. At best, it adds difficulty to installation and at worst, makes it impossible to fit a guardrail bolt through all the holes. Installation crews often have to cut a larger hole through the section, which is not an ideal installation procedure. Nevertheless, nested rail elements can often be seen in transition sections.



Figure 2.18. MGS with WP posts after the MASH Test 3-11 (17).

To avoid the installation difficulties, while also increasing the cross-sectional area of the rail, some designers will select a 10-gauge rail instead of the standard 12-gauge. The cross-sectional area of a 10-gauge W-beam and nested W-beam is 2.56 inches² and 4 inches², respectively. Therefore, the cross-sectional area of a 10-gauge W-beam is roughly 36% less than the cross-sectional area of a nested W-beam. Based on the comparison of cross-sectional areas, it would be expected that the tensile strength of a 10-gauge W-beam is roughly 36% less than that of a nested W-beam. However, the cross-sectional area of the 10-gauge may provide adequate tensile capacity without the additional 36% gained by using nested rail.

Assessment of Guardrail-Strengthening Techniques

As discussed previously, Rosson et al. investigated guardrail-strengthening techniques by full-scale crash testing according to Service Level 2 conditions of *NCHRP Report 230* (9) and by BARRIER VII computer simulations (10). Kansas DOT's (KDOT) standard W-beam guardrail with W6×8.5 steel posts was strengthened by nesting the W-beam and reducing the post spacing. Four rail variations were computer simulated and crash tested. The guardrail designated KSWB-1 (full-post spacing with single W-beam) formed the basis for comparison with the other three guardrail installations. Based on the full-scale crash-test results and computer simulation results, the study concluded that the strengthening technique of nesting the W-beam produces only marginal reductions in lateral deflection.

Barrier Deflection Characteristics of 31-Inch W-beam Guardrail Systems

As previously discussed, TTI conducted a research study to provide updated maximum deflection values based on simulations and crash-test results for installations of 31-inch W-beam guardrail systems (8). TTI researchers performed BARRIER VII simulations under MASH Test 3-11

Table 2.3. Results for nested W-beam guardrail system (8).

Strong-Post Nested W-Beam Guardrail	
Post Spacing	Maximum Barrier Deflection (inches)
Full	46
Half	26
Quarter	17

impact conditions to determine the maximum deflections for the nested W-beam guardrail system at full-post, half-post, and quarter-post spacing. The objective was to study the deflection characteristics of the guardrail system by changing the single W-beam BARRIER VII model to represent a nested W-beam barrier model. The results of the BARRIER VII simulation study for the nested W-beam guardrail system are summarized in Table 2.3.

Blockout Depth

Blockout Depth Comparison

With certain DOTs preferring the use of standard 8-inch blockouts rather than the 12-inch horizontal depth, a study was conducted to review and compare system performance and vehicle interaction in full-scale crash tests of 31-inch guardrail with 12-inch and 8-inch blockouts (18).

To identify similarities and dissimilarities from the use of the 12-inch and 8-inch blockout depths, data collected through crash tests were then compared to vehicle angular displacements (i.e., yaw, pitch, and roll angles), occupant risks [occupant impact velocities (OIV) and ridedown accelerations (RDA)], rail system deflections (dynamic and permanent), working width, and vehicle interaction with the guardrail system through the impact event. Engineering analysis and judgment, detailed film analysis review, and statistical analysis were employed to adequately compare results derived from groups of 31-inch guardrail tests utilizing 12-inch and 8-inch blockout depths (tests of 31-inch guardrail without blockouts were also included in the engineering analysis and comparison) (18).

Figure 2.19 shows dynamic deflections and means for each blockout depth category. Dynamic deflections recorded from full-scale crash tests on systems with 12-inch blockout depths have a calculated mean value of 49.45 inches. Dynamic deflections recorded from full-scale crash tests on systems with 8-inch blockout depths have a calculated mean value of 37.09 inches. The mean value for the dynamic deflection from 12-inch blockouts is 33.32% bigger than the mean value from 8-inch blockout tests. The dynamic deflections recorded from full-scale crash tests on systems with no use of blockouts have a calculated mean value of 31.52 inches, which represents a decrement of 36.26% from the mean value with 12-inch blockout depth tests (18).

Figure 2.20 shows working widths and means for each blockout depth category. Working width deflections recorded from full-scale crash tests on systems with 12-inch blockout depths have a calculated mean value of 61.55 inches. Working width deflections recorded from full-scale crash tests on systems with 8-inch blockout depths have a calculated mean value of 43.13 inches. The mean value for the working width deflection from 12-inch blockouts is 42.71% bigger than the mean value from 8-inch blockout tests. It is interesting to note that working width deflections recorded from full-scale crash tests on systems with no use of blockouts have a calculated mean value of 40.40 inches, which represents a decrement of 34.36% from the mean value with 12-inch blockout tests (18).

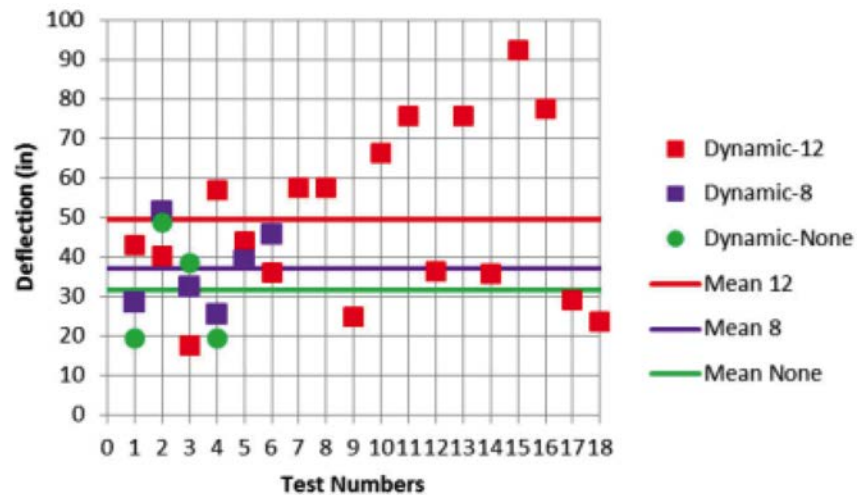


Figure 2.19. *Dynamic deflections with means for the investigated tests (18).*

When comparing the barrier deflection and working width, it was the opinion of the researchers that any difference observed between tests is not related to the type of blockouts used but rather to the test installation configuration and the actual impact conditions of the tests (18). Moreover, researchers concluded that the rail behavior does not depend on the blockout depth used in the system. Instead, it seems to be a function of the vehicle-system interaction. When the system is impacted by a pickup truck, the rail tends to generate vehicle deformation between the impacting tire and fender. When the system is impacted by a passenger car, the rail tends to be pushed upward, because of the engagement of the vehicle with the bottom of the rail.

Based on the evaluation reported in the conducted study, it was the opinion of the researchers that there is no significant difference between the use of 12-inch and 8-inch blockouts in terms of vehicle stability, occupant risk, rail system deflection, and interaction between the vehicle and guardrail system (18). This led to the recommendation that 8-inch-deep blockouts be considered

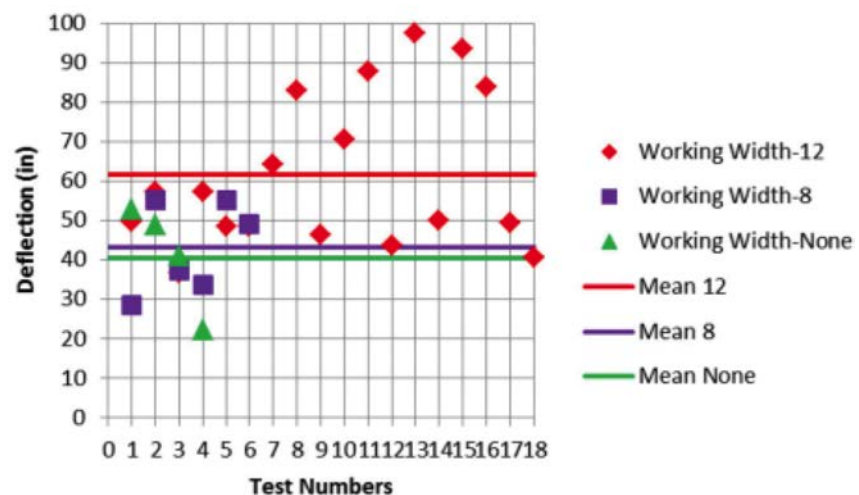


Figure 2.20. *Working width with means for the investigated tests (18).*

a crashworthy alternative for configurations initially tested with a 31-inch guardrail with 12-inch blockouts and midspan splices.

Midwest Guardrail System Without Blockouts

A study was conducted at MwRSF to compare results from 1100C small car and 2270P pickup truck tests for the standard (with blockout) and non-blockout versions of the MGS. The study showed lower dynamic deflection for the non-blockout systems in both pickup truck and small passenger car tests. The occupant risk in the non-blockout systems appeared to be higher than the standard MGS (19).

Backup Rails

Previous research efforts have investigated installing additional longitudinal rail elements, often referred to as “backup rails,” beyond the standard W-beam elements. Plaxico et al. studied the crashworthiness of Ohio DOT’s guardrail designs for mounting over a culvert (20). The various designs incorporated steel tubular members that nested inside the valleys of the W-beam. The research team performed detailed computer simulations of *NCHRP Report 350* Test 3-11 on the designs. The simulations showed a potential for tires to snag on the post because of the rigidity of the steel tubes. Therefore, the research team evaluated several retrofit options to mitigate the potential for wheel snag. After evaluation of the retrofits and transitions to the guardrail system, the research team received Federal Highway Administration (FHWA) acceptance on select systems.

AASHTO RDG Guardrail Stiffening Guidelines

The third edition of the AASHTO RDG provides the results of computer simulations using the Numerical Analysis of Roadside Design Program to determine maximum deflections for Standard SGR04a and SGR09 systems as well as the results of field testing conducted by the KDOT (21).

The MGS has successfully passed both MASH tests 3-11 and 3-10 under both the MASH and *NCHRP Report 350* evaluation criteria (2). Table 5-4 presented in the fourth edition of the AASHTO RDG summarizes the MGS applications with dynamic deflections, working widths, and post configurations (1). State DOTs use Table 5-4 to modify the MGS design for their necessary design applications based on dynamic deflections and working widths.

State Survey

Overview

A survey was designed to investigate current practices for stiffening guardrail systems. The survey questioned respondents on their state’s methods for reducing deflections of MGS. Each respondent was asked a series of questions regarding specific details of the state’s stiffening mechanisms. Furthermore, the respondents were asked to detail the methods used to transition these stiffening mechanisms.

The following survey was administered online using Qualtrics and was sent to all 50 state DOTs. A total of 21 state DOT agencies responded to the survey. The research team further engaged with several of the respondents regarding their submitted responses for the purposes of clarification or elaboration.

Survey Questions and Responses

Survey questions are not in numerical order, but instead are grouped by topic area.

Q4 - Does your agency use a stiffening mechanism to reduce guardrail deflections (MGS and non-MGS systems)?

[See Figure 2.21 for responses.]

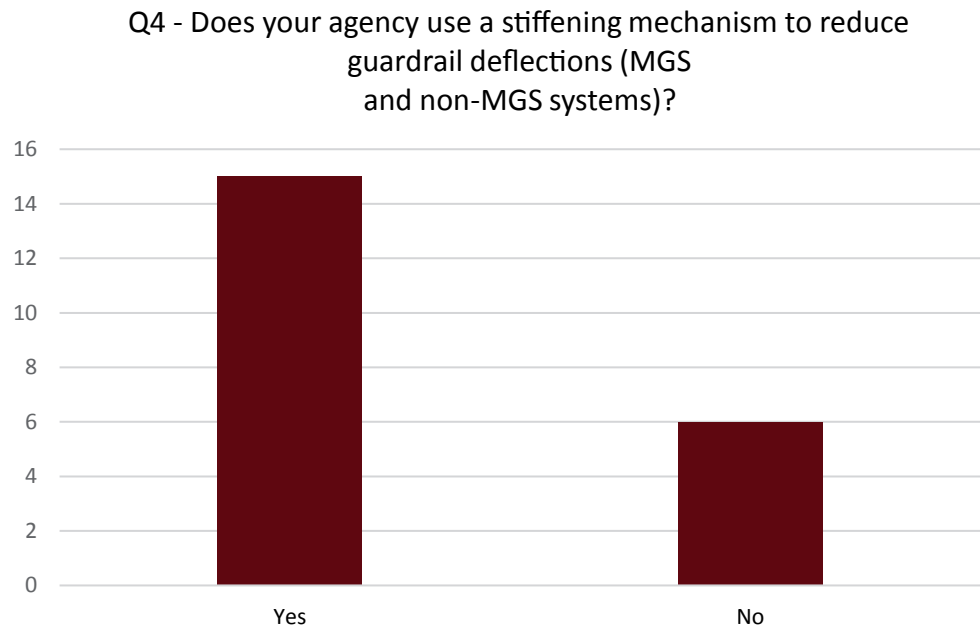


Figure 2.21. Question 4 responses.

Q5 - Which of the following components are used as part of this stiffening mechanism?
(Note: You will be given an opportunity to include other stiffening mechanisms later in the survey if you use more than one.) Select all that are used in this stiffening mechanism.

[See Figure 2.22 for responses.]

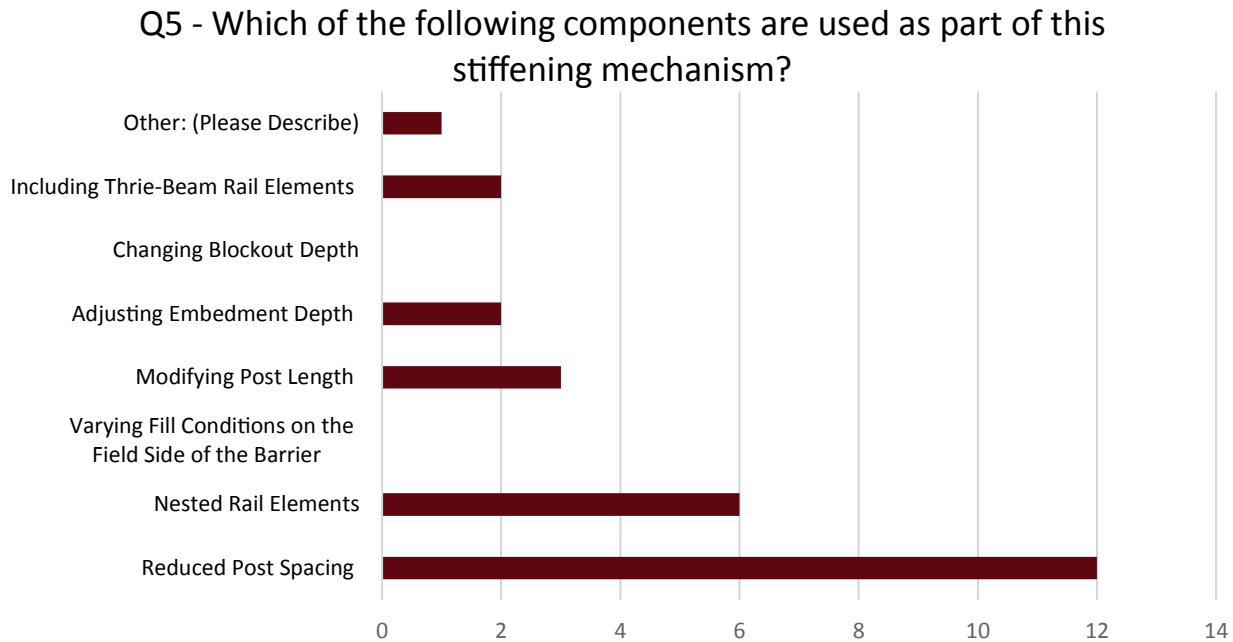
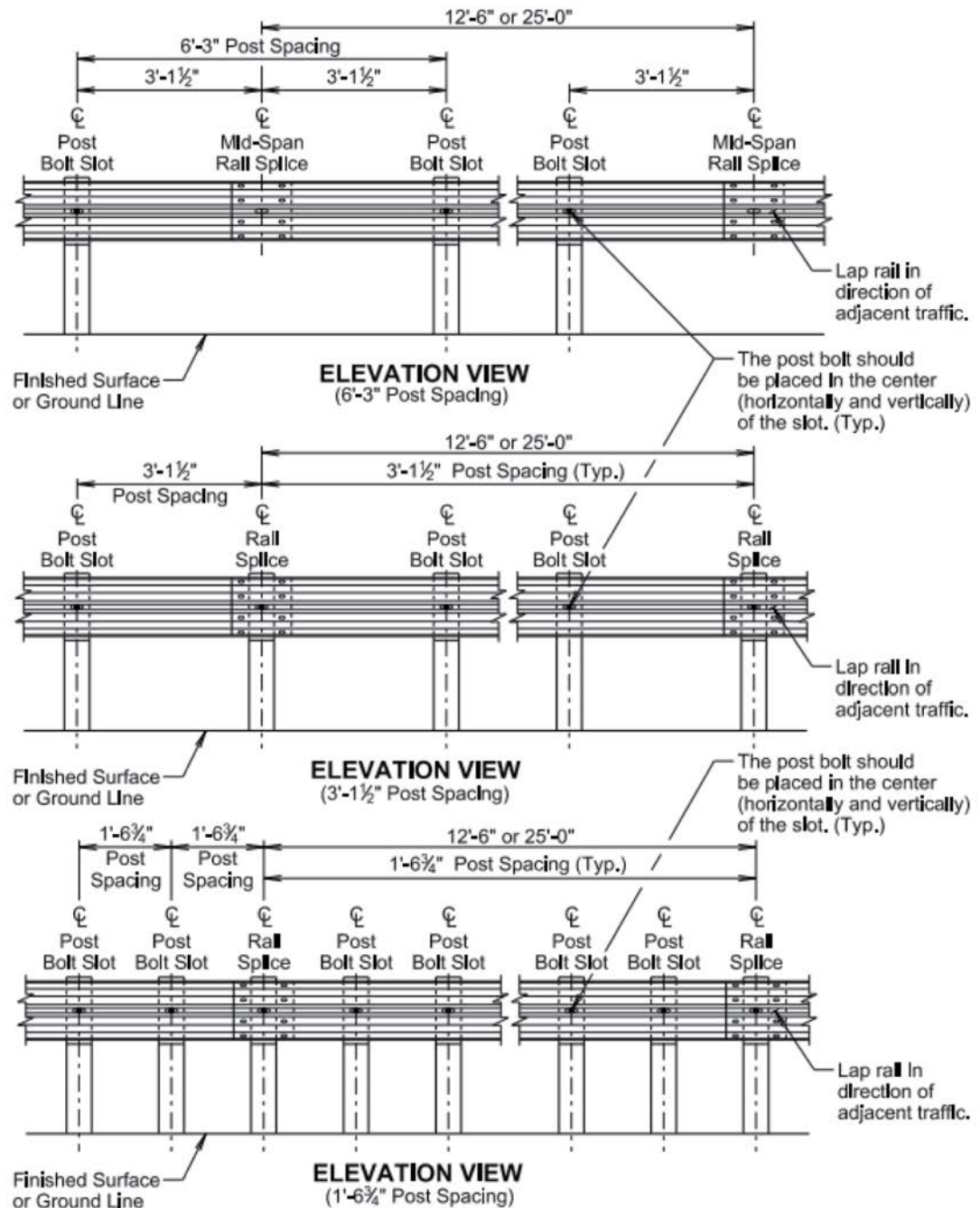


Figure 2.22. Question 5 responses.

Q66 - Please attach standard, drawing, or details for this guardrail stiffening mechanism. If you would like to submit multiple files, please collect them in a zipped folder and submit this zipped folder below.

[See Figures 2.23 through 2.31 and Table 2.4 for responses.]



Published Date: 4th Qtr. 2019	S D D O T	MIDWEST GUARDRAIL SYSTEM (MGS)	September 14, 2019 PLATE NUMBER 630.20 Sheet 4 of 6
-------------------------------	----------------------------------	---------------------------------------	--

Figure 2.23. South Dakota DOT response to Question 66.

NOTES:

1. INSTALLATION:

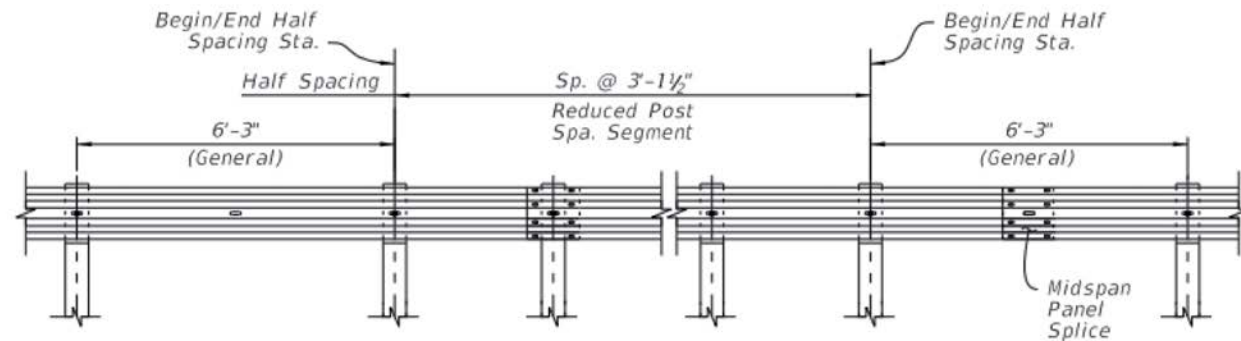
Work these details with the plans, where Stationing for Begin/End Half Spacing and Begin/End Quarter Spacing are indicated if required.

Where the Begin/End Stations indicated in the plans do not correspond exactly to post locations in construction, extend the Reduced Post Spacing segment to the nearest post(s) before the Begin Station and/or after the End Station called for.

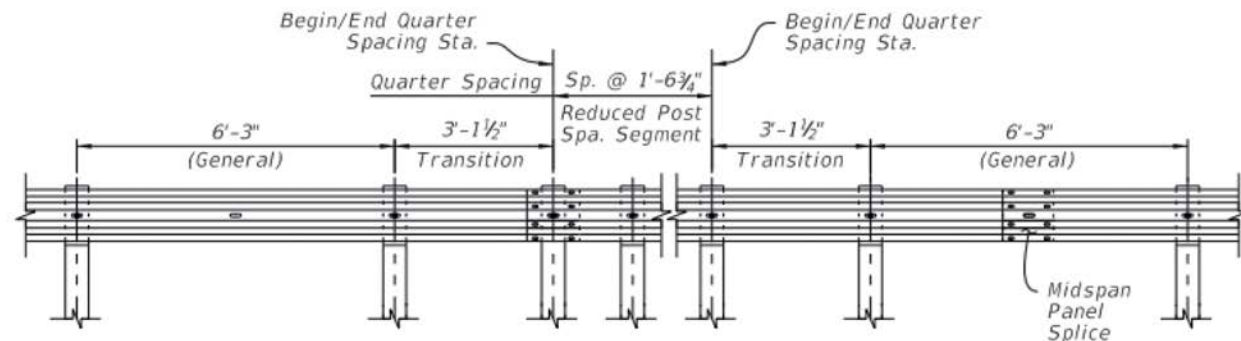
2. **PANEL SPLICES:** Midspan Panel Splices are not required in Transition and Reduced Post Spacing segments, however they are required for General segments. To place midspan splices in General segments, use one Non-General panel length (9'-4½" or 15'-7½") or add an additional Transition spaced post where required.

3. **LOW-SPEED GUARDRAIL:** For Reduced Post Spacing with Low-Speed Guardrail (12'-6" post spacing), the Reduced Spacing pattern requires a 6'-3" space between the 12'-6" and 3'-1½" spaces.

4. **PANEL POST BOLT SLOTS:** For Quarter Spacing configurations, punch additional ¾"x2½" Post Bolt Slots in the panels only where required for mounting and in accordance with Specification 536.



DETAIL 'S' - HALF SPACING ELEVATION
(AS REQD. PER THE PLANS)



DETAIL 'S' - QUARTER SPACING ELEVATION
(AS REQD. PER THE PLANS)

REDUCED POST SPACING FOR HAZARDS

Figure 2.24. Florida DOT response to Question 66.

NOTES:

1. SEE 805-001-XX FOR GENERAL NOTES. WORK APPROPRIATE SEMI-RIGID GUARDRAIL SHEETS (805-000-00 THROUGH 805-799-XX) TOGETHER.

2. USE THRIE-BEAM NESTED WITH CRITICAL OFFSET 1.5625' POST SPACING IN AREAS WHERE THE DISTANCE BETWEEN THE BACK OF THE POST AND THE OBSTRUCTION IS LESS THAN 24". DO NOT USE CRITICAL OFFSET POSTS TO SHIELD DROP OFF UNLESS STRUCTURE (WALL, CULVERT, ETC.) IS STRUCTURALLY SUFFICIENT TO SUPPORT RAIL LOADING.

3. STANDARD INSTALLATION IS SHOWN WITH STANDARD GUARDRAIL POSTS AND PROPER GRADING TO THE GUARDRAIL SHOULDER BREAK. IN AREAS WHERE PROPER GRADING TO GUARDRAIL SHOULDER BREAK CANNOT BE ACHIEVED, USE ADDITIONAL LENGTH POSTS (805-505-XX) AND COMPRESSED GUARDRAIL SHOULDER BREAK.

4. CAST-IN-PLACE VERTICAL CONCRETE WALLS (805-825-XX) ARE AN APPROPRIATE ALTERNATIVE TO THRIE-BEAM NESTED WITH CRITICAL OFFSET. THRIE BEAM BRIDGE CONNECTORS (805-330-XX) ARE ALSO REQUIRED FOR THIS ALTERNATIVE.

5. SEE AASHTO "A POLICY ON GEOMETRIC DESIGN"-UNDERPASS ROADWAYS-LATERAL CLEARANCES FOR ADDITIONAL APPLICATIONS.

6. MEASURE THRIE-BEAM NESTED WITH CRITICAL OFFSET IN LINEAR FEET TO PROJECT AT LEAST (2) $\frac{1}{2}X$ AND (2) $\frac{1}{2}X$ POST SPACES (9'-4 1/2") BEYOND EACH END OF THE OBSTRUCTION. ROUND UP (IN 12.5' INCREMENTS) THRIE-BEAM NESTED WITH CRITICAL OFFSET MEASUREMENT TO ELIMINATE THE NEED FOR FIELD CUTTING.

7. PAYMENT INCLUDES ALL MATERIAL (INCLUDING ADDITIONAL LENGTH POSTS IF REQUIRED) AND WORK REQUIRED TO COMPLETE INSTALLATION, AS SHOWN.

PAY ITEM:

8050150 OR THRIE-BEAM NESTED W/CRITICAL OFFSET POST-----LF [8051450]

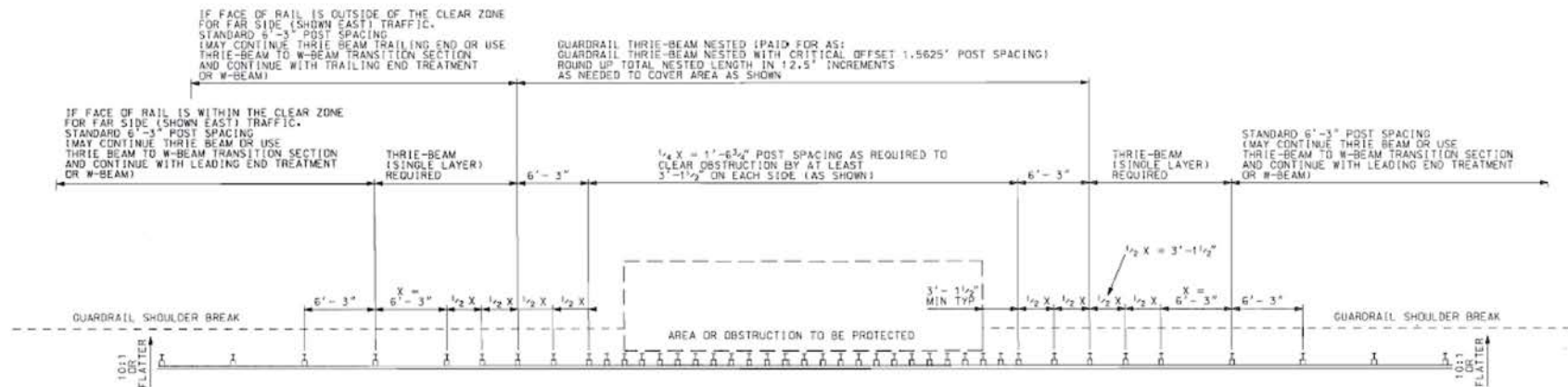
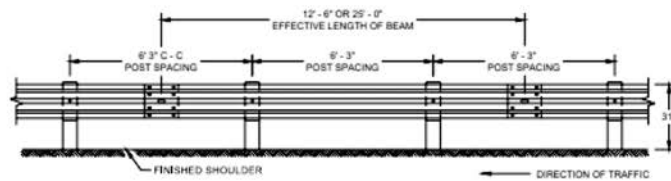
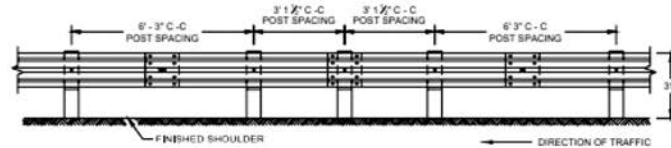


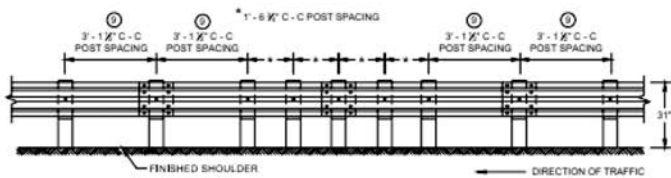
Figure 2.25. South Carolina DOT response to Question 66.



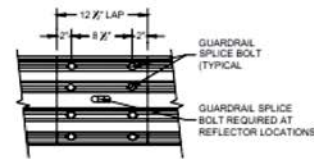
FRONT VIEW
POST SPACING STANDARD INSTALLATION



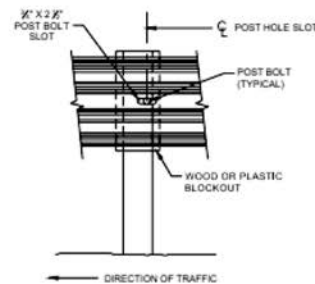
FRONT VIEW
HALF POST SPACING (HS) AND
HALF POST SPACING WITH LONGER POSTS (K)



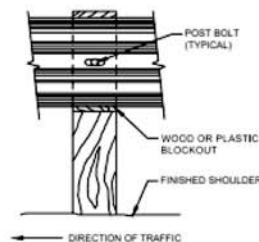
FRONT VIEW
QUARTER POST SPACING (QS)



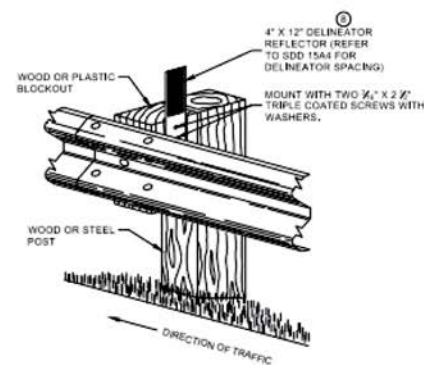
FRONT VIEW
MID-SPAN BEAM SPLICE



FRONT VIEW AT STEEL POST



FRONT VIEW AT WOOD POST



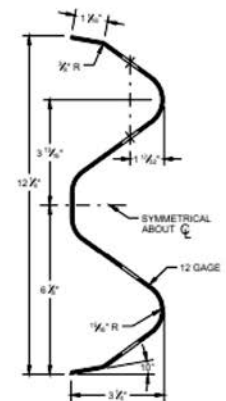
ONE SIDED REFLECTOR DETAIL
AND TYPICAL INSTALLATION

GENERAL NOTES

- ① DO NOT INSTALL REFLECTORS ON THE FIRST 50 FEET OF THE APPROACH END OF THE ENERGY ABSORBING TERMINAL. RAIL SPLICE LOCATIONS ARE THE ONLY ACCEPTABLE LOCATIONS FOR REFLECTORS.
- ② 25 FEET OF HALF POST SPACING IS REQUIRED ON APPROACH AND DEPARTURE ENDS OF QUARTER POST SPACING.

POST BOLTS ARE A 1/2" DIAMETER ASTM A307 GUARDRAIL BOLT. A POST BOLT REQUIRES 1/2" DIAMETER A563A DOUBLE RECESSED (DR) HEAVY HEX NUT AND 1/2" DIAMETER F844 FLAT WASHER. POST BOLTS MAY BE LONGER IF MULTIPLE BLOCKOUTS ARE BEING USED.

GUARD RAIL SPLICE BOLTS ARE A 1/2" DIAMETER ASTM A307 GUARDRAIL HEAD BOLT. A GUARDRAIL SPLICE BOLT REQUIRES 1/2" DIAMETER A563A DOUBLE RECESSED (DR) HEAVY HEX NUT.

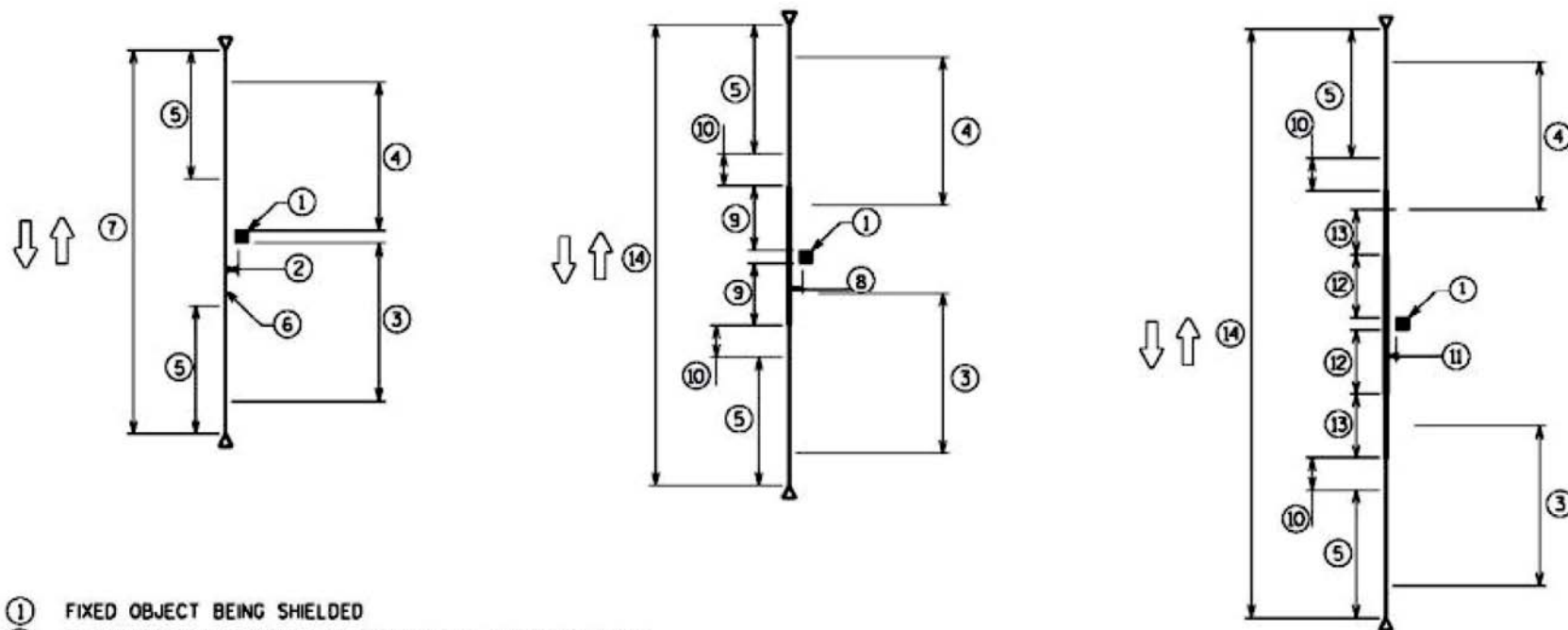


SECTION THRU W-BEAM RAIL

**MIDWEST GUARDRAIL SYSTEM
(MGS) GUARDRAIL**

STATE OF WISCONSIN
DEPARTMENT OF TRANSPORTATION

Figure 2.26. Wisconsin DOT response to Question 66 (1 of 2).



- ① FIXED OBJECT BEING SHIELDED
- ② APPROPRIATE WORKING WIDTH FOR OBJECT BEING SHIELDED
- ③ APPROACH LENGTH OF NEED (LON)
- ④ FAR SIDE LENGTH OF NEED (LON)
- ⑤ EAT LENGTH (SEE OTHER SECTIONS OF 11-45-2)
- ⑥ STANDARD POST SPACING FOR BEAM GUARD
- ⑦ TOTAL BARRIER SYSTEM LENGTH FOR NORMAL APPLICATIONS
- ⑧ HAZARD WITHIN THE WORKING WIDTH OF STANDARD BEAM GUARD
- ⑨ 25' OF HALF POST SPACING PRIOR HAZARD FOR BOTH DIRECTIONS OF TRAVEL
- ⑩ MIN. OF 12.5' OF STANDARD POST SPACING BETWEEN END OF TERMINAL AND START OF HALF POST SPACING.
- ⑪ BEAM GUARD QUARTER POST SPACING IS REQUIRED BECAUSE OF WORKING WIDTH OF NORMAL BEAM GUARD AND HALF POST SPACING BEAM GUARD IS TOO LARGE
- ⑫ 25' OF QUARTER POST SPACING PRIOR TO HAZARD FOR BOTH DIRECTIONS OF TRAVEL
- ⑬ 25' OF HALF POST SPACING PRIOR TO QUARTER POST SPACING
- ⑭ OVERALL LENGTH OF BARRIER SYSTEM MAY CHANGE DUE TO THE NEED FOR SMALLER WORKING WIDTHS

DRAWINGS NOT TO SCALE

DRAWINGS ARE INTENDED TO SHOW GENERAL ROADSIDE DESIGN CONCEPTS.

DESIGNERS ARE RESPONSIBLE FOR PROVIDING INDIVIDUAL CONSTRUCTION DETAILS FOR THEIR PROJECTS.

Figure 2.27. Wisconsin DOT response to Question 66 (2 of 2).

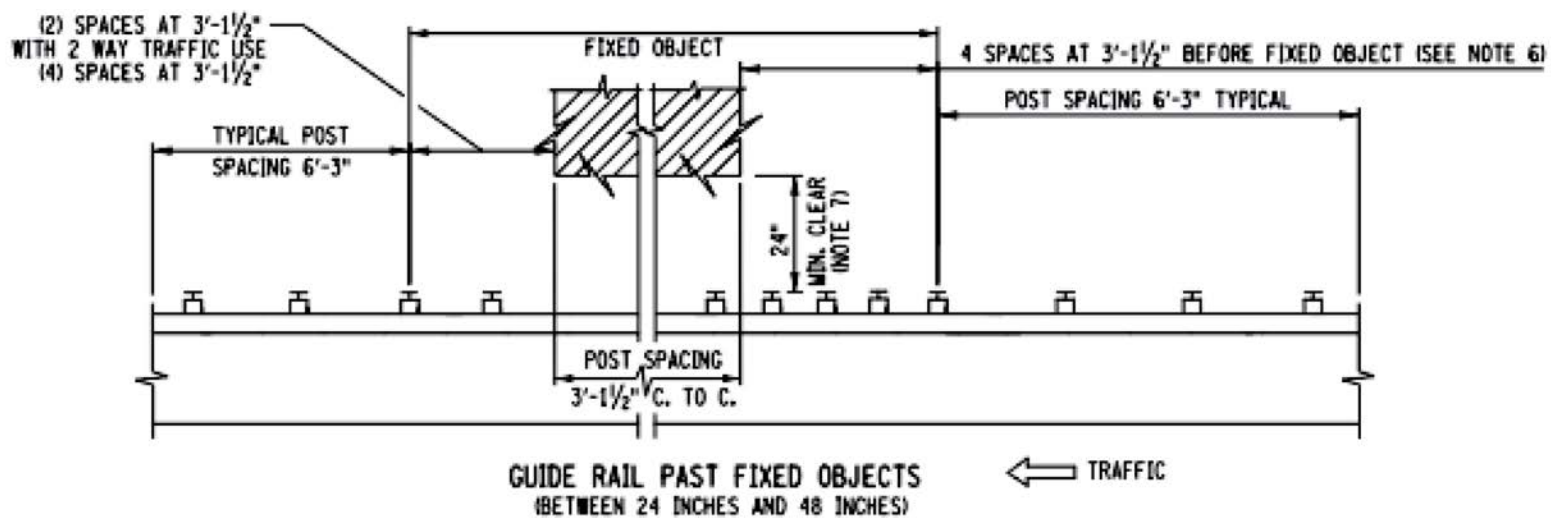
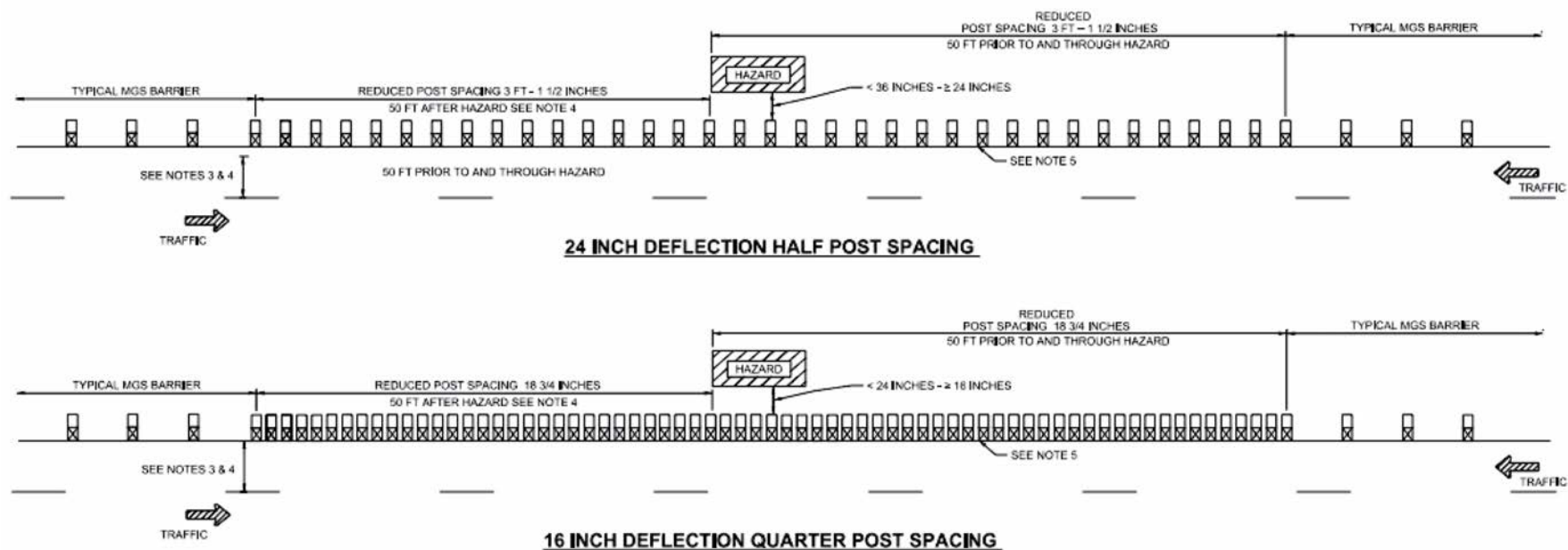


Figure 2.28. New York State DOT response to Question 66.



DESIGN-ONLY NOTES:

A. ALTERNATE BARRIER SYSTEM REQUIRED IF DEFLECTION DISTANCE IS LESS THAN 16 INCHES.

B. DO NOT USE WITH INITIAL LONG POST 2:1 FILL SLOPE INSTALLATIONS.

C. INDICATE LOCATIONS ON PLAN SET THAT REQUIRE REDUCED DEFLECTION CRITERIA. SPECIFY DEFLECTION DISTANCE FROM BACK OF POST TO FACE OF HAZARD.

NOTES:

1. USE TYPICAL 8 INCH WOOD OR COMPOSITE BLOCKS.

2. MEASURE DEFLECTION DISTANCE FROM BACK OF POST TO FACE OF HAZARD.

3. STIFFEN AS REQUIRED WHEN USED ON ROADWAYS WITH OPPOSING TRAFFIC AND THE NEAREST APPROACH LANE OF OPPOSING TRAFFIC IS LESS THAN THE MAXIMUM REQUIRED CLEAR ZONE.

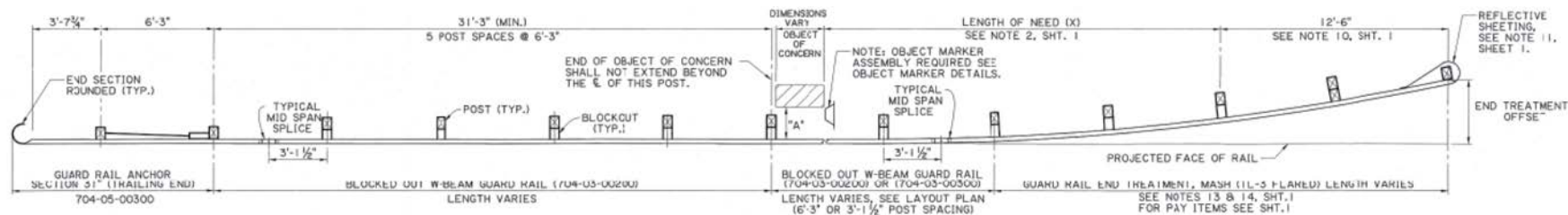
4. STIFFENING REQUIRED FOR 25 FT AFTER HAZARD WHEN USED ON ONE-WAY ROADWAYS.

5. BOLTS NOT REQUIRED THROUGH RAIL ELEMENTS FOR THOSE INSTALLATIONS REQUIRING ADDITIONAL POSTS.

6. STIFFENING NOT REQUIRED IF DEFLECTION DISTANCE IS GREATER THAN OR EQUAL TO 38 INCHES FROM BACK OF POST TO FACE OF HAZARD.

7. NOT TO BE USED ON INITIAL LONG POST 2:1 FILL SLOPE INSTALLATION.

Figure 2.29. Utah DOT response to Question 66.

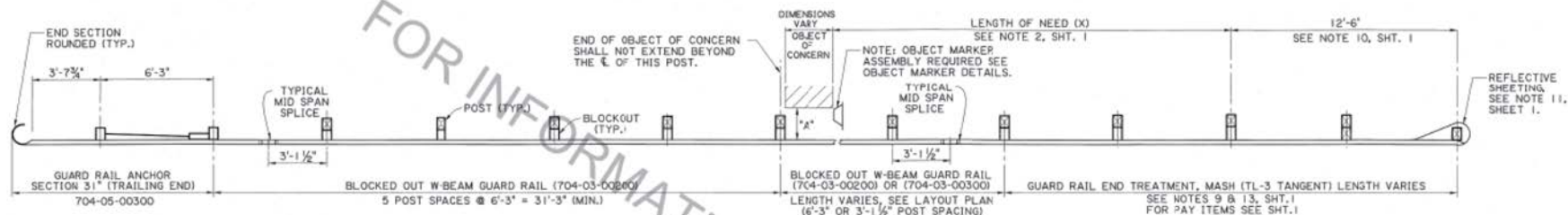


FOR TRAILING END TERMINAL DETAILS AND NOTES, SEE SHTS. 7 & 8.

BACK FACE OF GUARD RAIL TO FRONT FACE OF OBJECT = "A" = 5'-0" MIN.

PLAN - NON-BRIDGE END APPLICATION - FLARED

N.T.S.

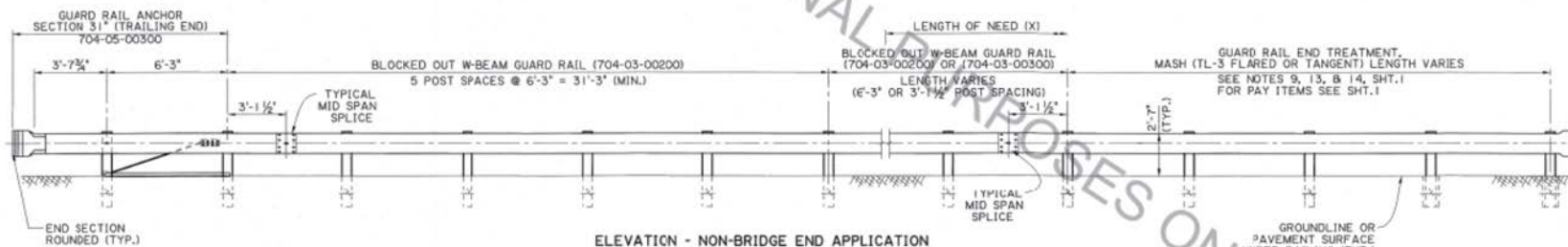


FOR TRAILING END TERMINAL DETAILS AND NOTES, SEE SHTS. 7 & 8.

BACK FACE OF GUARD RAIL TO FRONT FACE OF OBJECT = "A" = 5'-0" MIN.

PLAN - NON-BRIDGE END APPLICATION - TANGENT

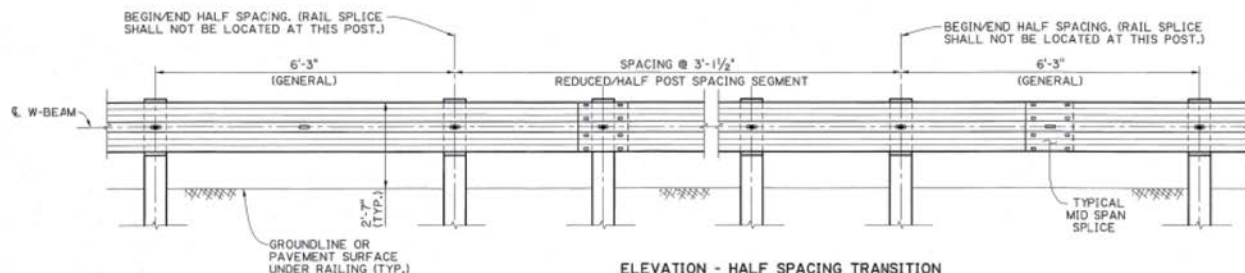
N.T.S.



ELEVATION - NON-BRIDGE END APPLICATION

FOR POST, BLOCKOUTS AND GUARD RAIL DETAILS, SEE SHTS. 6, 9, 10, & 11

N.T.S.



ELEVATION - HALF SPACING TRANSITION

(PCST SPACING 6'-3" TO 3'-1 1/2")

N.T.S.

PANEL SPLICES, FOR HALF POST SPACING TRANSITIONS

MIDSPAN PANEL SPLICES ARE NOT REQUIRED IN TRANSITION AND REDUCED POST SPACING SEGMENTS, HOWEVER THEY ARE REQUIRED FOR GENERAL SEGMENTS. TO PLACE MIDSPAN SPLICES IN GENERAL SEGMENTS NEAR A TRANSITION, USE ONE NON-GENERAL PANEL LENGTH (9'-0 1/2" or 15'-7 1/2") OR ADD AN ADDITIONAL TRANSITION SPACED POST WHERE REQUIRED.

Figure 2.30. Louisiana Department of Transportation and Development (DOTD) response to Question 66.

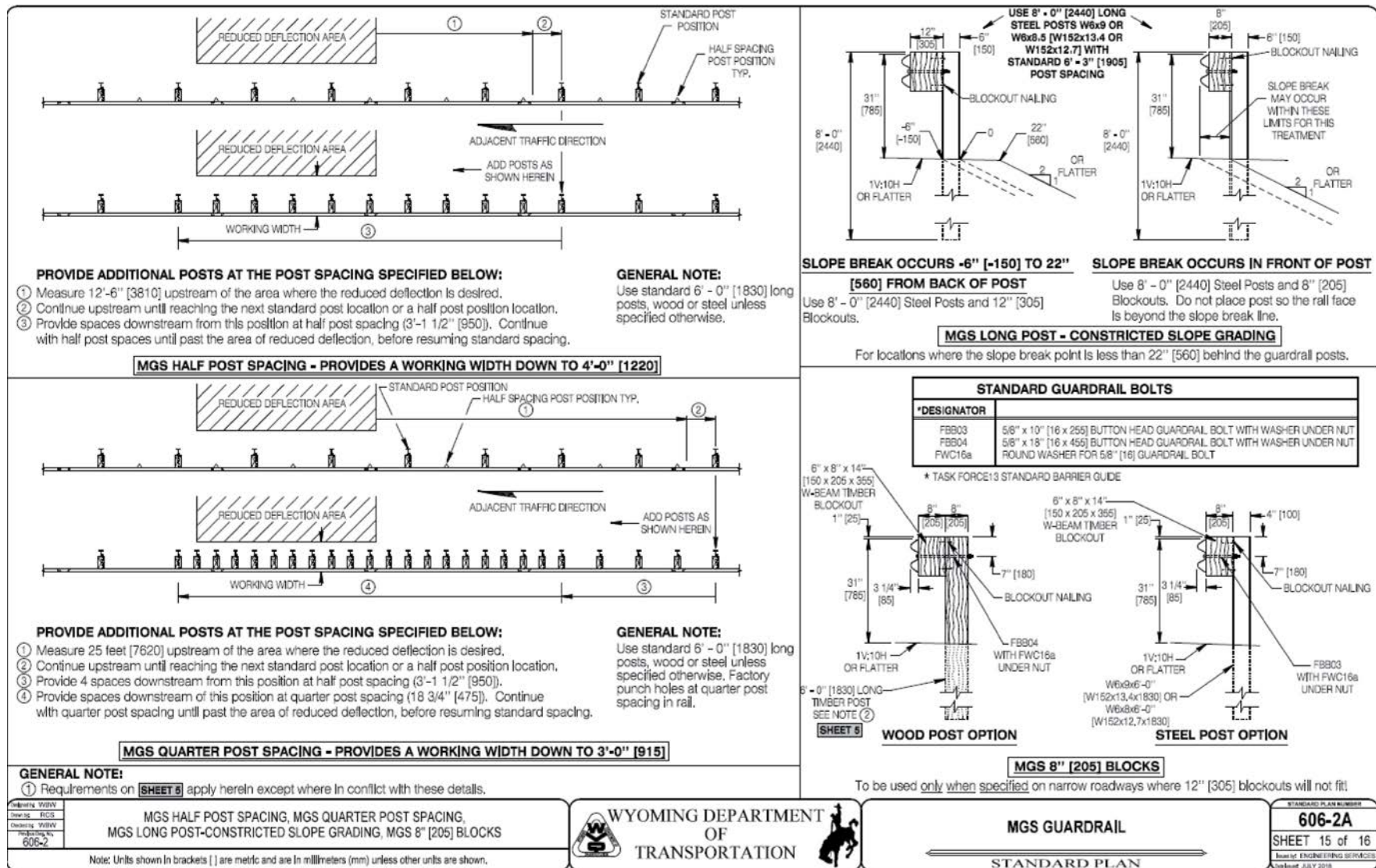


Figure 2.31. Wyoming DOT response to Question 66.

Table 2.4. Survey participants' written responses to Question 66.

Respondent	Response
North Dakota DOT (NDDOT)	Currently, for the 28" system, NDDOT guidance is 31 ½ "clearance with standard 6' 3" post spacing. With half-post spacing (3'-1 ½) "the clearance should be 24" and the reduced post spacing should extend for 25 ft in advance of the obstruction. For three-strand cable, the distance from cable to object shall be 11' or greater; this comes from the recent FAST Act guardrail training in ND.
West Virginia DOT	Methods for Reducing W-beam Deflection: Reduce post spacing to 3' – 1 ½". Reduce post spacing to 1' – 6 ¾". Double nest rail element. Any one stiffening method shall not exceed 25' in length. Any combination of stiffening methods shall not exceed 50' in length.

Q7 - What is the total length of this stiffening mechanism (not including transition zone)?

[See Table 2.5 for responses.]

Table 2.5. Survey participants' responses to Question 7.

Respondent	Response
Florida DOT	Depends on hazard length. 25' minimum.
Louisiana DOTD	Varies with length of hazard.
Michigan DOT	Varies.
New Mexico DOT	As needed.
New York State DOT	12'-6".
North Dakota DOT	The length of the obstruction with full 12'- 6 sections.
South Carolina DOT	Equal to width of hazard.
South Dakota DOT	As long as necessary.
Utah DOT	50' prior to hazard plus length of hazard.
West Virginia DOT	50 feet.
Wisconsin DOT	Depends on object length and direction of traffic.
Wyoming DOT	See standard drawing [earlier Figure 2.31].

Q8 - How far does the stiffening mechanism extend upstream of hazard (not including the transition zone)?

[See Table 2.6 for responses.]

Table 2.6. Survey participants' responses to Question 8.

Respondent	Response
Florida DOT	Minimum length is 12.5' both upstream and downstream of hazard.
Louisiana DOTD	No amount is specified in the standards although the drawing implies it extends for the full length of need minus the end treatment and transitions.
Michigan DOT	Varies.
New Mexico DOT	Length of need.
New York State DOT	15 degrees.
North Dakota DOT	25'.
South Carolina DOT	3' – 1.5' (PREMASH 805-015-00) [see earlier Figure 2.25].
South Dakota DOT	25' based on past crash testing.
Utah DOT	50'.
West Virginia DOT	44' to 47'.
Wisconsin DOT	25'.
Wyoming DOT	See standard drawing [earlier Figure 2.31].
Michigan DOT	Varies.

Q9 - How far does the stiffening mechanism extend downstream of hazard (not including the transition zone)?

[See Table 2.7 for responses.]

Table 2.7. Survey participants' responses to Question 9.

Respondent	Response
Florida DOT	Minimum length is 12.5' both upstream and downstream of hazard.
Louisiana DOTD	N/A. Stiffening mechanism is not required to extend past hazard although standard MGS is required to extend at least 31'-3" past the hazard with an appropriate trailing end anchor.
Michigan DOT	Varies.
New Mexico DOT	As needed.
New York State DOT	Same station +.
North Dakota DOT	No extra length of reduced post spacing is required downstream on locations of 1-way traffic – Install a 12'-6" long trailing end anchor – 2-way traffic would require the upstream transition to be mirrored.
South Carolina DOT	3' – 1.5' (PREMASH 805-015-00) [see earlier Figure 2.25].
South Dakota DOT	Extend to 5 posts downstream of object.
Utah DOT	25 ft if used on one-way roadways, 50 ft if located on a two-way roadway.
West Virginia DOT	3' to 6'.
Wisconsin DOT	25'.
Wyoming DOT	See standard drawing [earlier Figure 2.31].
Michigan DOT	Varies.

**Q10 - Which type of hazard is this stiffening mechanism intended to protect motorists from?
Select all that apply:**

[See Figure 2.32 and Table 2.8 for responses.]

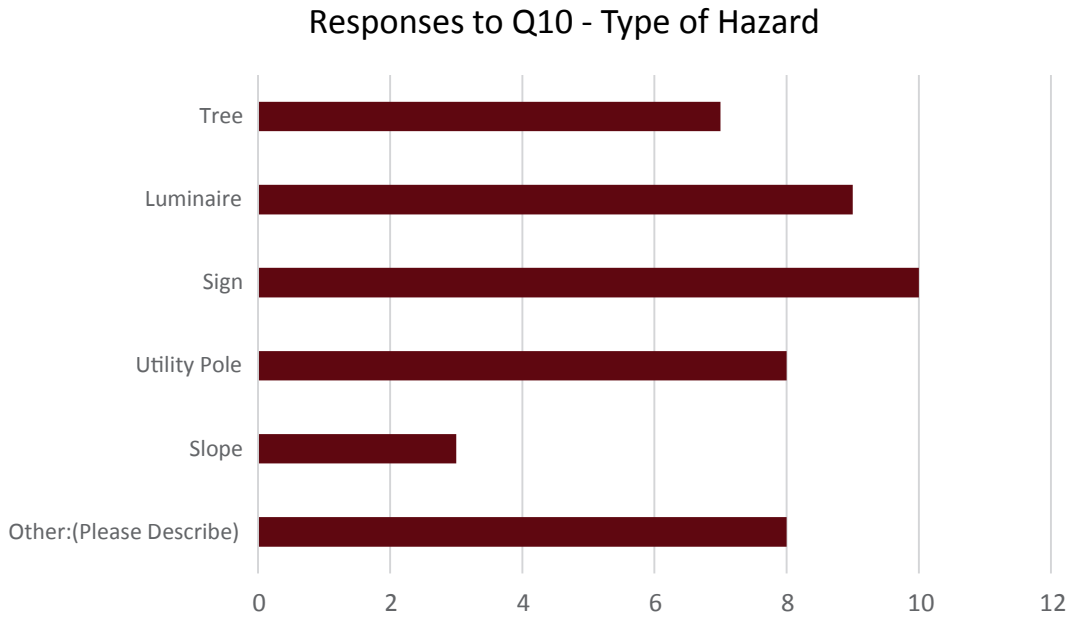


Figure 2.32. Question 10 responses.

Table 2.8. Survey participants' "Other" responses to Question 10.

Description of "Other" Responses to Question 10
Bridge abutments.
Typically, it is bridge piers/columns.
Bridge piers.
Any above-ground hazard, including those with breakaway mechanisms.
Bridge piers/columns.
Before 2016, bridge piers (this is still under review, particularly at lower speed and volume).
Piers, abutments, retaining walls.
As required.

Q13 - Which of the following components are used in the upstream transition to this stiffening mechanism? Select all that are used in this upstream transition:

[See Figure 2.33 and Table 2.9 for responses.]

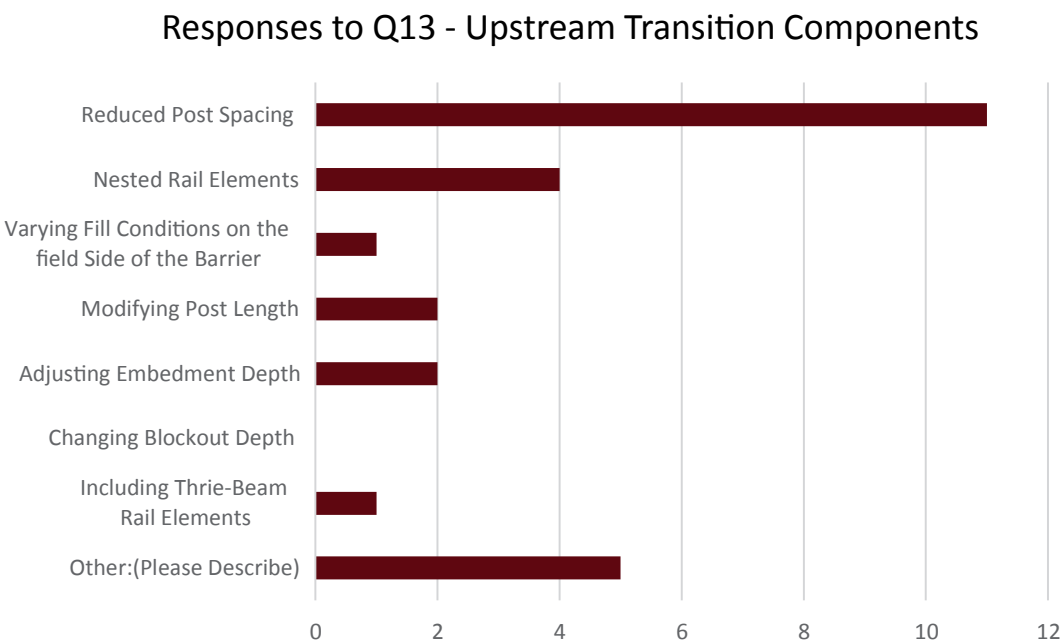


Figure 2.33. Question 13 responses.

Table 2.9. Survey participants’ “Other” responses to Question 13.

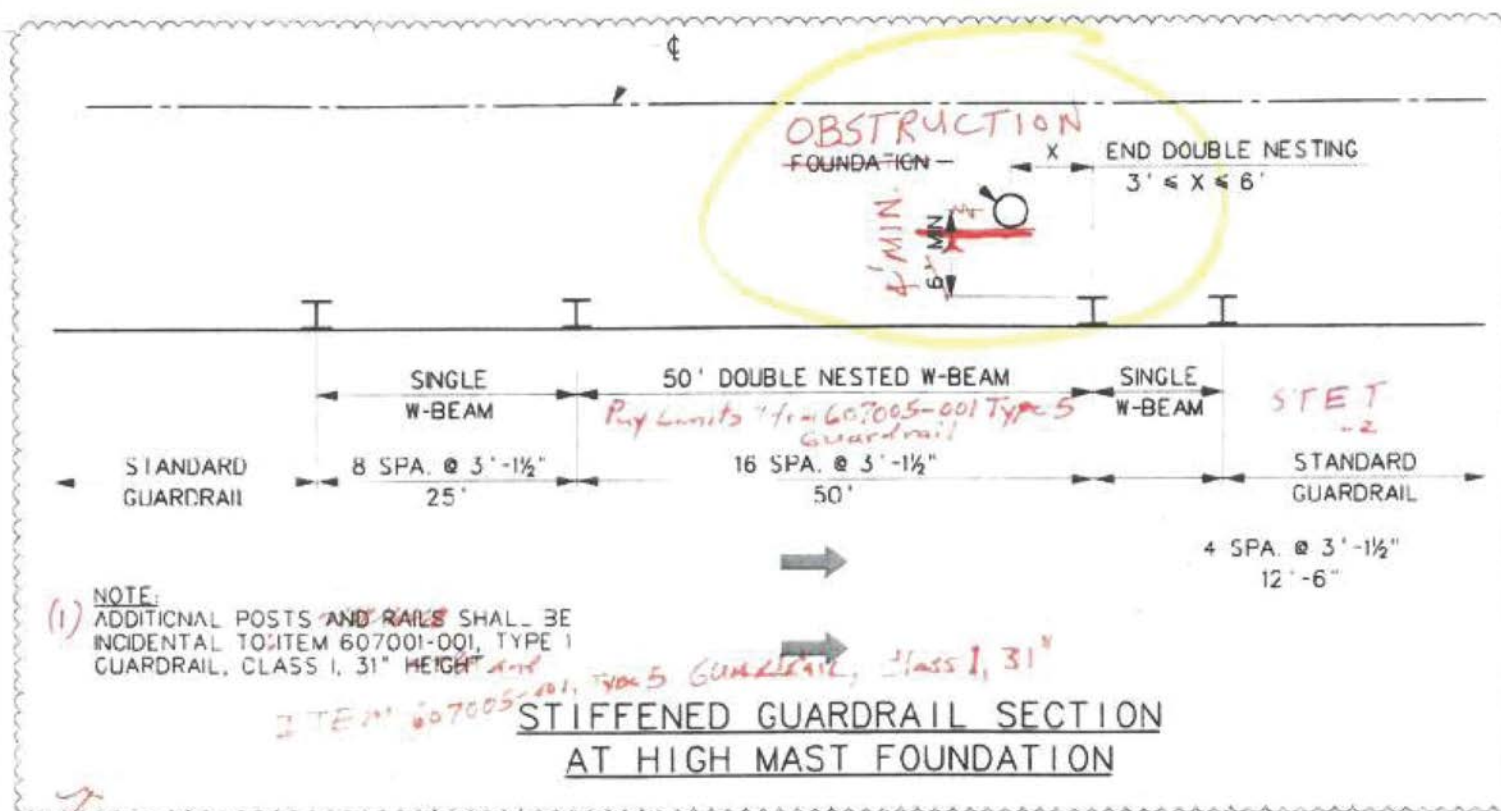
Description of “Other” Responses to Question 13
Transition not required at this time. This will be changed to match future test document.
Varying panel lengths to accommodate transition to midspan splice.
The standard plans require the half-post spacing to begin in certain segments relative to the rail splice.
Treated similar to stiffness transition to rigid barrier.
At this time none. Waiting for TTT’s Pooled Fund research to clarify situation.

Q67 - Please attach a link to standard, drawing, or details for this upstream transition. If you would prefer to attach a file, you will have the ability to do so next.

[See Table 2.10 and Figure 2.34 for responses.]

Table 2.10. Survey participants' responses to Question 67.

Respondent	Response
Florida DOT	See link above [earlier Figure 2.24].
Louisiana DOTD	Details Previously attached [earlier Figure 2.30].
New York State DOT	Same as Above [earlier Figure 2.28].
South Dakota DOT	We use the old rule shown in the <i>Roadside Design Guide</i> . The length of the stiffness transition is roughly 12 times the difference in the deflection distance. Our stiffening mechanism is always just post spacing, and nesting rail whether it be a thrie-beam system (we use longer posts and embedment for the nested thrie-beam transition) or MGS. We do not have standard drawings for all these transitions.
Utah DOT	See previous drawing provided earlier. [earlier Figure 2.29] At this time we do not have a transition detail. This will be changed to match future testing document.
Wyoming DOT	See standard drawing [earlier Figure 2.31].



- (2) Guardrail Element shall be bolted only at standard posts. At all additional posts the blockout shall be flush against the W-Beam.

Figure 2.34. West Virginia response to Question 67 – upstream transition.

Q17 - What is the total length of this upstream transition?

[See Table 2.11 for responses.]

Table 2.11. Survey participants' responses to Question 17.

Respondent	Response
Florida DOT	No transition for 1/2 post spacing. For quarter-post spacing, one half-posting post is added as transition.
New York DOT	12'-6".
North Dakota DOT	25'.
South Carolina DOT	Width of projected hazard.
West Virginia DOT	25'.
Wyoming DOT	See attached detail [earlier Figure 2.31].

**Q18 - Does the downstream transition repeat the same mechanisms as the upstream transition?
In other words, is the downstream transition a mirror image of the upstream transition?**

[See Figure 2.35 for responses.]

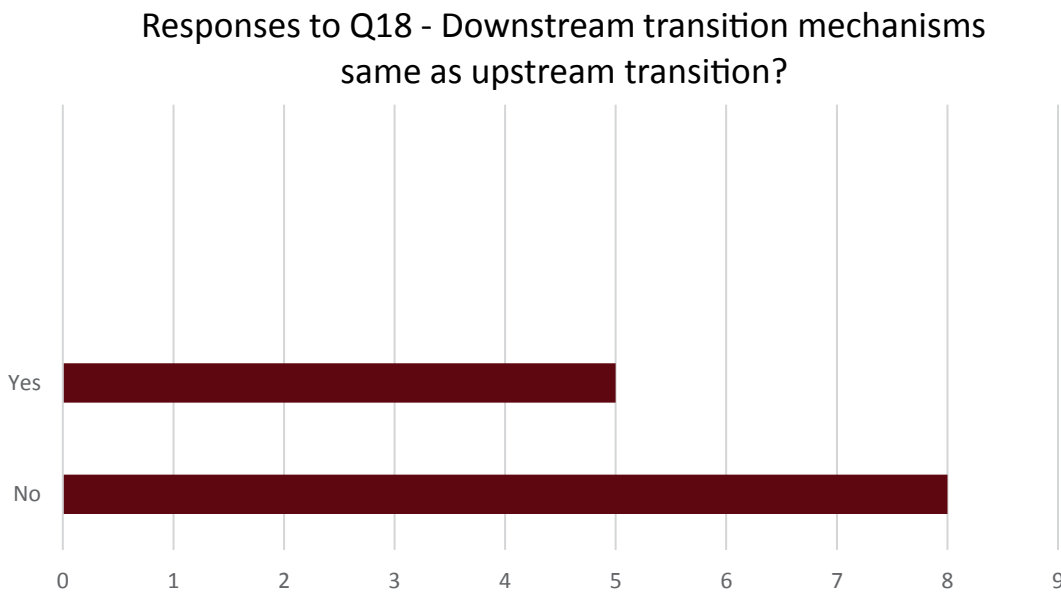


Figure 2.35. Question 18 responses.

Q15 - Which of the following components are used in the downstream transition to this stiffening mechanism? Select all that are used in this downstream transition:

[See Figure 2.36 and Table 2.12 for responses.]

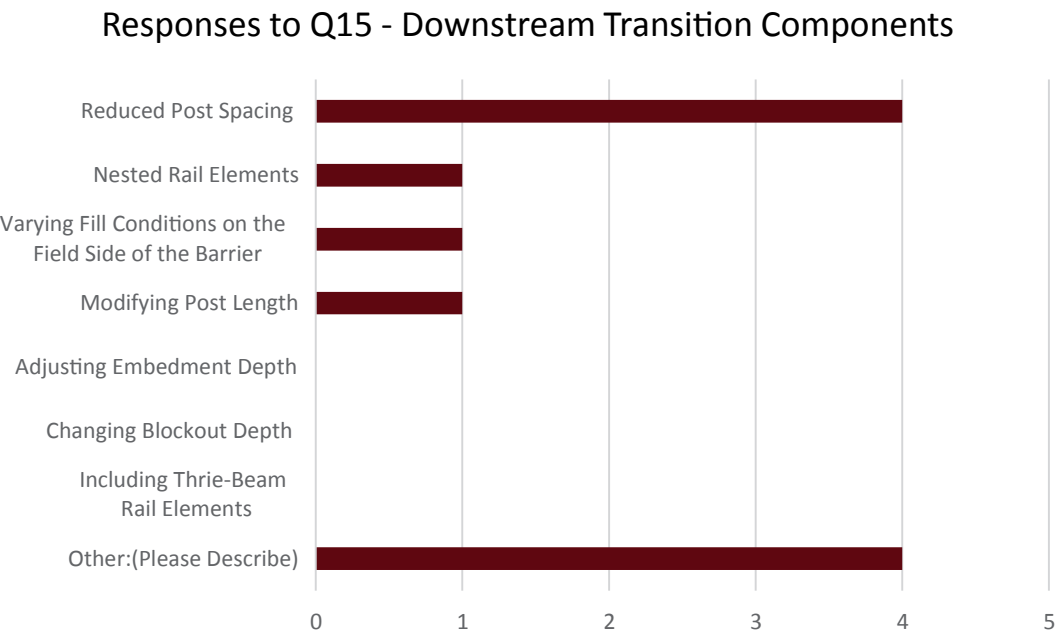


Figure 2.36. Question 15 responses.

Table 2.12. Survey participants’ “Other” responses to Question 15.

Description of “Other” Responses to Question 15
Depends if the roadway is one-way traffic or two-way traffic. If two-way traffic the upstream transition is mirrored and the downstream transition would be similar to the upstream transition.
Trailing end anchor for 1-way traffic - mirrored for 2-way traffic.
None provided at this time.
Waiting for TTI Pooled Fund Research.

Q68 - Please attach a link to standard, drawing, or details for this downstream transition. If you would prefer to attach a file, you will have the ability to do so next.

[See Table 2.13 for responses.]

Table 2.13. Survey participants' responses to Question 68.

Respondent	Response
New York State DOT	Same as above [earlier Figure 2.28].
West Virginia DOT	See STIFFENED GUARDRAIL SECTION detail [earlier Figure 2.34].
Wyoming DOT	See attached detail [earlier Figure 2.31].

Q19 - What is the total length of this downstream transition?

[See Table 2.14 for responses.]

Table 2.14. Survey participants' responses to Question 19.

Respondent	Response
New York State DOT	1'-6".
West Virginia DOT	12'-6".
Wyoming DOT	See attached detail [earlier Figure 2.31].
South Dakota DOT	Varies.
North Dakota DOT	The trailing end anchor is 12'-6" sections.
New Mexico DOT	As needed.

Q20 - Does your agency use another stiffening mechanism to reduce guardrail deflections (MGS and non-MGS systems)?

[See Figure 2.37 for responses.]

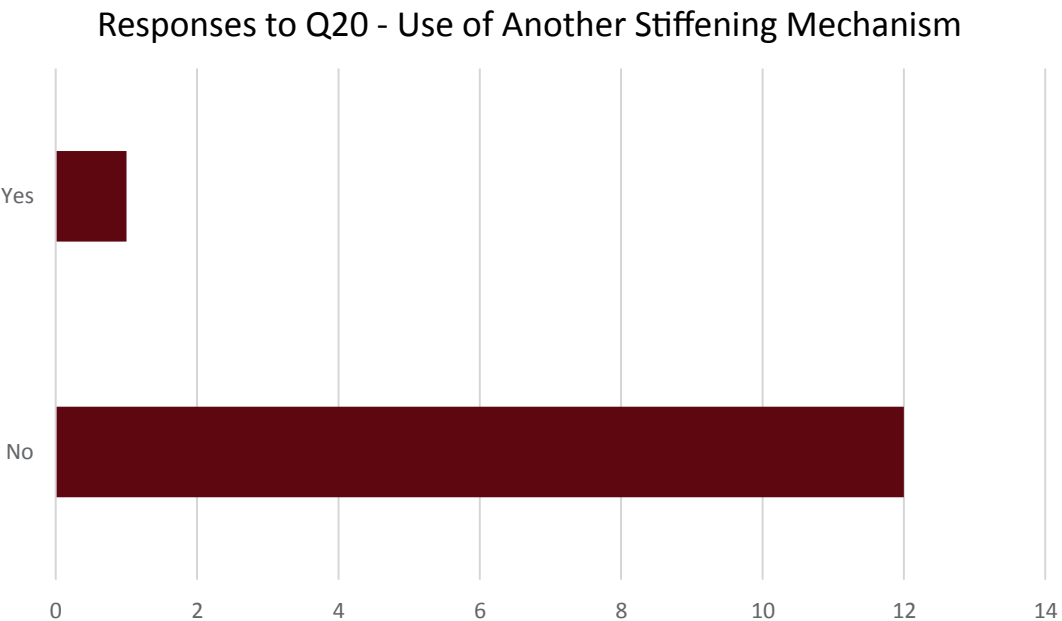


Figure 2.37. Question 20 responses.

Q23 - Which of the following components are used as part of this stiffening mechanism? (Note: You will be given an opportunity to include other stiffening mechanisms later in the survey if you use more than one.) Select all that are used in this stiffening mechanism:

[See Figure 2.38 for responses.]

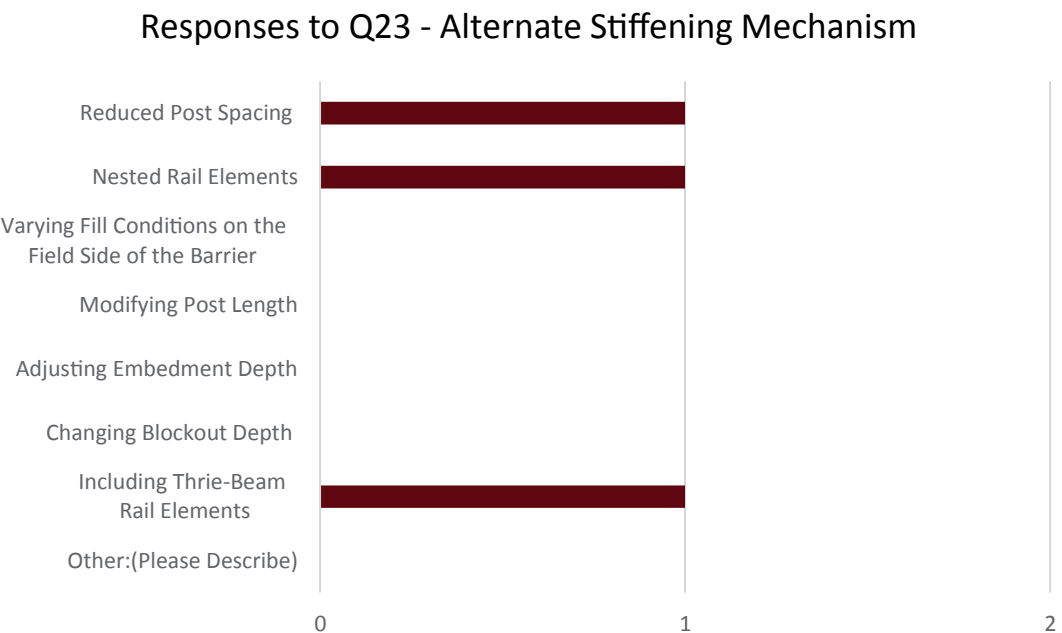


Figure 2.38. Question 23 responses.

Q71 - Please attach a link to standard, drawing, or details for this guardrail stiffening mechanism. If you would prefer to attach a file, you will have the ability to do so next.

[See Table 2.15 for responses.]

Table 2.15. Survey participants' response to Question 71.

Respondent	Response
Louisiana DOTD	We no longer use thrie-beam rail in our standards since adopting MASH. However, we have miles of thrie-beam rail currently in service.

Q24 - Please attach standard, drawing, or details for this guardrail stiffening mechanism.

If you would like to submit multiple files, please collect them in a zipped folder and submit this zipped folder below.

No responses were submitted.

Q25 - What is the total length of this stiffening mechanism (not including transition zone)?

[See Table 2.16 for responses.]

Table 2.16. Survey participants' response to Question 25.

Respondent	Response
Louisiana DOTD	Varies as needed to shield the hazard.

Q26 - How far does the stiffening mechanism extend upstream of hazard (not including the transition zone)?

[See Table 2.17 for responses.]

Table 2.17. Survey participants' response to Question 26.

Respondent	Response
Louisiana DOTD	We would typically extend the thrie-beam at least 25'-0" upstream of the hazard.

Q27 - How far does the stiffening mechanism extend downstream of hazard (not including the transition zone)?

[See Table 2.18 for responses.]

Table 2.18. Survey participants' response to Question 27.

Respondent	Response
Louisiana DOTD	It depends. If there was no approaching traffic from the opposite direction, the thrie-beam ended just beyond the hazard and used a thrie-beam anchor terminal. If approaching traffic from the opposite direction was a concern, then the downstream end mirrored the upstream side.

**Q28 - Which type of hazard is this stiffening mechanism intended to protect motorists from?
Select all that apply:**

[See Figure 2.39 and Table 2.19 for responses.]

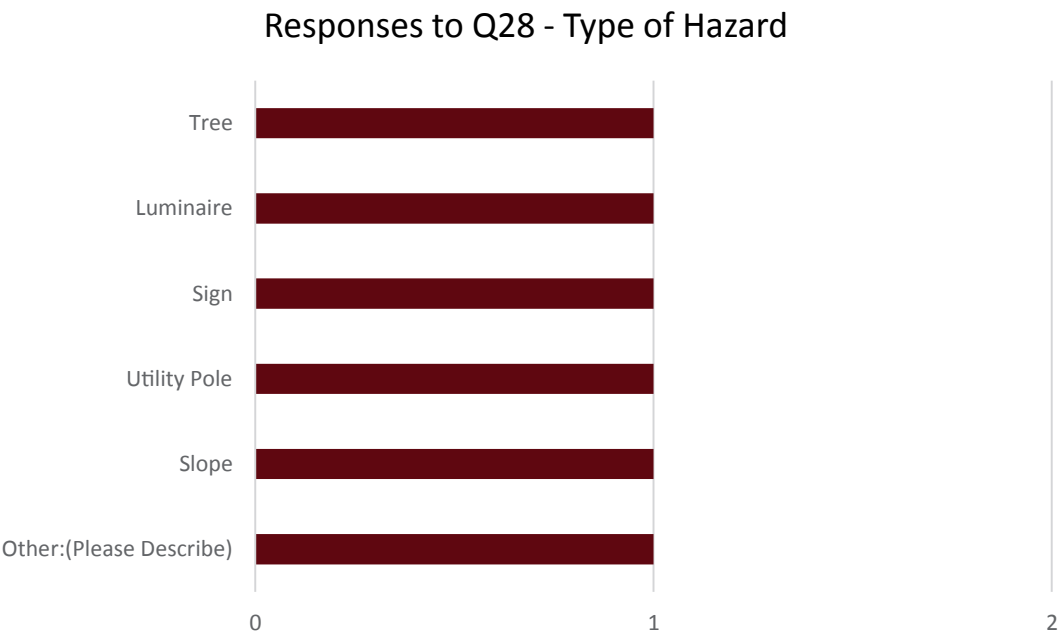


Figure 2.39. Question 28 responses.

Table 2.19. Survey participant’s “Other” response to Question 28.

Description of “Other” Responses to Question 28
Bridge Pier/Column

Q29 - Which of the following components are used in the upstream transition to this stiffening mechanism? Select all that are used in this upstream transition:

[See Figure 2.40 and Table 2.20 for responses.]

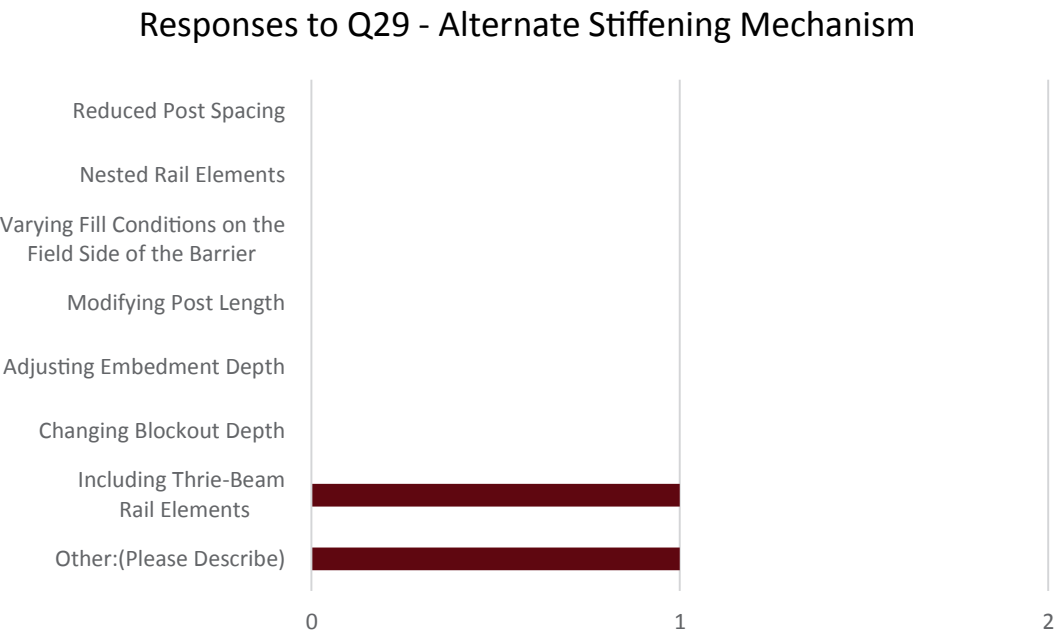


Figure 2.40. Question 29 responses.

Table 2.20. Survey participant’s “Other” responses to Question 29.

Description of “Other” Responses to Question 29
A 6’-3” W-beam to Thrie-Beam transition section was required.

Q72 - Please attach a link to standard, drawing, or details for this upstream transition. If you would prefer to attach a file, you will have the ability to do so next.

[See Table 2.21 for responses]

Table 2.21. Survey participants’ responses to Question 72.

Respondent	Response
Louisiana DOTD	Details previously attached [see earlier Figure 2.30].

Q31 - What is the total length of this upstream transition?

[See Table 2.22 for the response.]

Table 2.22. Survey participants’ responses to Question 31.

Respondent	Response
Louisiana DOTD	6’-3”.

Q32 - Does the downstream transition repeat the same mechanisms as the upstream transition? In other words, is the downstream transition a mirror image of the upstream transition?

[See Figure 2.41 for responses.]

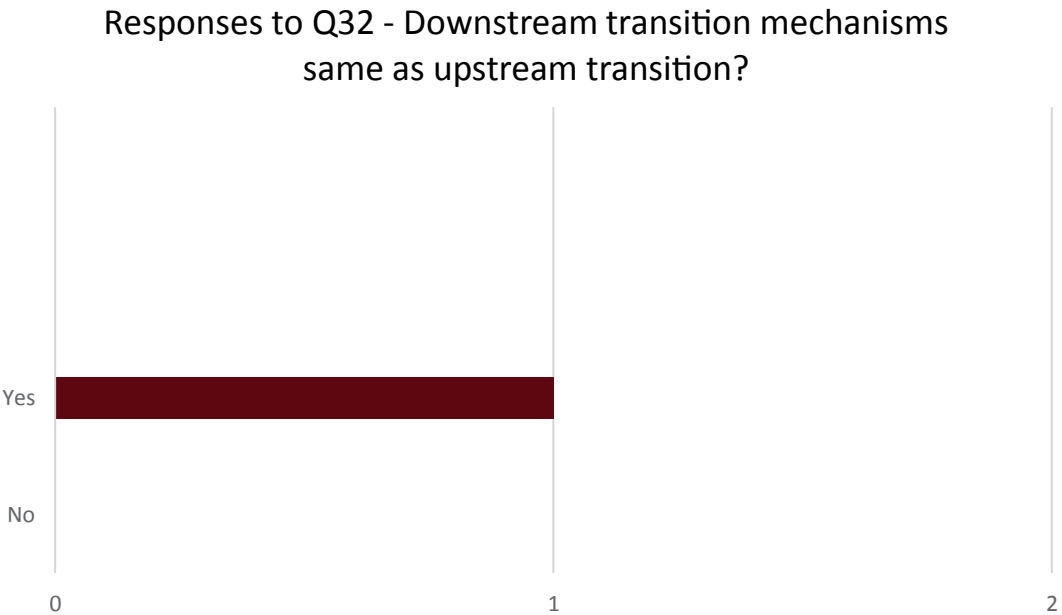


Figure 2.41. Question 32 response.

Q36 - Does your agency use another stiffening mechanism to reduce guardrail deflections (MGS and non-MGS systems)?

[See Figure 2.42 for the response.]

Responses to Q36 - Alternate stiffening mechanism

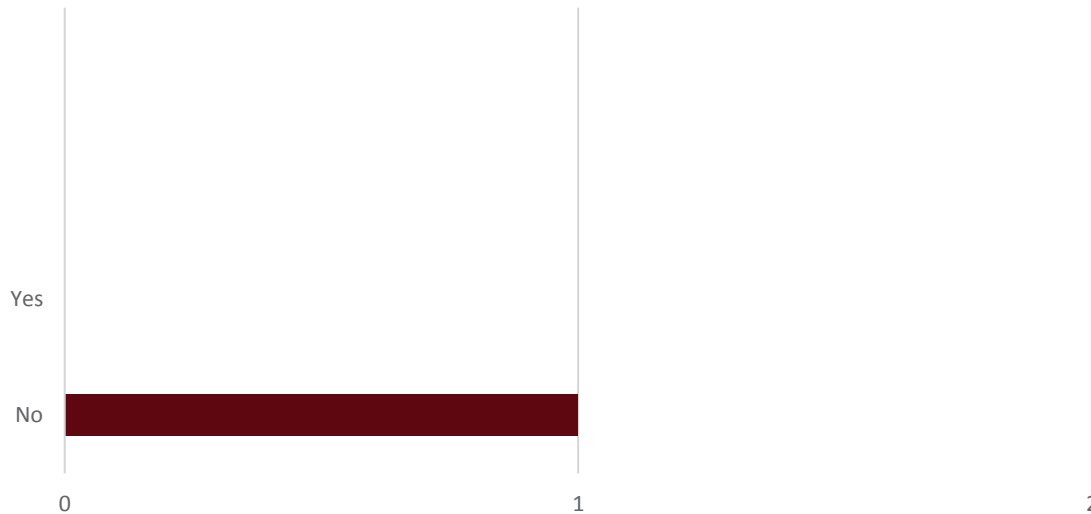


Figure 2.42. Question 36 response.

Q21 - What type of practice does your agency follow to address those locations where limited guardrail deflections are desired?

[See Table 2.23 for responses.]

Table 2.23. Survey participants' responses to Question 21.

Respondent	Response
Alabama DOT	We have traditionally used either nested elements or used a system other than traditional w beam guardrail (i.e., concrete barrier).
Arizona DOT	We have standard drawings for guardrail to concrete barrier transitions modeled after MwRSF reports. Our guidance for fixed objects behind barrier is copied below: FIXED OBJECTS BEHIND BARRIER: Avoid placing fixed objects within 59" behind guardrail face. When unavoidable, consider: Moving or eliminating fixed object Using steel posts (if fixed object is at least 50" behind face) Using double post spacing (every 3'-1½") Using concrete barrier.
Arkansas DOT	In locations where limited barrier deflection is desired, ARDOT's practice is to utilize rigid barriers (concrete barrier wall) in lieu of guardrail.
Georgia DOT	We allow for reduced post spacing (3' -1.5") in front of fixed objects that can meet the minimum deflection distance.
Iowa DOT	Reduced post spacing or nesting rail.
Massachusetts DOT	Since MassDOT has adopted MGS with 8" blockout, designers have been instructed not to place any non-breakaway devices within the zone of intrusion unless it is unfeasible to do so. In cases where it is unfeasible to remove or relocate the device, we will review the design to see what other options are available and will make a determination based upon what option presents the least amount of risk.

Q80 - Please attach a link to standard, drawing, or details. You will have the ability to attach a file instead next.

[See Figures 2.43 through 2.47 for responses.]

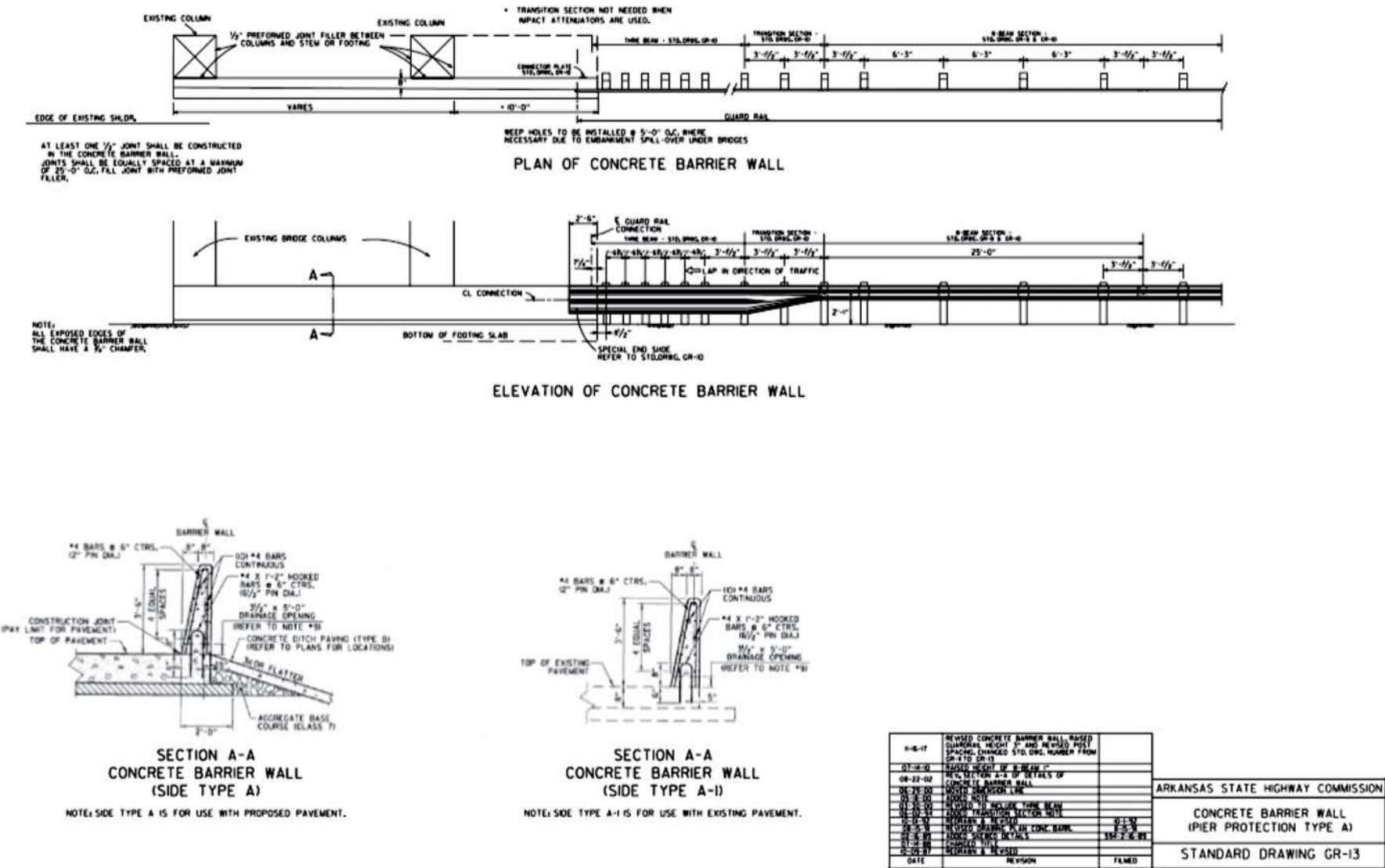


Figure 2.43. Arkansas DOT response to Question 80.

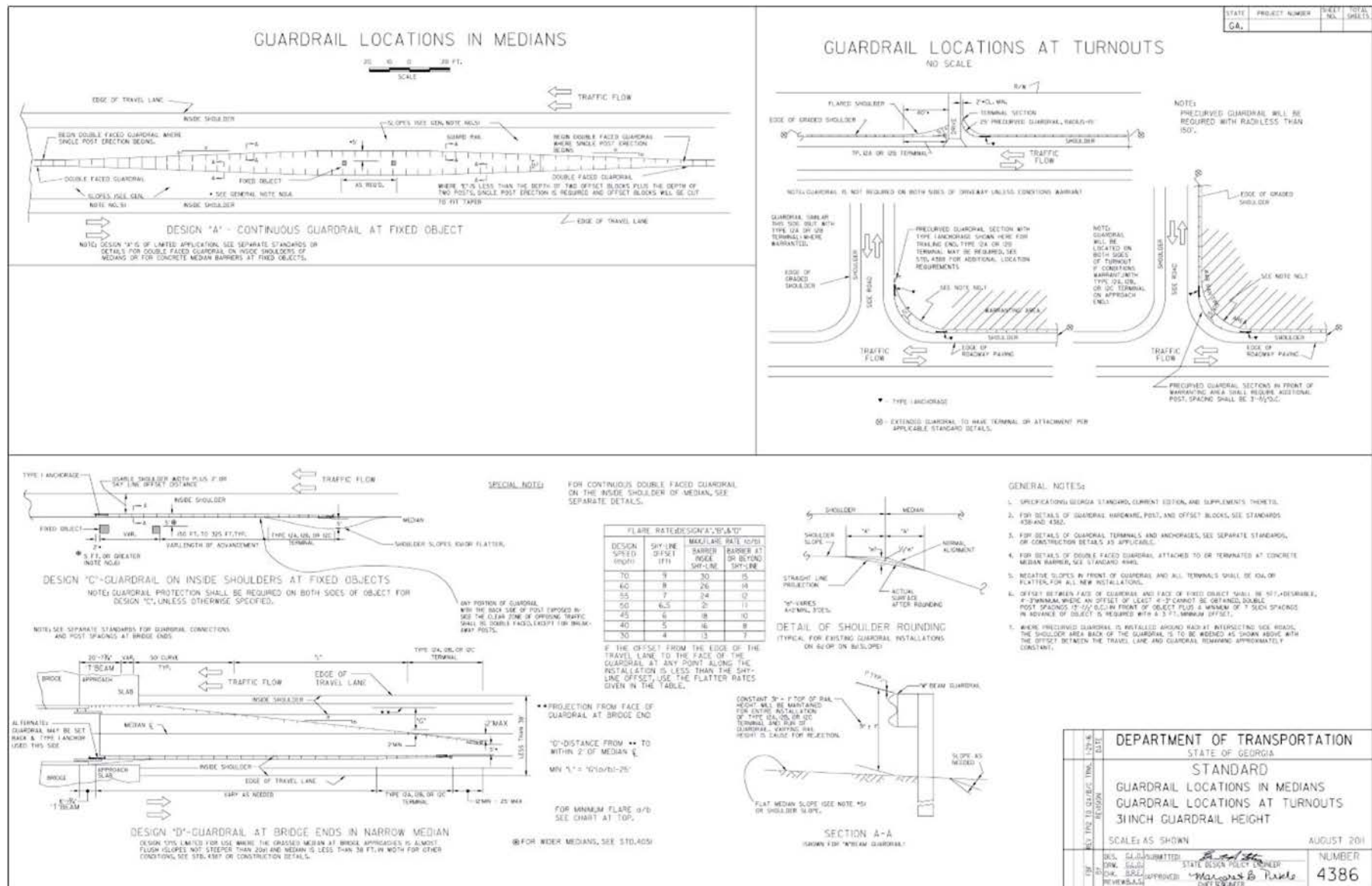


Figure 2.44. Georgia DOT response to Question 80 (1 of 4).

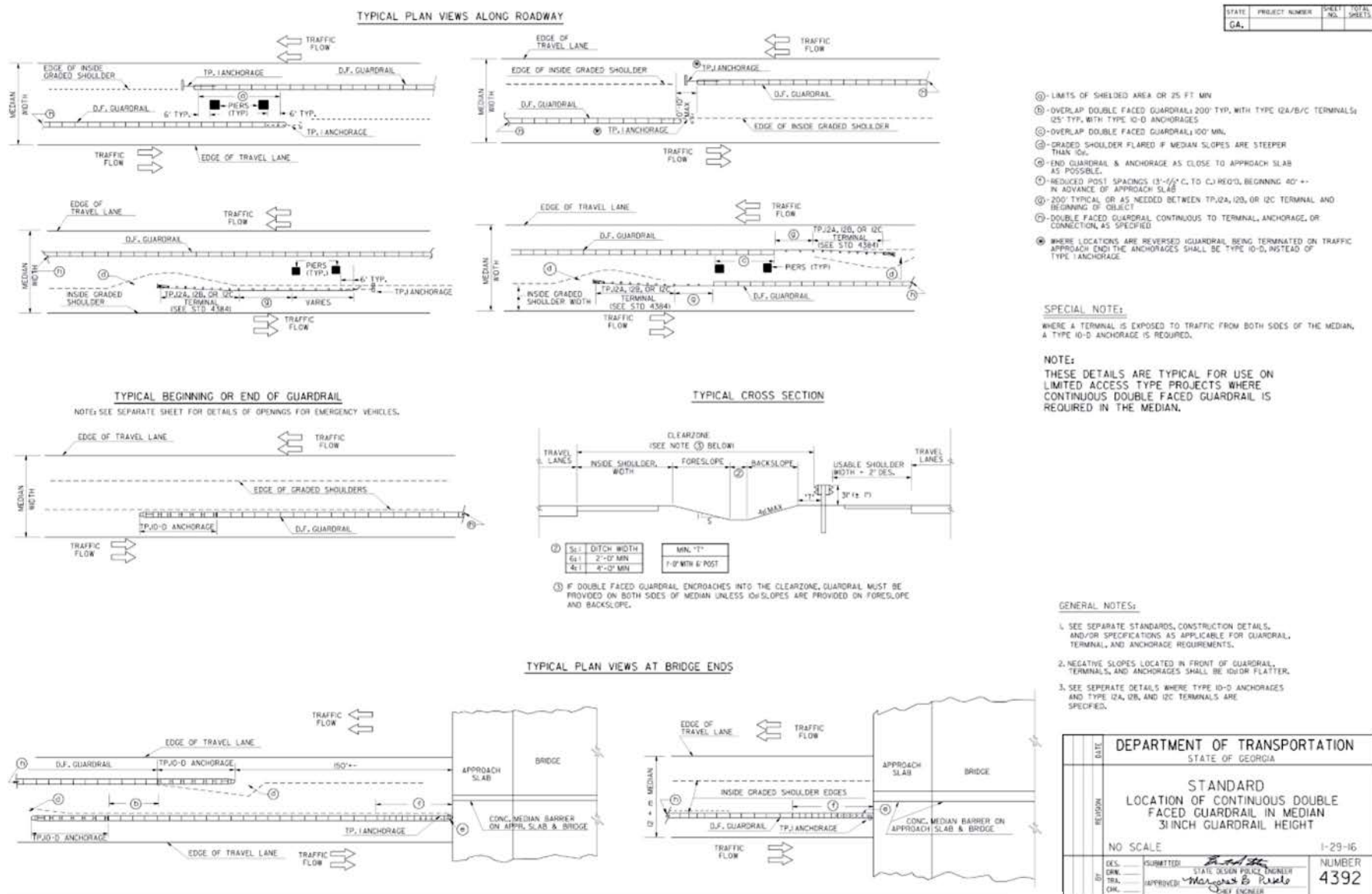
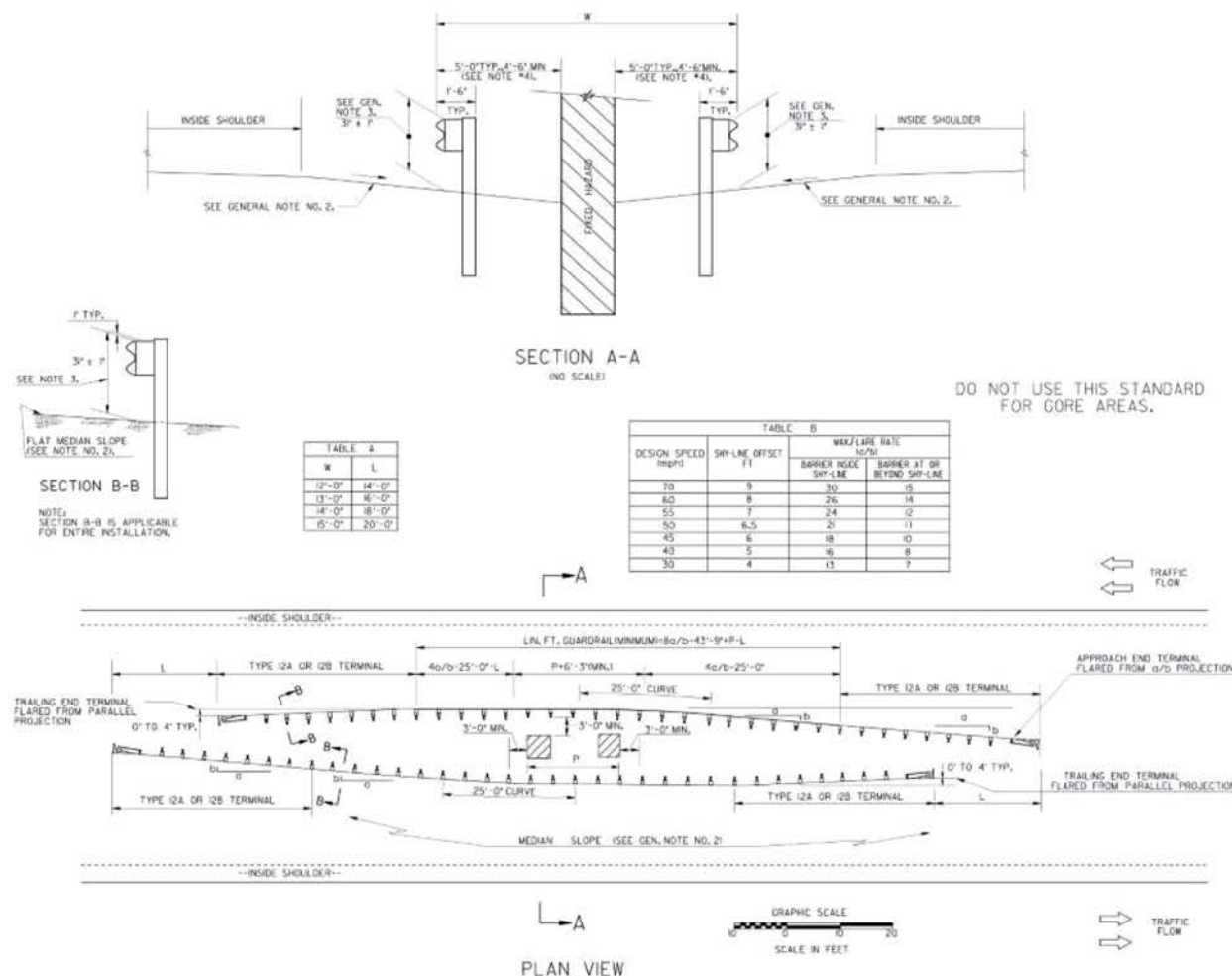


Figure 2.45. Georgia DOT response to Question 80 (2 of 4).

STATE	PROJECT NUMBER	SHEET NO.	TOTAL SHEETS
GA.			



GENERAL NOTES:

1. SPECIFICATIONS: GEORGIA STANDARD, CURRENT EDITION, AND SUPPLEMENTS THERE TO.
2. ALL MEDIAN SLOPES SHALL BE LOW OR FLATTER FOR THE ENTIRE INSTALLATION AND FOR AT LEAST 50 FT. IN ADVANCE ON BOTH SIDES.
3. THE HEIGHT OF "W"-BEAM RAIL TOP SHALL BE 3' ± 1", AS MEASURED TO THE GROUND LINE BELOW THE FACE OF RAIL AT ALL POINTS.
4. WHERE AN OFFSET OF AT LEAST 4'-6" CANNOT BE OBTAINED FROM RAIL FACE TO OBJECT FACE, DOUBLE POST SPACING (15'-0" O.C.) IN FRONT OF OBJECT PLUS A MINIMUM OF SEVEN SUCH SPACINGS IN ADVANCE OF OBJECT IS REQUIRED WITH A 3 FOOT (MIN.) OFFSET FROM RAIL FACE TO OBJECT FACE.

USER'S GUIDE:

- a. DETERMINE VALUE FOR "W" FROM DEPTH OF OBJECT AND OFFSETS, THEN SELECT "L" VALUE FROM TABLE A AT LEFT.
- b. FIND a/b FROM TABLE B AT LEFT.
- c. ESTABLISH "P" (OUTSIDE TO OUTSIDE OF OBJECT) AND ROUND TO MULTIPLE OF 6'-0" OR 12'-0".
- d. MINIMUM LINEAR FEET OF GUARDRAIL IS THEN EQUAL TO: $(60a/b) - 87' - 6" + 2P - 2L$.

ALSO FOUR TYPE 12A OR 12B TERMINALS IN ADDITION TO THE ABOVE.

SPECIAL NOTE:

STANDARD NO. 4389 IS APPLICABLE AT FIXED OBJECTS WHERE DOUBLE FACED GUARDRAIL IS NOT REQUIRED AND MEDIAN SLOPES ARE LOW OR FLATTER. DO NOT USE IN GORES.

DEPARTMENT OF TRANSPORTATION STATE OF GEORGIA	
STANDARD GUARDRAIL LOCATION AT FIXED OBJECTS IN MEDIAN 31 INCH GUARDRAIL HEIGHT	
SCALE AS SHOWN	AUGUST 2011
DES. SUBMITTER: <i>[Signature]</i> CHK. DATE: <i>[Signature]</i> APPROVED: <i>[Signature]</i> REVIEWER: <i>[Signature]</i>	NUMBER 4389

Figure 2.46. Georgia DOT response to Question 80 (3 of 4).

Literature Review and State Survey Conclusions

Overview

The research team analyzed the results of the literature review and the state survey. Based on these results, the research team developed a list of recommendations for selecting which stiffening mechanisms should progress into Phase II of this research project. Phase II involved performing computer simulations to evaluate the crashworthy behavior of stiffening mechanisms prior to full-scale crash testing. The research team recommended three of the mechanisms to be further evaluated in Phase II. The developed recommendations are listed below.

Post Spacing

The research team did not recommend continuing the evaluation of reduced post spacing during this research project. TTI was evaluating this stiffening mechanism for the Roadside Safety Pooled Fund, and it was estimated to be completed before the end of NCHRP Project 22-38. Therefore, the research team recommended ending the evaluation of reduced post spacing in Phase I.

Fill Condition

The research team did not recommend continuing the evaluation of the fill condition behind the barrier during this project. Both MwRSF and TTI have conducted considerable research on the installation of guardrail on slopes, and a summary of these projects was presented earlier. Consequently, the information found during Phase I of this project will be compiled in this project, but the research team did not recommend further evaluation of this stiffening mechanism during this research project.

Post Length and Embedment Depth

While TTI has completed research exploring embedment depths of guardrail posts, the research team recommended continuing the evaluation of embedment depth in Phase II. Embedding a post deeper in the soil would rigidize the post and decrease its deflection. However, this can only be achieved if the post does not yield or fracture. Researchers have seen the current W6×8.5 steel posts yielding with the current embedment depth. Therefore, choosing a deeper embedment depth would not provide any advantages to deflection if the same post were utilized. The research team recommended the evaluation of different post sizes while also increasing the embedment depth. The objective of this evaluation would be to determine cost-effective post sizes that would allow deeper embedment depths to provide reduced deflections.

Nested Rail Elements

While TTI has completed some research regarding nested rail elements, the research team recommended evaluating this stiffening mechanism through computer simulation with LS-DYNA. Despite many industry professionals' belief in using nested rail elements as a stiffening mechanism, previous research does not show promising results for reducing MGS deflections with nested rail elements. Additionally, the nested rails provide significant constructability issues, which could warrant the use of different stiffening mechanisms. Consequently, the research team recommended further evaluation of nested rail elements through detailed computer simulation.

10-Gauge W-Beam Rail

There has been limited research regarding thicker guardrail elements, and most of it has involved its use within transition sections. No recent research was found on the deflection-reducing capabilities of thicker rail sections. However, a thicker rail element should behave similarly to the nested rail elements without the constructability issues. Therefore, the research team recommended further evaluation through detailed computer simulation.

Blockout Depth

Previous research involving W-beam guardrail crash tests has used both 8-inch and 12-inch blockout depths. TTI completed a statistical study evaluating possible differences in crashworthy performance between these two blockout depths. The results showed no significant change in dynamic deflection between the two blockout depths. Therefore, the research team did not recommend further evaluation of blockout depth in this project.

Stiffening Mechanisms Selected for Computer Simulation Evaluation

After considering the research team's findings, it was determined which stiffening mechanisms would be evaluated in Phase II. This included much discussion on the stiffening mechanisms investigated in the literature review and others that were not included. Additional backup rails (steel members installed on the field side of the posts) and larger post sizes in conjunction with soil plates were two stiffening mechanisms added for consideration and prioritization. Furthermore, the research team acknowledged the benefits of including stiffening mechanism combinations in the simulation evaluation. Therefore, evaluating stiffening mechanism combinations was added to the computer simulation effort. Table 2.24 shows the ranking of the stiffening mechanisms, with the final selected mechanisms highlighted in the shaded area. From this ranking, post spacing, rub rails, 10-gauge rails, and backup rails were selected to be investigated with computer simulation. The following chapter discusses the computer simulation effort for these selected stiffening mechanisms.

Table 2.24. Stiffening mechanism prioritization results.

Stiffening Mechanism	Final Priority
Post Spacing	1
Rub Rail	2
10-Gauge Rail	2
Additional Backup Rail (e.g., HSS tube)	4
Post Size and Embedment Depth	5
Nested Rail	5
Post Size and Soil Plates	7

Computer Simulation and Modeling

The research team completed over 100 FEAs during their computer simulations, including simulations of MASH Tests 3-11, 3-10, 3-21, and 3-20. The following sections document this effort and are organized by stiffening mechanism.

Each stiffening mechanism was evaluated with a simulation of MASH Test 3-11 to determine its deflection-reducing capability. Because of budgetary and time constraints of the project, the research team could not perform simulations for all four MASH Tests (3-11, 3-10, 3-21, and 3-20) on every stiffening mechanism. Therefore, the research team selected the stiffening mechanisms to further investigate through additional simulations based on their deflection-reduction capability, similarity to other stiffening mechanisms, and previous crash tests.

The following sections in this chapter indicate whether a configuration successfully met MASH criteria. These statements only refer to the criteria able to be fully evaluated through computer simulation. Physical crash testing results are discussed in subsequent chapters.

Baseline Model and Validation

A detailed finite element (FE) model for the MGS with standard post spacing was developed. The system consists of a standard W-beam guardrail and standard W6×9 steel posts as shown in Figure 3.1.

A model verification effort of the MGS was performed using Crash Test 2214MG-2 from MwRSF Research Report No. TRP-03-171-06 (22) using the commercially available, nonlinear FE solver LS-DYNA. The simulation resulted in a maximum dynamic deflection of 43.4 inches, similar to the full-scale crash-test's deflection of 43.9 inches. Furthermore, an acceptable correlation between the crash test and the simulation was observed; the sequential frames are compared in Figure 3.2. Based on these results, the FE model of the system was considered to provide adequate predictions. This FE model was used as the baseline model for all the stiffening mechanisms considered in this project.

The original baseline model of the MGS system was further validated with the testing completed by MwRSF (22) through a Roadside Safety Verification and Validation Program (RSVVP) analysis. The research team used a multichannel, weighted approach to analyze the data signals from both the simulation and the actual crash test. The results of the RSVVP analysis can be seen below in Figure 3.2. The results of the qualitative and quantitative verification analyses provided the research team with a high level of confidence in the predictive capability of subsequent simulations (Figure 3.3).

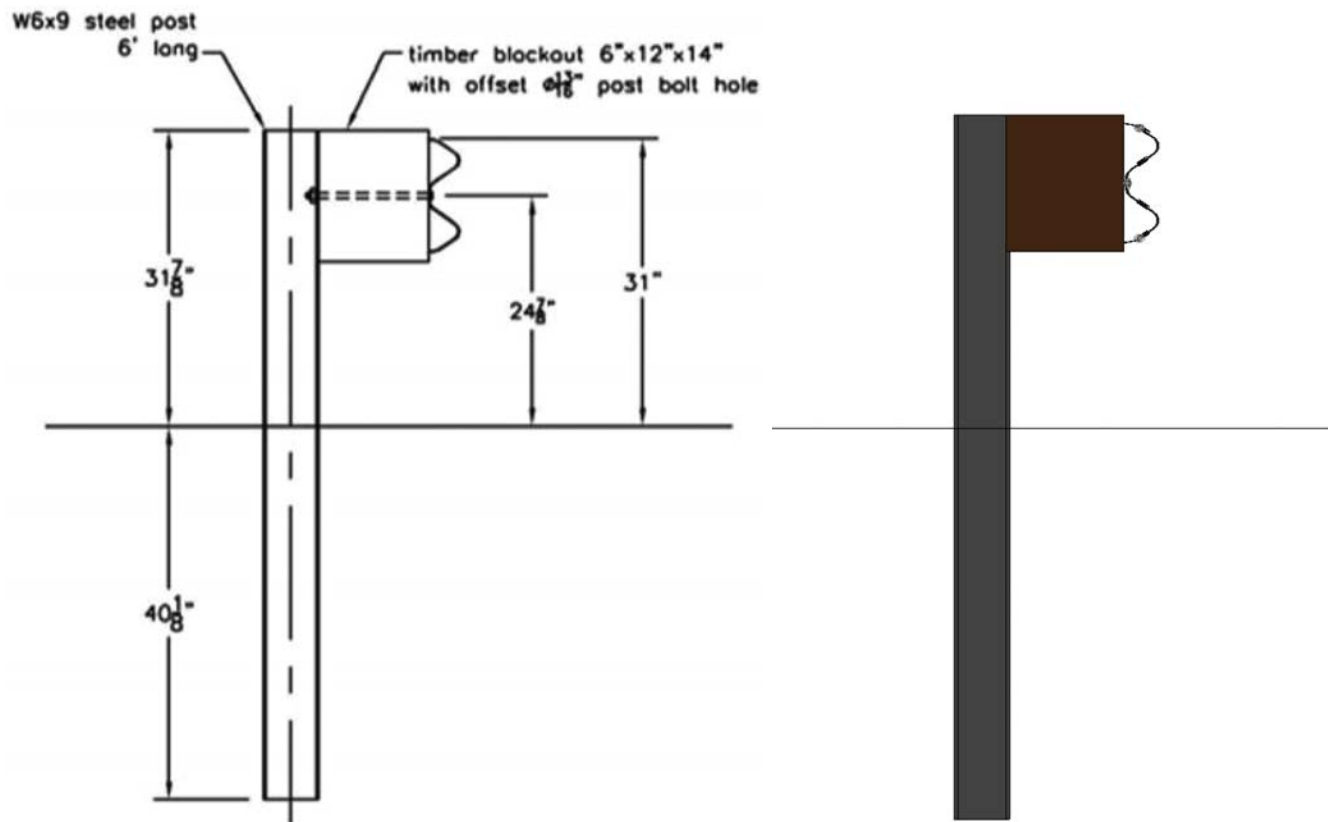


Figure 3.1. MGS section details and FE model (4).

This baseline model consisted of a standard MGS with 12-inch laterally deep blockouts. These blockouts were used in the MGS crash testing performed at MwRSF (22) and were therefore selected for the original model. Following the validation effort, the research team modified the model to include 8-inch laterally deep blockouts that would be used in future crash testing. As discussed in the literature review conducted in Phase I, TTI completed a statistical study evaluating potential differences in the crashworthy performance between these two blockout depths. The results of this study showed no significant change in dynamic deflection between the two blockout depths. Therefore, the research team did not anticipate a significant difference between the 12-inch and 8-inch laterally deep blockout simulations.

This new baseline model with 8-inch blockouts was evaluated with a computer simulation of the same impact conditions as the 12-inch blockout model. The research team then compared the results of the simulations with the 12-inch and 8-inch laterally deep blockouts. The only difference between these two models was the lateral depth of the blockout. The comparison showed minimal difference in the behavior of the vehicle between the 12-inch and 8-inch blockout. Figure 3.4 shows an overhead comparison of the two simulations. Figure 3.5 shows a downstream view comparison of the two simulations. The research team also used a multichannel, weighted approach to analyze the data signals from both simulations. Figure 3.6 shows the results of this RSVVP analysis. Based on the results of this analysis, the research team confirmed the validity of the 8-inch blockout baseline model and proceeded to use this design in subsequent simulations. A few simulations were performed in parallel with this effort, and, therefore, a few configurations incorporated the 12-inch blockout. However, the majority included the 8-inch blockout.



a.

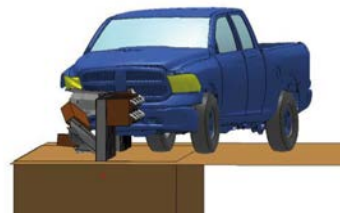


b.



c.

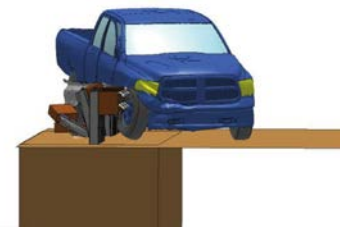
Crash-Test Sequence



d.



e.



f.

Simulation Sequence

Figure 3.2. Comparison between Crash Test 2214MG-2, sequenced in the left column, and simulation, sequenced in the right column (22).

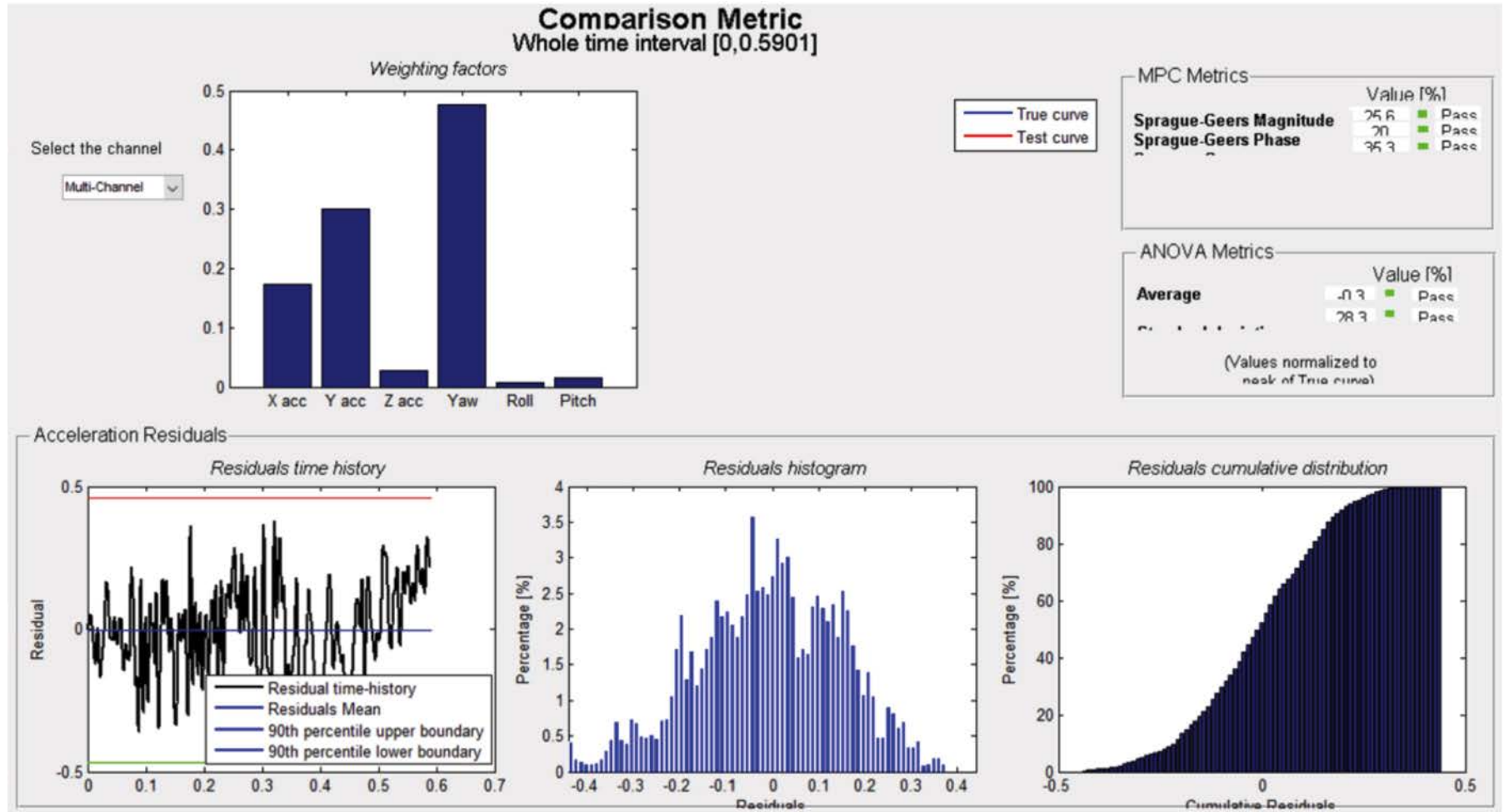


Figure 3.3. RSVVP analysis results of MGS crash test and simulation.

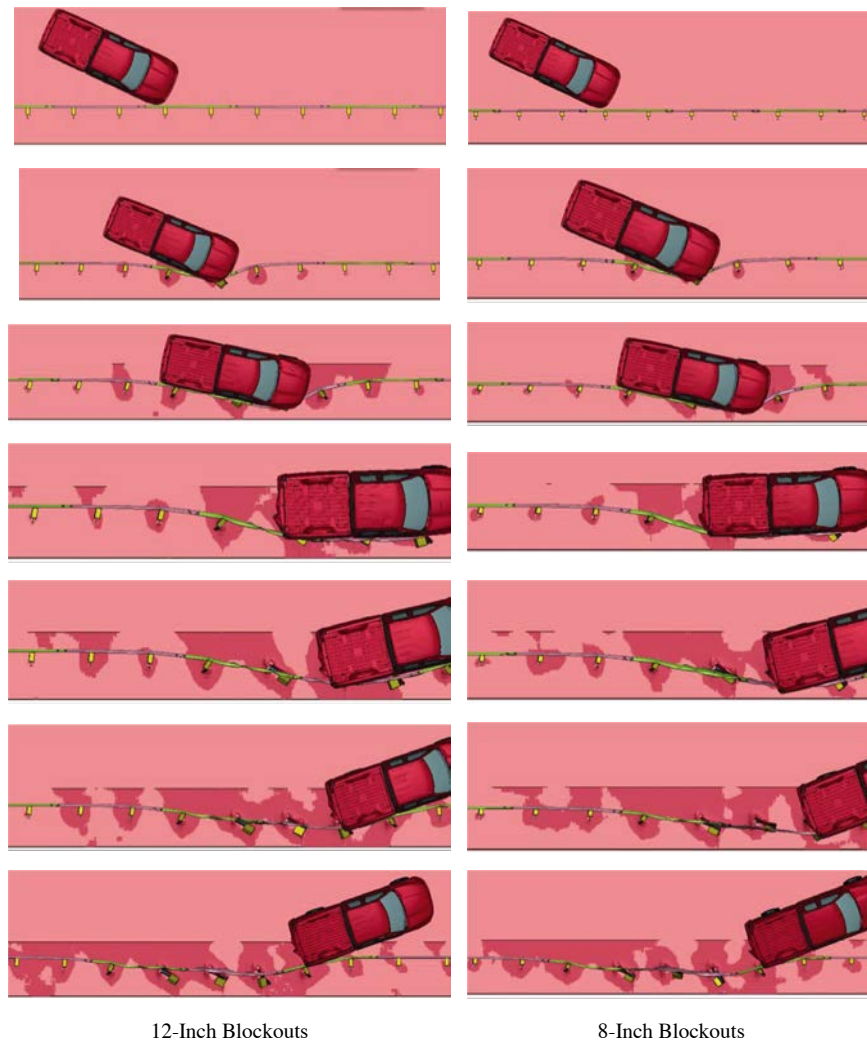


Figure 3.4. Overhead comparison of 12-inch and 8-inch laterally deep blockouts.

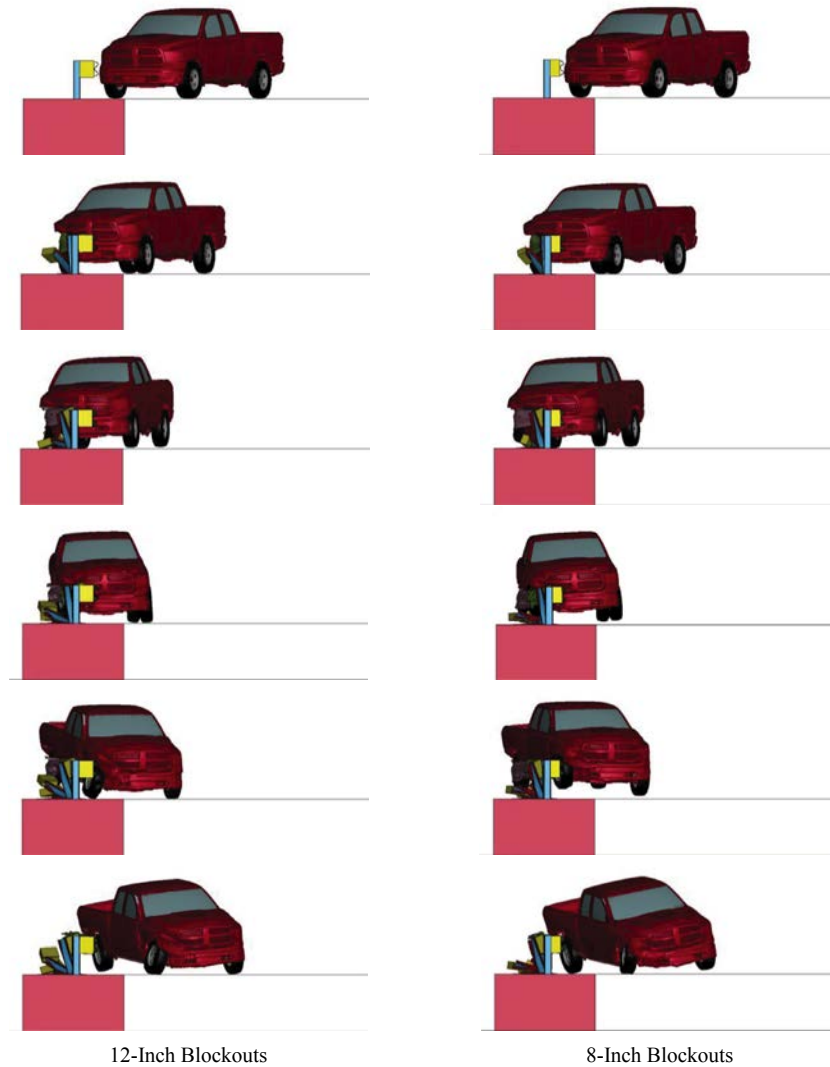


Figure 3.5. Downstream view comparison of 12-inch and 8-inch laterally deep blockouts.

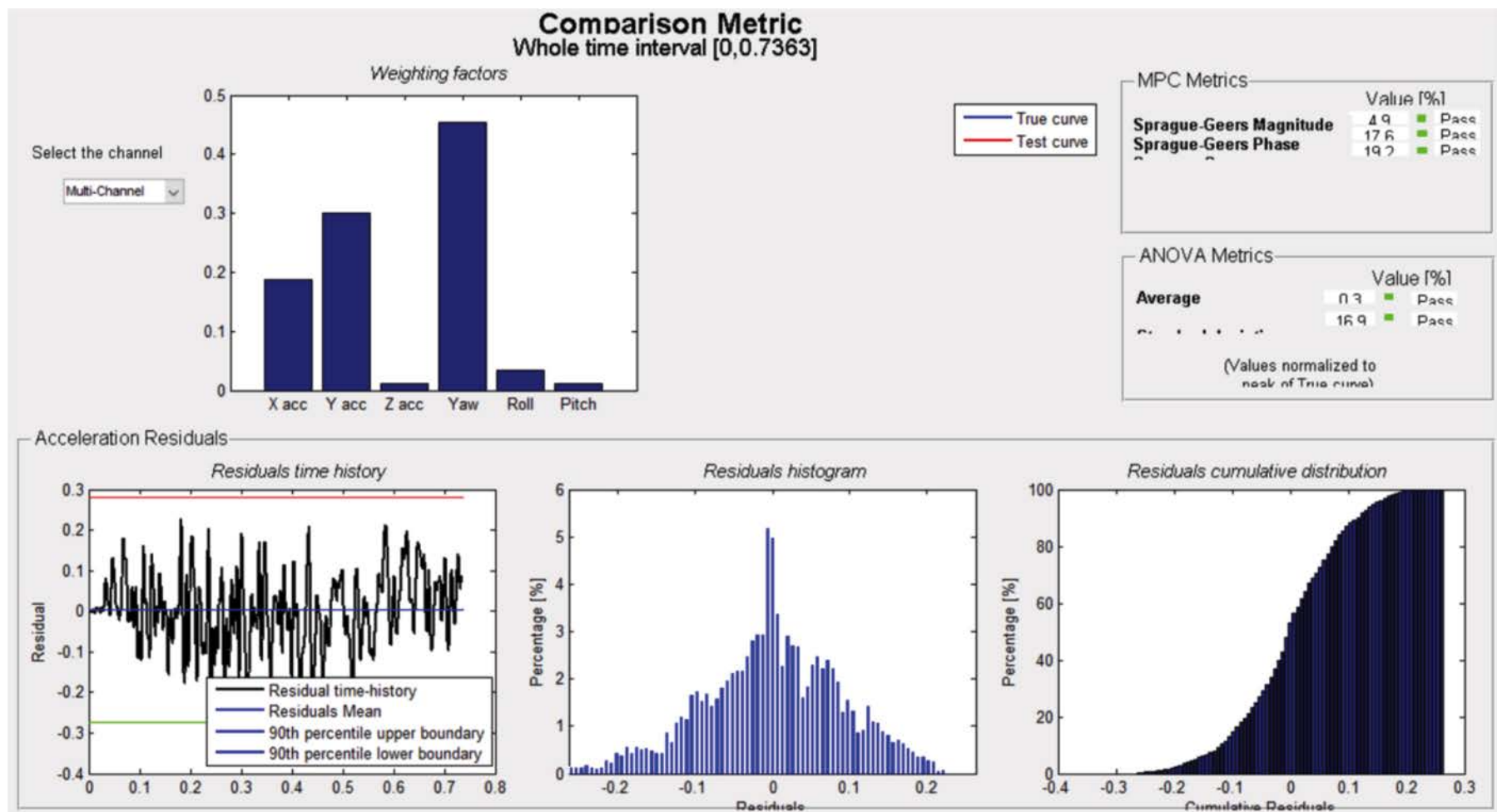


Figure 3.6. RSVVP analysis results of 12-inch and 8-inch blackout simulations.

Stiffening Mechanism Investigation

Reduced Post Spacing

Half-Post Spacing

Reduced post spacing systems have been successfully MASH crash tested prior to this simulation effort (7). Therefore, the objective of this portion of the simulation effort was the evaluation of a transition from MGS with full-post spacing to MGS with half-post spacing. This transition was modeled by modifying the verified baseline model discussed above. Additional posts were added to the downstream portion of the model to represent the half-post spacing. The half-post spacing portion of the model incorporated shortened blockouts (10-inch vertical height), which were utilized in the successful half-post spacing crash test (7). Figure 3.7 shows the transition portion of this model from an overhead perspective. Figure 3.8 shows the alignment of the shortened blockout with the W-beam rail.

MASH Test 3-21 Simulation

Figure 3.9, Figure 3.10, and Figure 3.11 show the sequential frames of MASH Test 3-21 on the transition to MGS with half-post spacing. The OIV was calculated to be 5.2 meters per second (m/s) (preferred limit is 9.1 m/s). The RDA was calculated to be 9.7 g (preferred limit is 15.0 g). This configuration passed MASH Test 3-21 by successfully containing and redirecting the vehicle.

10-Gauge W-Beam

The use of 10-gauge W-beam rail elements as stiffening mechanisms was prioritized at the end of Phase I. The most common W-beam rail is made from 12-gauge steel (thickness of 0.1046 inches), but the thickness is increased when replaced with a 10-gauge element (thickness of 0.1345 inches). To model this, the research team modified the W-beam elements of the baseline model to a 10-gauge thickness.

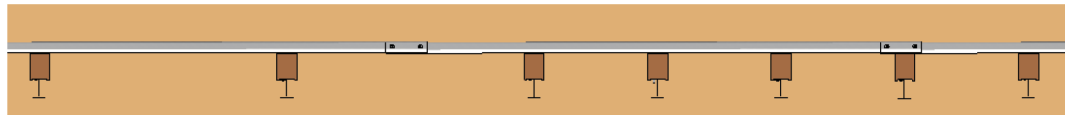


Figure 3.7. Overhead view of transition to MGS with half-post spacing and shortened 10-inch blockout.

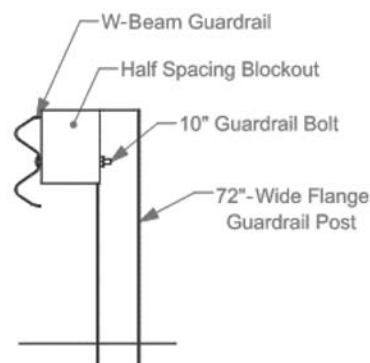


Figure 3.8. Profile view of MGS with half-post spacing and shortened 10-inch blockout with W-beam rail (7).

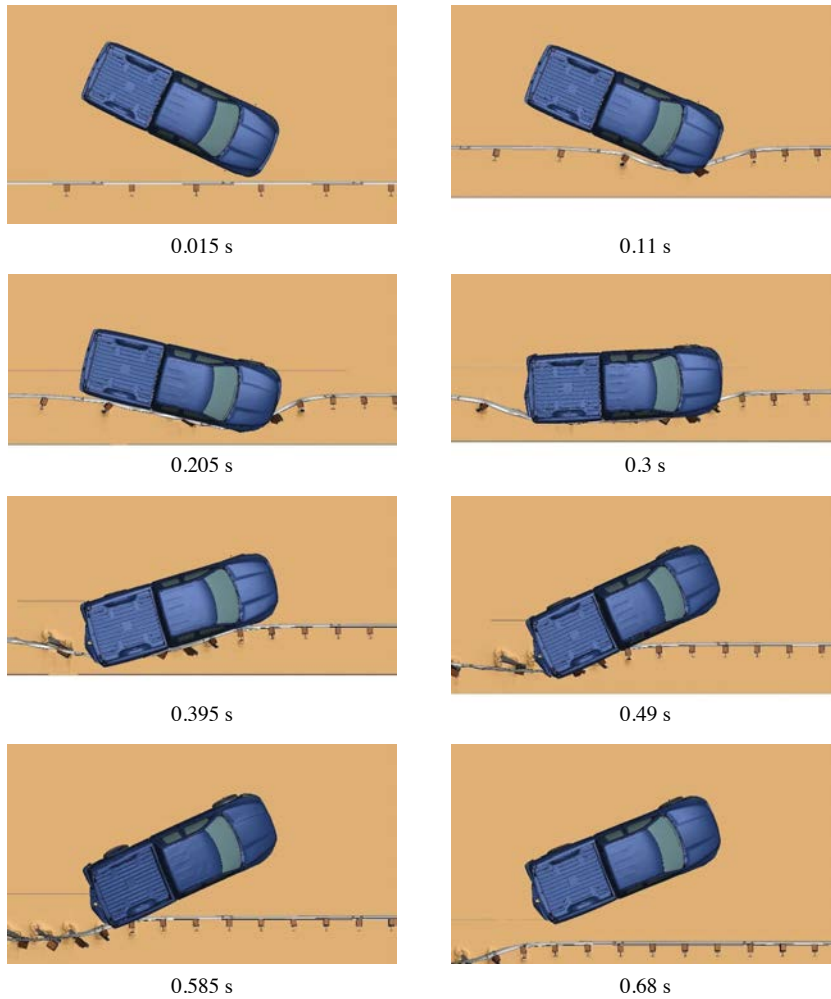


Figure 3.9. *Transition to MGS with half-post spacing – overhead view of MASH Test 3-21.*

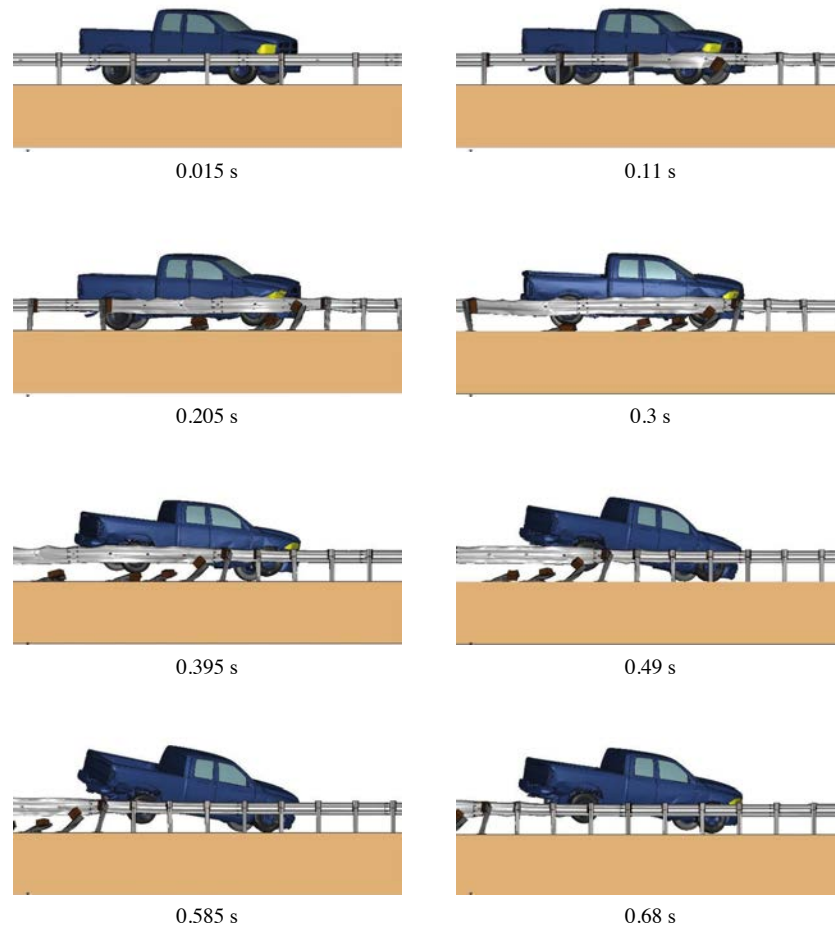


Figure 3.10. Transition to MGS with half-post spacing – field-side view of MASH Test 3-21.

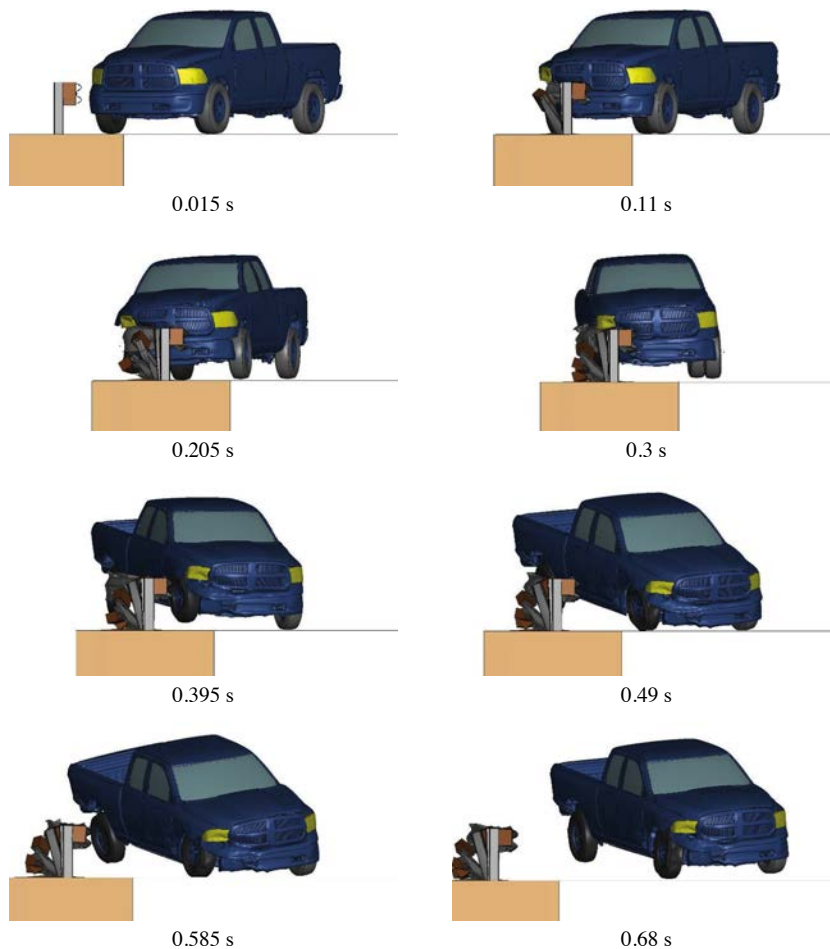


Figure 3.11. Transition to MGS with half-post spacing – downstream view of MASH Test 3-21.

The baseline MGS model was modified with the inclusion of a thicker 10-gauge steel W-beam guardrail in place of the standard 12-gauge element. This configuration can be seen in Figure 3.12. Full-scale dynamic simulations for MASH Tests 3-11, 3-10, and 3-21 were performed on this system configuration.

MASH Test 3-11 Simulation

Figure 3.13, Figure 3.14, and Figure 3.15 show the sequential frames of MASH Test 3-11 on MGS with a 10-gauge W-beam. In this simulation, the maximum dynamic deflection was 39.2 inches, the working width was 52.1 inches, and the working width height was 48.1 inches. The OIV was calculated to be 4.8 m/s (preferred limit is 9.1 m/s). The RDA was calculated to be 11.7 g (preferred limit is 15 g). This configuration passed MASH Test 3-11 by successfully containing and redirecting the vehicle.

MASH Test 3-10 Simulation

Figure 3.16, Figure 3.17, and Figure 3.18 show the sequential frames of MASH Test 3-10 on MGS with a 10-gauge W-beam. The OIV was calculated to be 6.5 m/s (preferred limit is 9.1 m/s). The RDA was calculated to be 20.2 g (maximum limit is 20.49 g). This configuration passed MASH Test 3-10 by successfully containing and redirecting the vehicle.

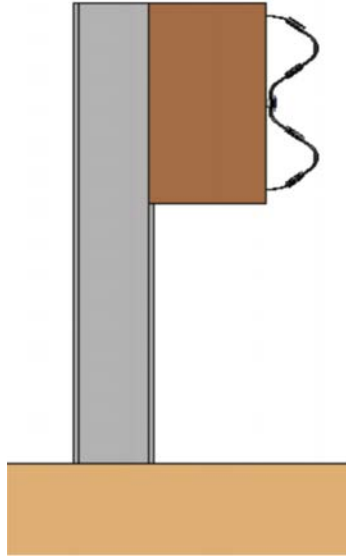


Figure 3.12. Profile view of MGS with a 10-gauge W-beam.

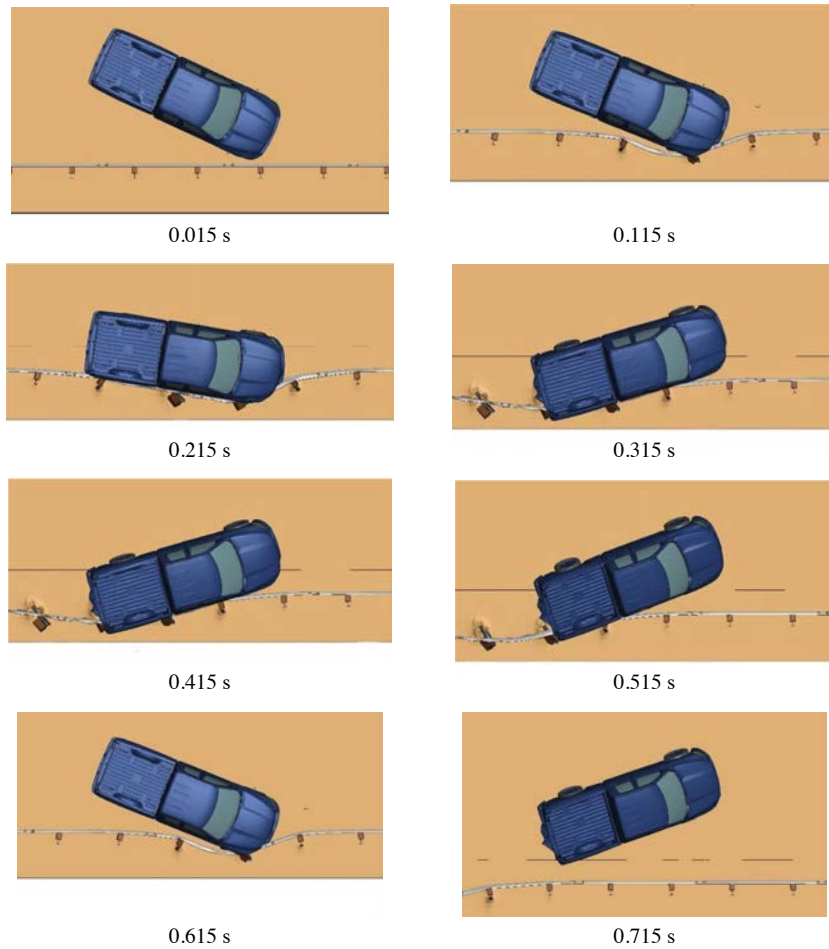


Figure 3.13. MGS with 10-gauge W-beam – overhead view of MASH Test 3-11.

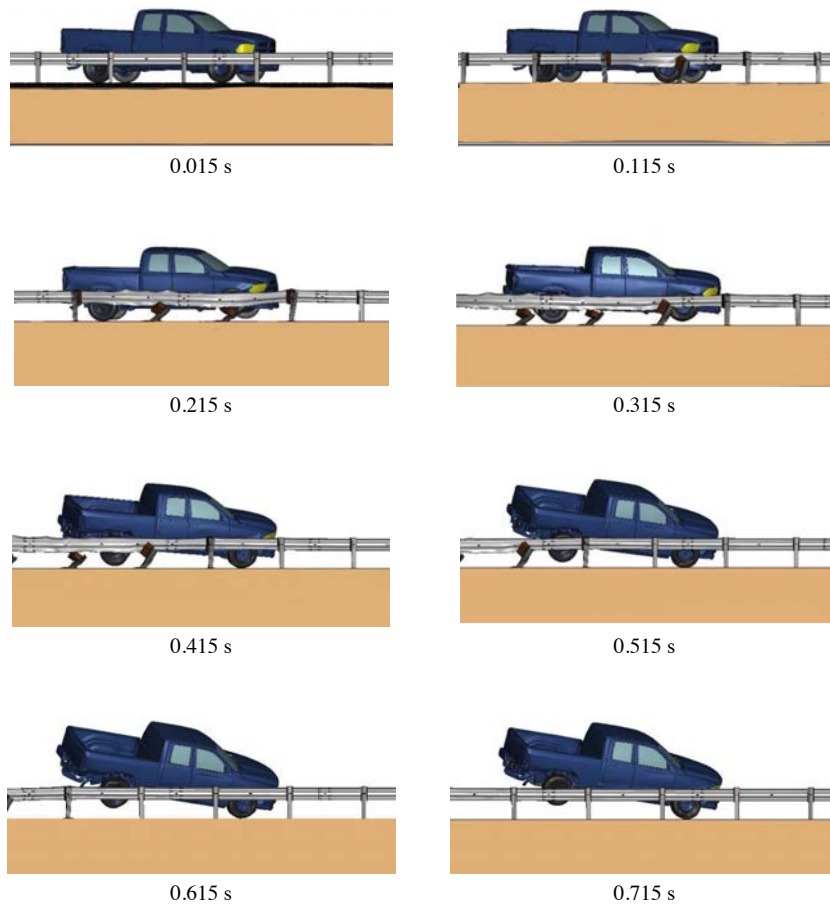


Figure 3.14. MGS with 10-gauge W-beam – field-side view of MASH Test 3-11.

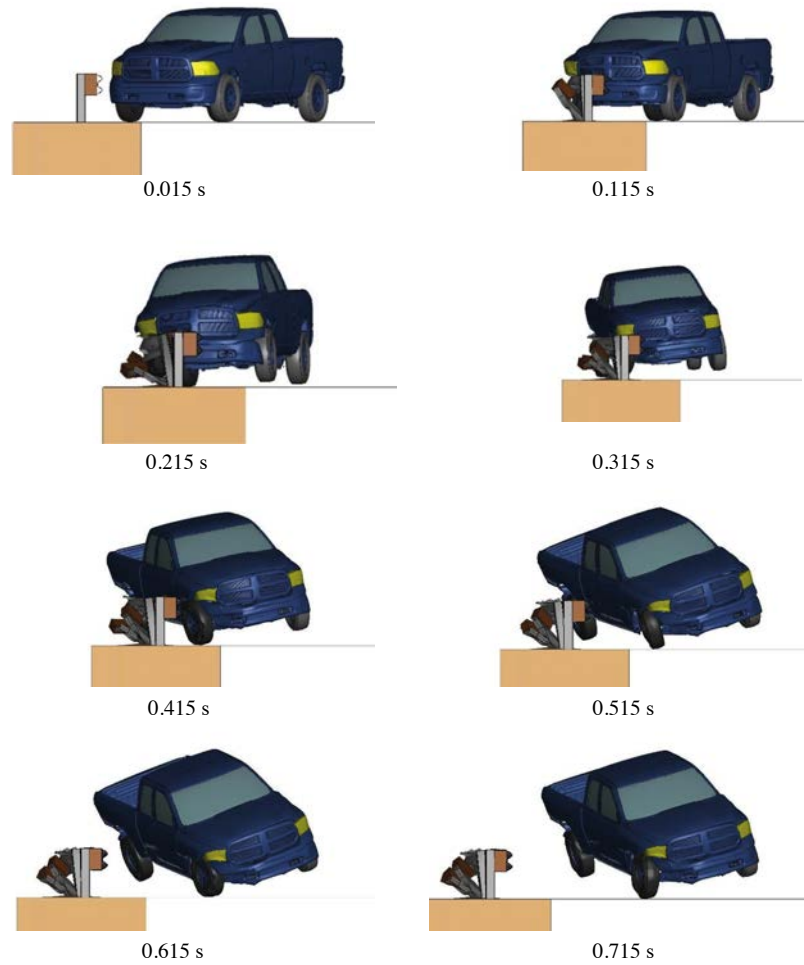


Figure 3.15. MGS with 10-gauge W-beam – downstream view of MASH Test 3-11.

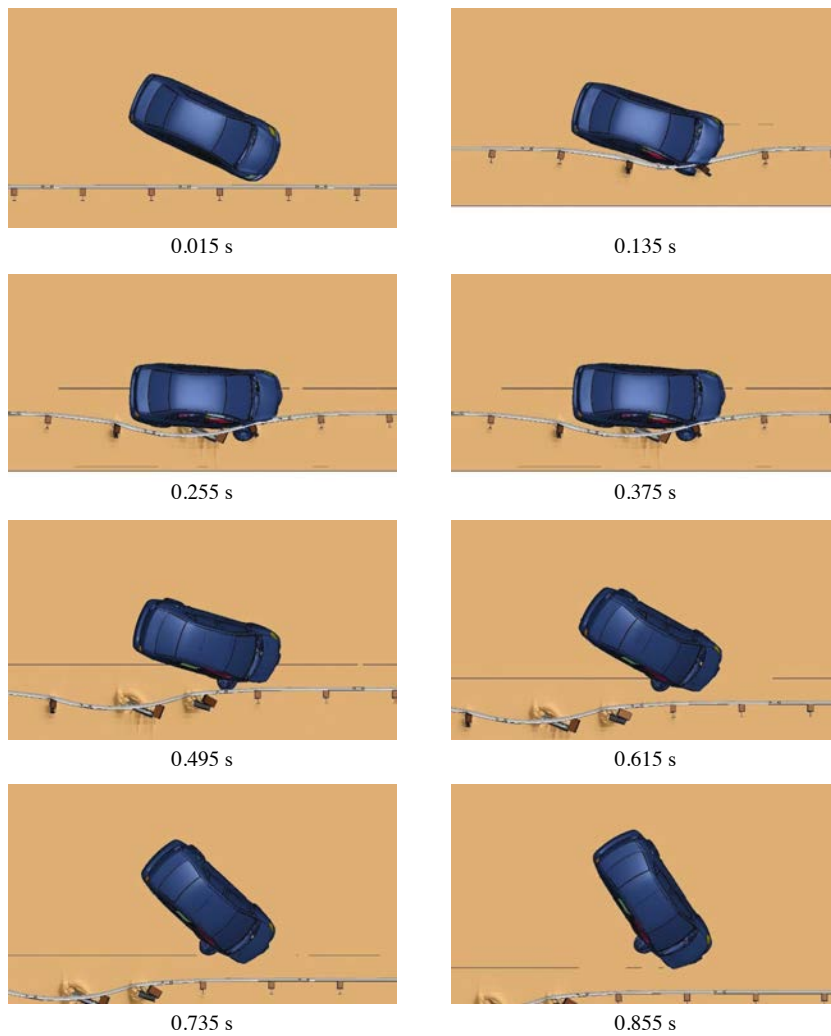


Figure 3.16. MGS with 10-gauge W-beam – overhead view of MASH Test 3-10.

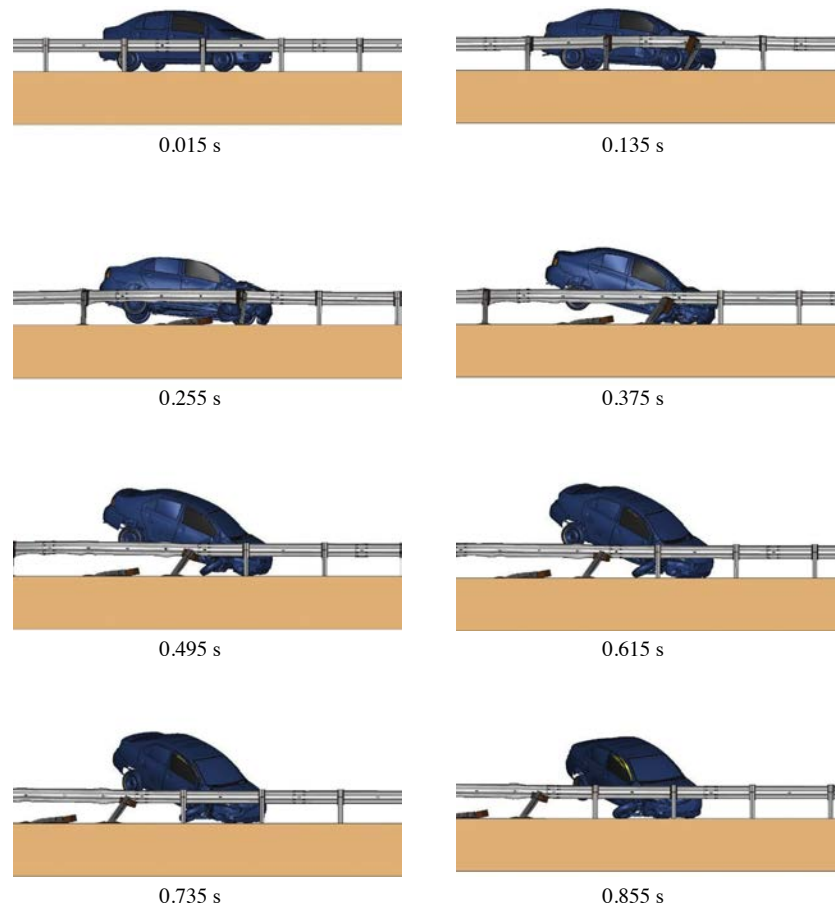


Figure 3.17. MGS with 10-gauge W-beam – field-side view of MASH Test 3-10.

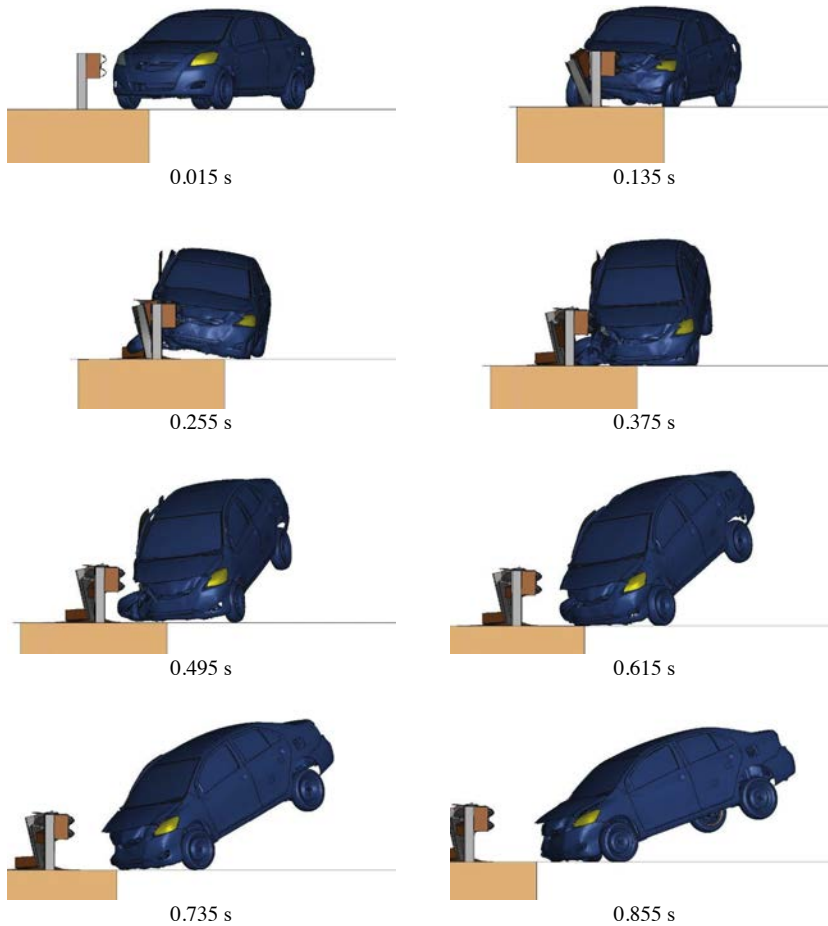


Figure 3.18. MGS with 10-gauge W-beam – downstream view of MASH Test 3-10.

MASH Test 3-21 Simulation

The transition to MGS with a 10-gauge W-beam is shown below in Figure 3.19. This transition includes the simple ending of the 12-gauge W-beam and the start of the 10-gauge W-beam.

Figure 3.20, Figure 3.21, and Figure 3.22 show the sequential frames of MASH Test 3-21 on the transition to MGS with a 10-gauge W-beam. The OIV was calculated to be 4.9 m/s (preferred limit is 9.1 m/s). The RDA was calculated to be 14.8 g (preferred limit is 15 g). This configuration passed MASH Test 3-21 by successfully containing and redirecting the vehicle.

Rub Rail

C6×8.2 Rub Rail Mounted 12 Inches Above Grade

The baseline MGS model was modified with the inclusion of a C6×8.2 rub rail mounted 12 inches above grade as shown in Figure 3.23. A full-scale dynamic simulation for MASH Test 3-11 was performed on this system configuration.



Figure 3.19. Overhead view of transition to MGS with 10-gauge W-beam.

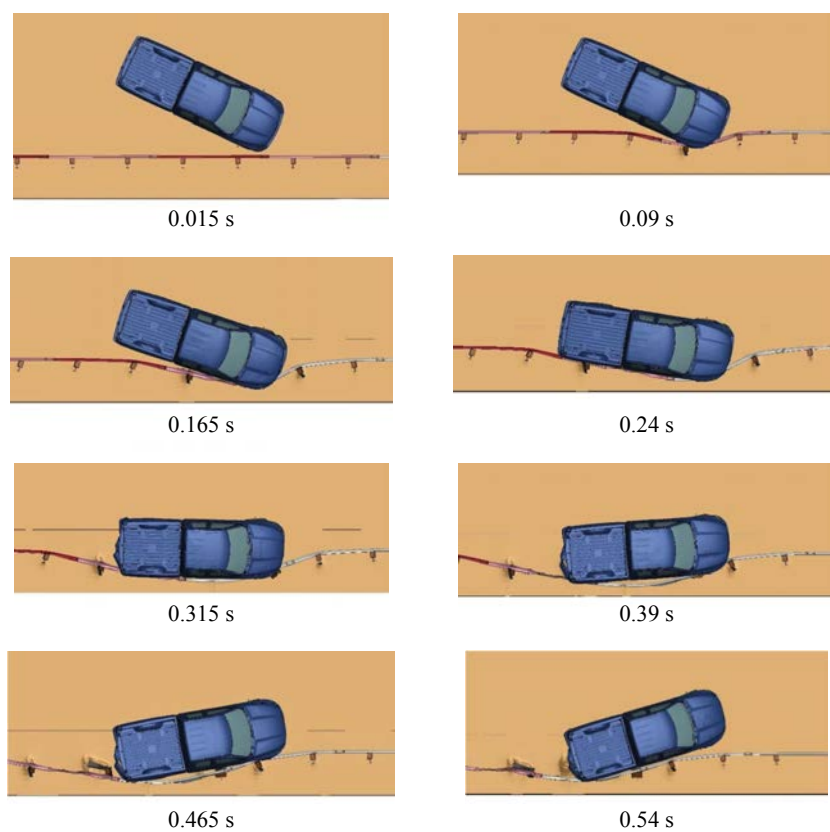


Figure 3.20. MGS with 10-gauge W-beam – overhead view of MASH Test 3-21.

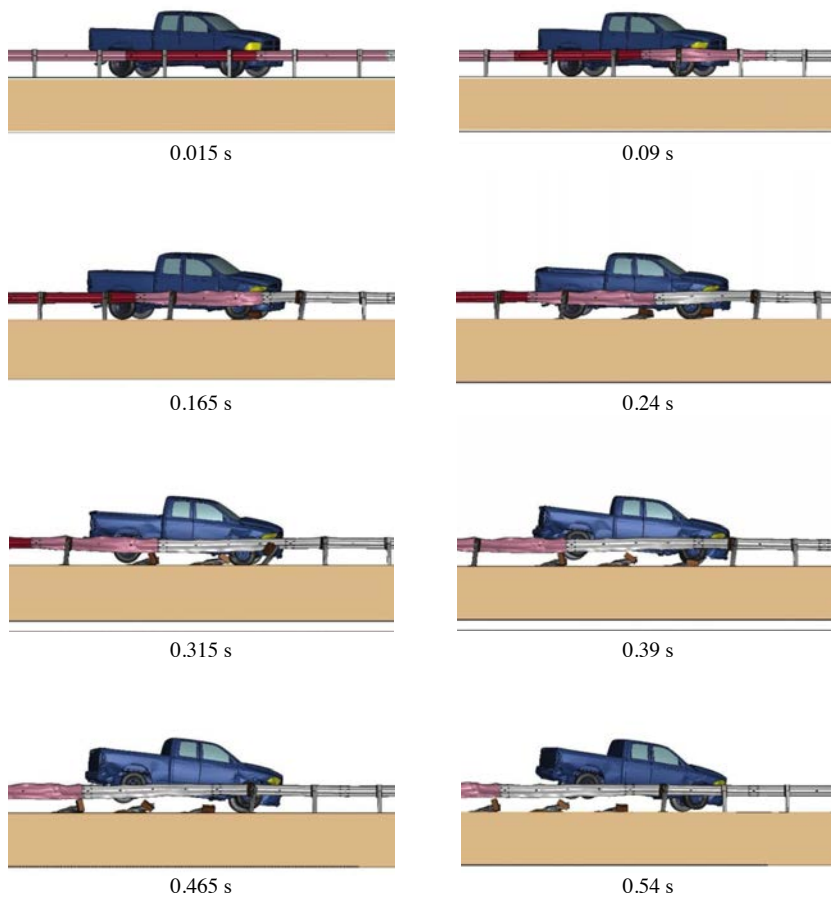


Figure 3.21. MGS with 10-gauge W-beam – field-side view of MASH Test 3-21.



Figure 3.22. MGS with 10-gauge W-beam – downstream view of MASH Test 3-21.

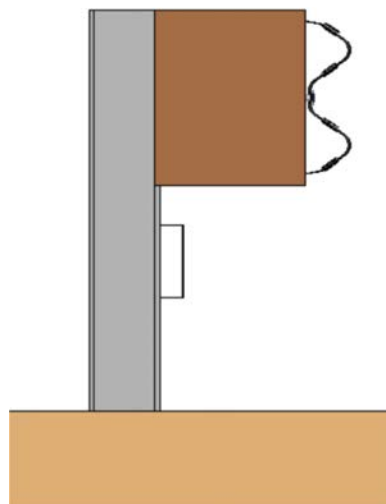


Figure 3.23. Profile view of MGS with C6×8.2 rub rail mounted 12 inches above grade.

MASH Test 3-11 Simulation

Figure 3.24, Figure 3.25, and Figure 3.26 show the sequential frames of MASH Test 3-11 on MGS with a C6×8.2 rub rail mounted 12 inches above grade. In this simulation, the maximum dynamic deflection was 34.7 inches, the working width was 48.8 inches, and the working width height was 19.8 inches. The OIV was calculated to be 6.0 m/s (preferred limit is 9.1 m/s). The RDA was calculated to be 9.6 g (preferred limit is 15.0 g). This configuration passed MASH Test 3-11 by successfully containing and redirecting the vehicle.

C6×8.2 Rub Rail Mounted 6 Inches Above Grade

The baseline MGS model was modified with the inclusion of a C6×8.2 rub rail mounted 6 inches above grade as shown in Figure 3.27. A full-scale dynamic simulation for MASH Test 3-11 was performed on this system configuration.

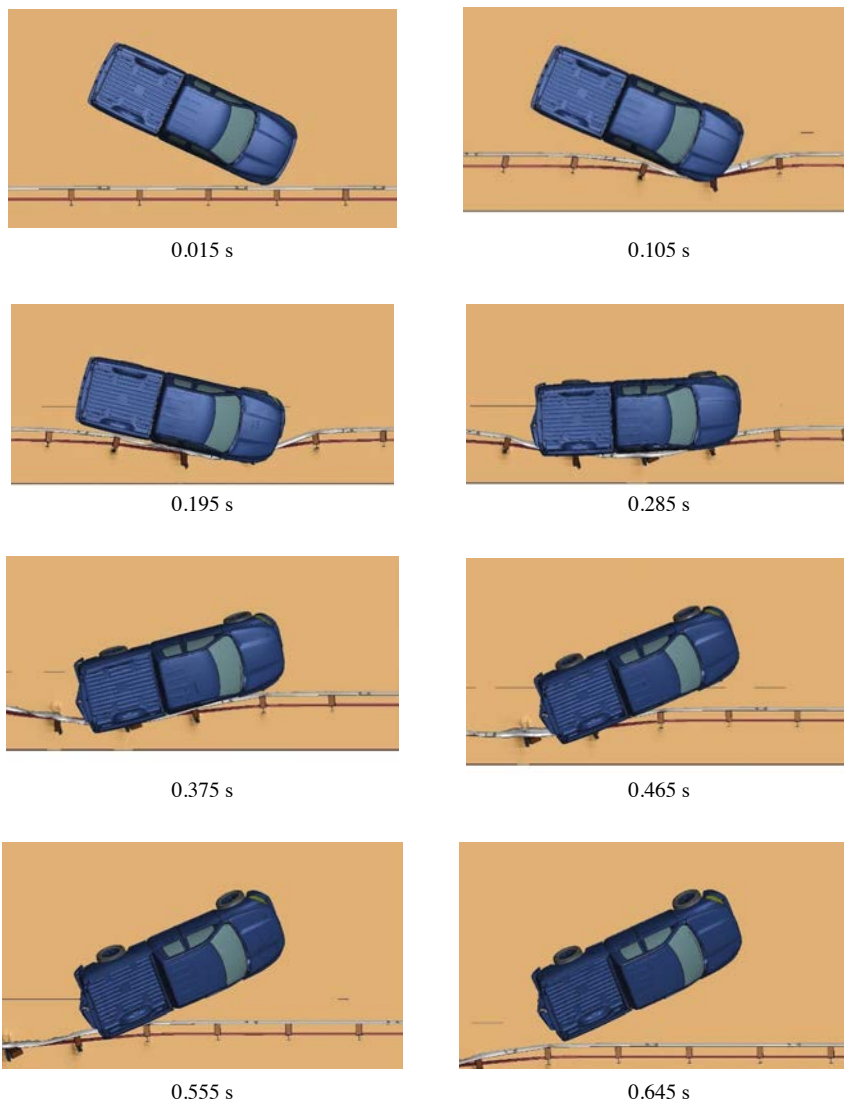


Figure 3.24. MGS with C6×8.2 rub rail mounted 12 inches above grade – overhead view of MASH Test 3-11.

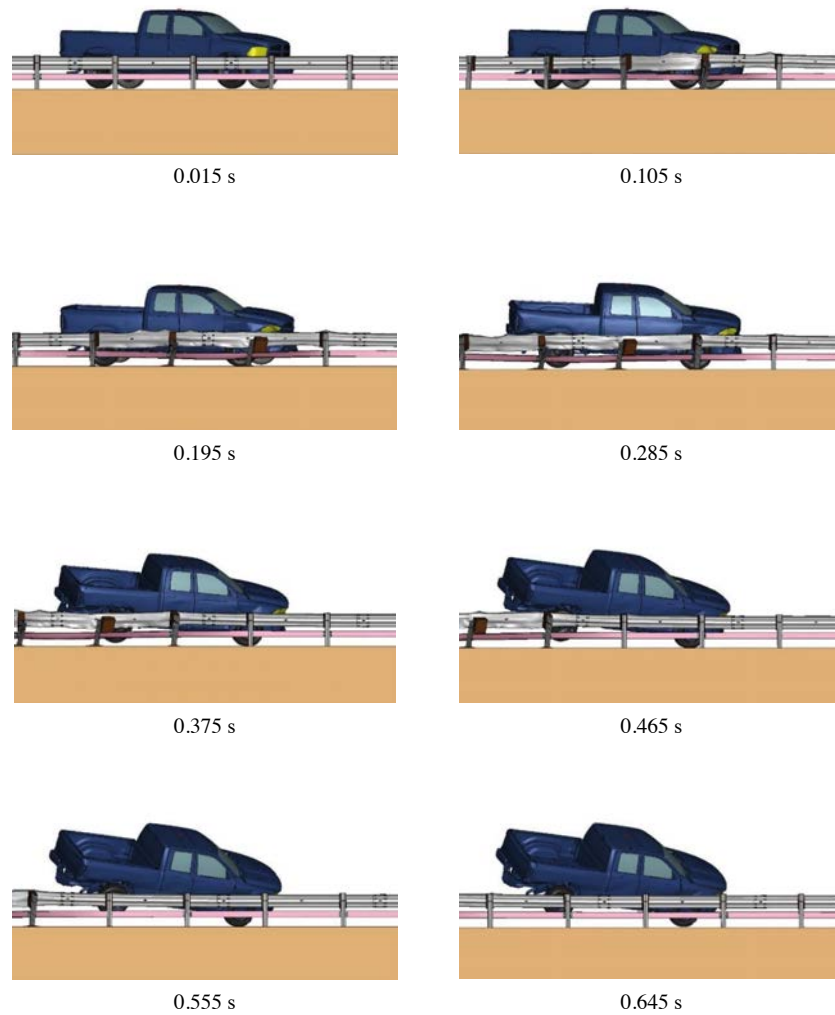


Figure 3.25. MGS with C6×8.2 rub rail mounted 12 inches above grade – field-side view of MASH Test 3-11.

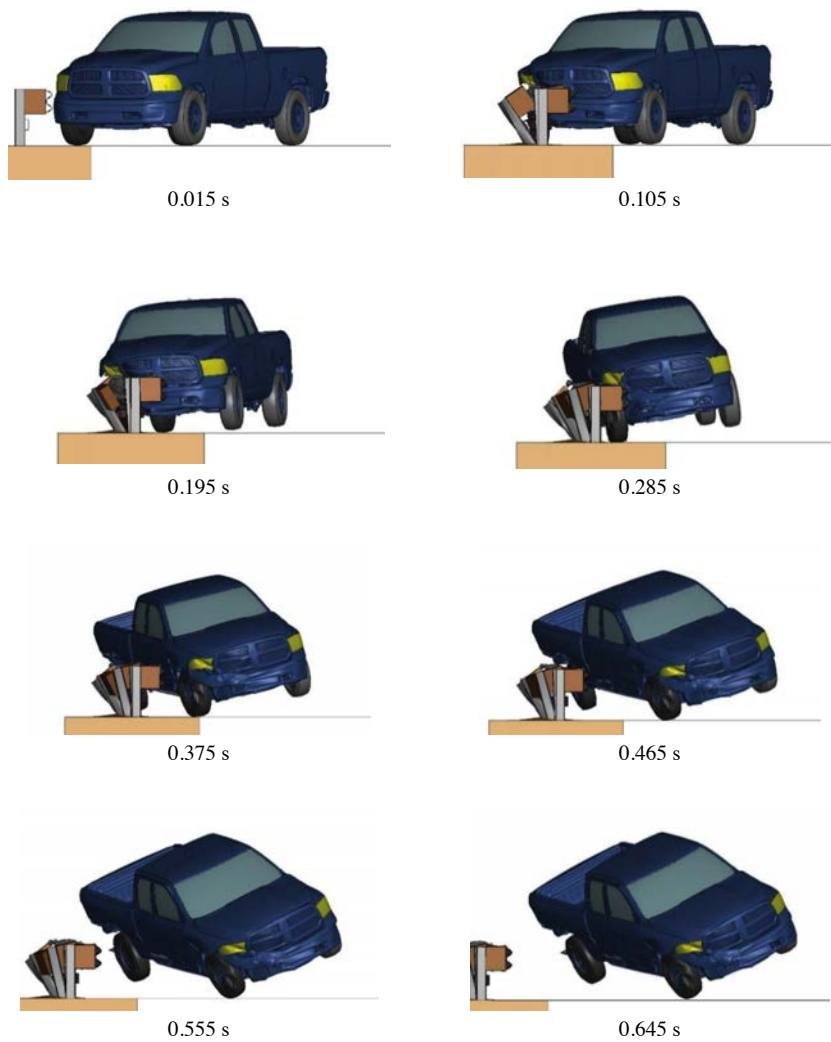


Figure 3.26. MGS with C6×8.2 rub rail mounted 12 inches above grade – downstream view of MASH Test 3-11.

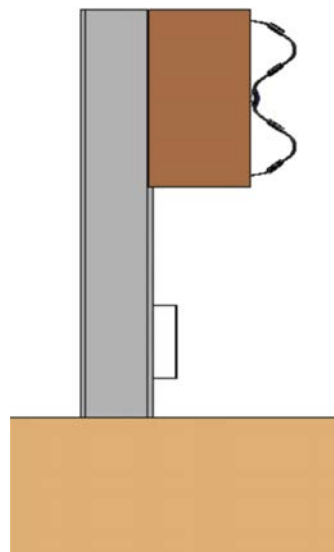


Figure 3.27. Profile view of MGS with C6×8.2 rub rail mounted 6 inches above grade.

MASH Test 3-11 Simulation

Figure 3.28, Figure 3.29, and Figure 3.30 show the sequential frames of MASH Test 3-11 on MGS with a C6×8.2 rub rail mounted 6 inches above grade. In this simulation, the maximum dynamic deflection was 36.0 inches, the working width was 47.0 inches, and the working width height was 37.0 inches. The OIV was calculated to be 5.2 m/s (preferred limit is 9.1 m/s). The RDA was calculated to be 12.0 g (preferred limit is 15.0 g). This configuration passed MASH Test 3-11 by successfully containing and redirecting the vehicle.

HSS4×4×¼ Rub Rail Mounted 12 Inches Above Grade

The baseline MGS model was modified with the inclusion of the HSS4×4×¼ rub rail mounted 12 inches above grade as shown in Figure 3.31. A full-scale dynamic simulation for MASH Test 3-11 was performed on this system configuration.

MASH Test 3-11 Simulation

Figure 3.32, Figure 3.33, and Figure 3.34 show the sequential frames of MASH Test 3-11 on MGS with HSS4×4×¼ rub rail mounted 12 inches above grade. This configuration failed MASH Test 3-11 because the vehicle exhibited rollover as it exited the system.

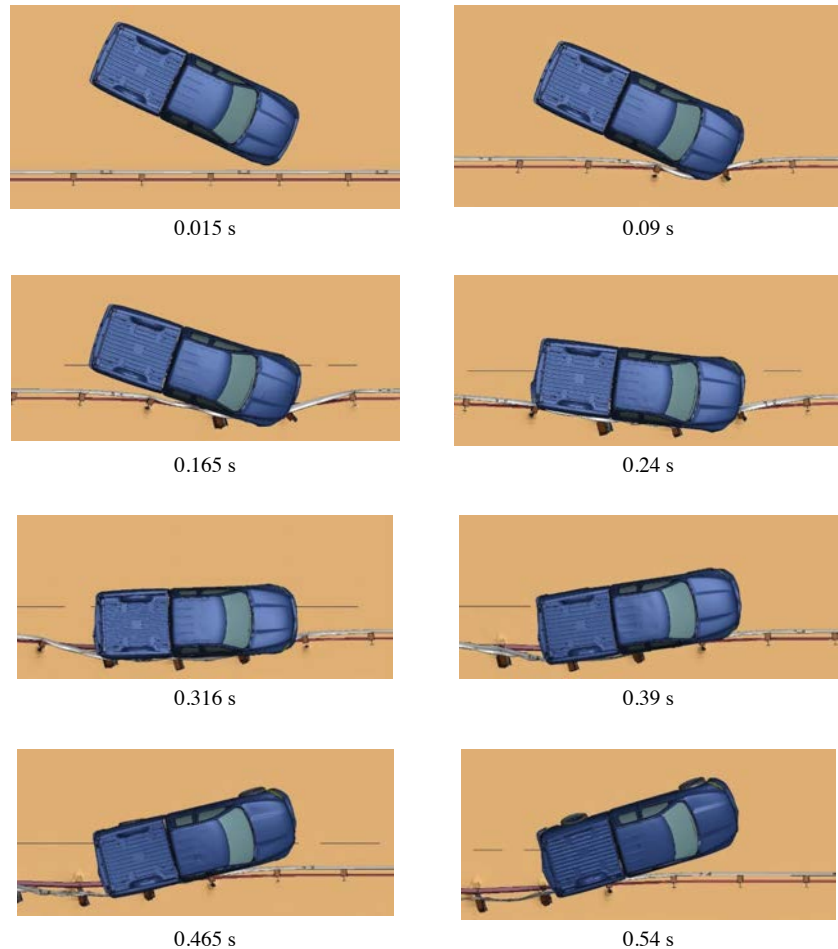


Figure 3.28. MGS with C6×8.2 rub rail mounted 6 inches above grade – overhead view of MASH Test 3-11.

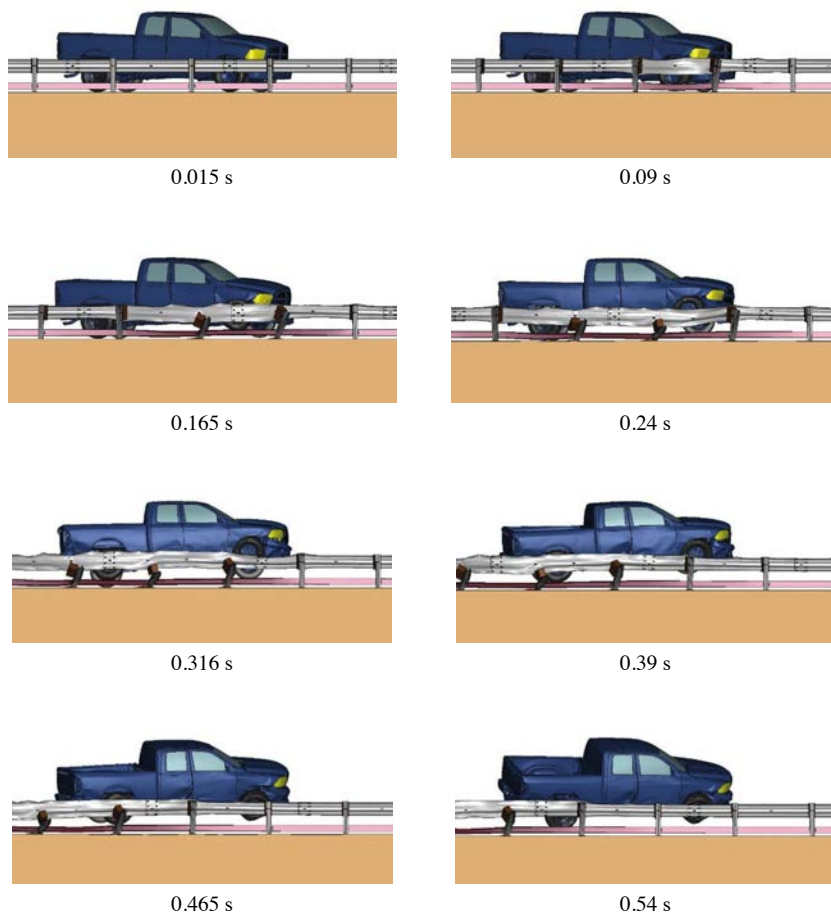


Figure 3.29. MGS with C6×8.2 rub rail mounted 6 inches above grade – field-side view of MASH Test 3-11.



Figure 3.30. MGS with C6×8.2 rub rail mounted 6 inches above grade – downstream view of MASH Test 3-11.

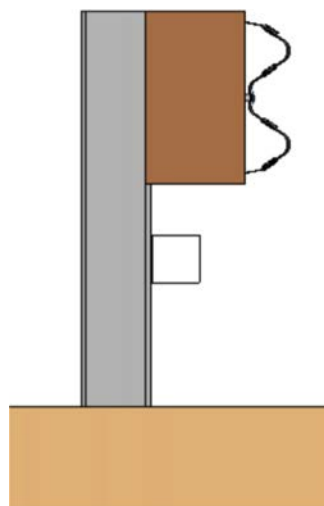


Figure 3.31. Profile view of MGS with HSS4×4×¼ rub rail mounted 12 inches above grade.

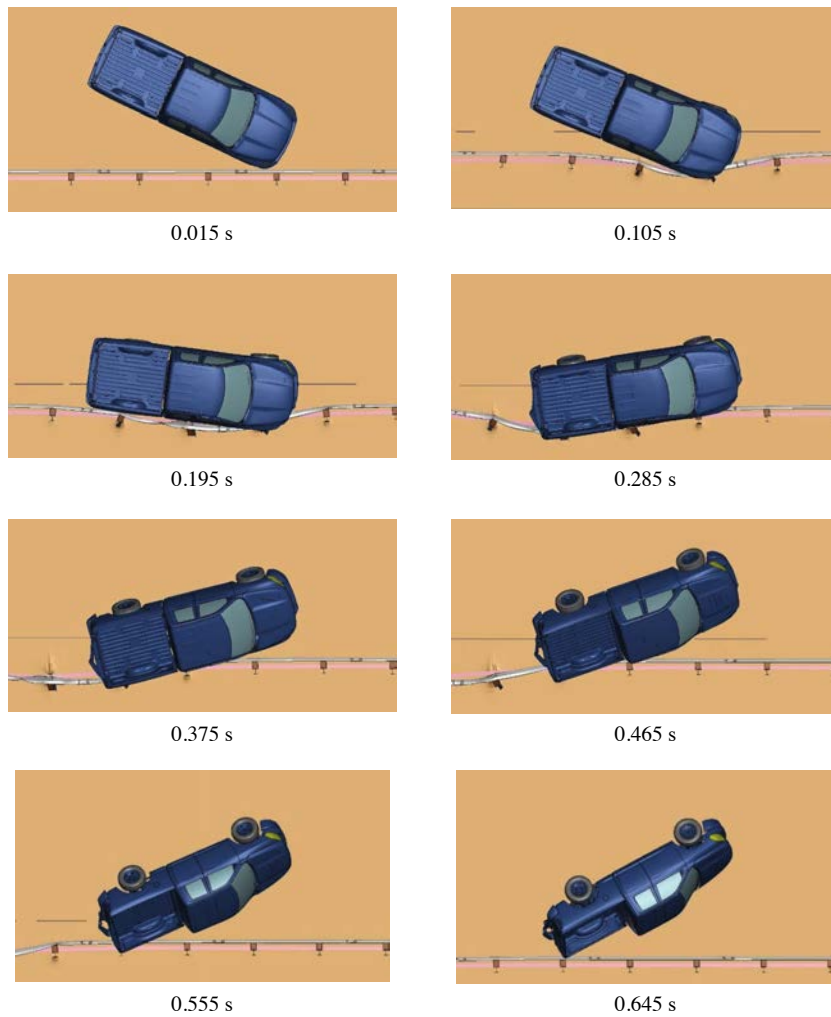


Figure 3.32. MGS with HSS4×4×¼ rub rail mounted 12 inches above grade – overhead view of MASH Test 3-11.

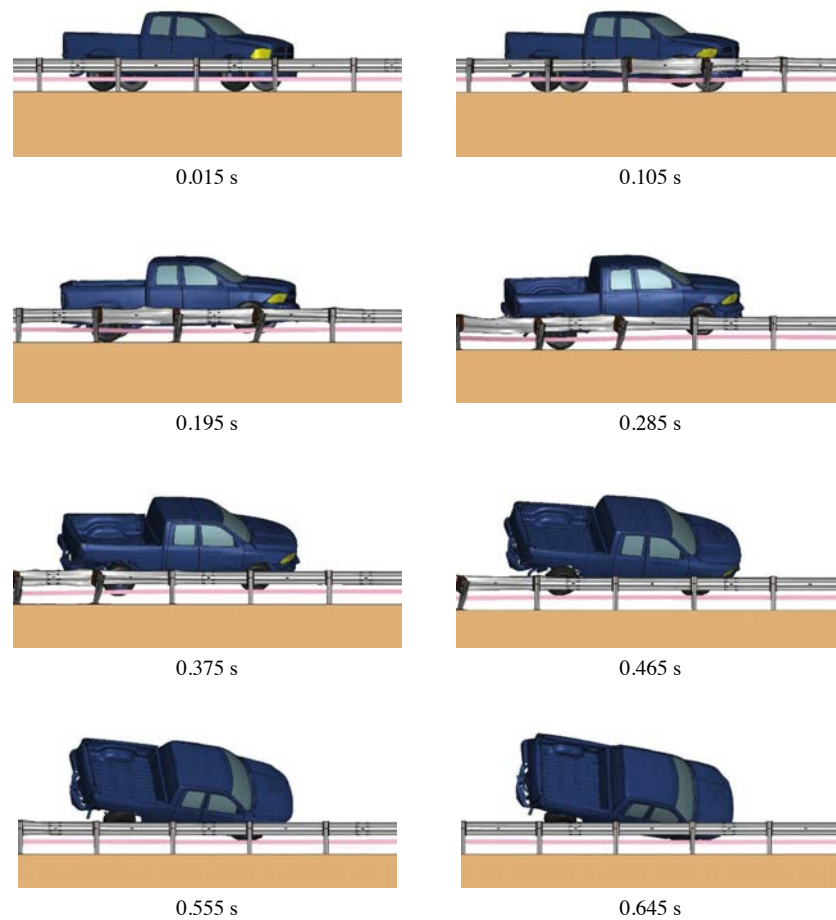


Figure 3.33. MGS with HSS4×4×¼ rub rail mounted 12 inches above grade – field-side view of MASH Test 3-11.

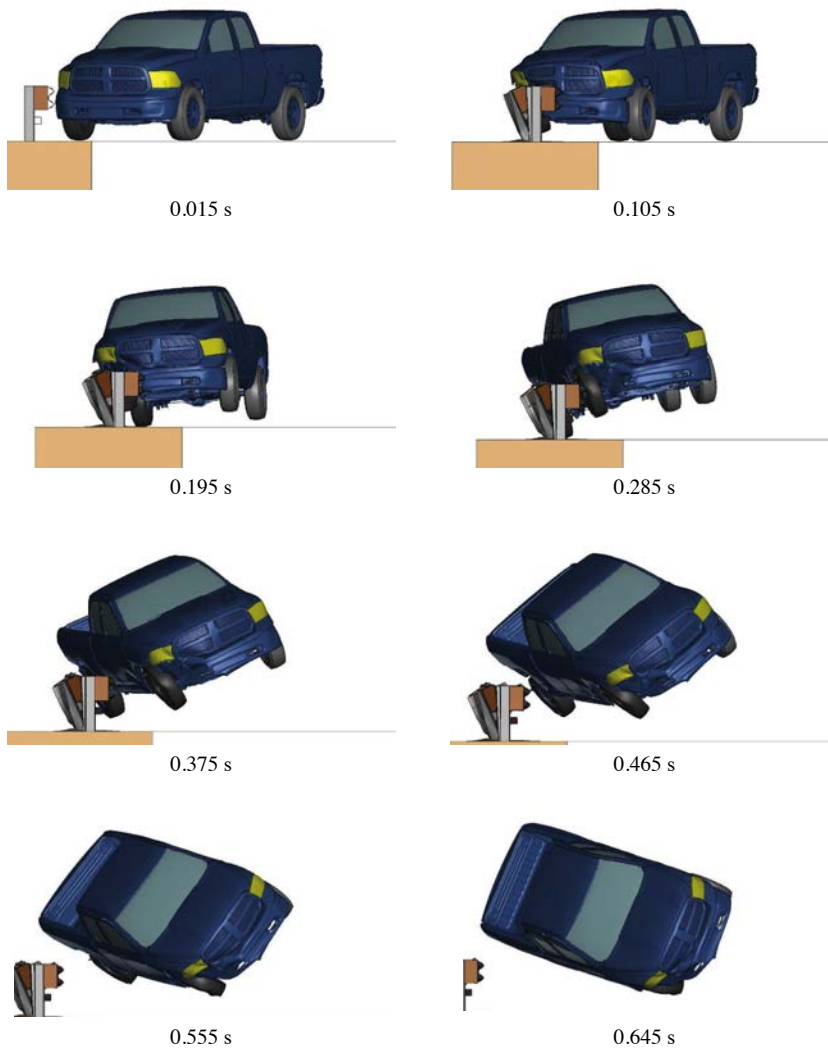


Figure 3.34. MGS with HSS4×4×¼ rub rail mounted 12 inches above grade – downstream view of MASH Test 3-11.

HSS4×4×¼ Rub Rail Mounted 6 Inches Above Grade

The baseline MGS model was modified with the inclusion of a HSS4×4×¼ rub rail mounted 6 inches above grade as shown in Figure 3.35. A full-scale dynamic simulation for MASH Test 3-11 was performed on this system configuration.

MASH Test 3-11 Simulation

Figure 3.36, Figure 3.37, and Figure 3.38 show the sequential frames of MASH Test 3-11 on MGS with HSS4×4×¼ rub rail mounted 6 inches above grade. This configuration failed MASH Test 3-11 because the rub rail acted as a ramp for the vehicle to rise and roll over.

HSS10×10×¼ Rub Rail Mounted 12 Inches Above Grade

The baseline MGS model was modified with the inclusion of a HSS10×10×¼ rub rail mounted 12 inches above grade as shown in Figure 3.39. A full-scale dynamic simulation for MASH Test 3-11 was performed on this system configuration.

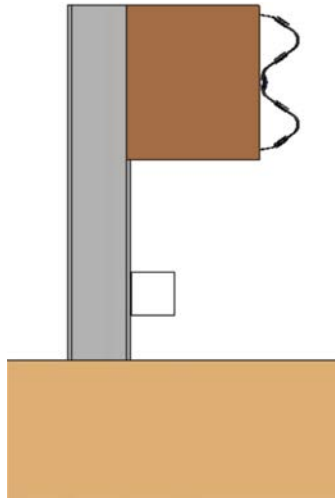


Figure 3.35. Profile view of MGS with HSS4×4×¼ rub rail mounted 6 inches above grade.

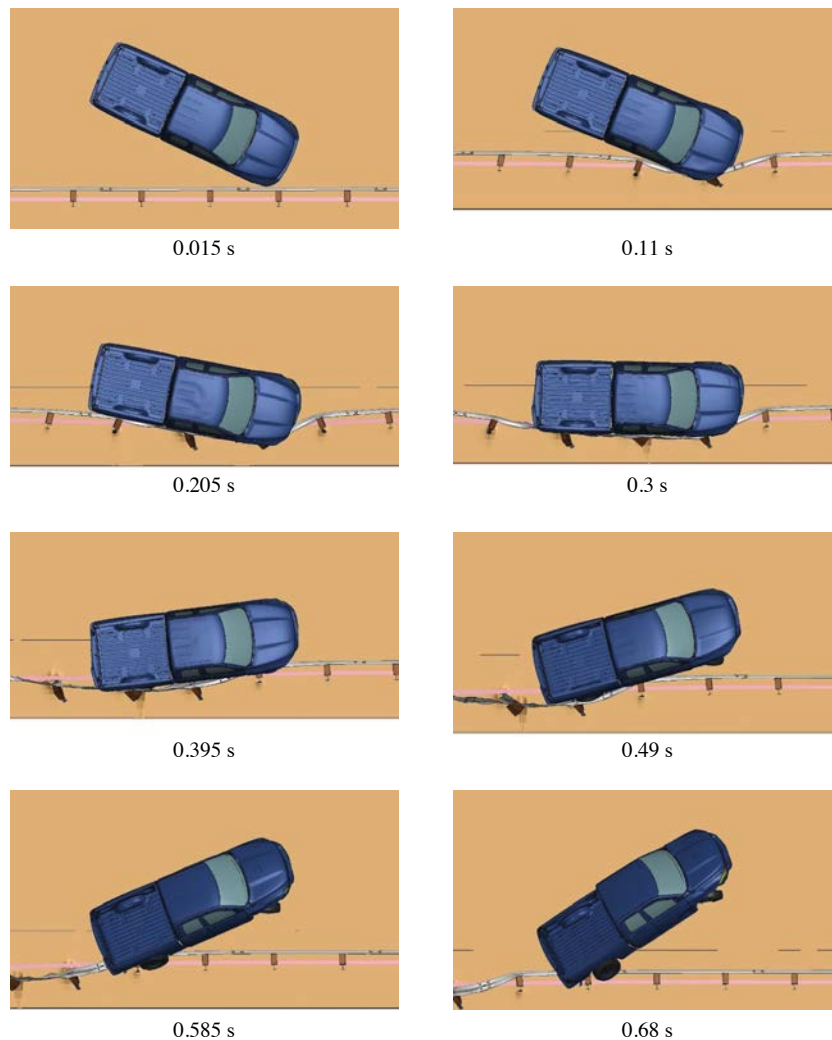


Figure 3.36. MGS with HSS4×4×¼ rub rail mounted 6 inches above grade – overhead view of MASH Test 3-11.

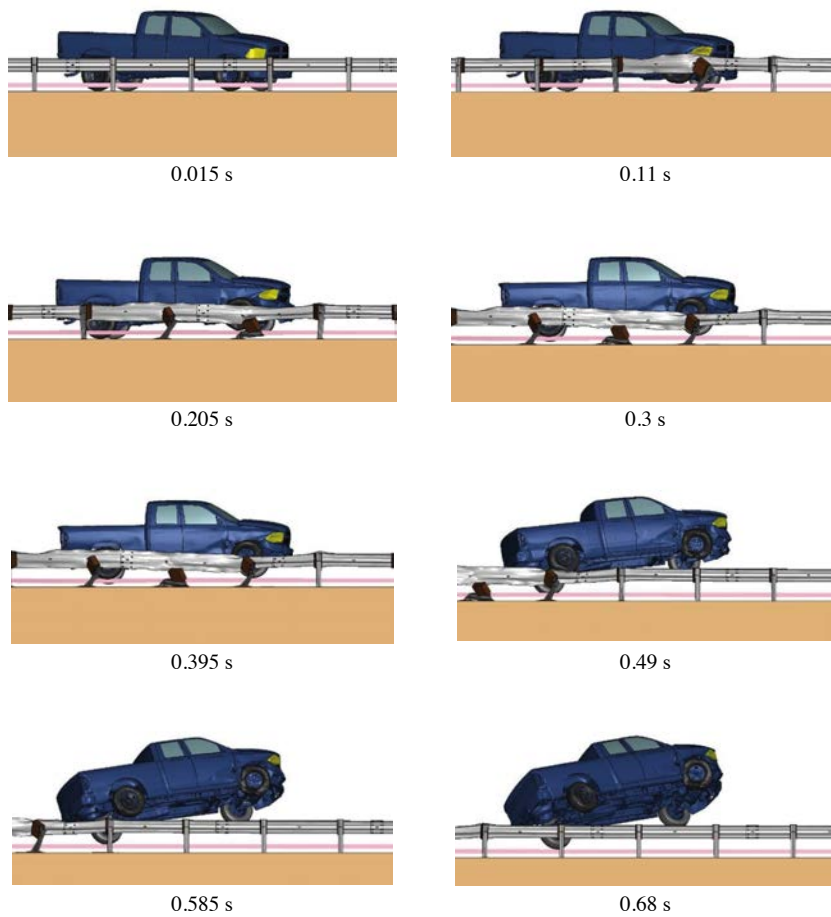


Figure 3.37. MGS with HSS4×4×¼ rail mounted 6 inches above grade – field-side view of MASH Test 3-11.



Figure 3.38. MGS with HSS4×4×¼ rub rail mounted 6 inches above grade – downstream view of MASH Test 3-11.

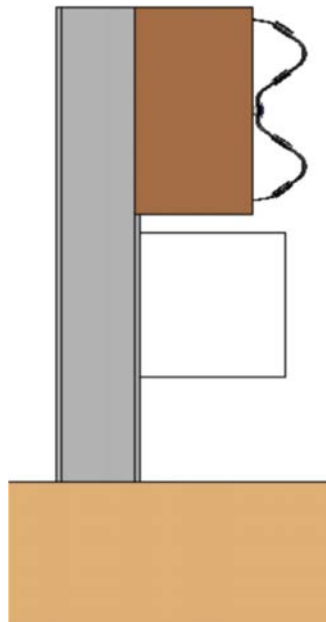


Figure 3.39. Profile view of MGS with HSS10×10×¼ rub rail mounted 12 inches above grade.

MASH Test 3-11 Simulation

Figure 3.40, Figure 3.41, and Figure 3.42 show the sequential frames of MASH Test 3-11 on MGS with HSS10×10×¼ rub rail mounted 12 inches above grade. This configuration failed MASH Test 3-11 because the rub rail acted as a ramp for the vehicle to rise and roll over.

8HU12×135 Rub Rail Mounted 8 Inches Above Grade

The baseline MGS model was modified with the inclusion of an 8HU12×135 rub rail mounted 8 inches above grade as shown in Figure 3.43. A full-scale dynamic simulation for MASH Test 3-11 was performed on this system configuration.

MASH Test 3-11 Simulation

Figure 3.44, Figure 3.45, and Figure 3.46 show the sequential frames of MASH Test 3-11 on MGS with 8HU12×135 rub rail mounted 8 inches above grade. This configuration failed MASH Test 3-11 because the rub rail system provided a ramp for the vehicle to rise and roll over.

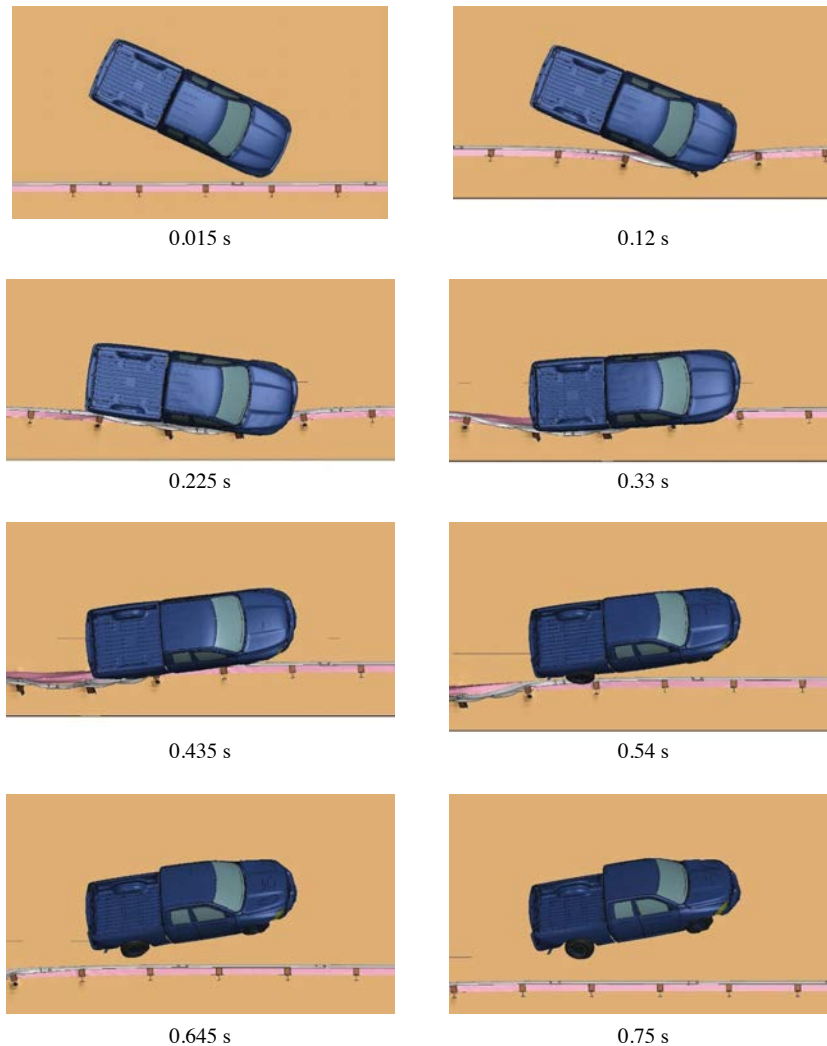


Figure 3.40. MGS with HSS10×10×¼ rub rail mounted 12 inches above grade – overhead view of MASH Test 3-11.

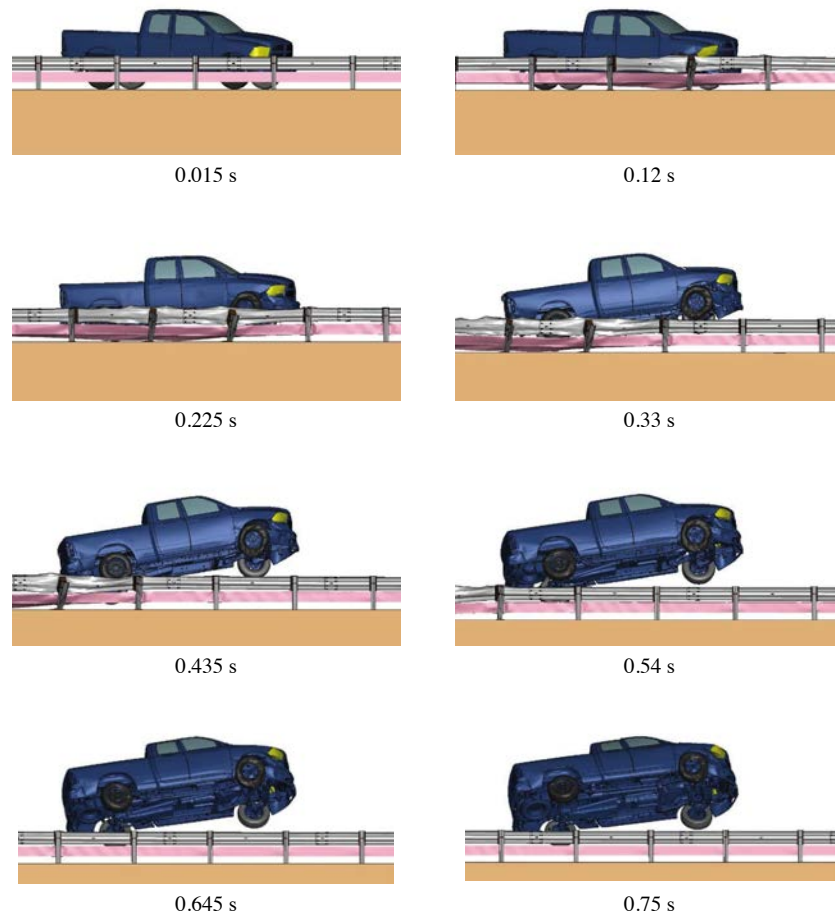


Figure 3.41. MGS with HSS10×10×¼ rub rail mounted 12 inches above grade – field-side view of MASH Test 3-11.



Figure 3.42. MGS with HSS10×10×¼ rub rail mounted 12 inches above grade – downstream view of MASH Test 3-11.

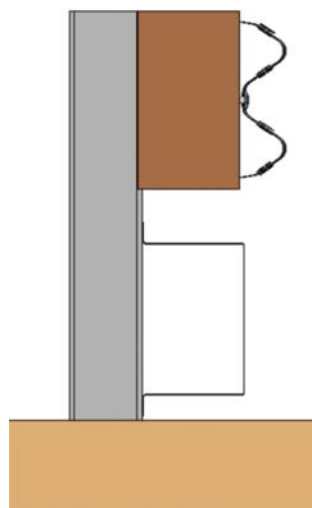


Figure 3.43. Profile view of MGS with 8HU12×135 rub rail mounted 8 inches above grade.

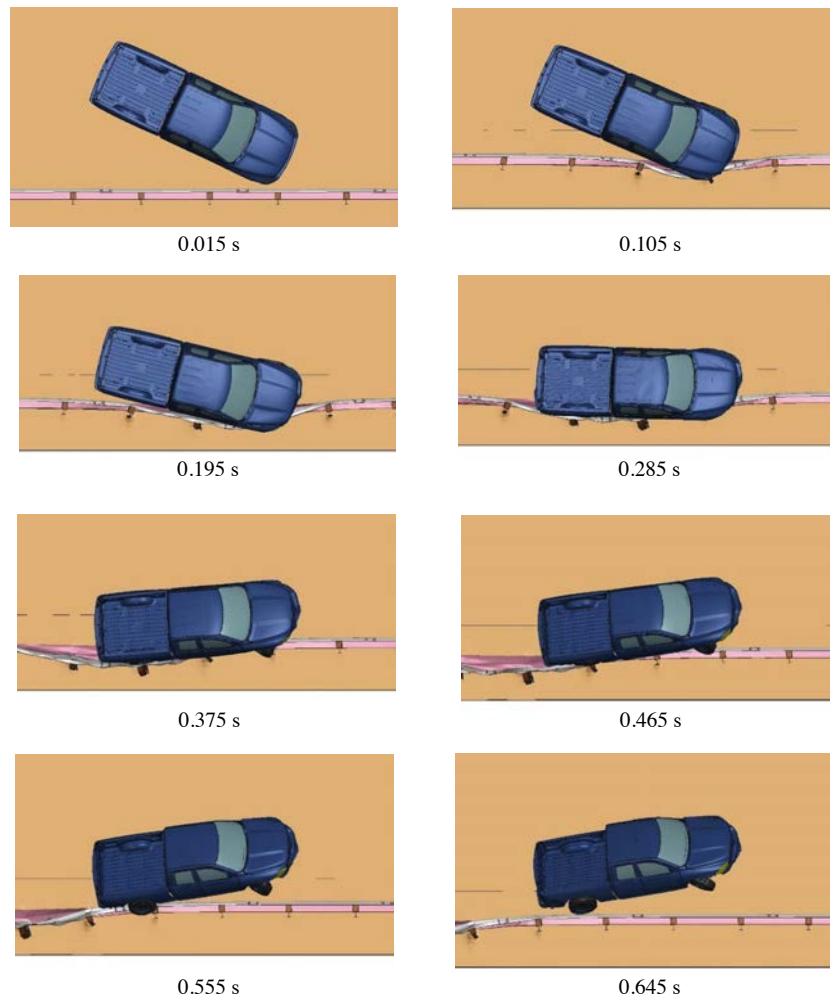


Figure 3.44. MGS with 8HU12×135 rub rail mounted 8 inches above grade – overhead view of MASH Test 3-11.

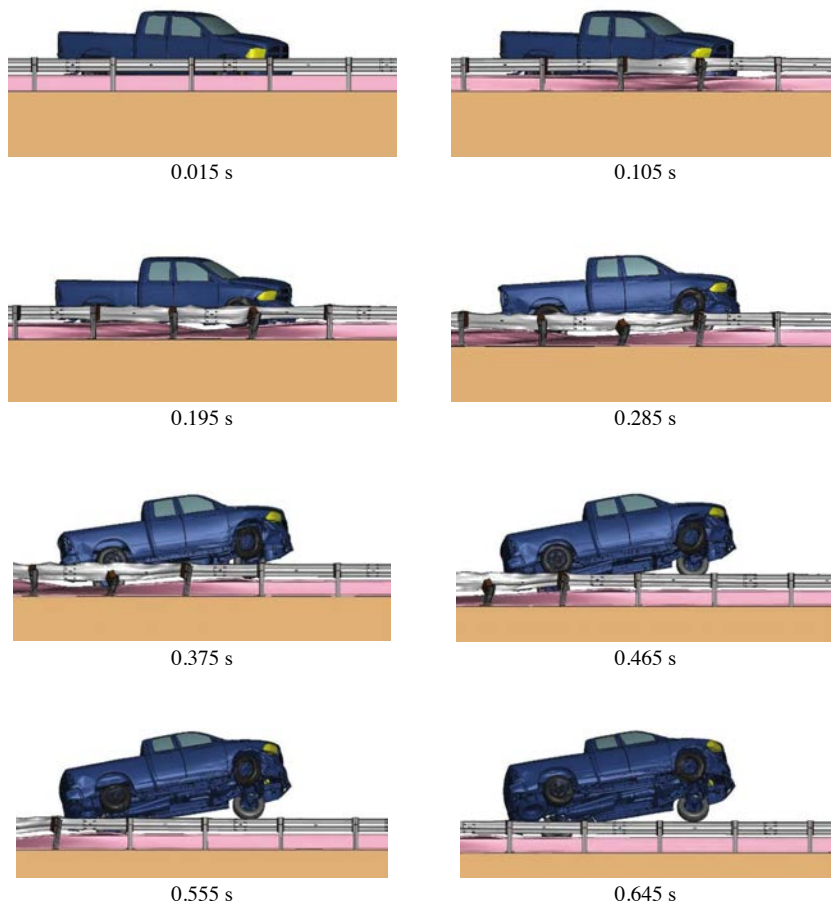


Figure 3.45. MGS with 8HU12×135 rub rail mounted 8 inches above grade – field-side view of MASH Test 3-11.



Figure 3.46. MGS with 8HU12×135 rub rail mounted 8 inches above grade – downstream view of MASH Test 3-11.

10HU5×075 Rub Rail Mounted 12 Inches Above Grade

The baseline MGS model was modified with the inclusion of a 10HU5×075 rub rail mounted 12 inches above grade as shown in Figure 3.47. A full-scale dynamic simulation for MASH Test 3-11 was performed on this system configuration.

MASH Test 3-11 Simulation

Figure 3.48, Figure 3.49, and Figure 3.50 show the sequential frames of MASH Test 3-11 on MGS with 10HU5×075 Rub Rail mounted 12 inches above grade. In this simulation, the maximum dynamic deflection was 31.5 inches, the working width was 45.6 inches, and the working width height was 22.7 inches. The OIV was calculated to be 5.3 m/s (preferred limit is 9.1 m/s). The RDA was calculated to be 13.7 g (preferred limit is 15.0 g). This configuration passed MASH Test 3-11 by successfully containing and redirecting the vehicle.

Backup Rail

C6×8.2 Backup Rail Mounted In-Line with W-beam

The baseline MGS model was modified with the inclusion of a C6×8.2 backup rail mounted in-line with a W-beam as shown in Figure 3.51. A full-scale dynamic simulation for MASH Test 3-11 was performed on this system configuration.

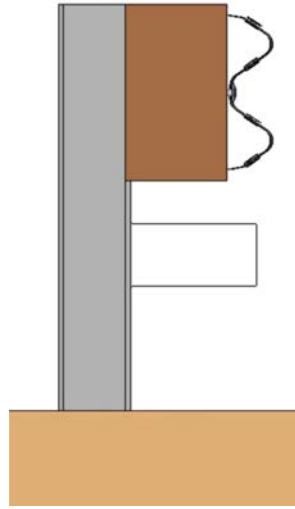


Figure 3.47. Profile view of MGS with 10HU5×075 rub rail mounted 12 inches above grade.

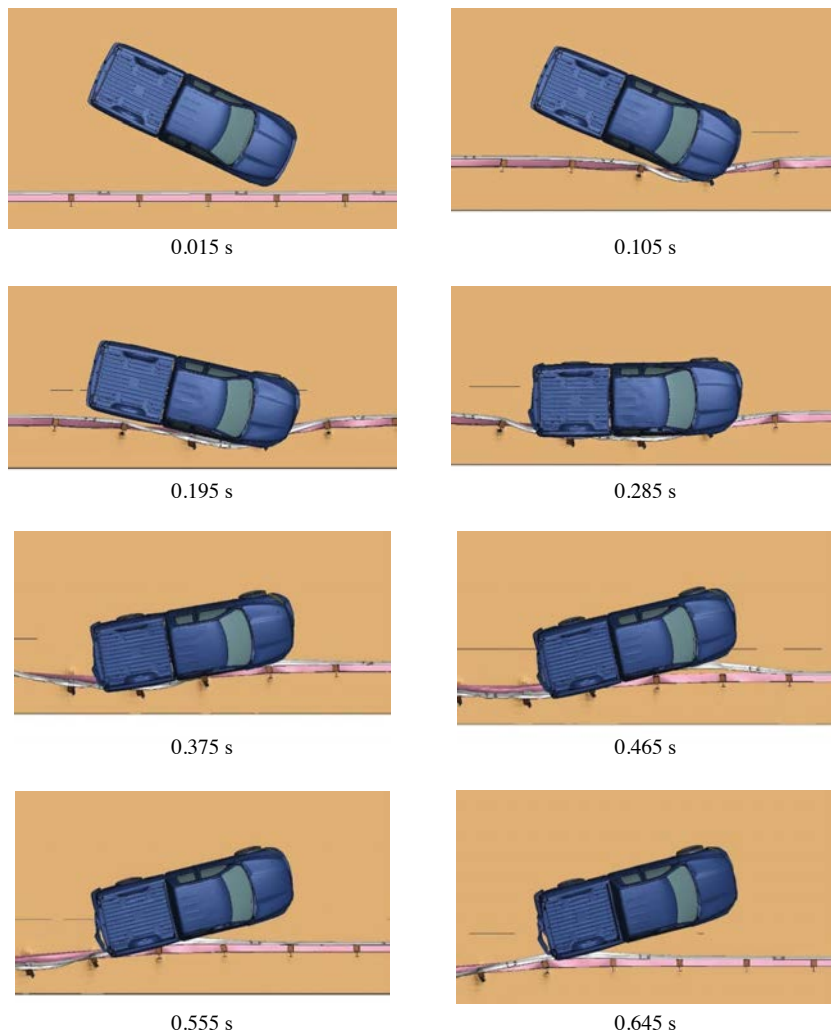


Figure 3.48. MGS with 10HU5×075 rub rail mounted 12 inches above grade – overhead view of MASH Test 3-11.

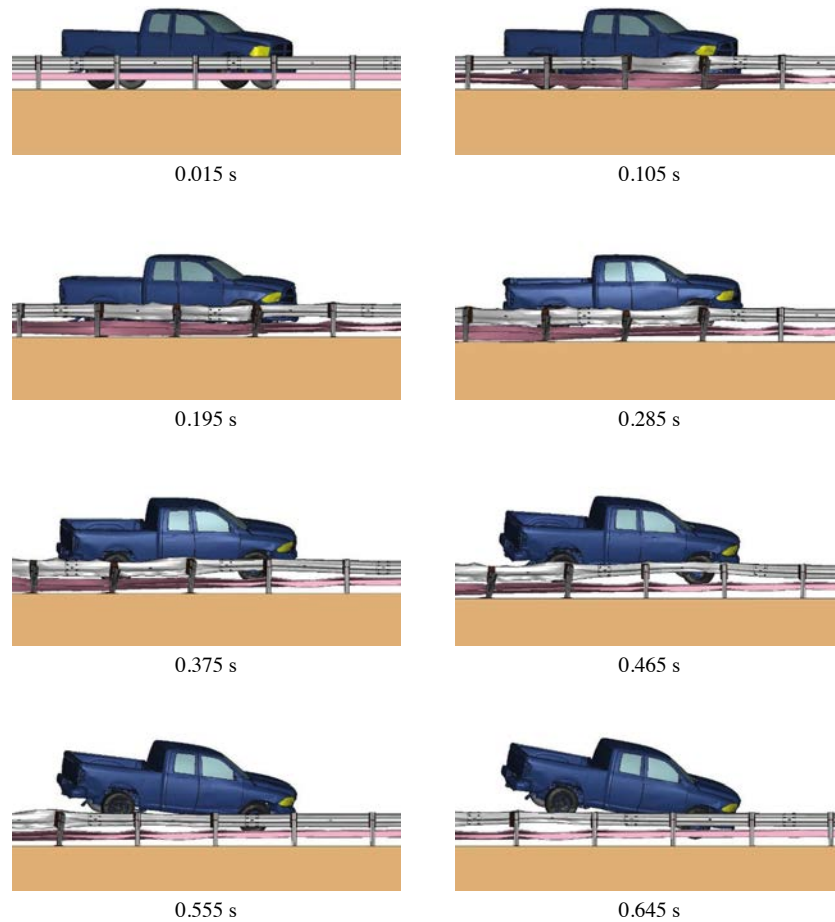


Figure 3.49. MGS with 10HU5×075 rub rail mounted 12 inches above grade – field-side view of MASH Test 3-11.



Figure 3.50. MGS with 10HU5×075 rub rail mounted 12 inches above grade – downstream view of MASH Test 3-11.

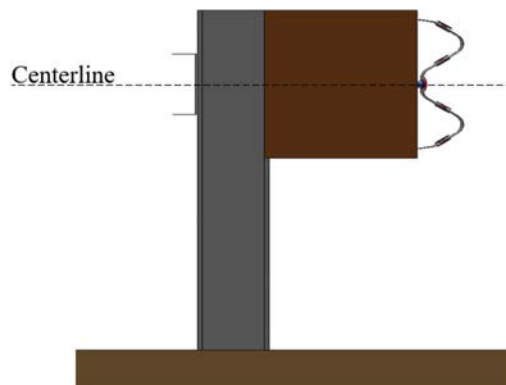


Figure 3.51. Profile view of MGS with C6×8.2 backup rail mounted in-line with W-beam.

MASH Test 3-11 Simulation

Figure 3.52 shows the sequential frames of MASH Test 3-11 on MGS with a C6×8.2 backup rail mounted in-line with the W-beam. In this simulation, the maximum dynamic deflection was 36.4 inches. The OIV was calculated to be 7.2 m/s (preferred limit is 9.1 m/s). The RDA was calculated to be 15.9 g (maximum limit is 20.49 g). This configuration passed MASH Test 3-11 by successfully containing and redirecting the vehicle.

C6×8.2 Backup Rail Mounted 17.5 Inches Above Grade

The baseline MGS model was modified with the inclusion of a C6×8.2 backup rail mounted 17.5 inches above grade as shown in Figure 3.53. A full-scale dynamic simulation for MASH Test 3-11 was performed on this system configuration.

MASH Test 3-11 Simulation

Figure 3.54 shows the sequential frames of MASH Test 3-11 on MGS with a C6×8.2 backup rail mounted 17.5 inches above grade. This configuration failed MASH Test 3-11 because the vehicle exhibited rollover after exiting the system.

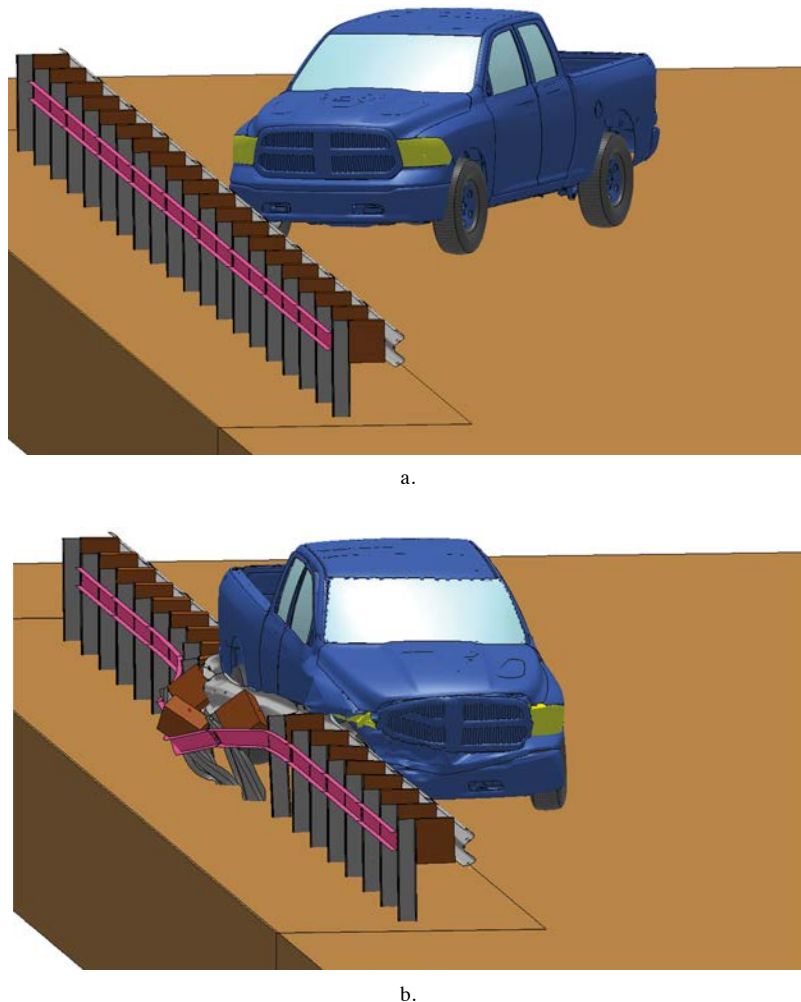


Figure 3.52. MGS with C6×8.2 backup rail mounted in-line with W-beam – isometric view of MASH Test 3-11.

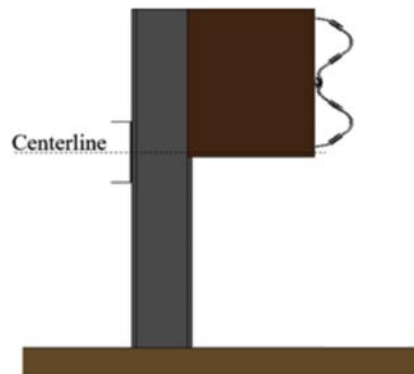
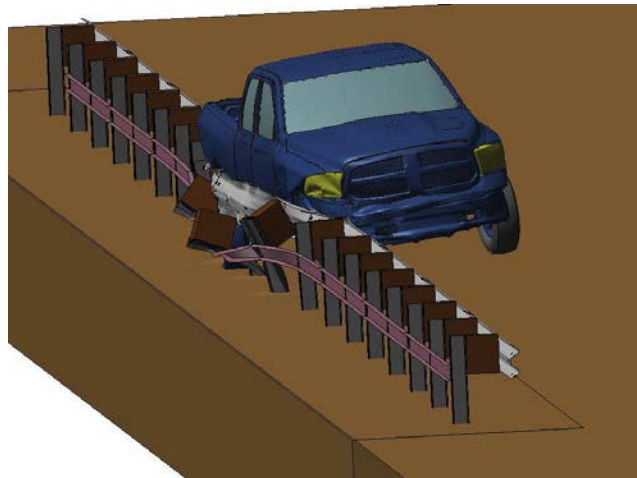
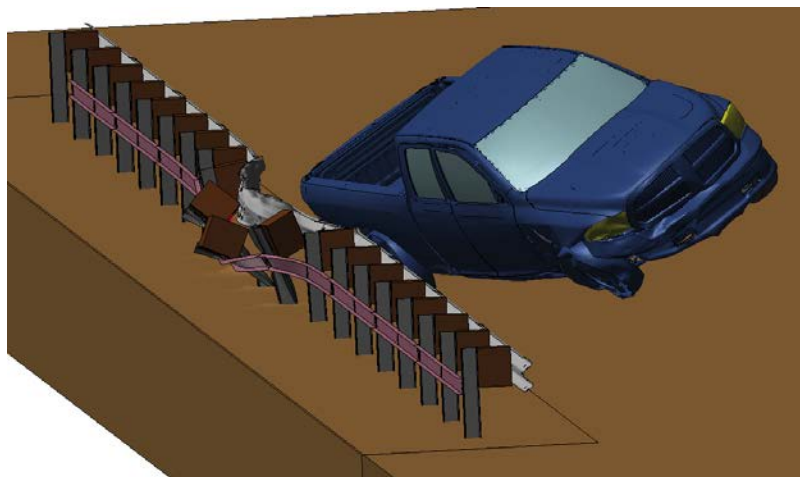


Figure 3.53. Profile view of MGS with C6×8.2 backup rail mounted 17.5 inches above grade.



a.



b.

Figure 3.54. MGS with C6×8.2 backup rail mounted 17.5 inches above grade – isometric view of MASH Test 3-11.

C6×8.2 Backup Rail Mounted 12 Inches Above Grade

The baseline MGS model was modified with the inclusion of a C6×8.2 backup rail mounted 12 inches above grade as shown in Figure 3.55. A full-scale dynamic simulation for MASH Test 3-11 was performed on this system configuration.

MASH Test 3-11 Simulation

Figure 3.56 and Figure 3.57 show the sequential frames of MASH Test 3-11 on MGS with a C6×8.2 backup rail mounted 12 inches above grade. In this simulation, the maximum dynamic deflection was 38.8 inches, the working width was 43.7 inches, and the working width height was 64.3 inches. The OIV was calculated to be 4.9 m/s (preferred limit is 9.1 m/s). The RDA was calculated to be 10.1 g (preferred limit is 15.0 g). This configuration passed MASH Test 3-11 by successfully containing and redirecting the vehicle.

HSS4×4×¼ Backup Rail Mounted 17.5 Inches Above Grade

The baseline MGS model was modified with the inclusion of an HSS4×4×¼ backup rail mounted 17.5 inches above grade as shown in Figure 3.58. A full-scale dynamic simulation for MASH Test 3-11 was performed on this system configuration.

MASH Test 3-11 Simulation

Figure 3.59 and Figure 3.60 show the sequential frames of MASH Test 3-11 on MGS with an HSS4×4×¼ backup rail system mounted 17.5 inches above grade. In this simulation, the maximum dynamic deflection was 31.1 inches, the working width was 36.7 inches, and the working width height was 33.4 inches. The OIV was calculated to be 7.1 m/s (preferred limit is 9.1 m/s). The RDA was calculated to be 13.7 g (preferred limit is 15.0 g). This configuration passed MASH Test 3-11 by successfully containing and redirecting the vehicle.

HSS4×4×¼ Backup Rail Mounted 12 Inches Above Grade

The baseline model was modified with the inclusion of an HSS4×4×¼ backup rail mounted 12 inches above grade as shown in Figure 3.61. A full-scale dynamic simulation for MASH Test 3-11 was performed on this system configuration.

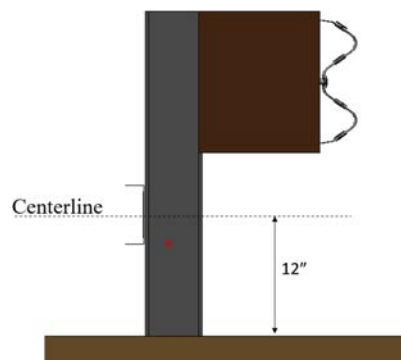
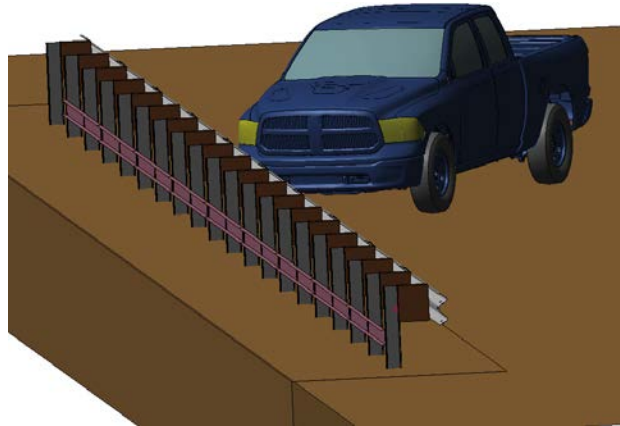
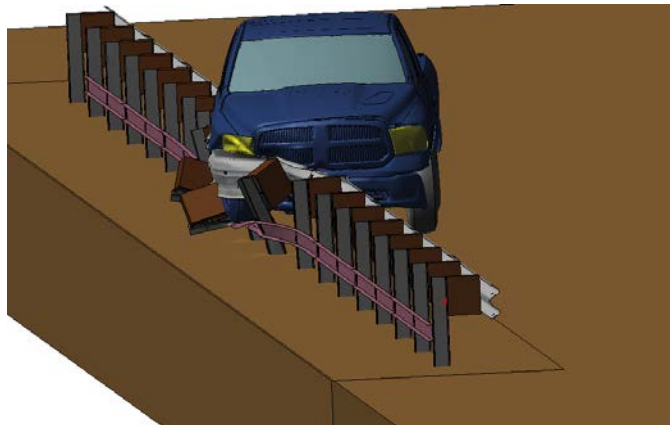


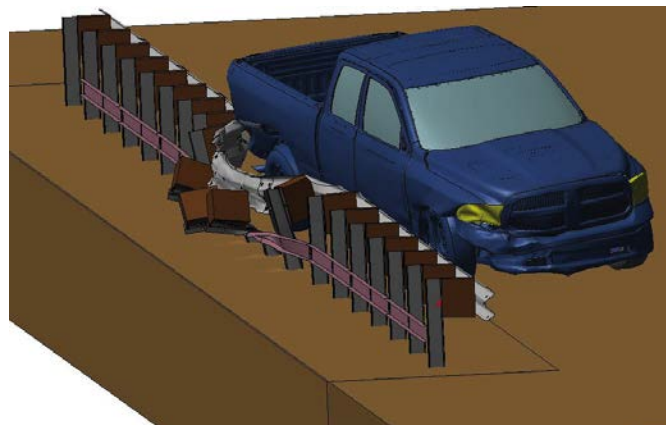
Figure 3.55. Profile view of MGS with C6×8.2 backup rail mounted 12 inches above grade.



a.

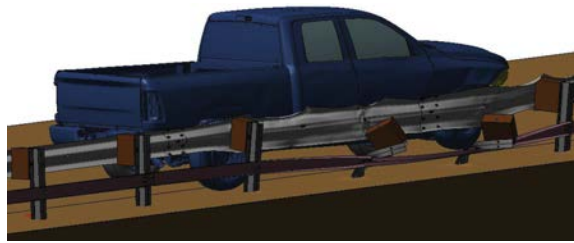


b.



c.

Figure 3.56. MGS with C6×8.2 backup rail mounted 12 inches above grade – isometric view of MASH Test 3-11.



a.



b.

Figure 3.57. MGS with C6×8.2 backup rail mounted 12 inches above grade – additional views of MASH Test 3-11 at approximate maximum deflection.

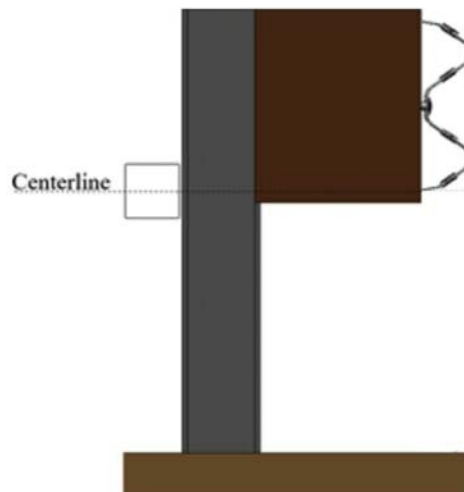


Figure 3.58. Profile view of MGS with HSS4×4×¼ backup rail mounted 17.5 inches above grade.

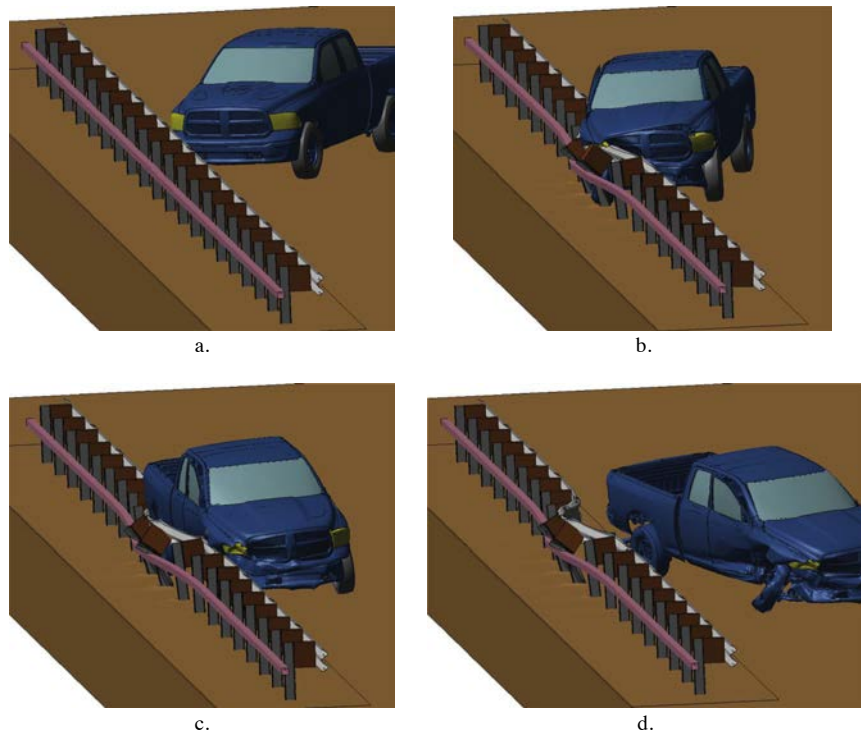


Figure 3.59. MGS with HSS4×4×¼ backup rail mounted 17.5 inches above grade – isometric view of MASH Test 3-11.

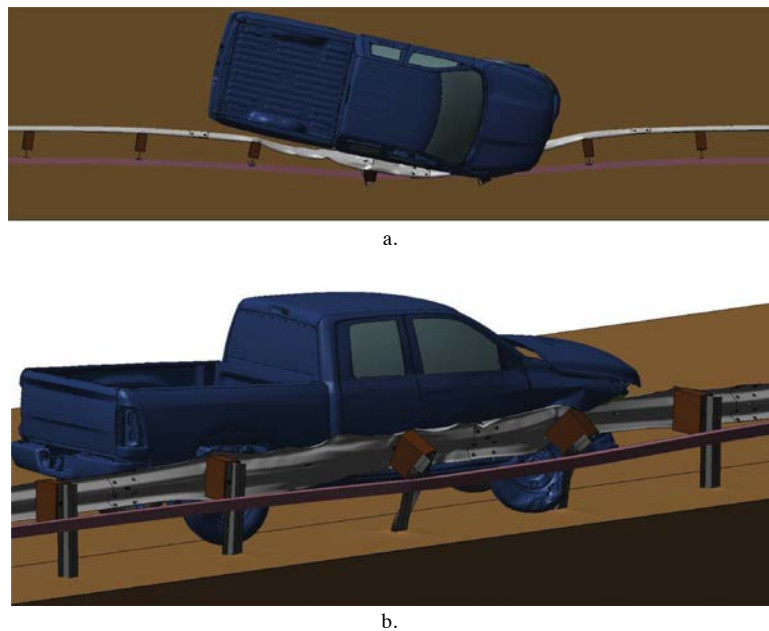


Figure 3.60. MGS with HSS4×4×¼ backup rail mounted 17.5 inches above grade – additional views of MASH Test 3-11 at maximum deflection.

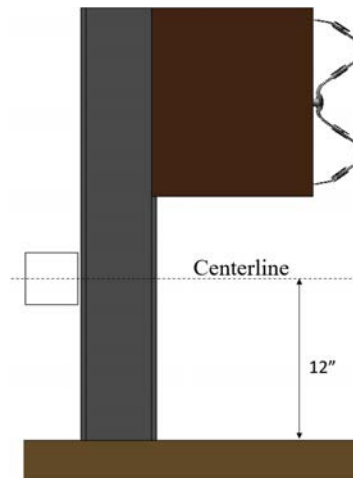


Figure 3.61. Profile view of MGS with HSS4×4× $\frac{1}{4}$ backup rail mounted 12 inches above grade.

MASH Test 3-11 Simulation

Figure 3.62 and Figure 3.63 show the sequential frames of MASH Test 3-11 on MGS with an HSS4×4× $\frac{1}{4}$ backup rail mounted 12 inches above grade. This configuration failed MASH Test 3-11 because the vehicle exhibited rollover after exiting the system.

HSS4×4× $\frac{1}{4}$ Backup Rail Mounted In-Line with W-Beam

The baseline MGS model was modified with the inclusion of an HSS4×4× $\frac{1}{4}$ backup rail mounted in-line with the W-beam as shown in Figure 3.64. Full-scale dynamic simulations for MASH Tests 3-11 and 3-10 were performed on this system configuration.

MASH Test 3-11 Simulation

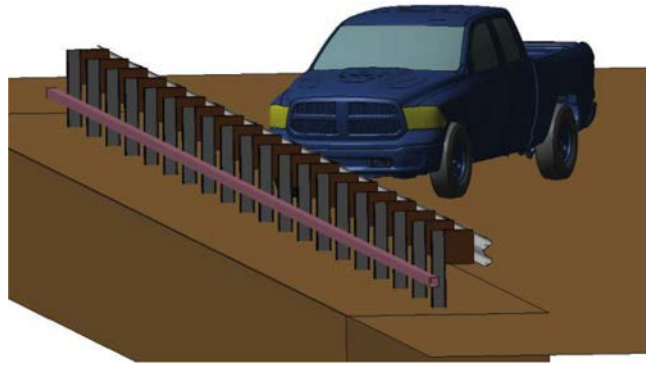
Figure 3.65, Figure 3.66, and Figure 3.67 show the sequential frames of MASH Test 3-11 on MGS with an HSS4×4× $\frac{1}{4}$ backup rail mounted in-line with the W-beam. In this simulation, the maximum dynamic deflection was 33.7 inches, the working width was 38.9 inches, and the working width height was 31.8 inches. The OIV was calculated to be 6.2 m/s (preferred limit is 9.1 m/s). The RDA was calculated to be 18.2 g (maximum limit is 20.49 g). This configuration passed MASH Test 3-11 by successfully containing and redirecting the vehicle.

MASH Test 3-10 Simulation

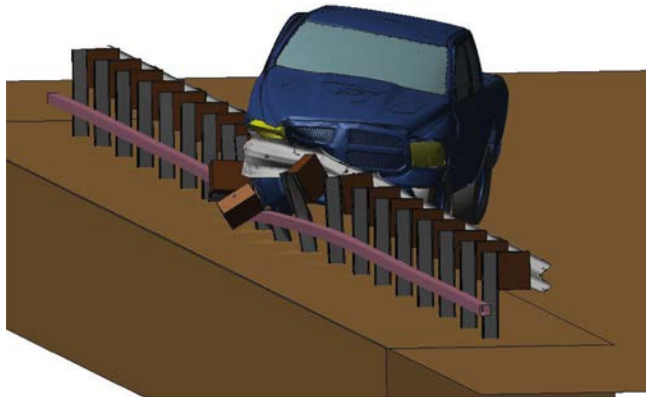
Figure 3.68, Figure 3.69, and Figure 3.70 show the sequential frames of MASH Test 3-10 on MGS with HSS4×4× $\frac{1}{4}$ backup rail mounted in-line with W-beam. The OIV was calculated to be 9.1 m/s (maximum limit is 12.2 m/s). The RDA was calculated to be 14.3 g (preferred limit is 15.0 g). This configuration successfully passed MASH Test 3-10 by containing and redirecting the vehicle.

HSS5×5× $\frac{5}{16}$ Backup Rail Mounted In-Line with W-Beam

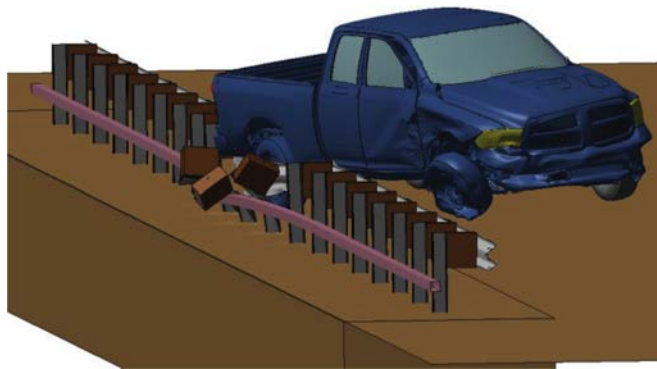
The baseline MGS model was modified with the inclusion of an HSS5×5× $\frac{5}{16}$ backup rail mounted in-line with the W-beam as shown in Figure 3.71. A full-scale dynamic simulation for MASH Test 3-11 was performed on this system configuration.



a.



b.

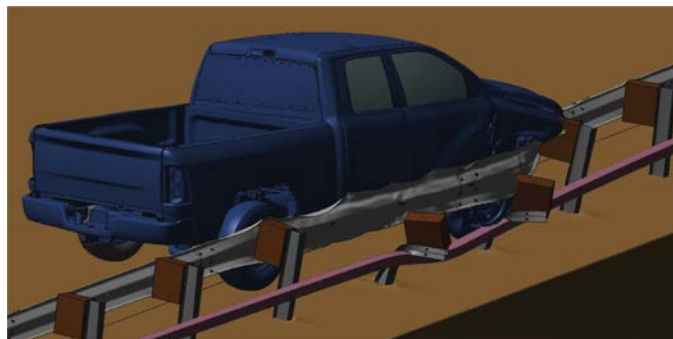


c.



d.

Figure 3.62. MGS with HSS4×4×¼ backup rail mounted 12 inches above grade – isometric views of MASH Test 3-11.



a.



b.

Figure 3.63. MGS with HSS4×4×¼ backup rail mounted 12 inches above grade – additional views of MASH Test 3-11 at maximum deflection.

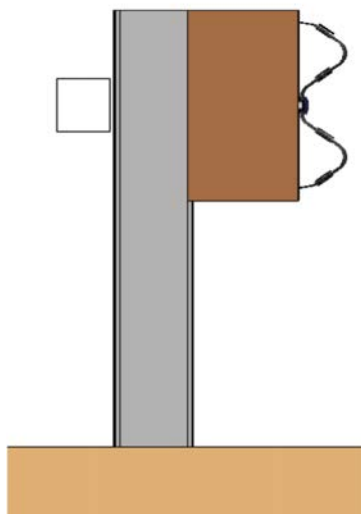


Figure 3.64. Profile view of MGS with HSS4×4×¼ backup rail mounted in-line with W-beam.

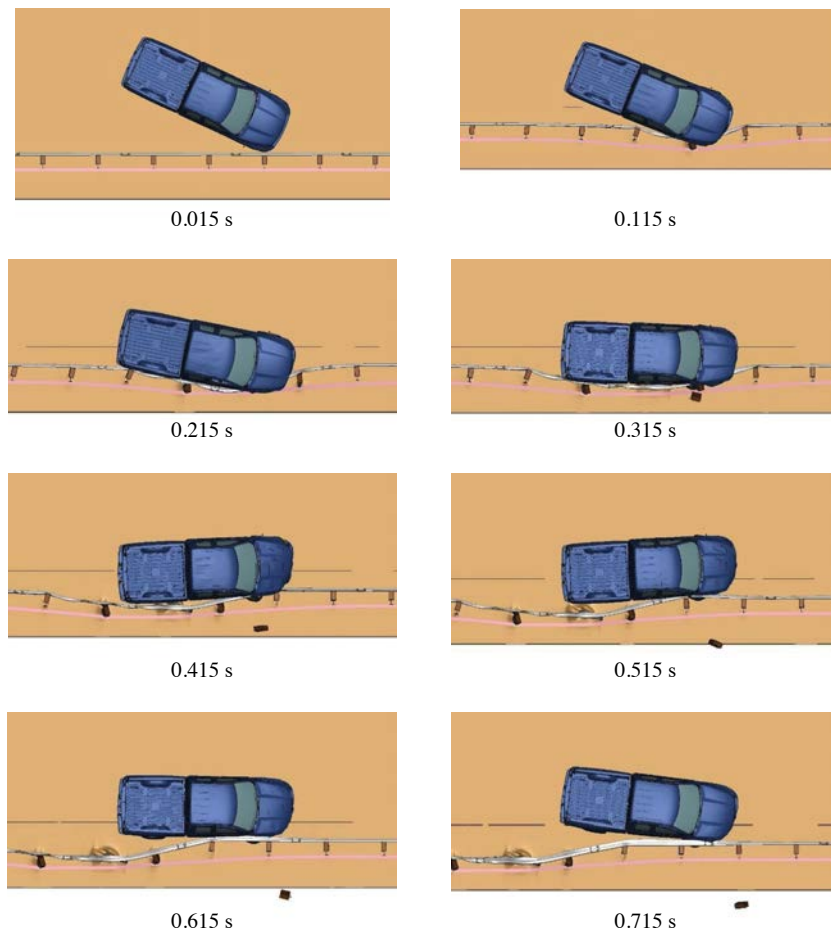


Figure 3.65. MGS with HSS4×4×¼ backup rail mounted in-line with W-beam – overhead view of MASH Test 3-11.

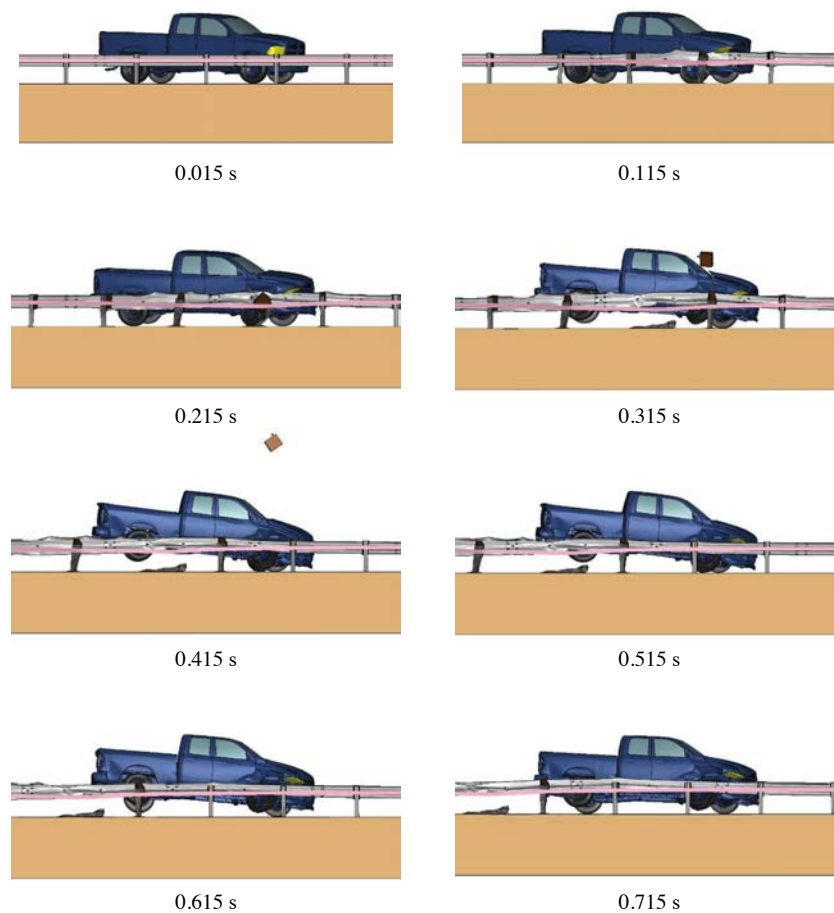


Figure 3.66. MGS with HSS4×4×¼ backup rail mounted in-line with W-beam – field-side view of MASH Test 3-11.

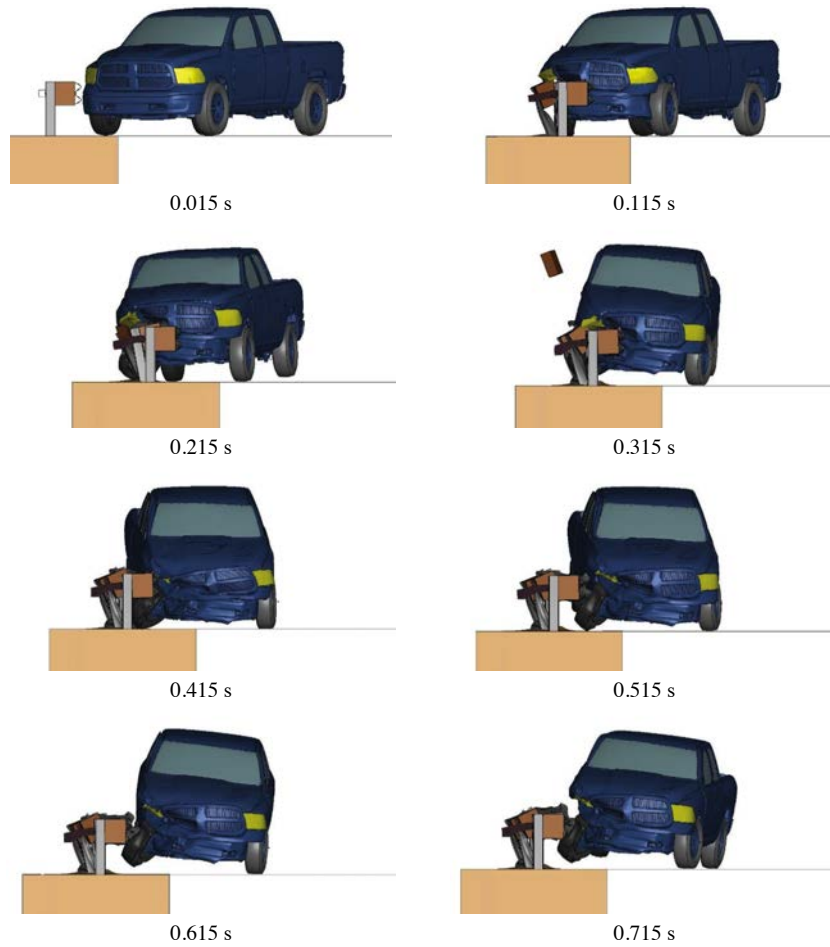


Figure 3.67. MGS with HSS4×4×¼ backup rail mounted in-line with W-beam – downstream view of MASH Test 3-11.

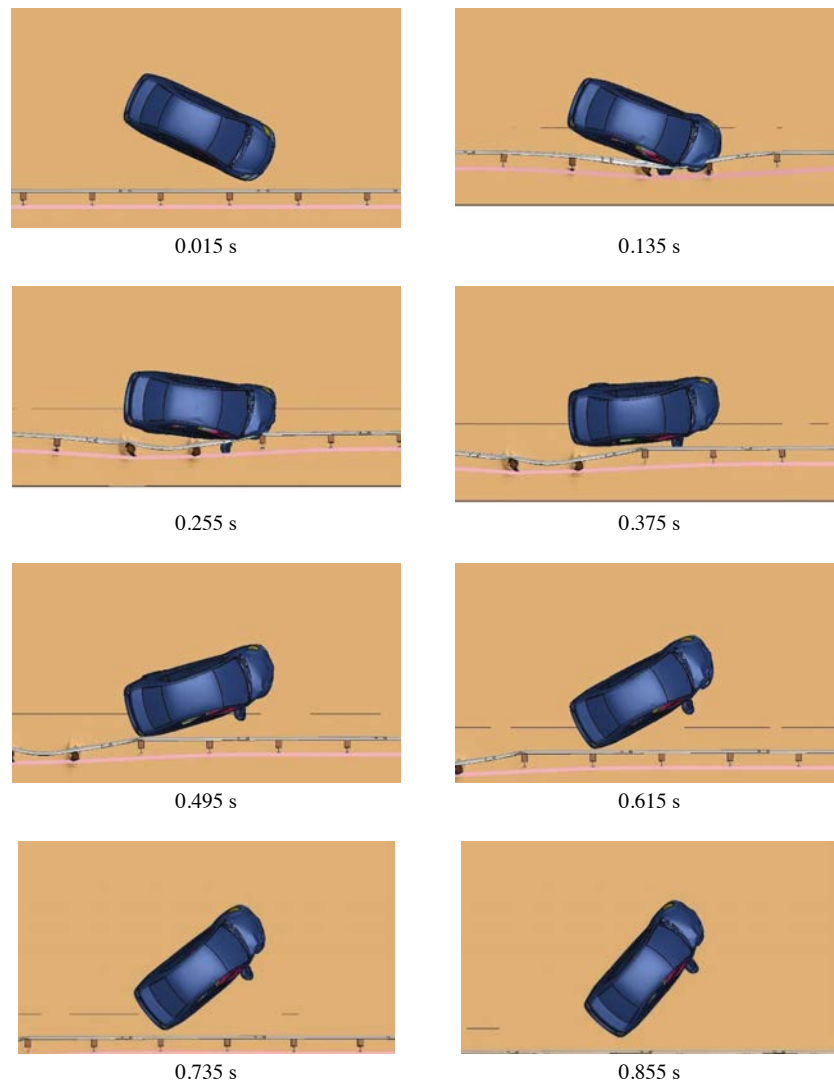


Figure 3.68. MGS with HSS4×4×¼ backup rail mounted in-line with W-beam – overhead view of MASH Test 3-10.

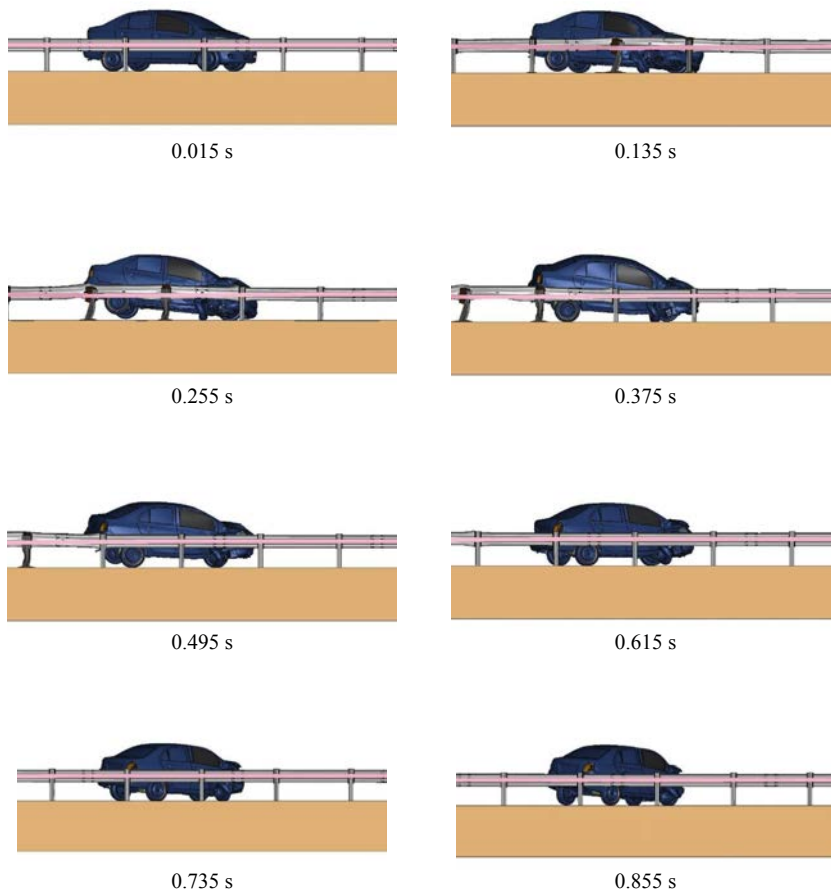


Figure 3.69. MGS with HSS4×4×¼ backup rail mounted in-line with W-beam – field-side view of MASH Test 3-10.



Figure 3.70. MGS with HSS4×4×¼ backup rail mounted in-line with W-beam – downstream view of MASH Test 3-10.

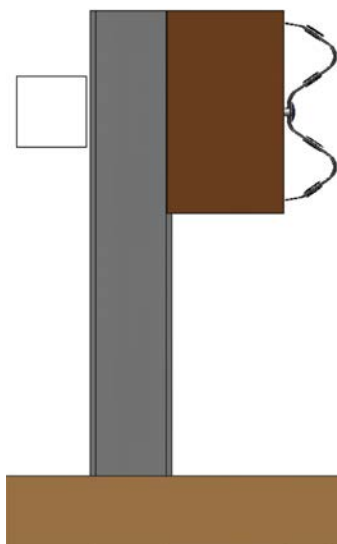


Figure 3.71. Profile view of MGS with HSS5×5×5/16 backup rail mounted in-line with W-beam.

MASH Test 3-11 Simulation

Figure 3.72, Figure 3.73, and Figure 3.74 show the sequential frames of MASH Test 3-11 on MGS with HSS5×5× $\frac{5}{16}$ backup rail mounted in-line with W-beam. This configuration failed MASH Test 3-11 because the vehicle exhibited rollover after exiting the system.

HSS6×6× $\frac{3}{8}$ Backup Rail Mounted In-Line with W-Beam

The baseline MGS model was modified with the inclusion of an HSS6×6× $\frac{3}{8}$ backup rail mounted in-line with the W-beam as shown in Figure 3.75. Full-scale dynamic simulations for MASH Tests 3-11 and 3-10 were performed on this system configuration.

MASH Test 3-11 Simulation

Figure 3.76, Figure 3.77, and Figure 3.78 show the sequential frames of MASH Test 3-11 on MGS with HSS6×6× $\frac{3}{8}$ backup rail mounted in-line with W-beam. In this simulation, the maximum dynamic deflection was 23.5 inches, the working width was 36.1 inches, and the working width height was 39.7 inches. The OIV was calculated to be 9.0 m/s (preferred limit is 9.1 m/s). The RDA was calculated to be 18.5 g (maximum limit is 20.49 g). This configuration passed MASH Test 3-11 by successfully containing and redirecting the vehicle.

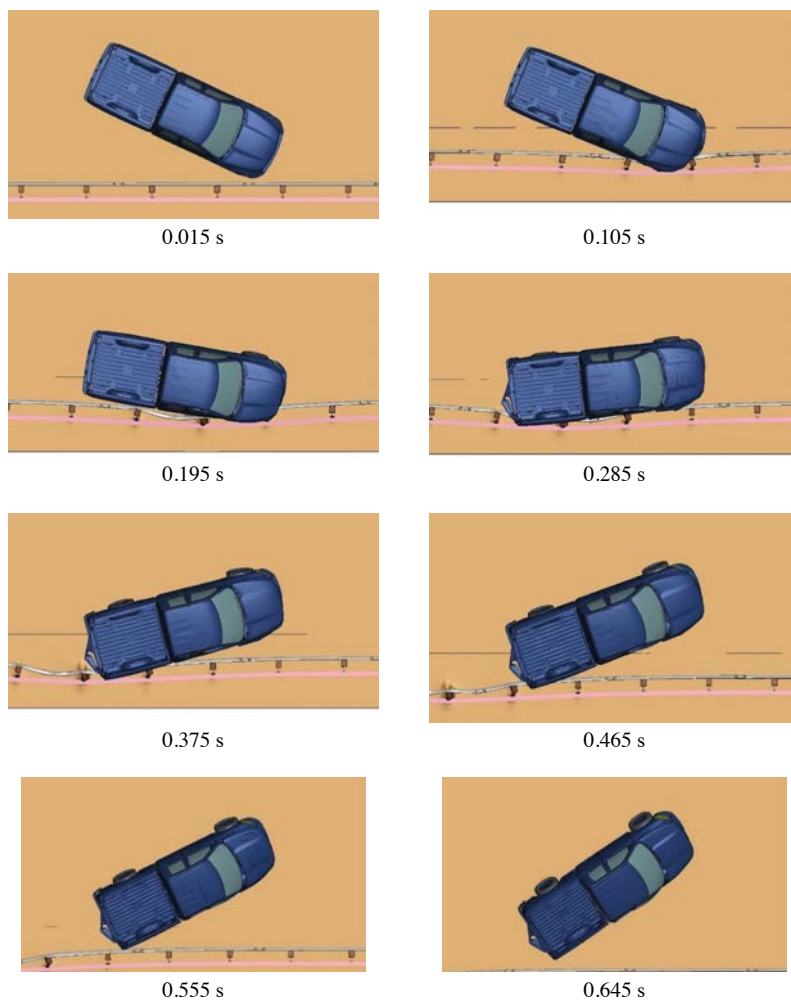


Figure 3.72. MGS with HSS5×5× $\frac{5}{16}$ mounted in-line with W-beam – overhead view of MASH Test 3-11.

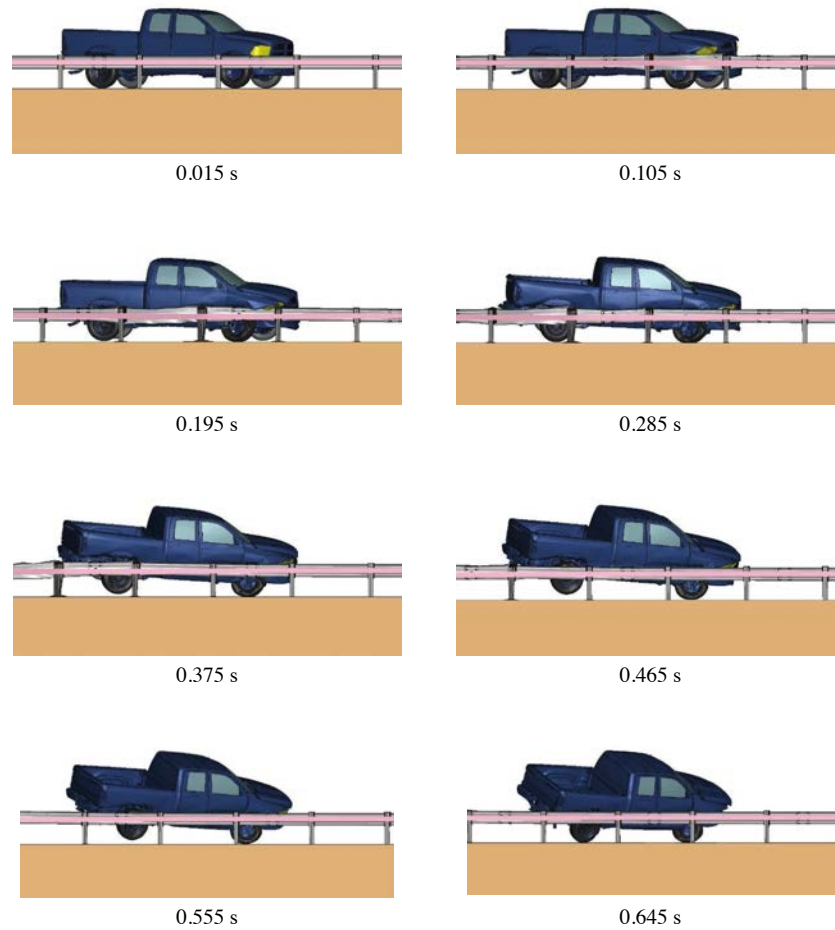


Figure 3.73. MGS with $HSS5 \times 5 \times \frac{5}{16}$ mounted in-line with W-beam – field-side view of MASH Test 3-11.



Figure 3.74. MGS with $HSS5 \times 5 \times \frac{5}{16}$ mounted in-line with W-beam – downstream view of MASH Test 3-11.

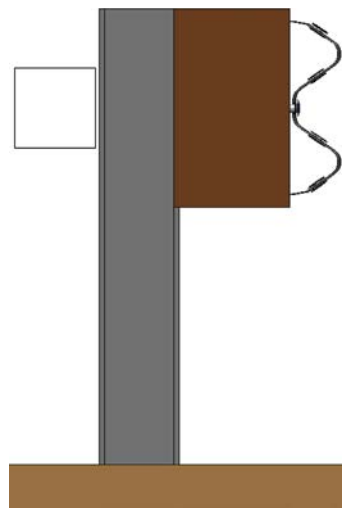


Figure 3.75. Profile view of MGS with $HSS6 \times 6 \times \frac{3}{8}$ backup rail mounted in-line with W-beam.

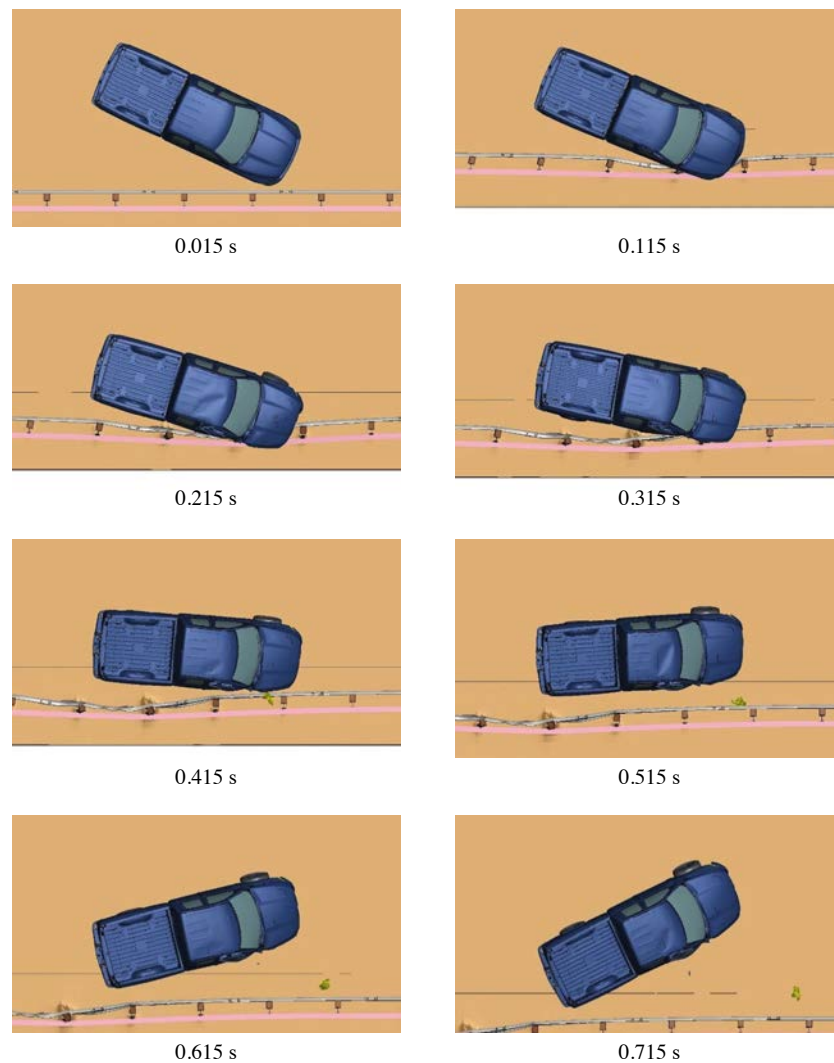


Figure 3.76. MGS with HSS6×6×³/₈ backup rail mounted in-line with W-beam – overhead view of MASH Test 3-11.

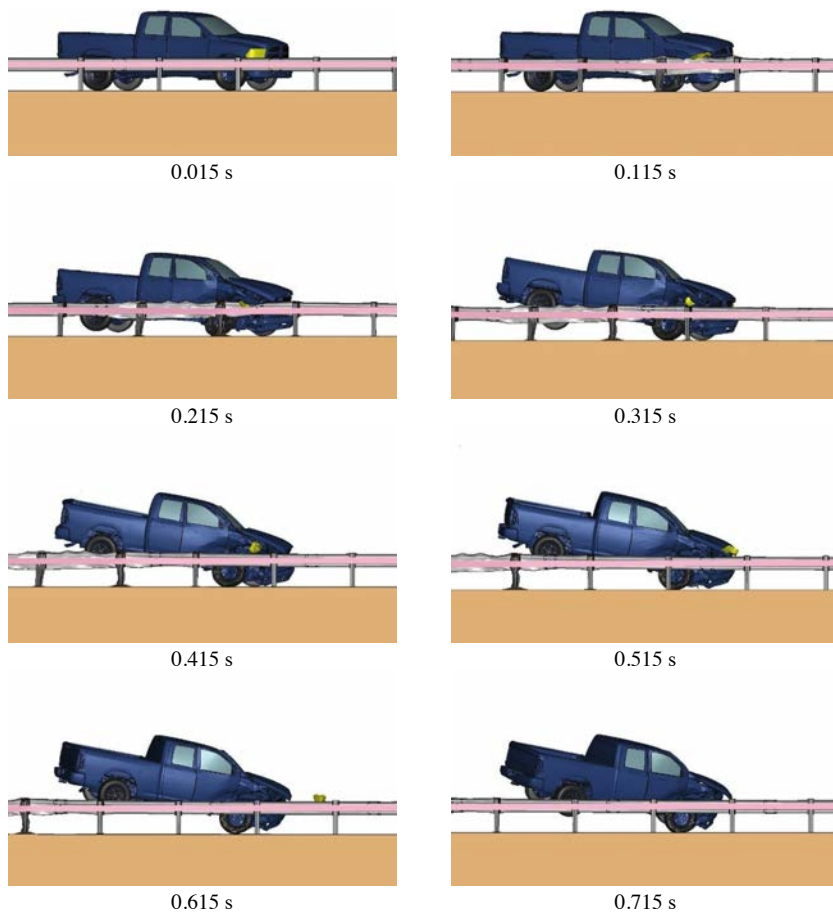


Figure 3.77. MGS with HSS6×6×³/₈ backup rail mounted in-line with W-beam – field-side view of MASH Test 3-11.

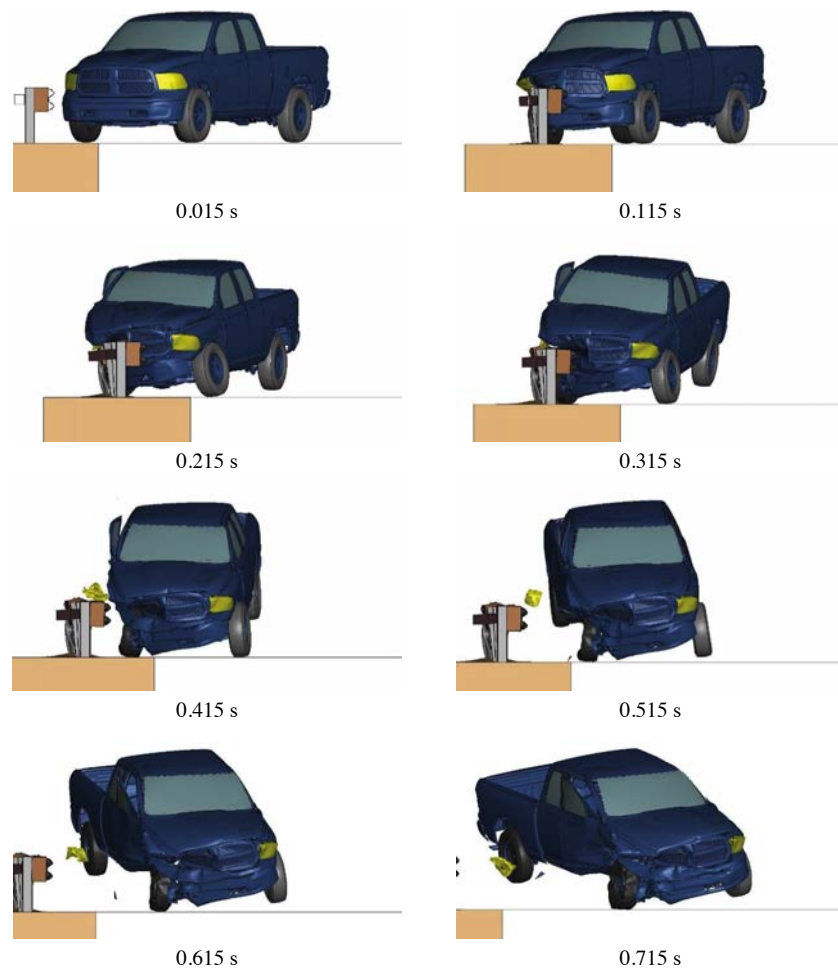


Figure 3.78. MGS with HSS6×6× $\frac{3}{8}$ backup rail mounted in-line with W-beam – downstream view of MASH Test 3-11.

MASH Test 3-10 Simulation

Figure 3.79, Figure 3.80, and Figure 3.81 show the sequential frames of MASH Test 3-10 on MGS with HSS6×6× $\frac{3}{8}$ backup rail mounted in-line with W-beam. The OIV was calculated to be 8.9 m/s (preferred limit is 9.1 m/s). The RDA was calculated to be 27.1 g (maximum limit is 20.49 g). This configuration failed MASH Test 3-10 by failing to meet the maximum RDA limit.

HSS10×10× $\frac{1}{4}$ Backup Rail Mounted In-Line with W-Beam

The baseline MGS model was modified with the inclusion of an HSS10×10× $\frac{1}{4}$ backup rail mounted in-line with the W-beam as shown in Figure 3.82. A full-scale dynamic simulation for MASH Test 3-11 was performed on this system configuration.

MASH Test 3-11 Simulation

Figure 3.83, Figure 3.84, and Figure 3.85 show the sequential frames of MASH Test 3-11 on MGS with HSS10×10× $\frac{1}{4}$ backup rail mounted in-line with W-beam. The OIV was calculated to be 8.7 m/s (preferred limit is 9.1 m/s). The RDA was calculated to be 21.0 g (maximum limit is 20.49 g). This configuration failed MASH Test 3-11 because it exceeded the RDA limit.

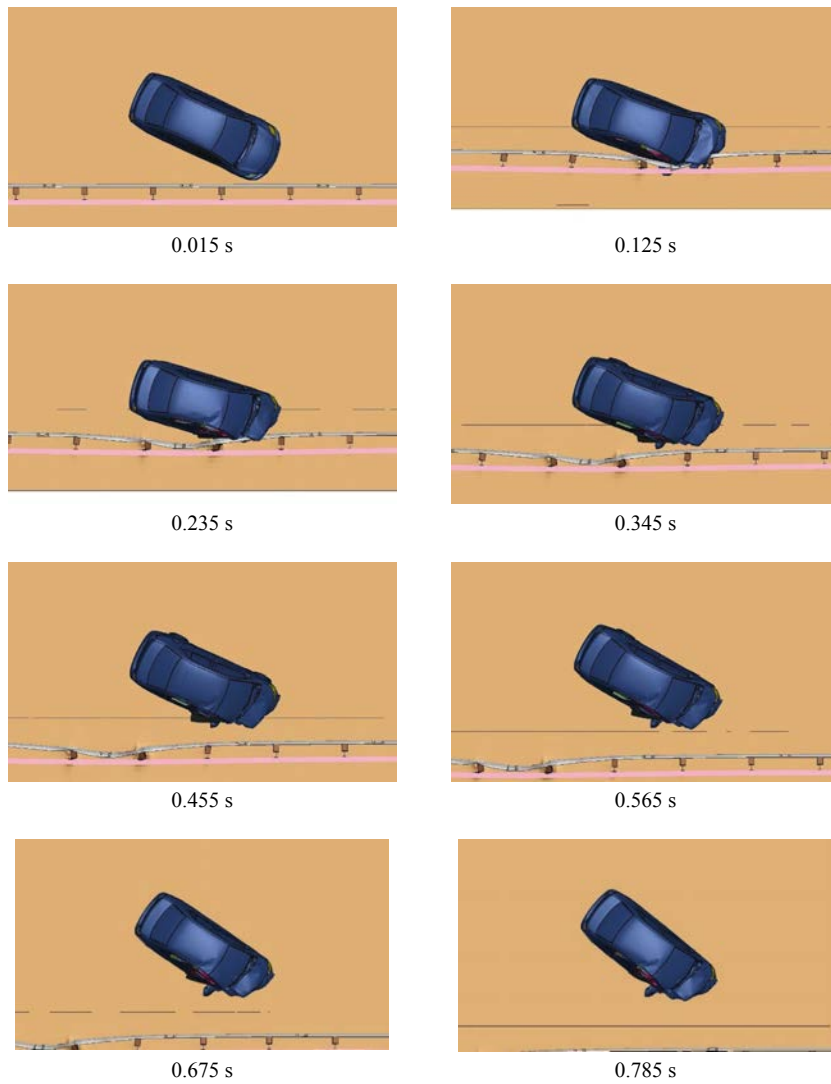


Figure 3.79. MGS with HSS6×6× $\frac{3}{8}$ backup rail mounted in-line with W-beam – overhead view of MASH Test 3-10.

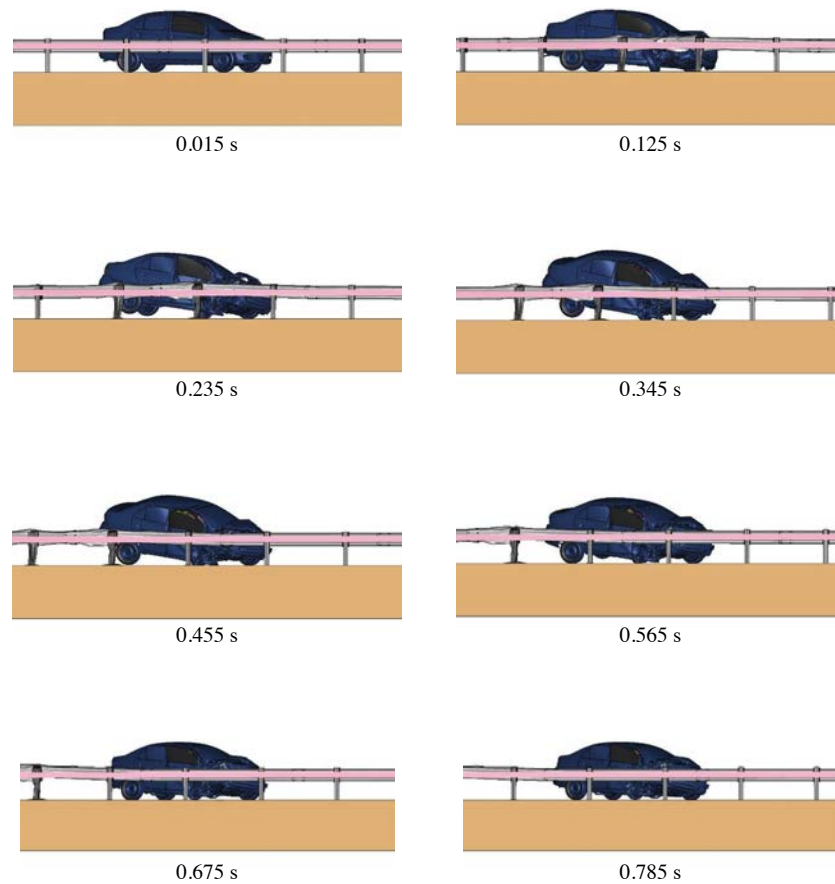


Figure 3.80. MGS with HSS6×6×³/₈ backup rail mounted in-line with W-beam – field-side view of MASH Test 3-10.

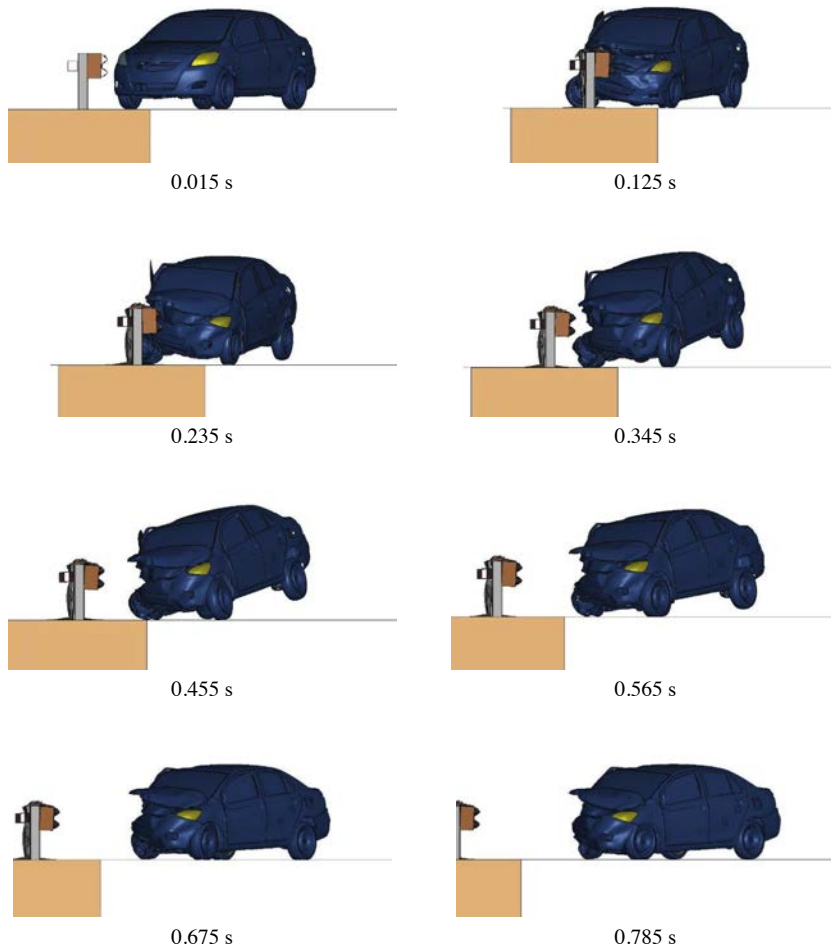


Figure 3.81. MGS with HSS6×6× $\frac{3}{8}$ backup rail mounted in-line with W-beam – downstream view of MASH Test 3-10.

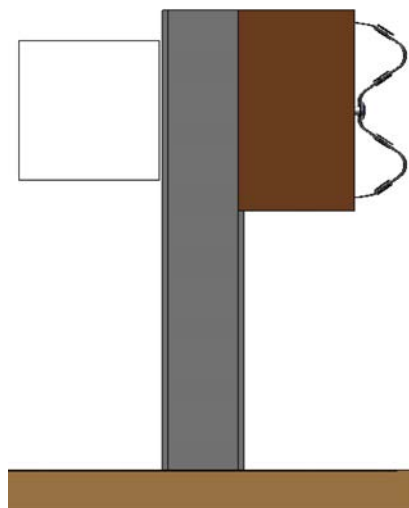


Figure 3.82. Profile view of MGS with HSS10×10× $\frac{1}{4}$ backup rail mounted in-line with W-beam.

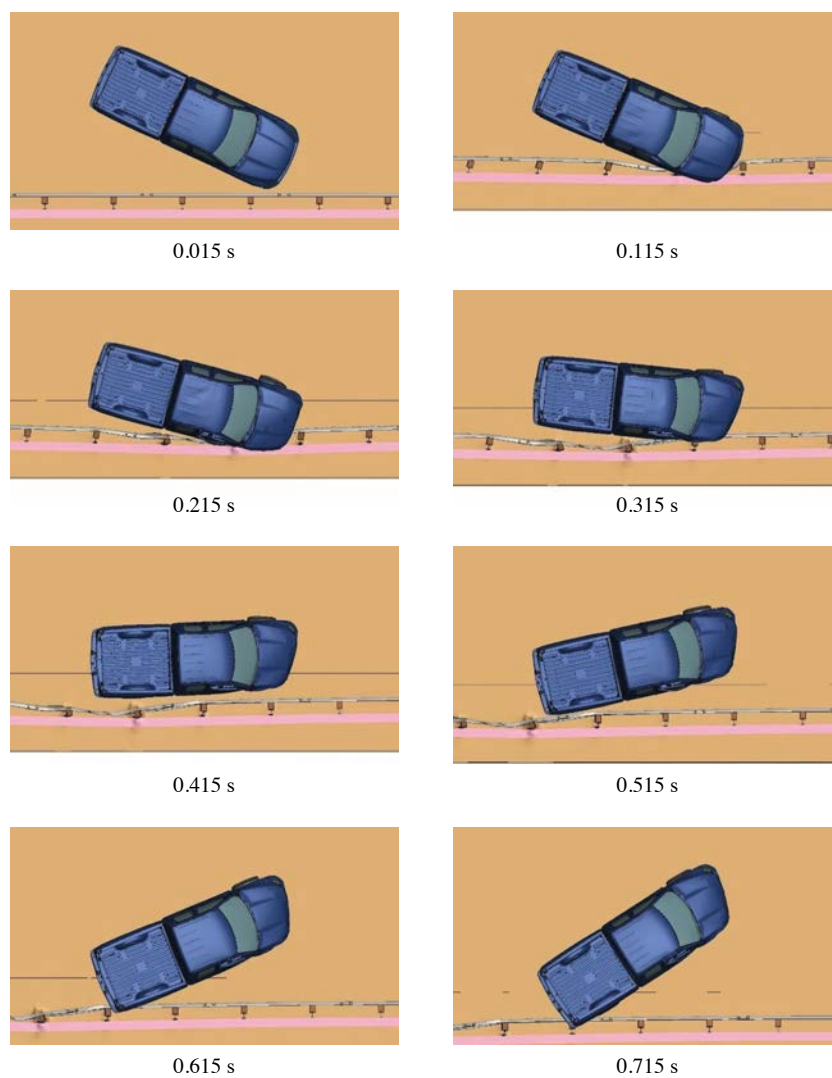


Figure 3.83. MGS with HSS10×10×¼ backup rail mounted in-line with W-beam – overhead view of MASH Test 3-11.

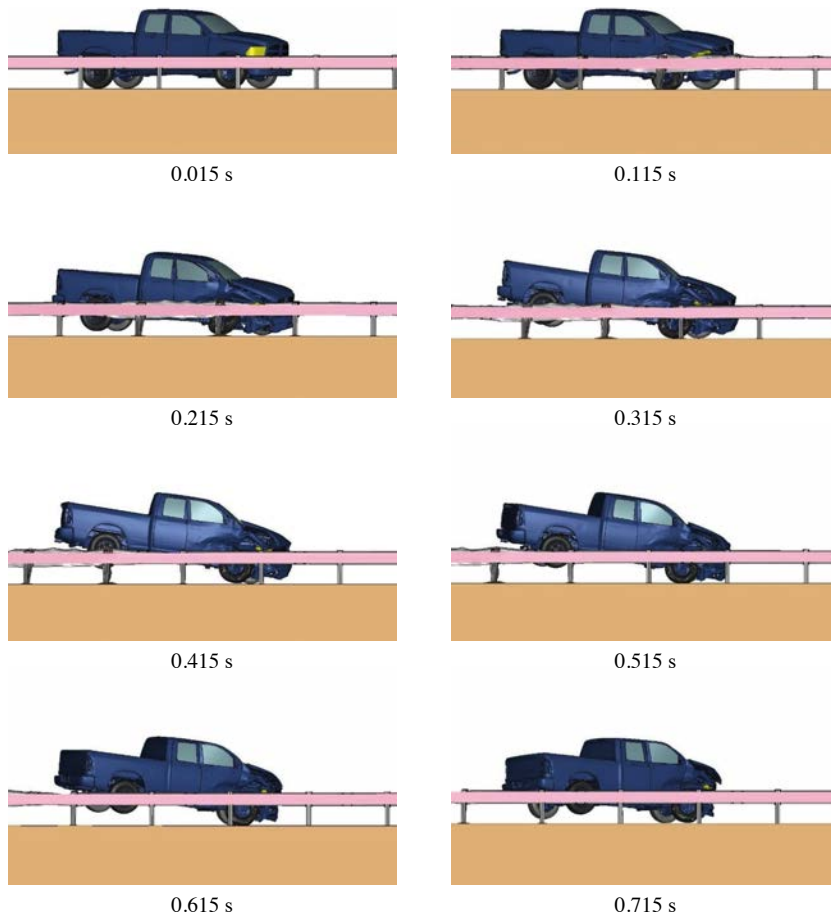


Figure 3.84. MGS with HSS10×10×¼ backup rail mounted in-line with W-beam – field-side view of MASH Test 3-11.

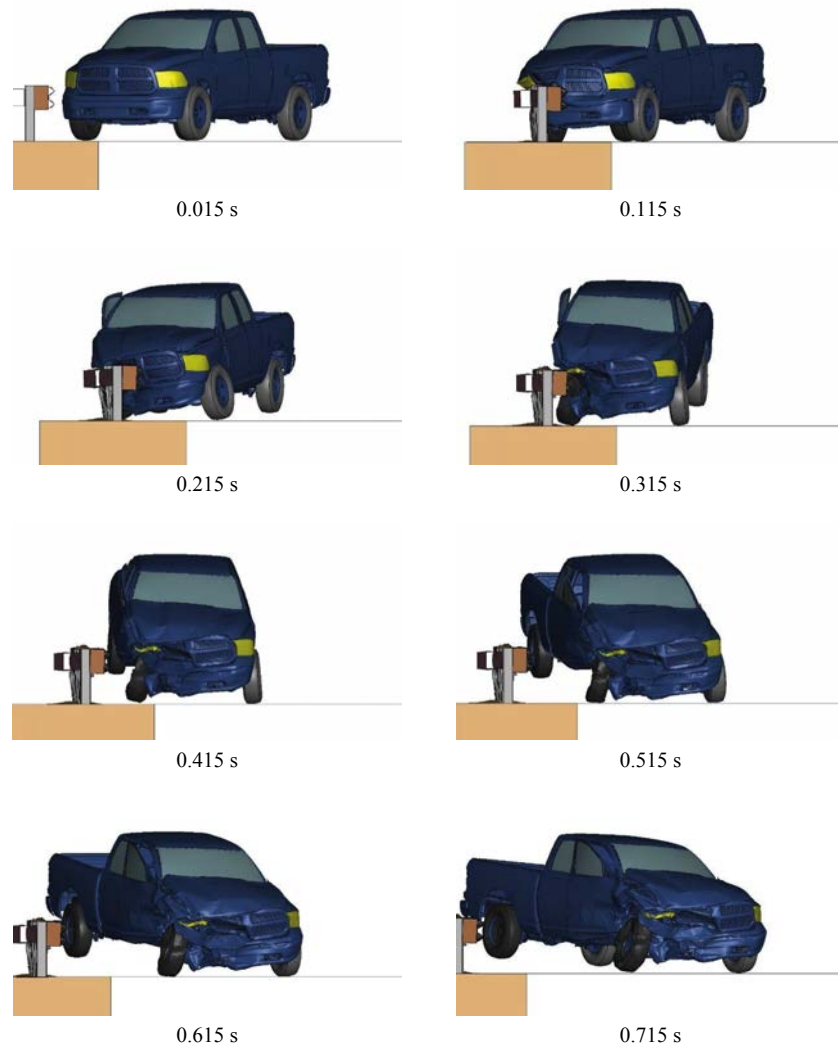


Figure 3.85. *MGS with HSS10×10×¼ backup rail mounted in-line with W-beam – downstream view of MASH Test 3-11.*

10HU5×075 Backup Rail Mounted In-Line with W-Beam

The baseline MGS model was modified with the inclusion of a 10HU5×075 backup rail mounted in-line with the W-beam as shown in Figure 3.86. A full-scale dynamic simulation for MASH Test 3-11 was performed on this system configuration.

MASH Test 3-11 Simulation

Figure 3.87, Figure 3.88, and Figure 3.89 show the sequential frames of MASH Test 3-11 on MGS with 10HU5×075 backup rail mounted in-line with W-beam. This configuration failed MASH Test 3-11 because the vehicle exhibited rollover after exiting the system.

8HU12×135 Backup Rail Mounted In-Line with W-Beam

The baseline MGS model was modified with the inclusion of an 8HU12x135 backup rail mounted in-line with the W-beam as shown in Figure 3.90. Full-scale dynamic simulations for MASH Test 3-11 and 3-10 were performed on this system configuration.

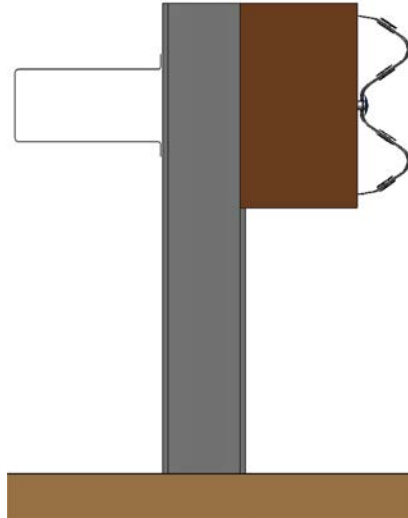


Figure 3.86. Profile view of MGS with 10HU5×075 backup rail mounted in-line with W-beam.

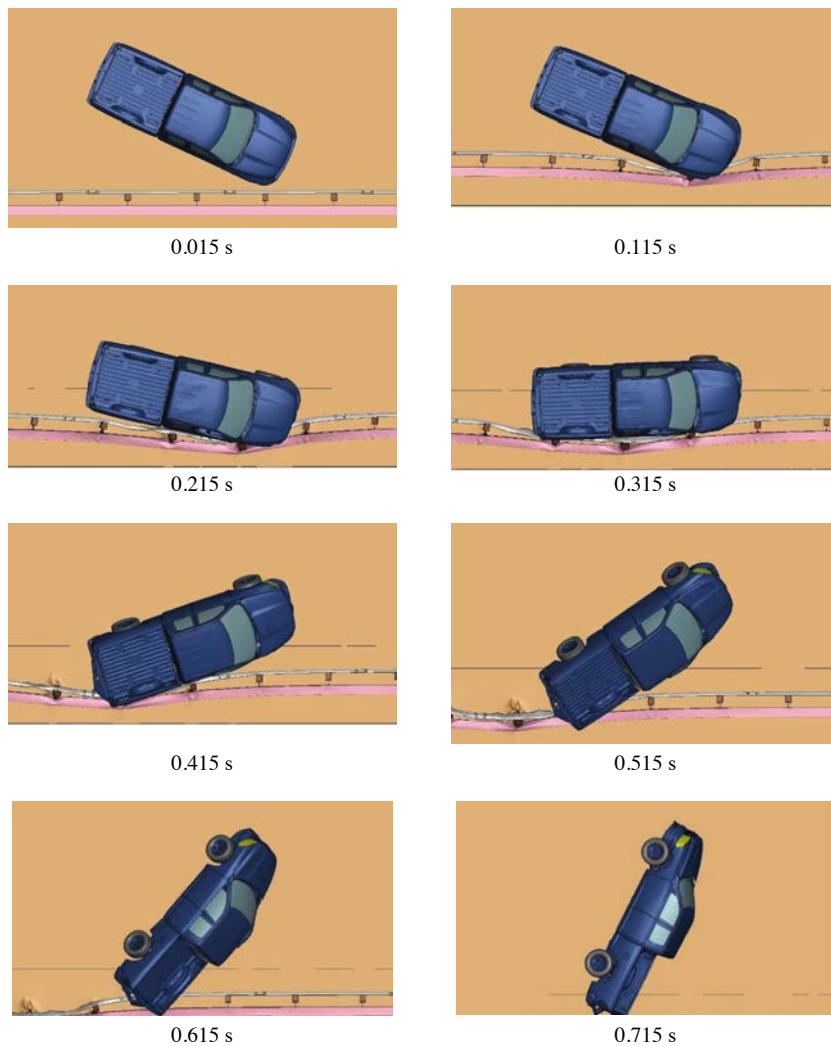


Figure 3.87. MGS with 10HU5×075 backup rail mounted in-line with W-beam – overhead view of MASH Test 3-11.

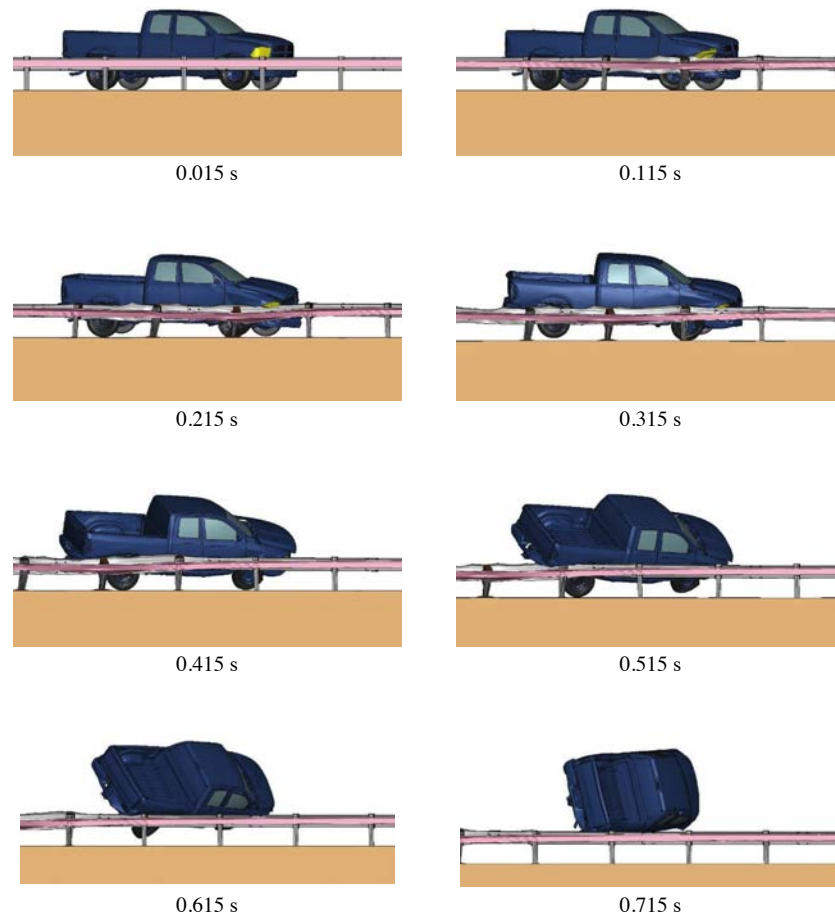


Figure 3.88. MGS with 10HU5×075 backup rail mounted in-line with W-beam – field-side view of MASH Test 3-11.



Figure 3.89. MGS with 10HU5×075 backup rail mounted in-line with W-beam – downstream view of MASH Test 3-11.

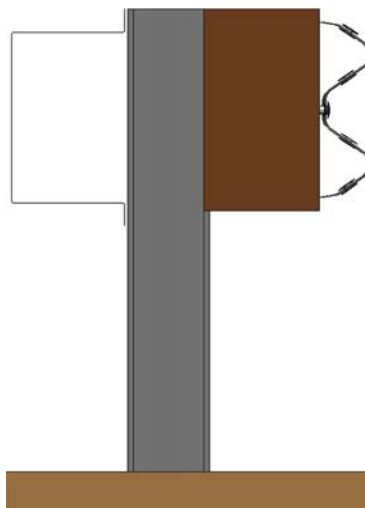


Figure 3.90. Profile view of MGS with 8HU12×135 backup rail mounted in-line with W-beam.

MASH Test 3-11 Simulation

Figure 3.91, Figure 3.92, and Figure 3.93 show the sequential frames of MASH Test 3-11 on MGS with 8HU12×135 backup rail mounted in-line with W-beam. In this simulation, the maximum dynamic deflection was 25.4 inches, the working width was 33.8 inches, and the working width height was 38.3 inches. The OIV was calculated to be 9.6 m/s (maximum limit is 12.2 m/s). The RDA was calculated to be 18.2 g (maximum limit is 20.49 g). This configuration passed MASH Test 3-11 by successfully containing and redirecting the vehicle.

MASH Test 3-10 Simulation

Figure 3.94, Figure 3.95, and Figure 3.96 show the sequential frames of MASH Test 3-10 on MGS with 8HU12×135 backup rail mounted in-line with W-beam. The OIV was calculated to be 11.9 m/s (maximum limit is 12.2 m/s). The RDA was calculated to be 20.0 g (maximum limit is 20.49 g). This configuration passed MASH Test 3-10 by successfully containing and redirecting the vehicle.

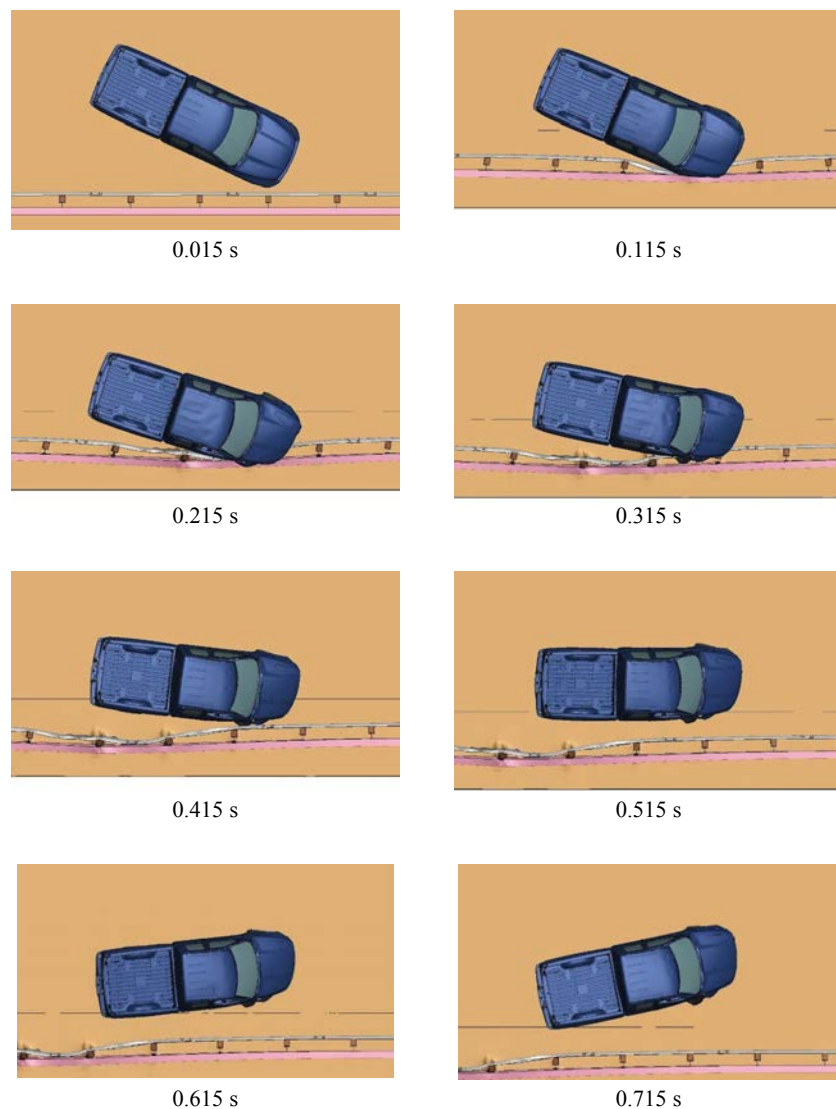


Figure 3.91. MGS with 8HU12×135 backup rail mounted in-line with W-beam – overhead view of MASH Test 3-11.

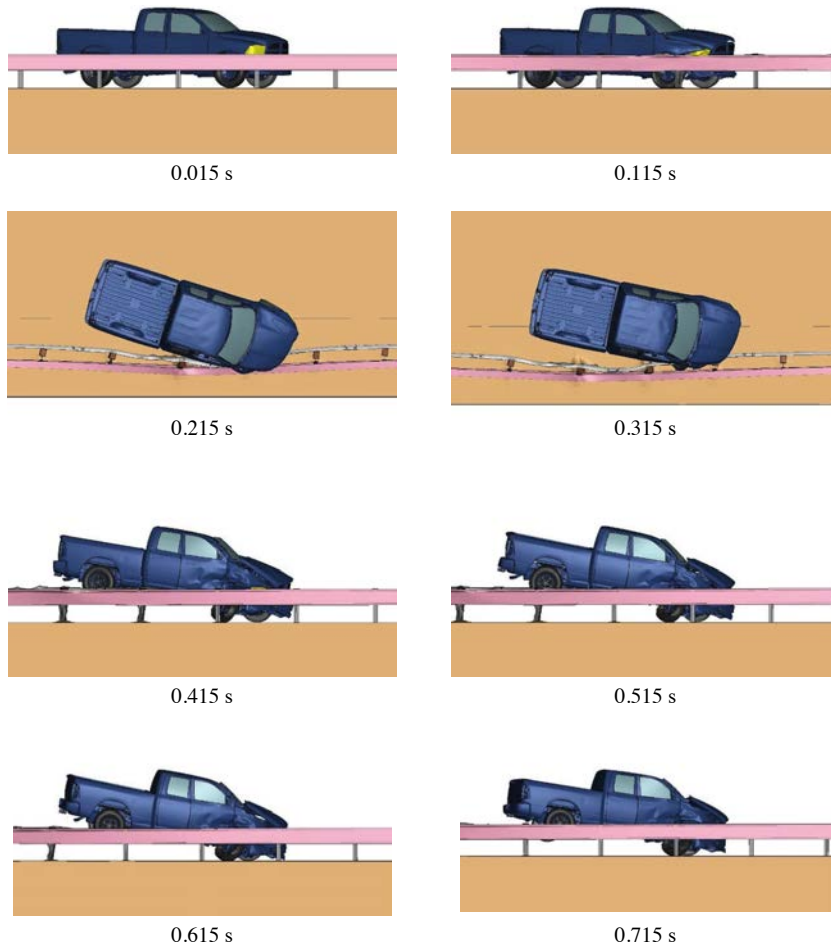


Figure 3.92. MGS with 8HU12×135 backup rail mounted in-line with W-beam – field-side view of MASH Test 3-11.



Figure 3.93. MGS with 8HU12×135 backup rail mounted in-line with W-beam – downstream view of MASH Test 3-11.

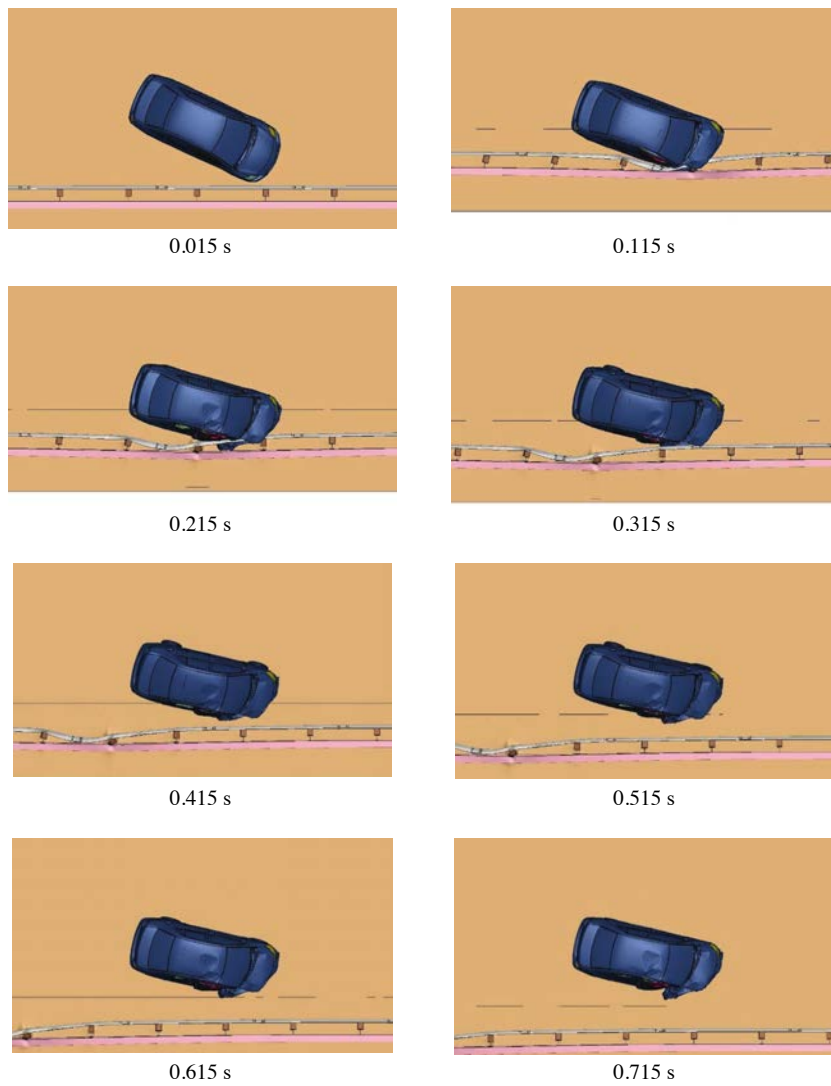


Figure 3.94. MGS with 8HU12×135 backup rail mounted in-line with W-beam – overhead view of MASH Test 3-10.

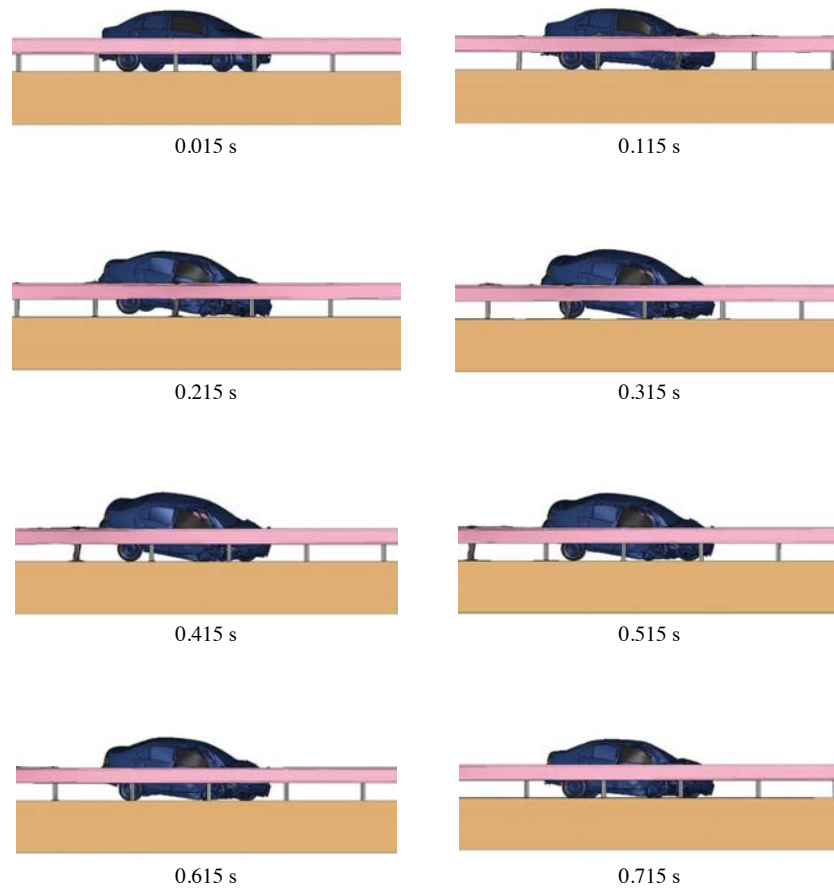


Figure 3.95. MGS with 8HU12×135 backup rail mounted in-line with W-beam – field-side view of MASH Test 3-10.

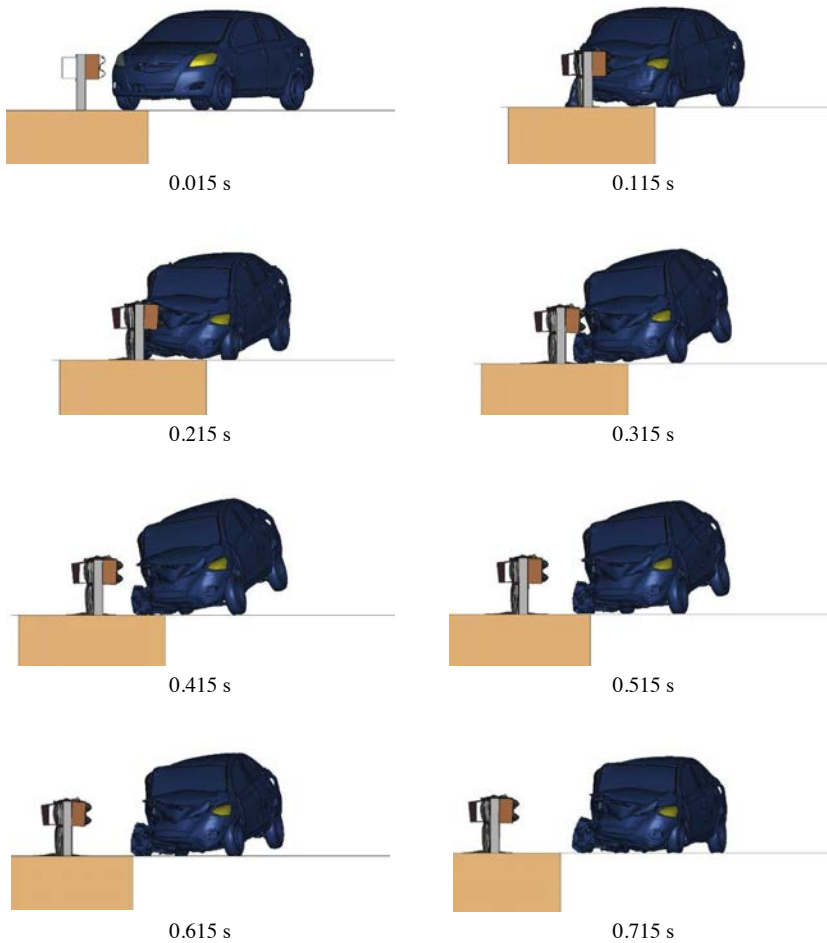


Figure 3.96. MGS with 8HU12×135 backup rail mounted in-line with W-beam – downstream view of MASH Test 3-10.

HSS8×8×¼ Blockout Replacement Rail

The baseline MGS model was modified with the inclusion of a HSS8×8×¼ blockout replacement rail as shown in Figure 3.97. Full-scale dynamic simulations for MASH Tests 3-11, 3-10, 3-21, and 3-20 were performed on this system configuration.

MASH Test 3-11 Simulation

Figure 3.98 shows the sequential frames of MASH Test 3-11 on MGS with HSS8×8×¼ blockout replacement rail. In this simulation, the maximum dynamic deflection was 15.4 inches, the working width was 35.4 inches, and the working width height was 30.5 inches. The OIV was calculated to be 7.0 m/s (preferred limit is 9.1 m/s). The RDA was calculated to be 11.8 g (preferred limit is 15 g). This configuration passed MASH Test 3-11 by successfully containing and redirecting the vehicle.

MASH Test 3-10 Simulation

Figure 3.99, Figure 3.100, and Figure 3.101 show the sequential frames of MASH Test 3-10 on MGS with HSS8×8×¼ blockout replacement rail. The OIV was calculated to be 8.2 m/s (preferred limit is 9.1 m/s). The RDA was calculated to be 17.3 g (maximum limit is 20.49 g). This configuration passed MASH Test 3-10 by successfully containing and redirecting the vehicle.

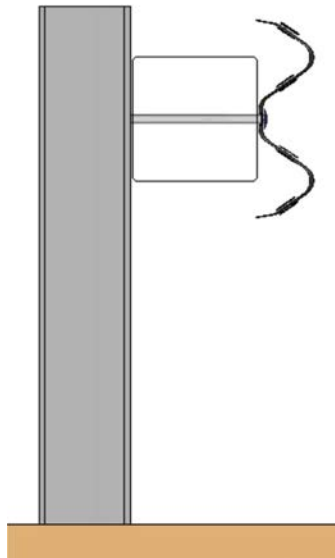
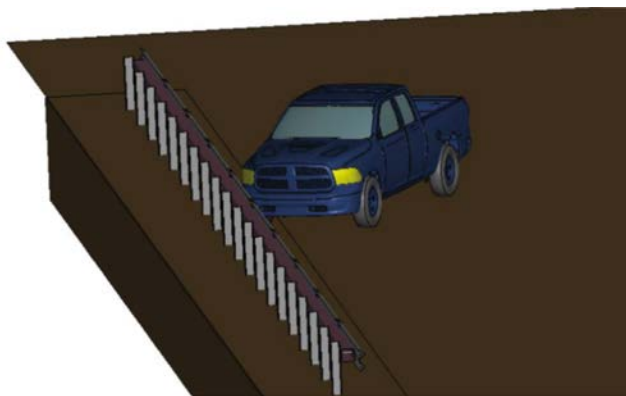
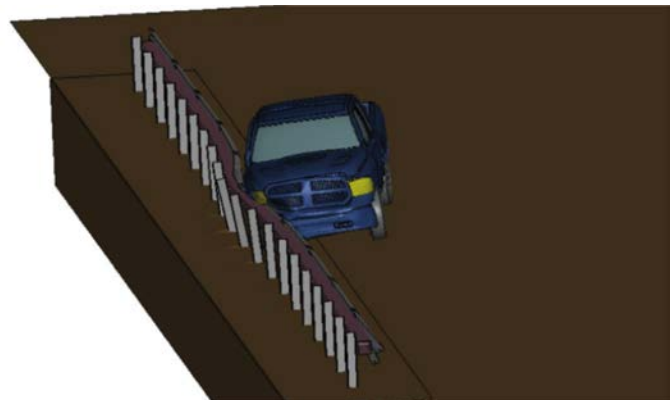


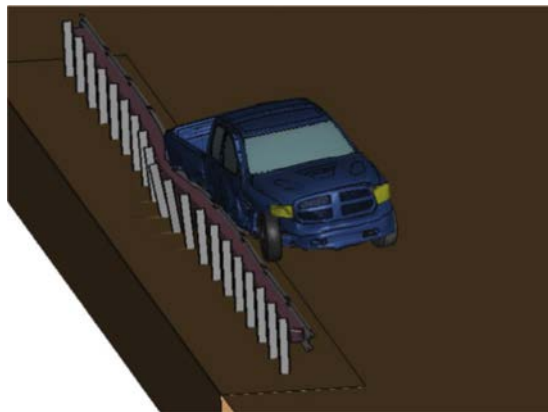
Figure 3.97. Profile view of MGS with HSS8×8×¼ blockout replacement rail.



a.



b.



c.

Figure 3.98. MGS with HSS8×8×¼ blockout replacement rail – isometric view of MASH Test 3-11.

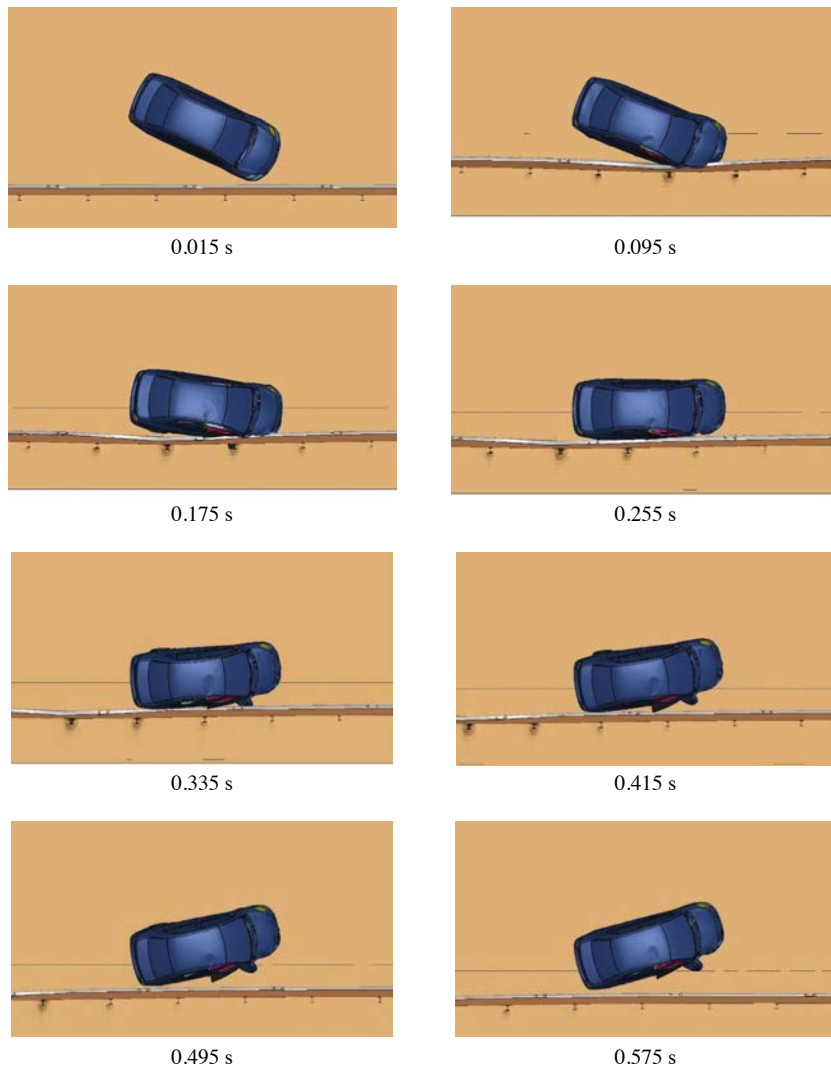


Figure 3.99. MGS with HSS8×8×¼ blockout replacement rail – overhead view of MASH Test 3-10.

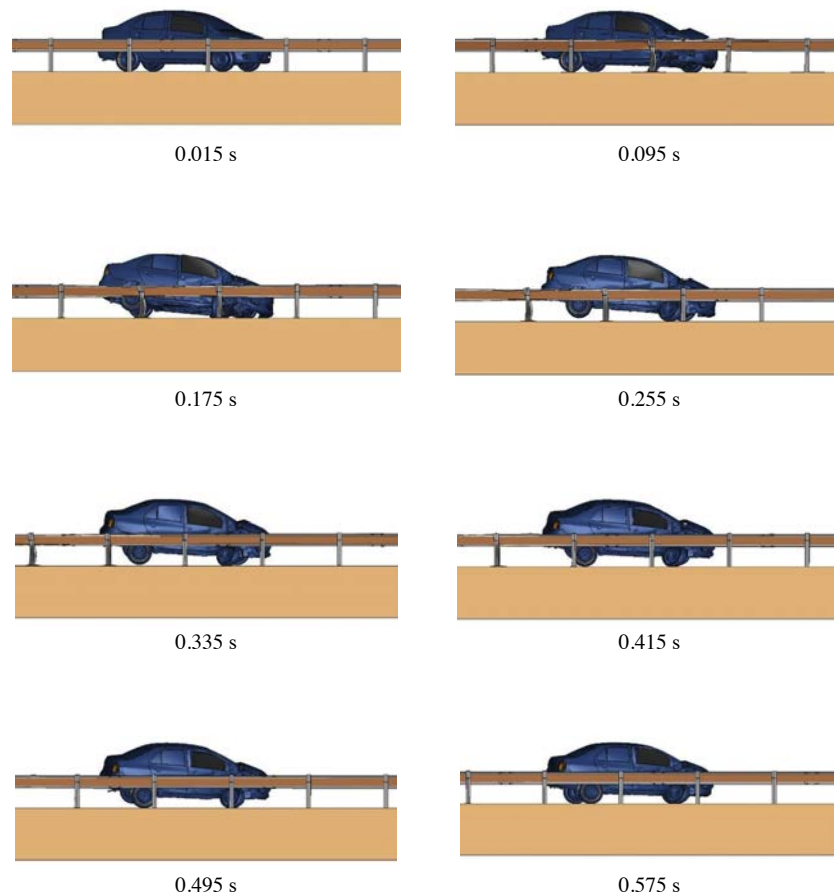


Figure 3.100. MGS with HSS8×8×¼ blackout replacement rail – field-side view of MASH Test 3-10.



Figure 3.101. MGS with HSS8×8×¼ blockout replacement rail – downstream view of MASH Test 3-10.

MASH Test 3-21 Simulation

The transition from standard MGS to the stiffened section is shown in Figure 3.102. This transition includes varying the post spacing and tapering the edge of the blockout replacement rail.

Figure 3.103, Figure 3.104, and Figure 3.105 show the sequential frames of MASH Test 3-21 on the transition to MGS with HSS8×8×¼ blockout replacement rail. The OIV was calculated to be 6.2 m/s (preferred limit is 9.1 m/s). The RDA was calculated to be 10.6 g (preferred limit is 15.0 g). This configuration passed the MASH Test 3-21 by successfully containing and redirecting the vehicle.

MASH Test 3-20 Simulation

The transition from standard MGS to the stiffened section is shown in Figure 3.106. This transition includes varying the post spacing and tapering the edge of the blockout replacement rail.

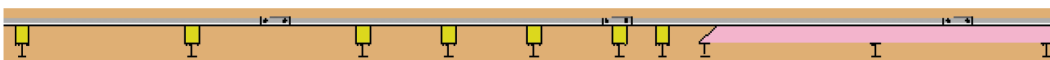


Figure 3.102. Overhead view of the transition to MGS with HSS8×8×¼ blockout replacement rail.

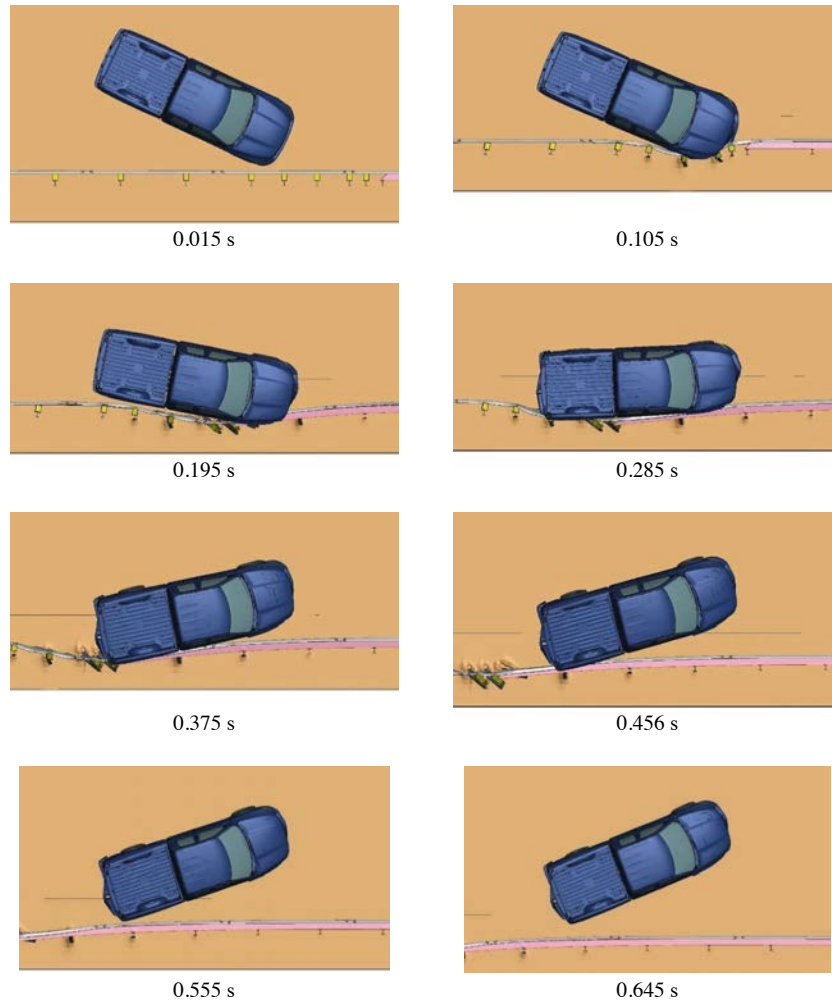


Figure 3.103. Transition to MGS with HSS8×8×¼ blockout replacement rail – overhead view of MASH Test 3-21.

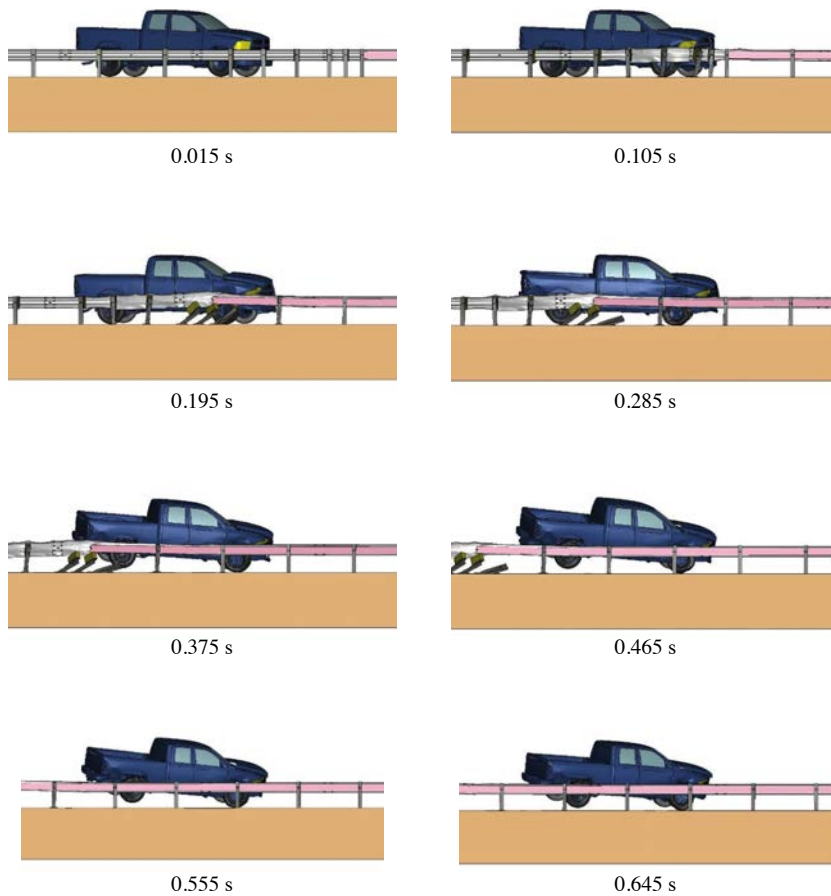


Figure 3.104. Transition to MGS with HSS8×8×¼ blockout replacement rail – field-side view of MASH Test 3-21.

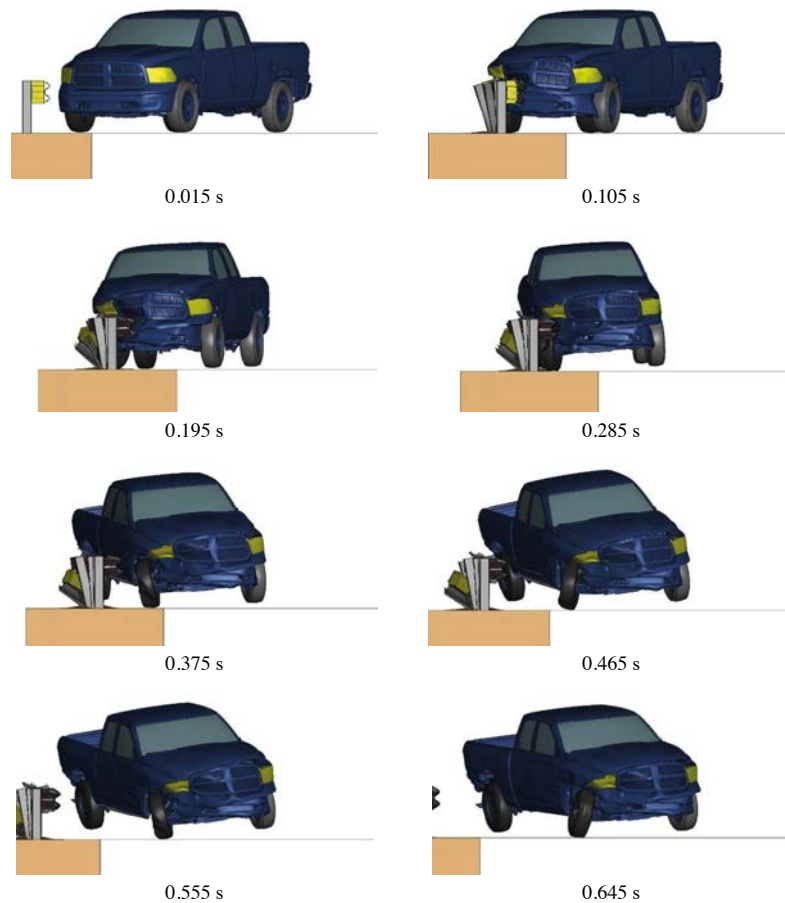


Figure 3.105. Transition to MGS with HSS8×8× $\frac{1}{4}$ blackout replacement rail – downstream view of MASH Test 3-21.

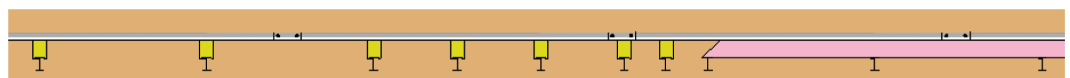


Figure 3.106. Overhead view of the transition to MGS with HSS8×8× $\frac{1}{4}$ blackout replacement rail.

Figure 3.107, Figure 3.108, and Figure 3.109 show the sequential frames of MASH Test 3-20 on the transition to MGS with HSS8×8× $\frac{1}{4}$ blackout replacement rail. The OIV was calculated to be 8.5 m/s (preferred limit is 9.1 m/s). The RDA was calculated to be 15.4 g (maximum limit is 20.49 g). This transition system passed MASH Test 3-20 by successfully containing and redirecting the vehicle.

Anchored Backup Rail Study

For all the MGS system configurations shown previously, the backup rails are modeled as unanchored at the ends. To evaluate the anchorage condition's impact on barrier deflection, the research team evaluated the performance of two configurations with backup rails anchored at the ends. The first configuration consisted of the HSS4×4× $\frac{1}{4}$ as the backup rail, and the second consisted of the combination of the HSS5×5× $\frac{5}{16}$ with the 10-gauge W-beam. A summary of data and how the anchored simulations compare with the unanchored configurations is presented in Table 3.1. The results showed anchoring the backup rail does not provide significant improvement in the deflection-reducing performance of the system.

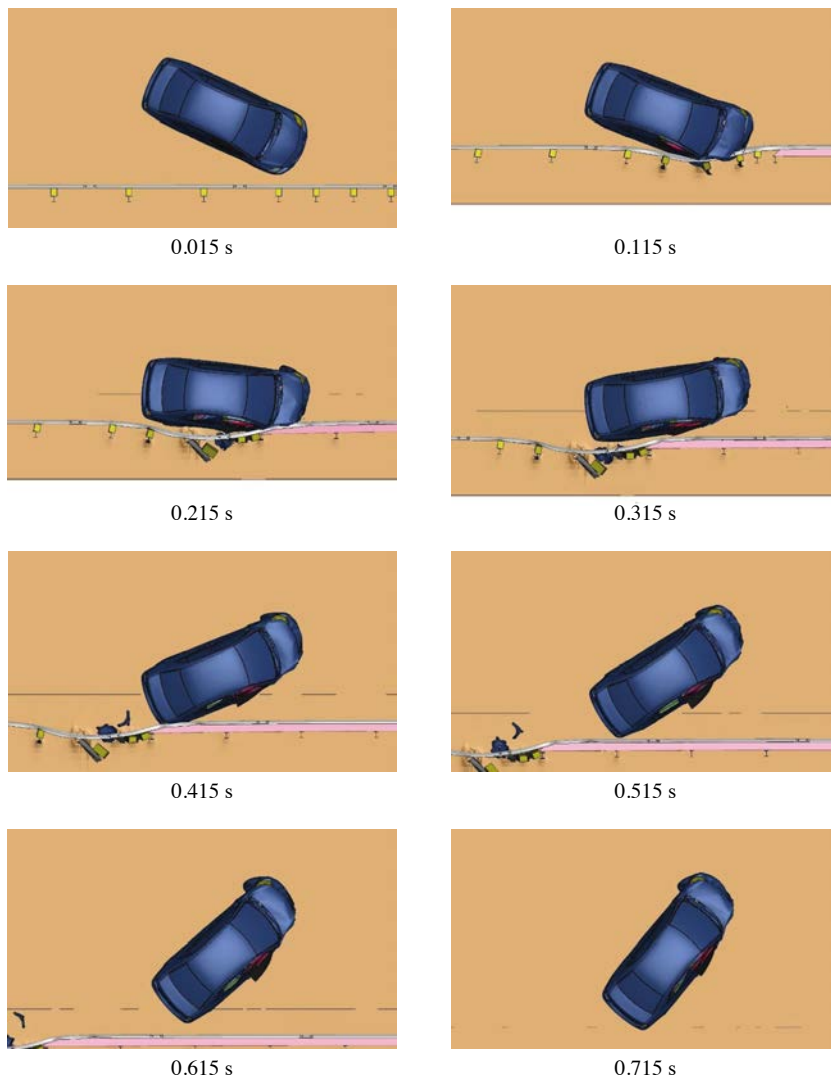


Figure 3.107. Transition to MGS with HSS8×8×¼ blockout replacement rail – overhead view of MASH Test 3-20.

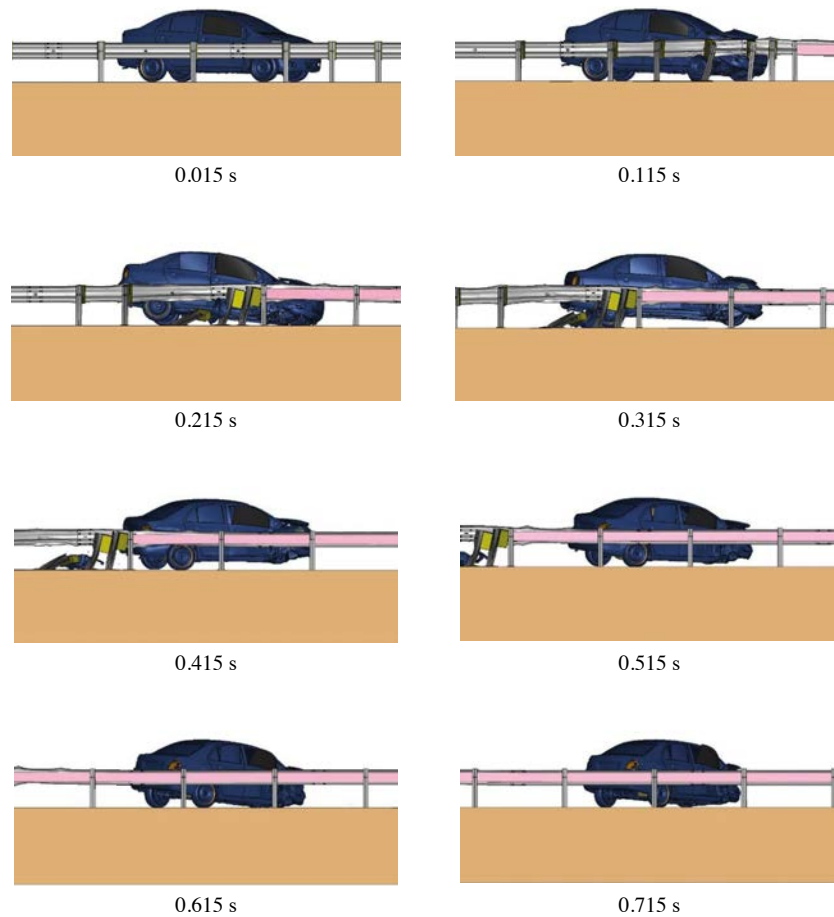


Figure 3.108. *Transition to MGS with HSS8×8×¼ blackout replacement rail – field-side view of MASH Test 3-20.*

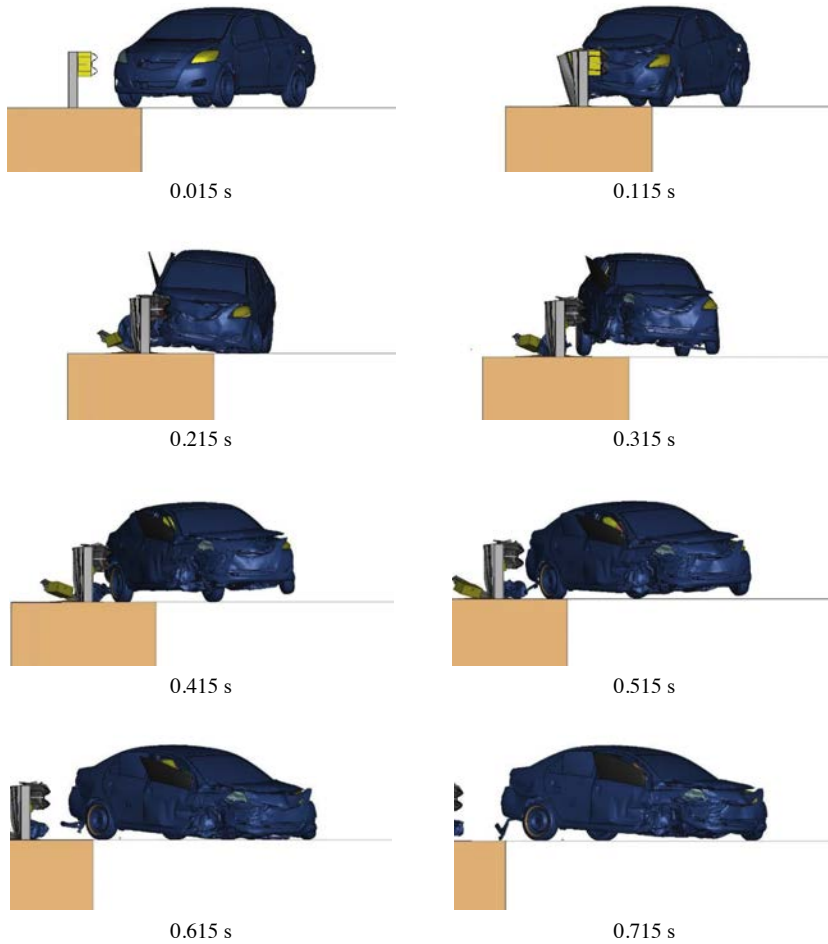


Figure 3.109. Transition to MGS with HSS8×8×¼ blockout replacement rail – downstream view of MASH Test 3-20.

Table 3.1. Summary results of MGS configurations with anchored backup rails.

Backup Rail Section	Max. Dynamic Deflection (inches)		MASH Test 3-11 Results	
	Unanchored	Anchored	Unanchored	Anchored
HSS4x4x1/4	33.7	33.5	Pass	Pass
HSS5x5x5/16 with 10-Gauge W-beam	21.8	21.6	Pass	Pass

Combination Rails

Combined Backup Rail and 10-Gauge W-Beam

In some of the simulations presented previously, the W-beam rail locally deformed around the guardrail posts. The research team chose to investigate if a slightly more robust rail element (10-gauge) would mitigate this local deformation while also improving crashworthiness and reducing deflection.

Sections HSS5×5×⁵/₁₆ and HSS6×6×³/₈ were selected to be evaluated in combination with a 10-gauge W-beam. The sections were attached to the post in-line with the W-beam. A summary

Table 3.2. Summary results for combined backup rails and 10-gauge W-beam.

Backup Rail Section	Maximum Dynamic Deflection (inches)		MASH Test 3-11	
	With 10-Gauge W-Beam	With 12-Gauge W-Beam	With 10-Gauge W-Beam	With 12-Gauge W-Beam
HSS5x5x5/16	21.8	26.1	Fail	Fail
HSS6x6x3/8	20.8	23.5	Pass	Pass

of the resulting data and how they compare with the 12-gauge W-beam combination are presented in Table 3.2. The results show an improvement in the dynamic deflection of the systems. However, the thicker W-beam failed to change the outcome of the MASH test for the HSS5x5x5/16 configuration, as the vehicle still similarly interacted with the system and exhibited rollover.

Combination of Half-Post Spacing and HSS4x4x1/4 Backup Rail Mounted In-Line with W-Beam

The baseline MGS model was modified with the inclusion of half-post spacing and an HSS4x4x1/4 backup rail mounted in-line with a W-beam as shown in Figure 3.110. A full-scale dynamic simulation for MASH Test 3-11 was performed on this system configuration.

MASH Test 3-11 Simulation

Figure 3.111, Figure 3.112, and Figure 3.113 show the sequential frames of MASH Test 3-11 on MGS with a combination of half-post spacing and HSS4x4x1/4 backup rail mounted in-line with W-beam. The configuration failed MASH Test 3-11 because the vehicle exhibited rollover after exiting the system.

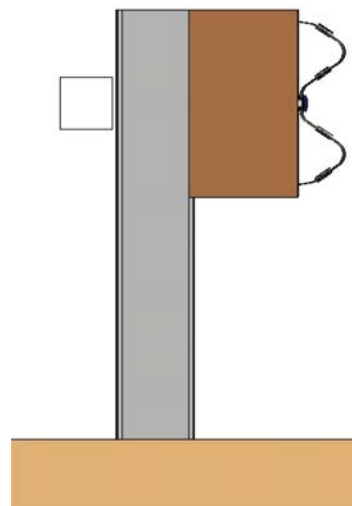


Figure 3.110. Profile view of MGS with a combination of half-post spacing and HSS4x4x1/4 backup rail mounted in-line with W-beam.

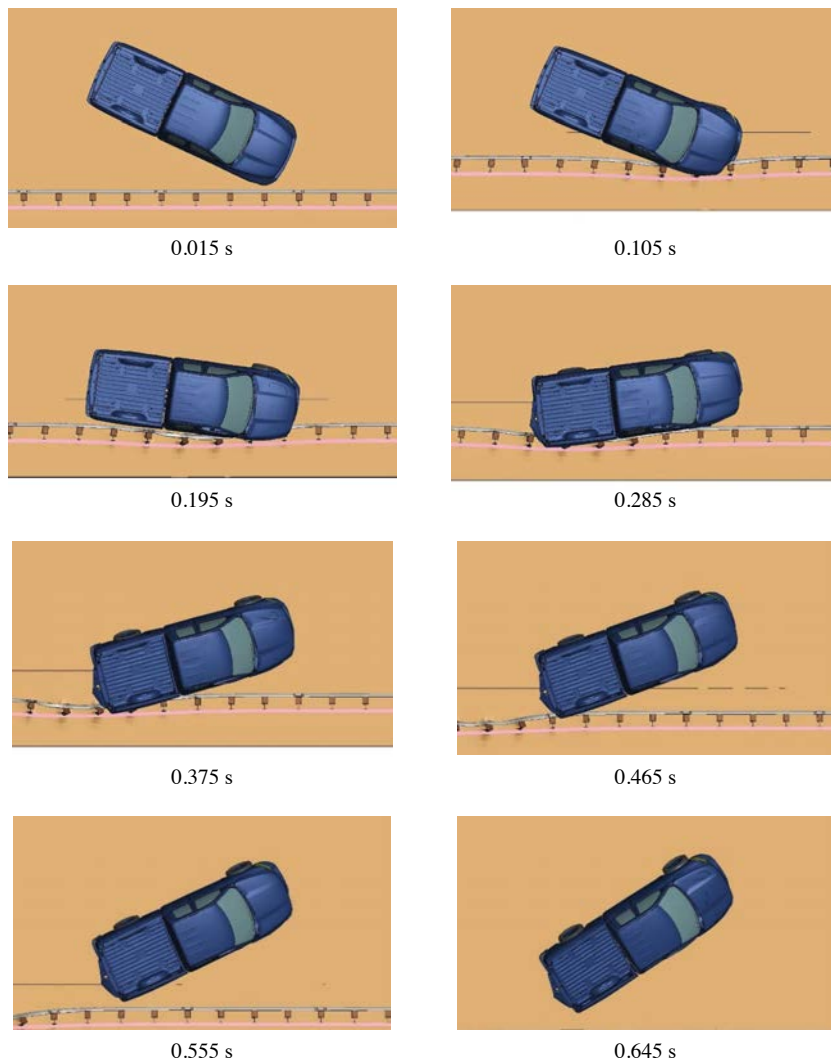


Figure 3.111. MGS with a combination of half-post spacing and HSS4×4×¼ backup rail mounted in-line with W-beam – overhead view of MASH Test 3-11.

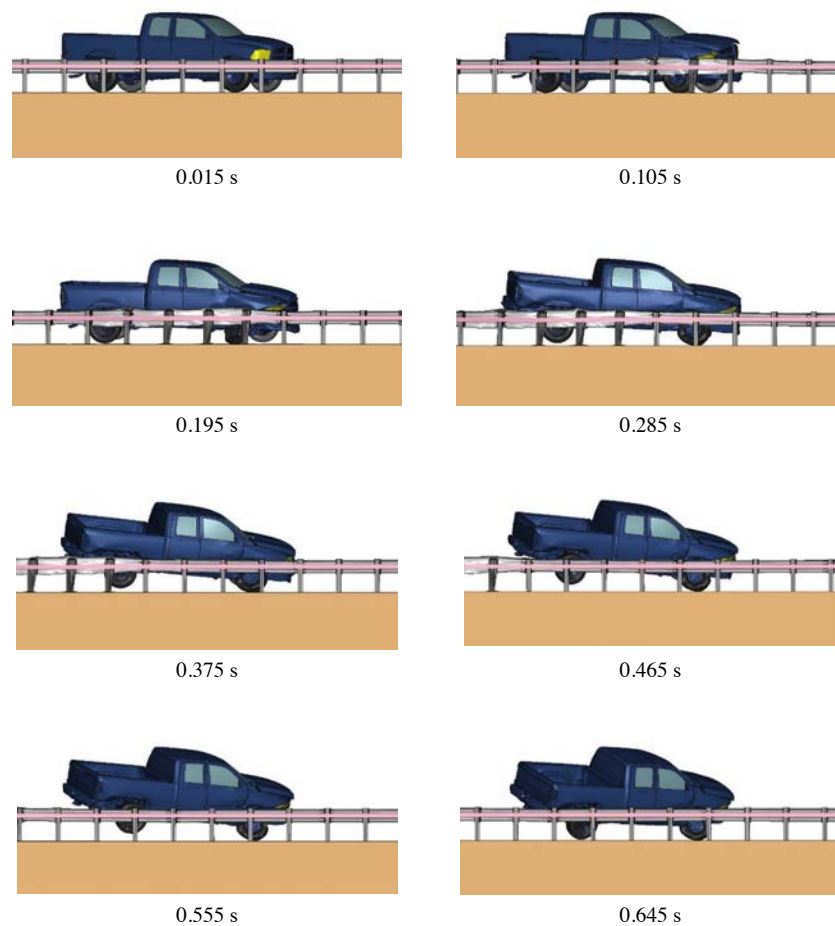


Figure 3.112. MGS with a combination of half-post spacing and HSS4×4×¼ backup rail mounted in-line with W-beam – field-side view of MASH Test 3-11.



Figure 3.113. MGS with a combination of half-post spacing and HSS4×4×¼ backup rail mounted in-line with W-beam – downstream view of MASH Test 3-11.

Combination of Quarter-Post Spacing and HSS4×4×¼ Backup Rail Mounted In-Line with W-Beam

The baseline MGS model was modified with the inclusion of quarter-post spacing and an HSS4×4×¼ backup rail mounted in-line with a W-beam as shown in Figure 3.114. Full-scale dynamic simulations for MASH Test 3-11, 3-10, 3-21, and 3-20 were performed on this system configuration.

MASH Test 3-11 Simulation

Figure 3.115, Figure 3.116, and Figure 3.117 show the sequential frames of MASH Test 3-11 on MGS with a combination of quarter-post spacing and HSS4×4×¼ backup rail mounted in-line with W-beam. In this simulation, the maximum dynamic deflection was 10.1 inches, the working width was 26.5 inches, and the working width height was 26.6 inches. The OIV was calculated to be 7.1 m/s (preferred limit is 9.1 m/s). The RDA was calculated to be 13.2 g (preferred limit is 15 g). This configuration passed MASH Test 3-11 by successfully containing and redirecting the vehicle.

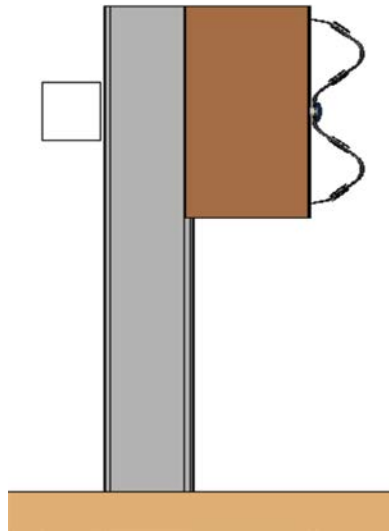


Figure 3.114. Profile view of MGS with a combination of quarter-post spacing and HSS4×4× $\frac{1}{4}$ backup rail mounted in-line with W-beam.

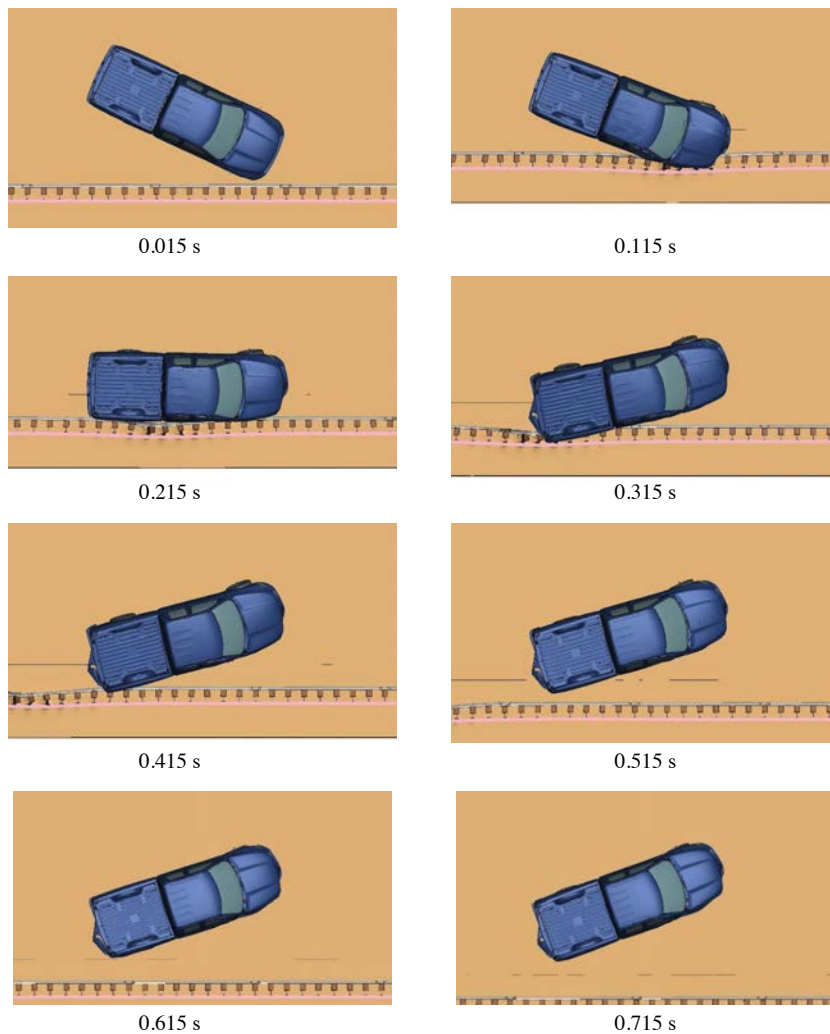


Figure 3.115. MGS with a combination of quarter-post spacing and HSS4×4× $\frac{1}{4}$ backup rail mounted in-line with W-beam – overhead view of MASH Test 3-11.

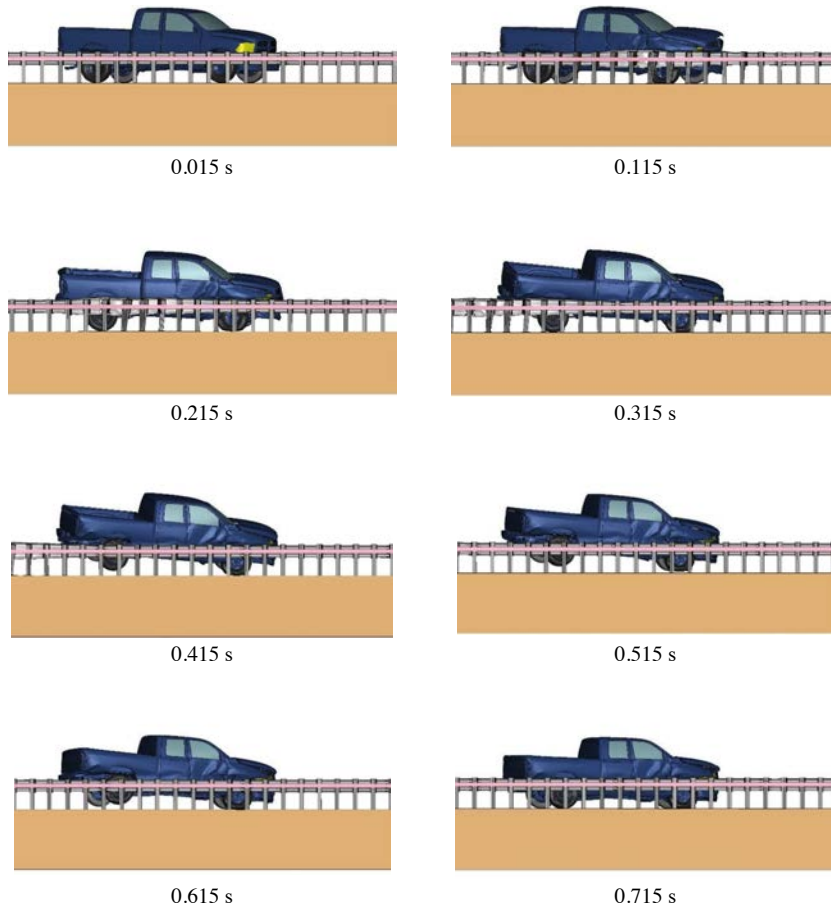


Figure 3.116. MGS with a combination of quarter-post spacing and HSS4×4× $\frac{1}{4}$ backup rail mounted in-line with W-beam – field-side view of MASH Test 3-11.

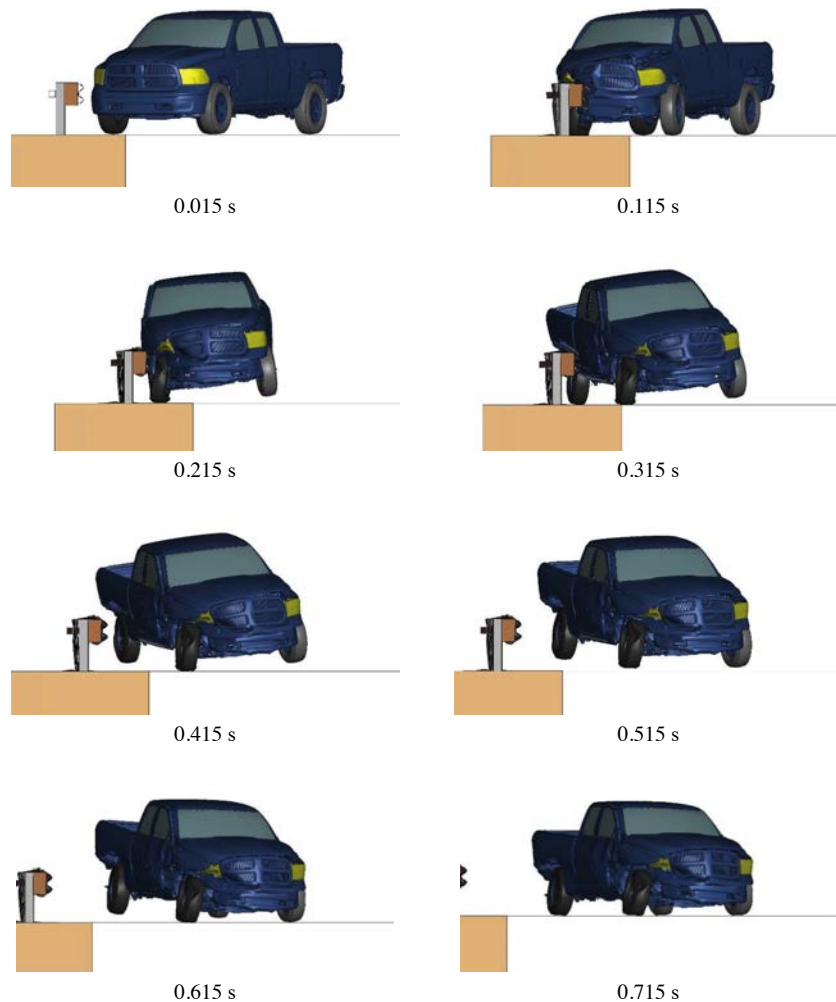


Figure 3.117. MGS with a combination of quarter-post spacing and HSS4×4×¼ backup rail mounted in-line with W-beam – downstream view of MASH Test 3-11.

MASH Test 3-10 Simulation

Figure 3.118, Figure 3.119, and Figure 3.120 show the sequential frames of MASH Test 3-10 on MGS with a combination of quarter-post spacing and HSS4×4×¼ backup rail mounted in-line with W-beam. The OIV was calculated to be 11.6 m/s (maximum limit is 12.2 m/s). The RDA was calculated to be 15.0 g (maximum limit is 20.49 g). This configuration passed MASH Test 3-10 by successfully containing and redirecting the vehicle.

MASH Test 3-21 Simulation

The transition from standard MGS to the stiffened section is shown in Figure 3.121. This transition includes varying the post spacing adjacent to the stiffened section.

Figure 3.122, Figure 3.123, and Figure 3.124 show the sequential frames of MASH Test 3-21 on the transition to MGS with combined HSS4×4×¼ backup rail and quarter-post spacing. The OIV was calculated to be 6.7 m/s (preferred limit is 9.1 m/s). The RDA was calculated to be 14.8 g (preferred limit is 15.0 g). This configuration passed MASH Test 3-21 by successfully containing and redirecting the vehicle.

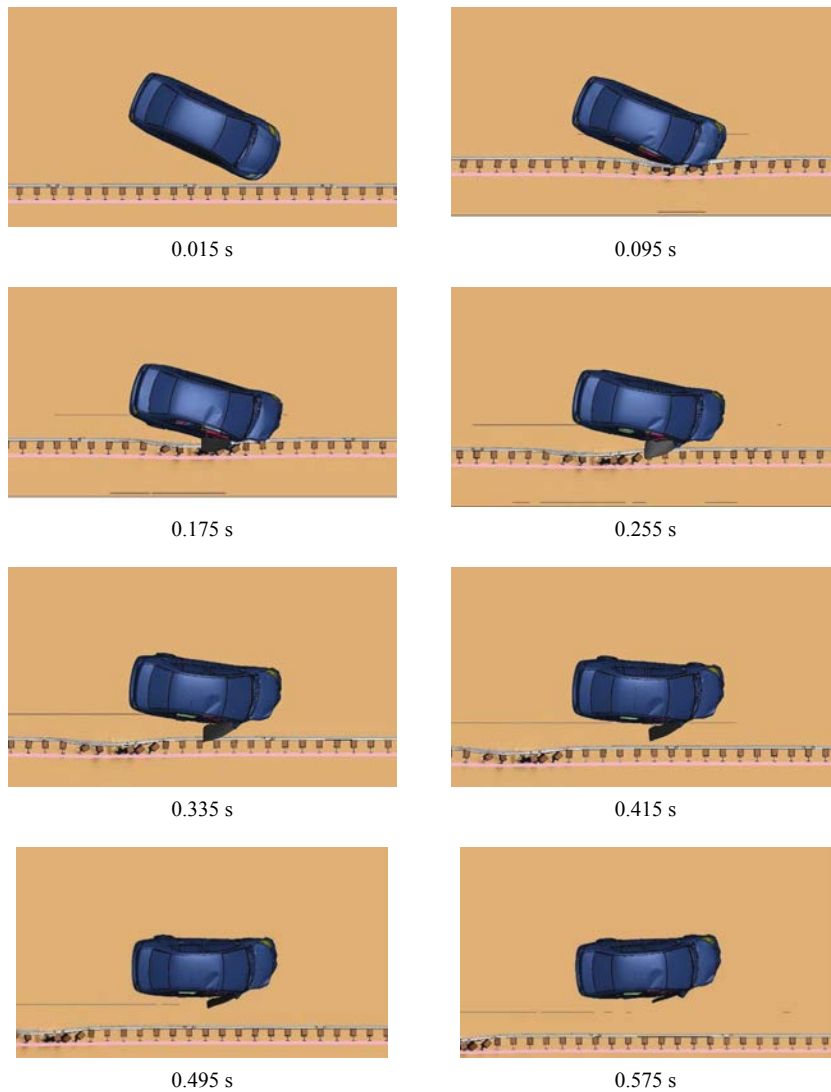


Figure 3.118. MGS with a combination of quarter-post spacing and HSS4×4×¼ backup rail mounted in-line with W-beam – overhead view of MASH Test 3-10.

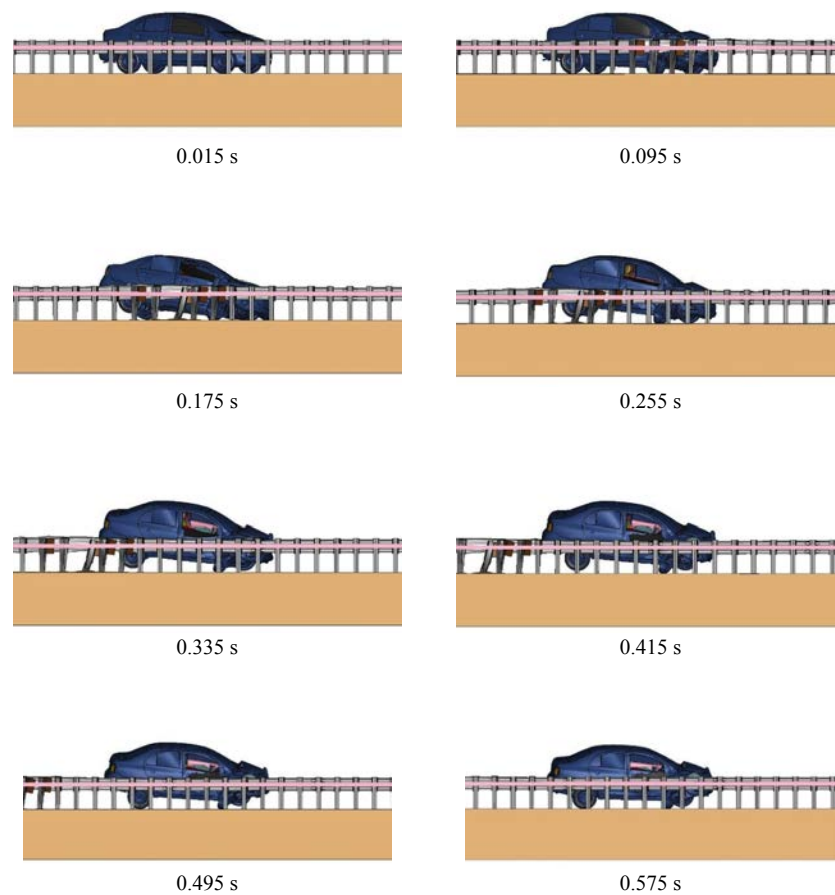


Figure 3.119. MGS with a combination of quarter-post spacing and HSS4×4× $\frac{1}{4}$ backup rail mounted in-line with W-beam – field-side view of MASH Test 3-10.

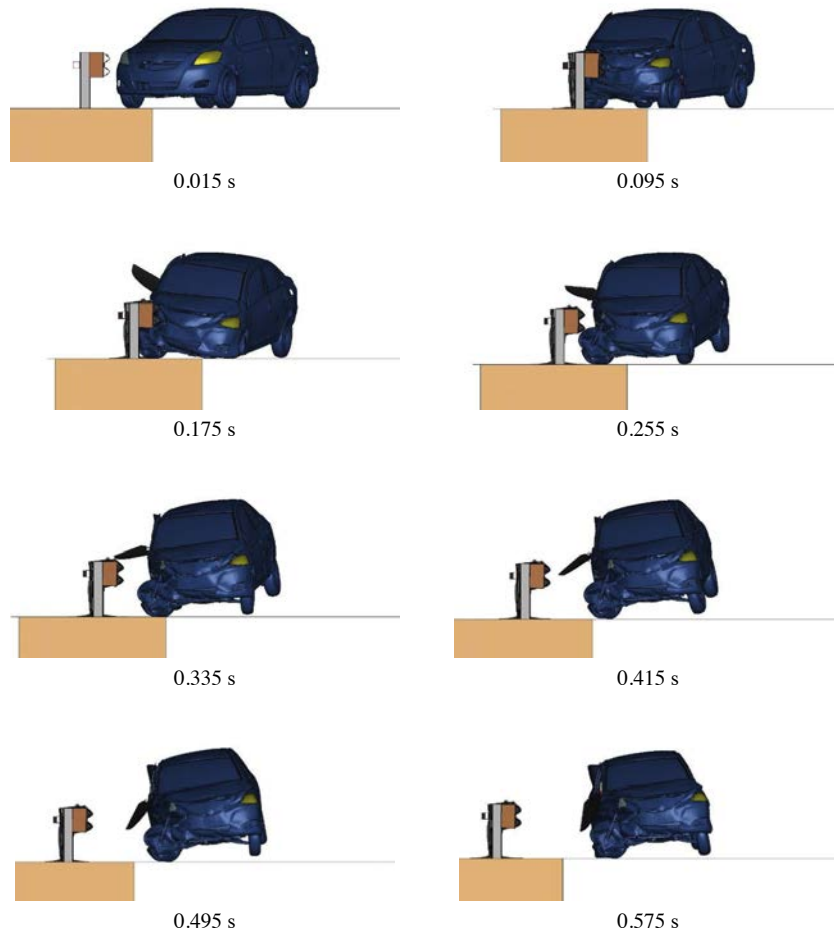


Figure 3.120. MGS with a combination of quarter-post spacing and HSS4×4×¼ backup rail mounted in-line with W-beam – downstream view of MASH Test 3-10.

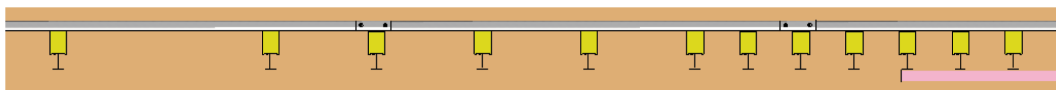


Figure 3.121. Overhead view of the transition to MGS with a combination of quarter-post spacing and HSS4×4×¼ backup rail mounted in-line with W-beam.

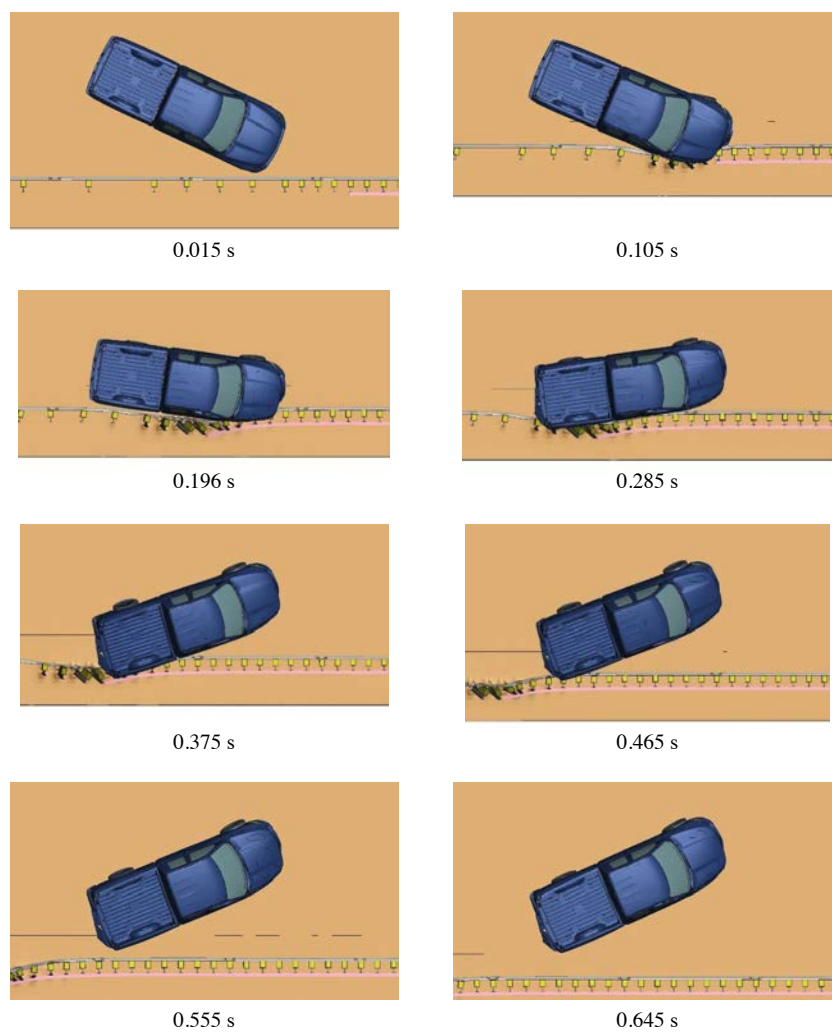


Figure 3.122. *Transition to MGS with a combination of quarter-post spacing and HSS4×4×¼ backup rail mounted in-line with W-beam – overhead view of MASH Test 3-21.*

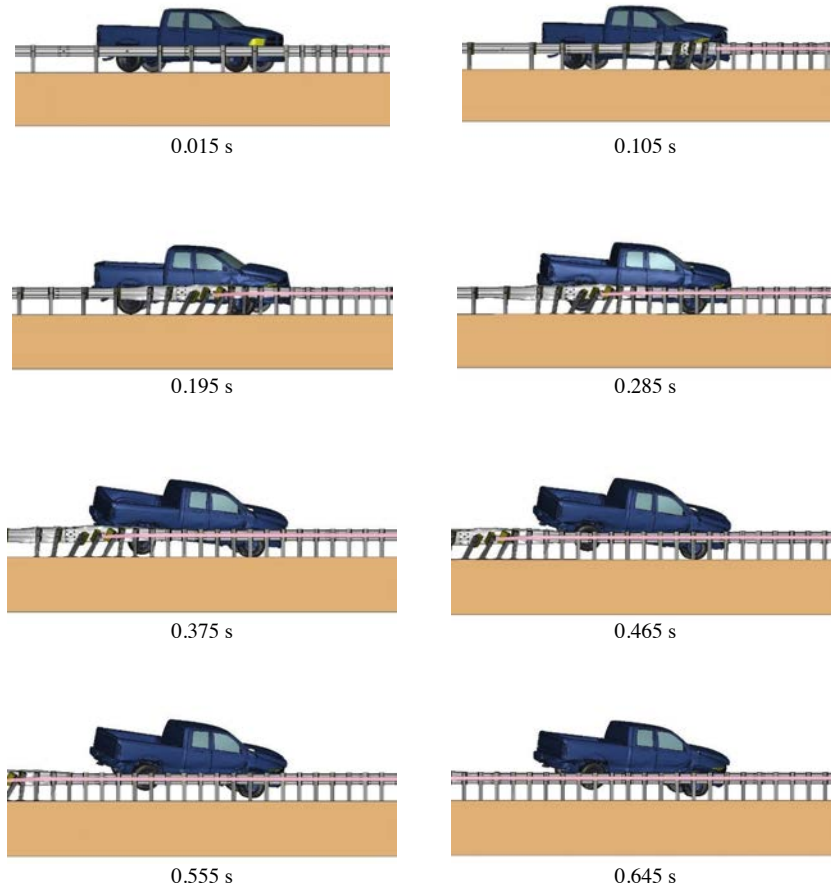


Figure 3.123. Transition to MGS with a combination of quarter-post spacing and HSS4×4×¼ backup rail mounted in-line with W-beam – field-side view of MASH Test 3-21.

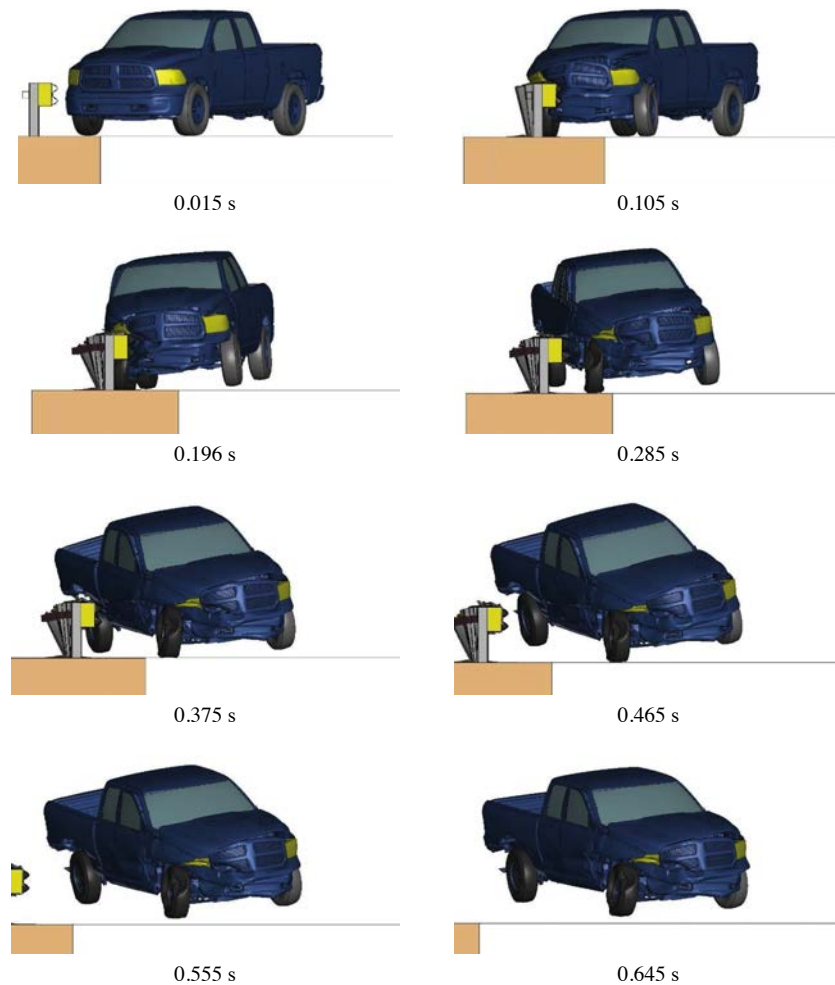


Figure 3.124. Transition to MGS with a combination of quarter-post spacing and HSS4×4×¼ backup rail mounted in-line with W-beam – downstream view of MASH Test 3-21.

MASH Test 3-20 Simulation

The transition from standard MGS to the stiffened section is shown in Figure 3.125. This transition includes varying the post spacing adjacent to the stiffened section.

Figure 3.126, Figure 3.127, and Figure 3.128 show the sequential frames of MASH Test 3-20 on the transition to MGS with a combination of quarter-post spacing and HSS4×4×¼ backup rail mounted in-line with W-beam. The OIV was calculated to be 8.8 m/s (preferred limit is 9.1 m/s). The RDA was calculated to be 18.7 g (maximum limit is 20.49 g). This transition system passed MASH Test 3-20 by successfully containing and redirecting the vehicle.



Figure 3.125. Overhead view of the transition to MGS with a combination of quarter-post spacing and HSS4×4×¼ backup rail mounted in-line with W-beam.

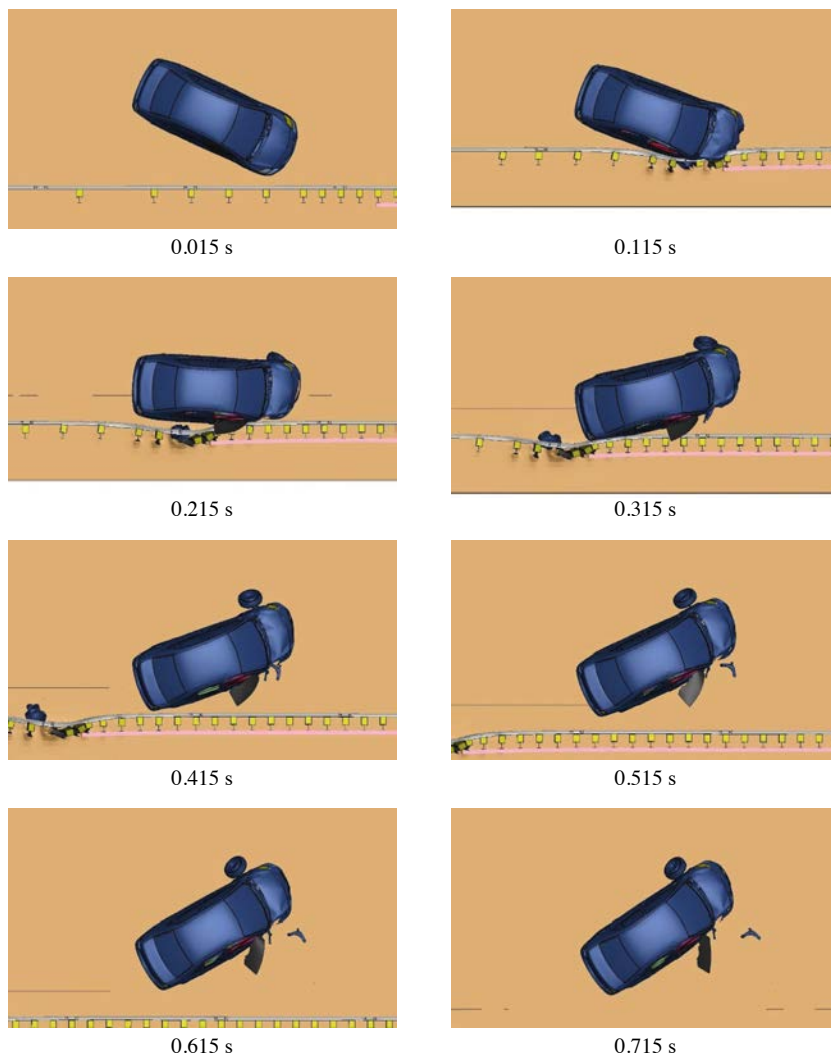


Figure 3.126. Transition to MGS with a combination of quarter-post spacing and HSS4×4×¼ backup rail mounted in-line with W-beam – overhead view of MASH Test 3-20.

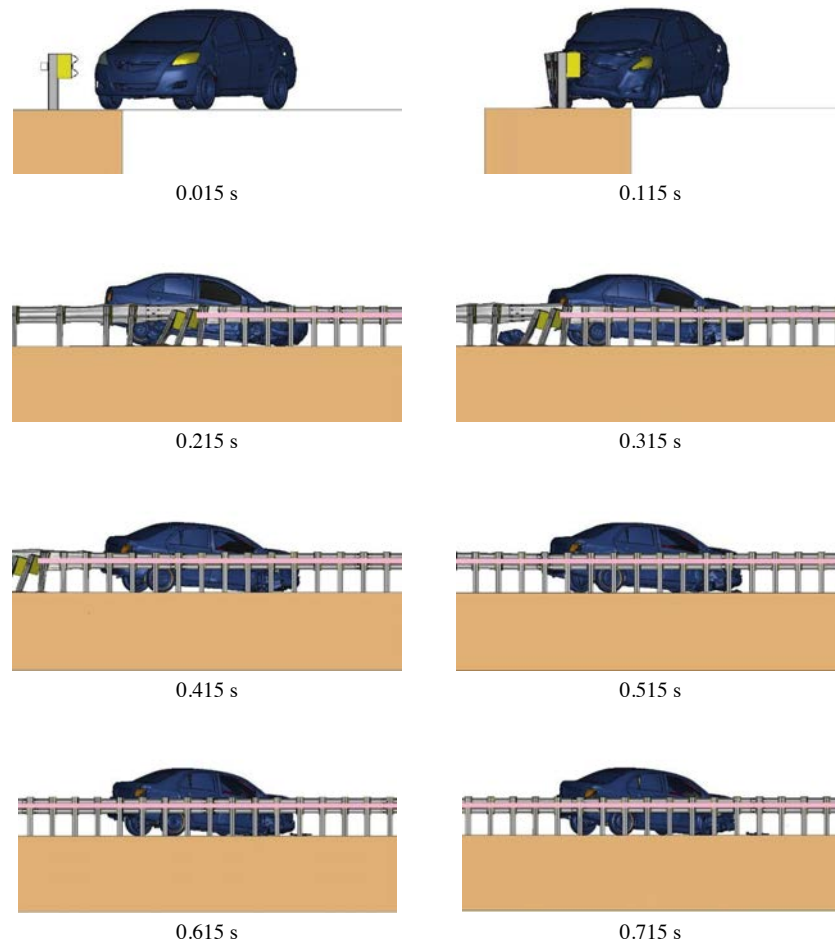


Figure 3.127. Transition to MGS with a combination of quarter-post spacing and HSS4×4×¼ backup rail mounted in-line with W-beam – field-side view of MASH Test 3-20.

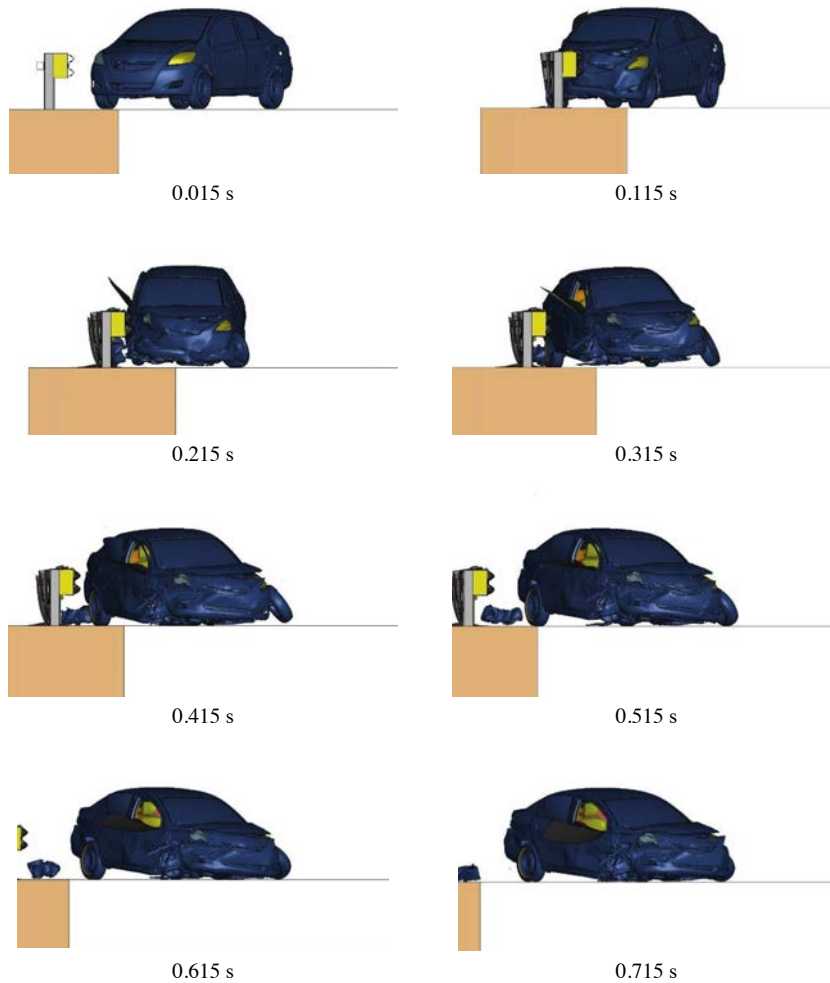


Figure 3.128. Transition to MGS with a combination of quarter-post spacing and HSS4×4×¼ backup rail mounted in-line with W-beam – downstream view of MASH Test 3-20.

Combination of Half-Post Spacing and HSS8×8×¼ Blockout Replacement Rail

The baseline MGS model was modified with the inclusion of half-post spacing and an HSS8×8×¼ blockout replacement rail as seen in Figure 3.129. A full-scale dynamic simulation for MASH Test 3-11 was performed on this system configuration.

MASH Test 3-11 Simulation

Figure 3.130, Figure 3.131, and Figure 3.132 show the sequential frames of MASH Test 3-11 on MGS with a combination of half-post spacing and HSS8×8×¼ blockout replacement rail. In this simulation, the maximum dynamic deflection was 10.0 inches, the working width was 23.3 inches, and the working width height was 32.5 inches. The OIV was calculated to be 8 m/s (preferred limit is 9.1 m/s). The RDA was calculated to be 8.6 g (preferred limit is 15.0 g). This configuration passed MASH Test 3-11 by successfully containing and redirecting the vehicle.

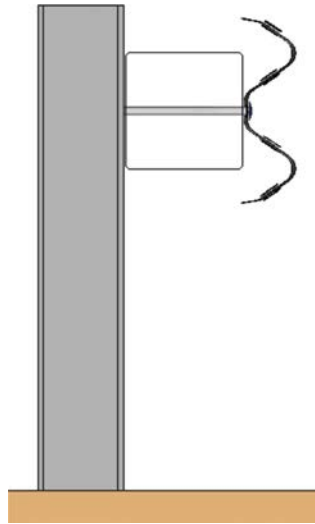


Figure 3.129. Profile view of MGS with a combination of half-post spacing and HSS8×8×¼ blockout replacement rail.

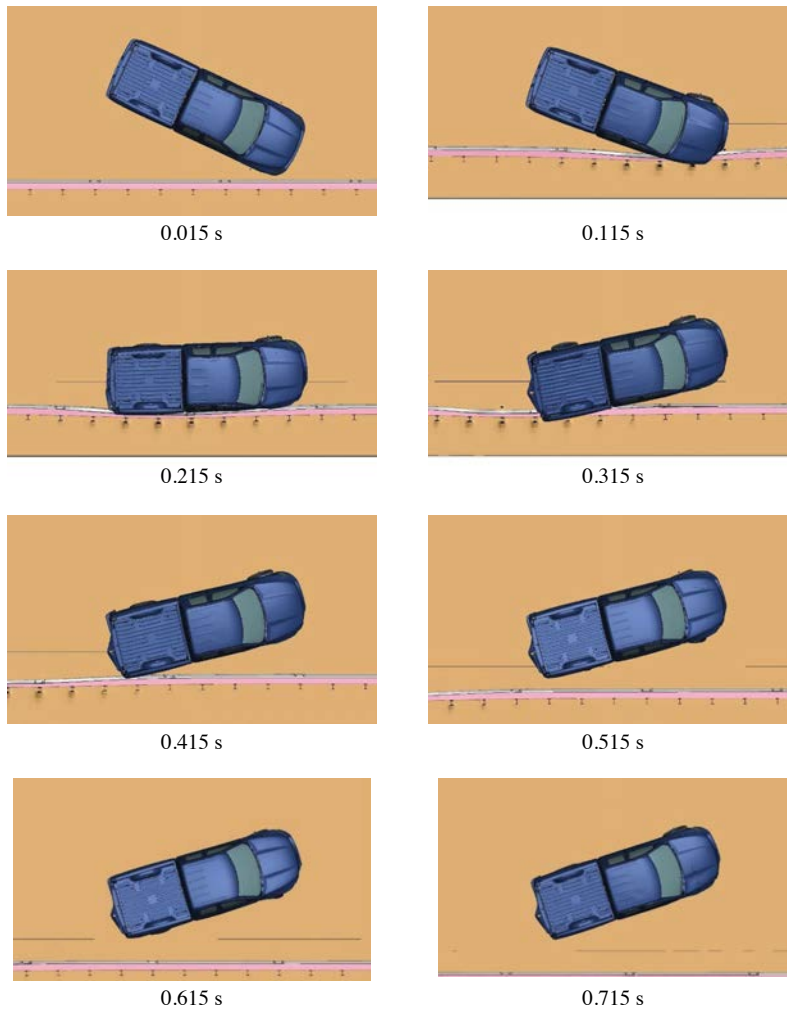


Figure 3.130. MGS with a combination of half-post spacing and HSS8×8×¼ blockout replacement rail – overhead view of MASH Test 3-11.

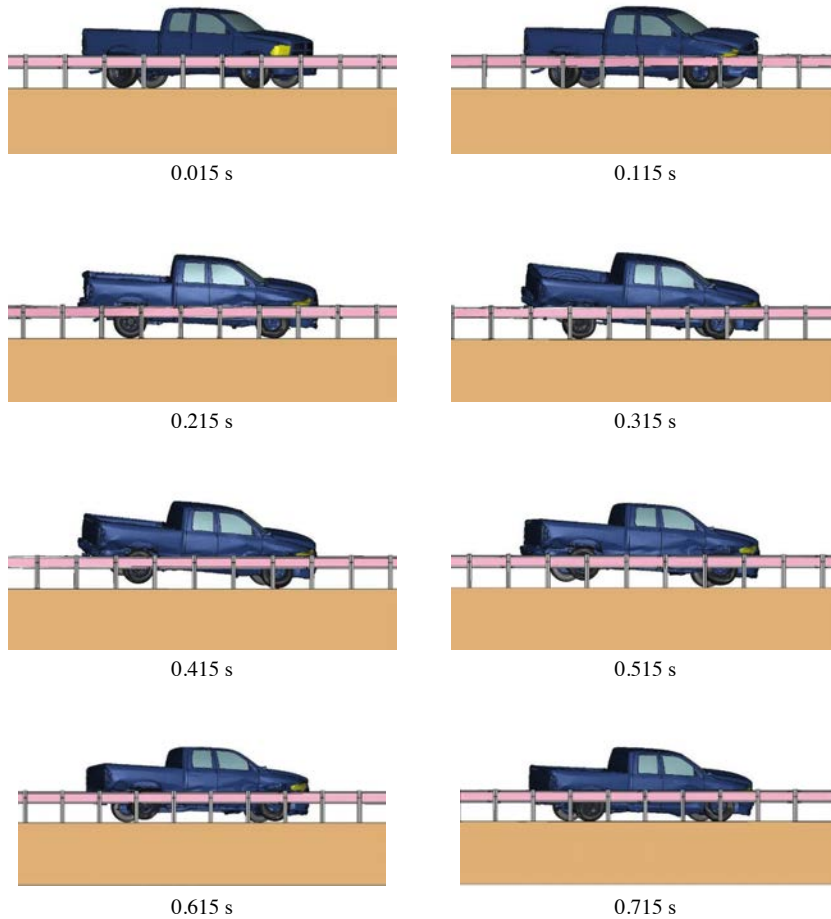


Figure 3.131. MGS with a combination of half-post spacing and HSS8×8×¼ blockout replacement rail – field-side view of MASH Test 3-11.

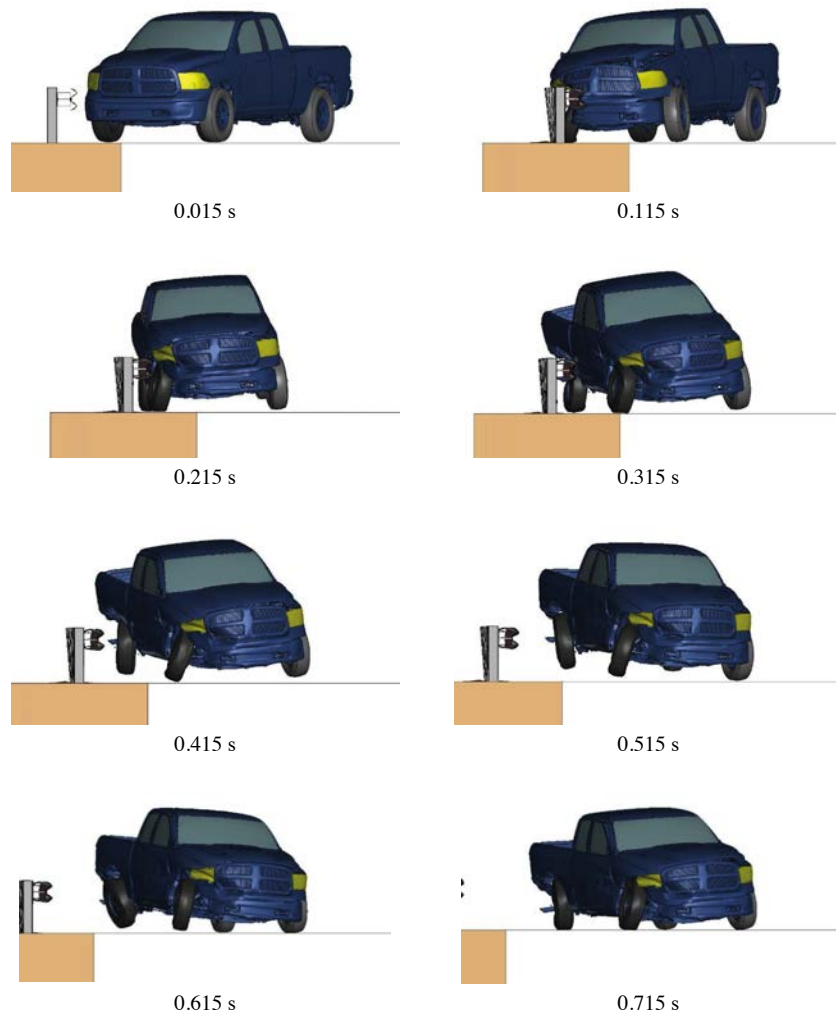


Figure 3.132. MGS with a combination of half-post spacing and HSS8×8×¼ blockout replacement rail – downstream view of MASH Test 3-11.

Combination of Quarter-Post Spacing and HSS8×8×¼ Blockout Replacement Rail

The baseline MGS was modified with the inclusion of quarter-post spacing and an HSS8×8×¼ blockout replacement rail as shown in Figure 3.133. Full-scale dynamic simulations for MASH Tests 3-11, 3-10, 3-21, and 3-20 were performed on this system configuration.

MASH Test 3-11 Simulation

Figure 3.134, Figure 3.135, and Figure 3.136 show the sequential frames of MASH Test 3-11 on MGS with a combination of quarter-post spacing and HSS8×8×¼ blockout replacement rail. In this simulation, the maximum dynamic deflection was 7.4 inches, the working width was 20.9 inches, and the working width height was 32.4 inches. The OIV was calculated to be 8.4 m/s (preferred limit is 9.1 m/s). The RDA was calculated to be 8.1 g (preferred limit is 15.0 g). This configuration passed MASH Test 3-11 by successfully containing and redirecting the vehicle.

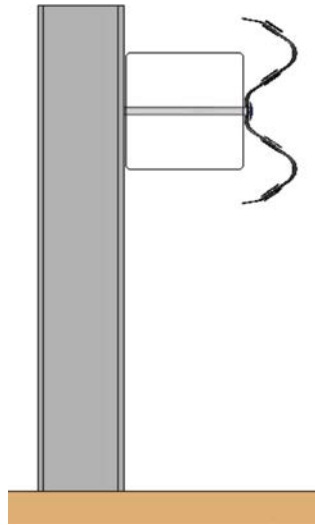


Figure 3.133. Profile view of MGS with a combination of quarter-post spacing and HSS8×8×¼ blockout replacement rail.

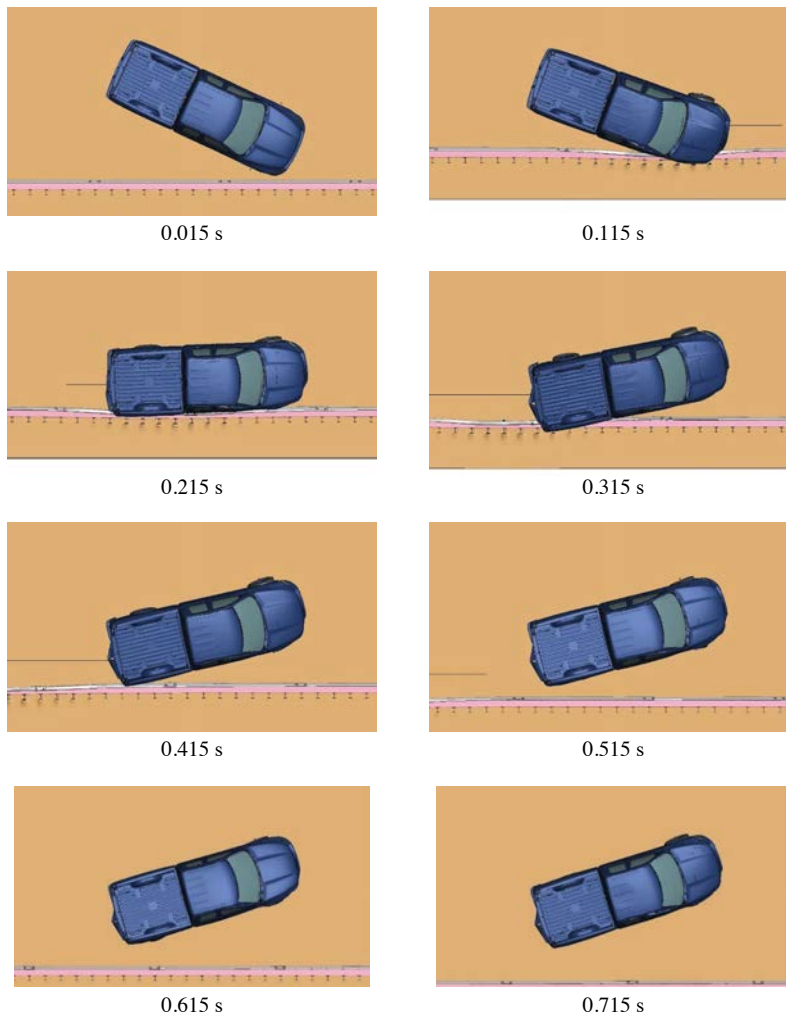


Figure 3.134. MGS with a combination of quarter-post spacing and HSS8×8×¼ blockout replacement rail – overhead view of MASH Test 3-11.

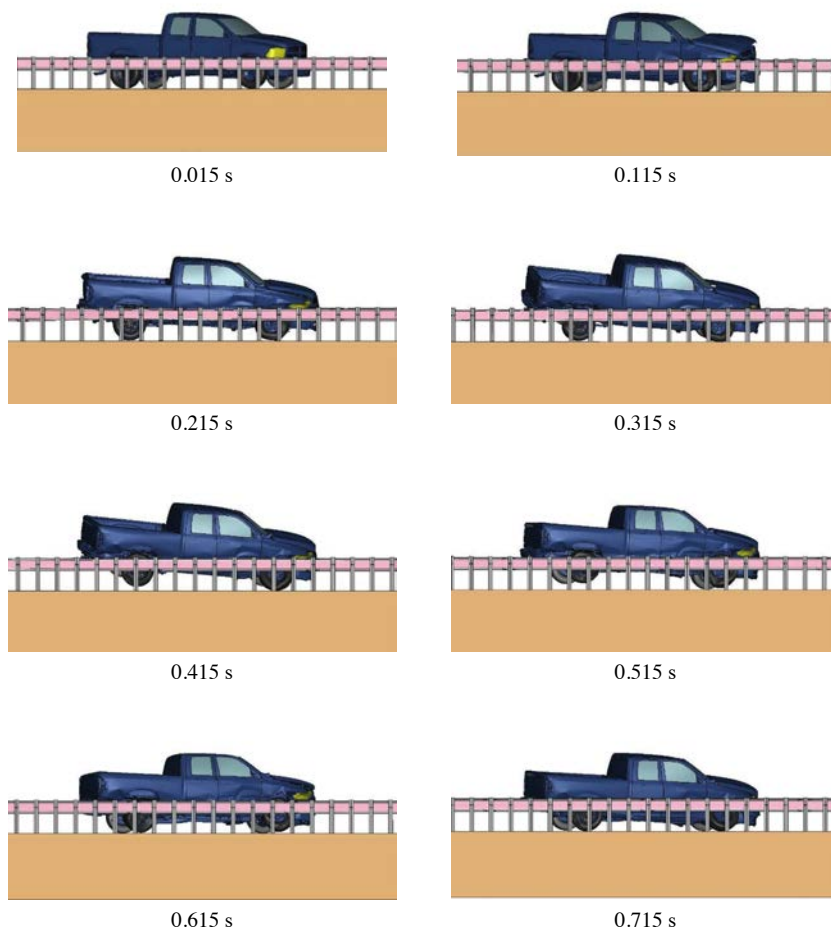


Figure 3.135. MGS with a combination of quarter-post spacing and HSS8×8×¼ blackout replacement rail – field-side view of MASH Test 3-11.

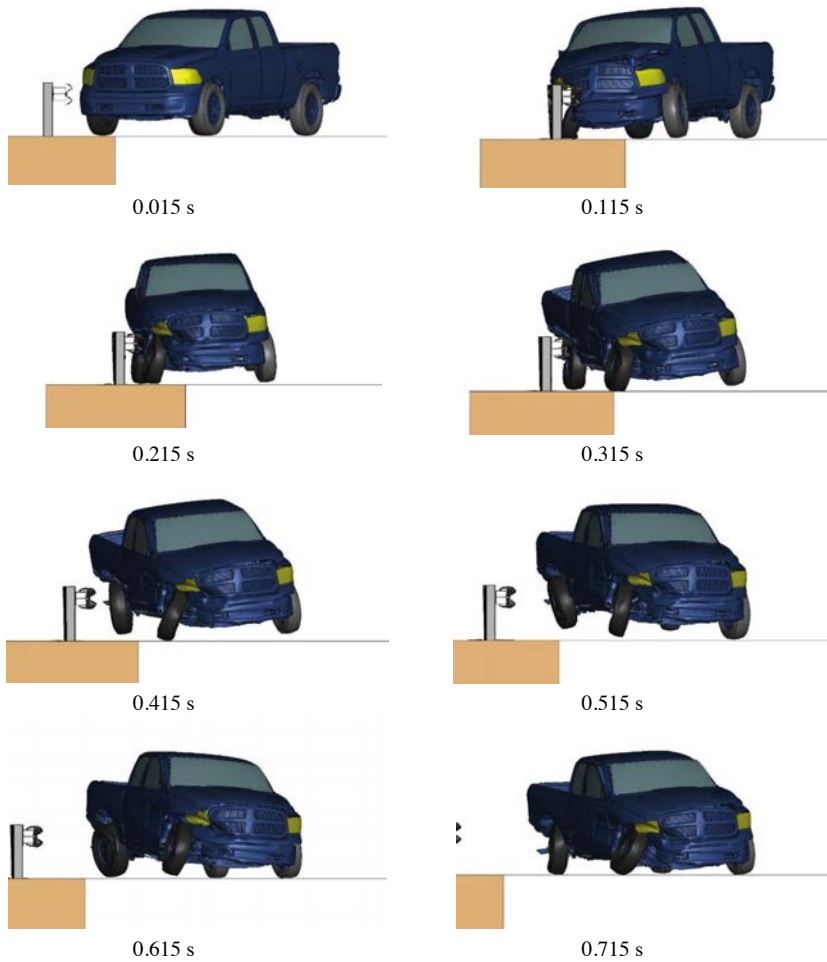


Figure 3.136. MGS with a combination of quarter-post spacing and HSS8×8×¼ blockout replacement rail – downstream view of MASH Test 3-11.

MASH Test 3-10 Simulation

Figure 3.137, Figure 3.138, and Figure 3.139 show the sequential frames of MASH Test 3-10 on MGS with a combination of quarter-post spacing and HSS8×8×¼ blockout replacement rail. The OIV was calculated to be 9.4 m/s (maximum limit is 12.2 m/s). The RDA was calculated to be 13.9 g (preferred limit is 15.0 g). This configuration passed MASH Test 3-10 by successfully containing and redirecting the vehicle.

MASH Test 3-21 Simulation

The transition from standard MGS to the stiffened section is shown in Figure 3.140. This transition includes varying the post spacing adjacent and tapering the edge of the blockout replacement rail.

Figure 3.141, Figure 3.142, and Figure 3.143 show the sequential frames of MASH Test 3-21 on the transition to MGS with a combination of quarter-post spacing and HSS8×8×¼ blockout replacement rail. The OIV was calculated to be 6.4 m/s (preferred limit is 9.1 m/s). The RDA was calculated to be 15.9 g (maximum limit is 20.49 g). This configuration passed MASH Test 3-21 by successfully containing and redirecting the vehicle.

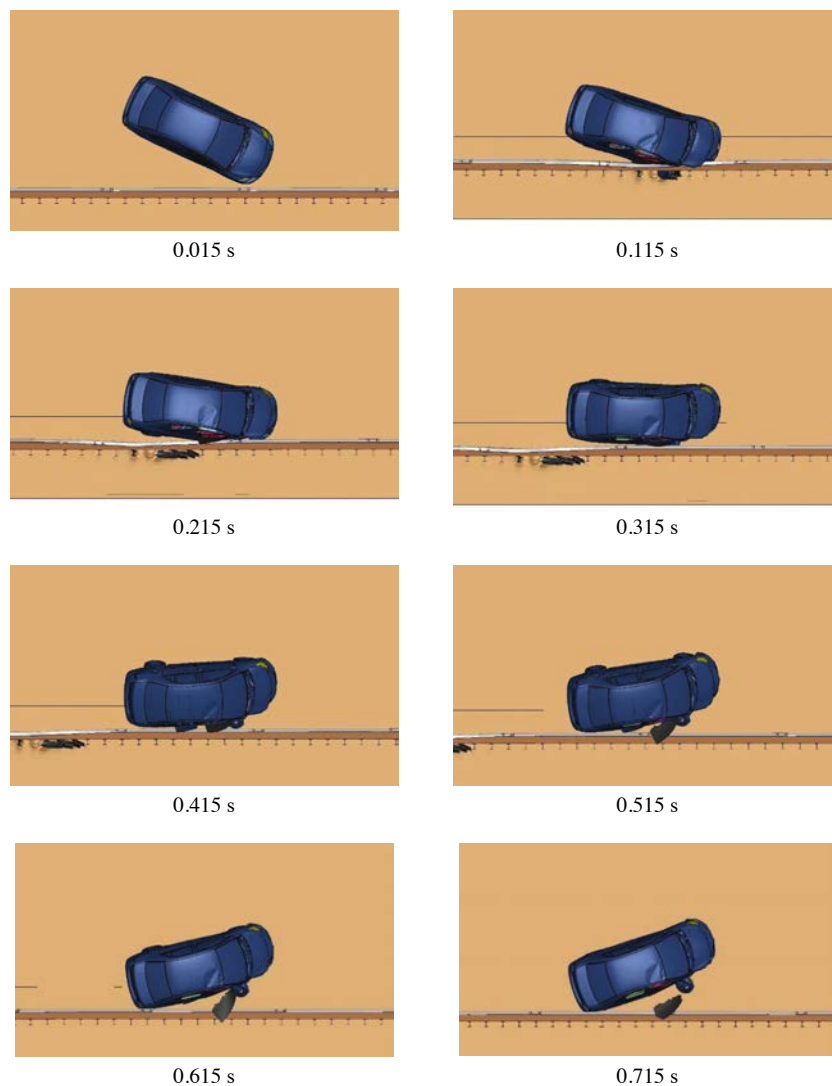


Figure 3.137. *MGS with a combination of quarter-post spacing and HSS8×8× $\frac{1}{4}$ blockout replacement rail – overhead view of MASH Test 3-10.*

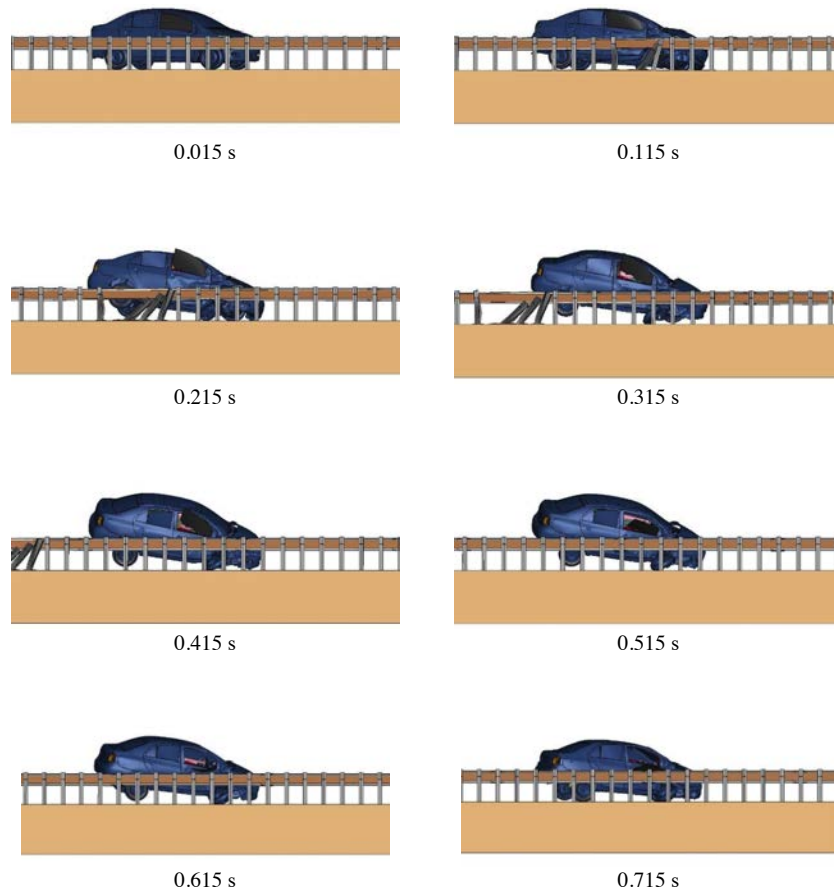


Figure 3.138. MGS with a combination of quarter-post spacing and HS8×8×¼ blockout replacement rail – field-side view of MASH Test 3-10.



Figure 3.139. MGS with a combination of quarter-post spacing and HSS8×8×¼ blackout replacement rail – downstream view of MASH Test 3-10.



Figure 3.140. Overhead view of the transition to MGS with a combination of quarter-post spacing and HSS8×8×¼ blackout replacement rail.

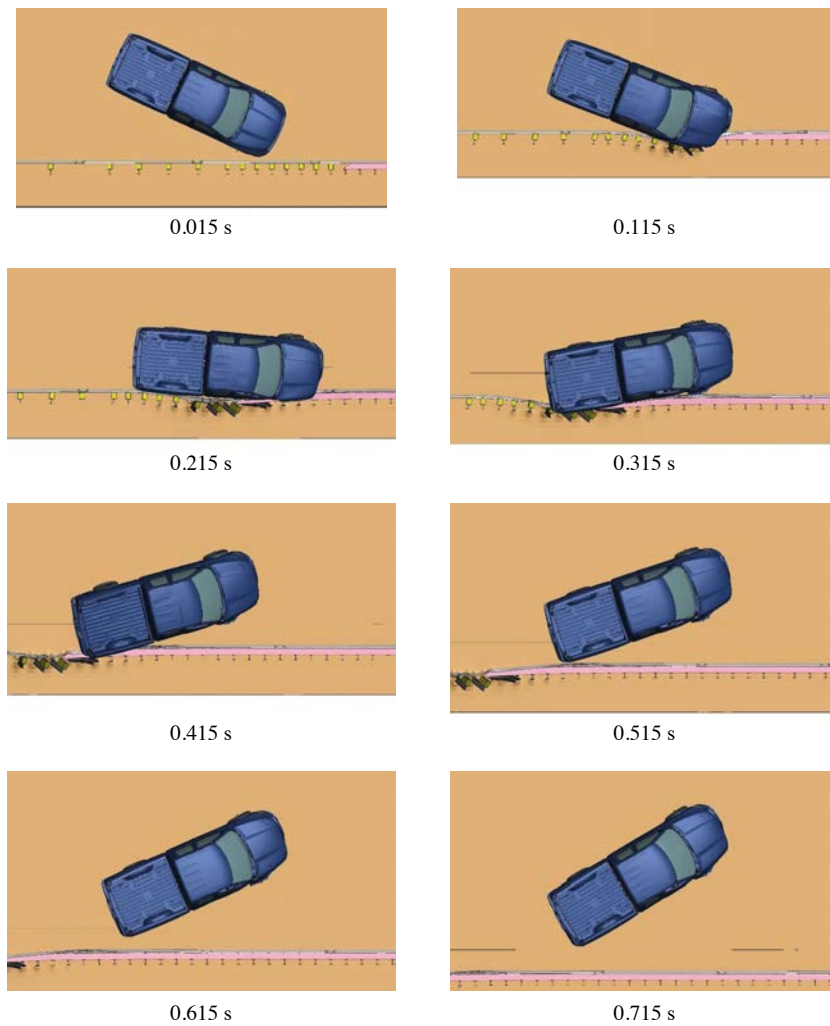


Figure 3.141. Transition to MGS with a combination of quarter-post spacing and HSS8×8×¼ blockout replacement rail – overhead view of MASH Test 3-21.

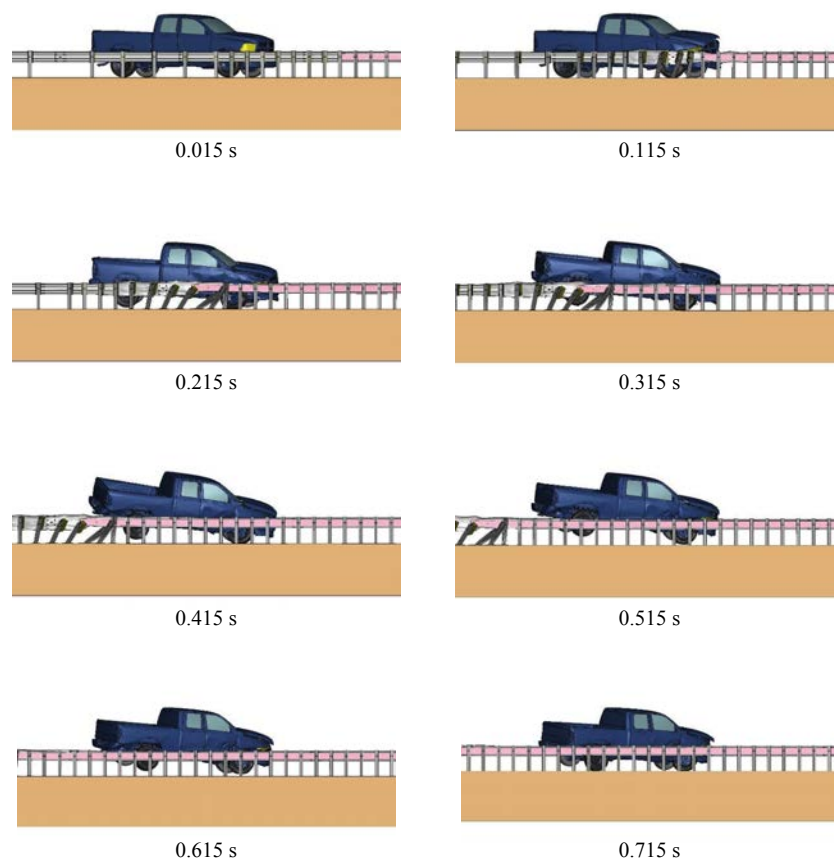


Figure 3.142. Transition to MGS with a combination of quarter-post spacing and HSS8×8×¼ blockout replacement rail – field-side view of MASH Test 3-21.

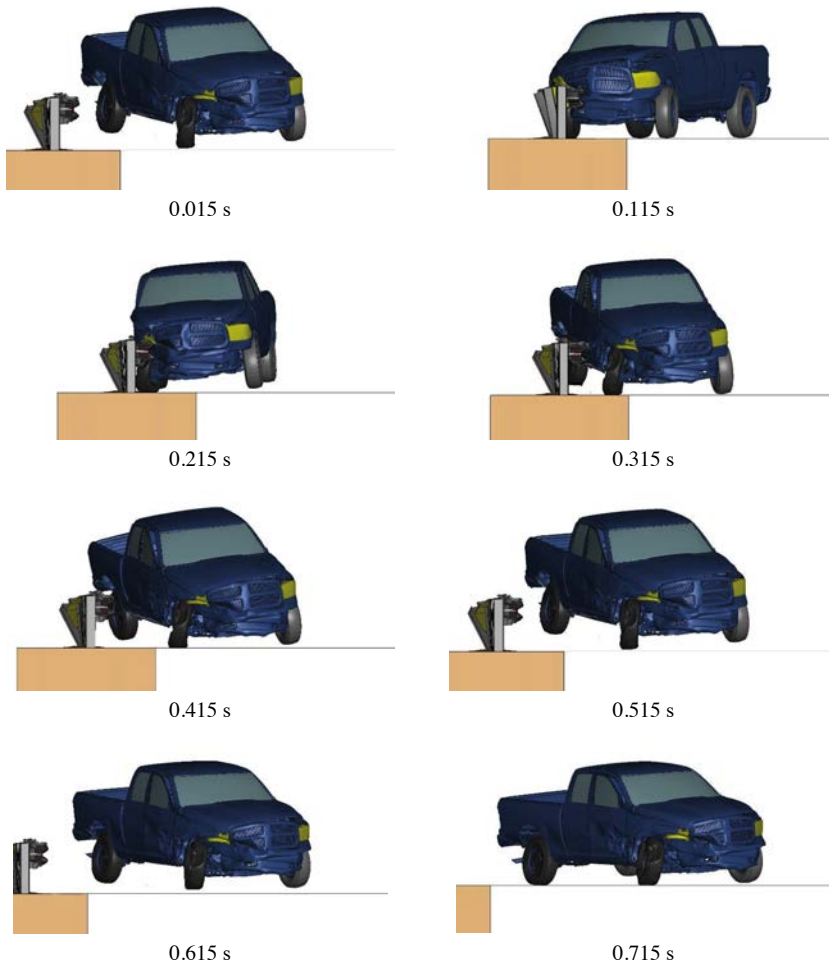


Figure 3.143. Transition to MGS with a combination of quarter-post spacing and HSS8×8×¼ blackout replacement rail – downstream view of MASH Test 3-21.

MASH Test 3-20 Simulation

The transition from standard MGS to the stiffened section is shown in Figure 3.144. This transition includes varying the post spacing adjacent and tapering the edge of the breakout replacement rail.

Figure 3.145, Figure 3.146, and Figure 3.147 show the sequential frames of MASH Test 3-20 on the transition to MGS with a combination of quarter-post spacing and HSS8×8×¼ blackout replacement rail. The OIV was calculated to be 10.1 m/s (maximum limit is 12.0 m/s). The RDA was calculated to be 17.7 g (maximum limit is 20.49 g). This configuration passed MASH Test 3-20 by successfully containing and redirecting the vehicle.

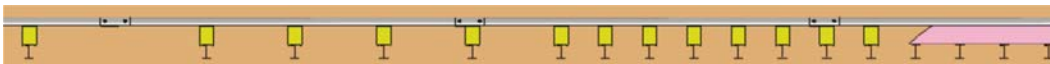


Figure 3.144. Overhead view of the transition to MGS with a combination of quarter-post spacing and HSS8×8×¼ blackout replacement rail.

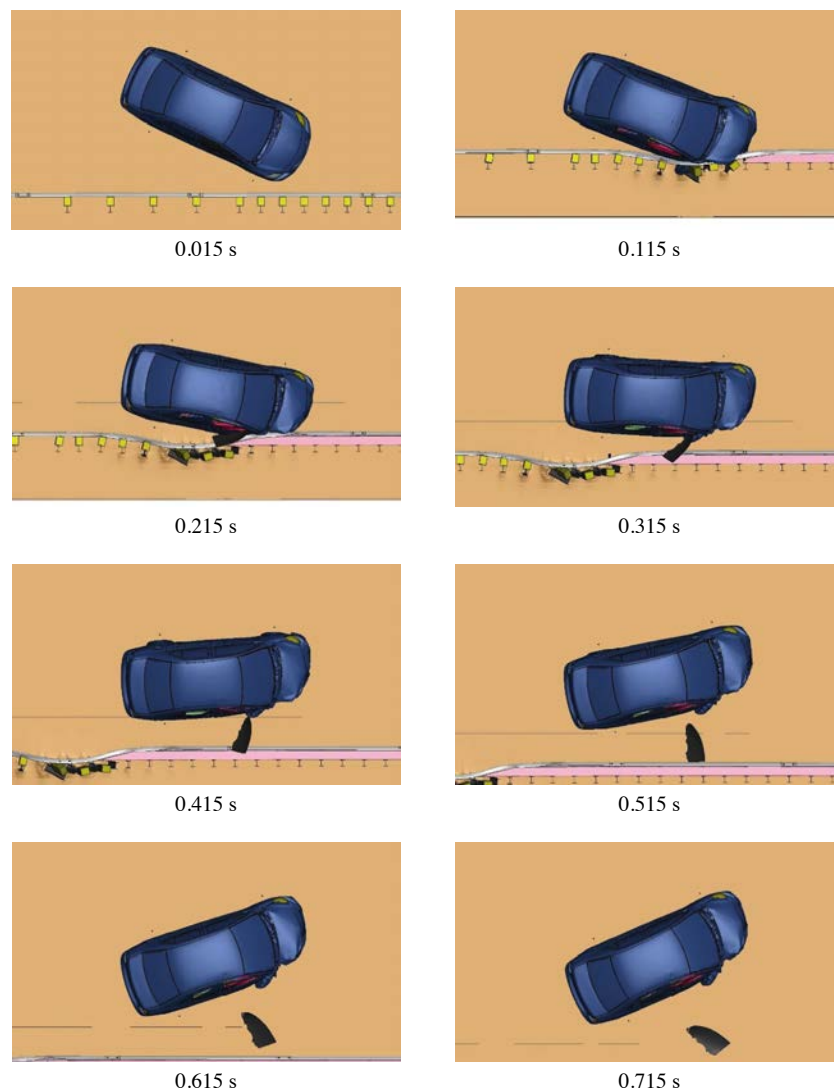


Figure 3.145. Transition to MGS with a combination of quarter-post spacing and HSS8×8×¼ blockout replacement rail – overhead view of MASH Test 3-20.

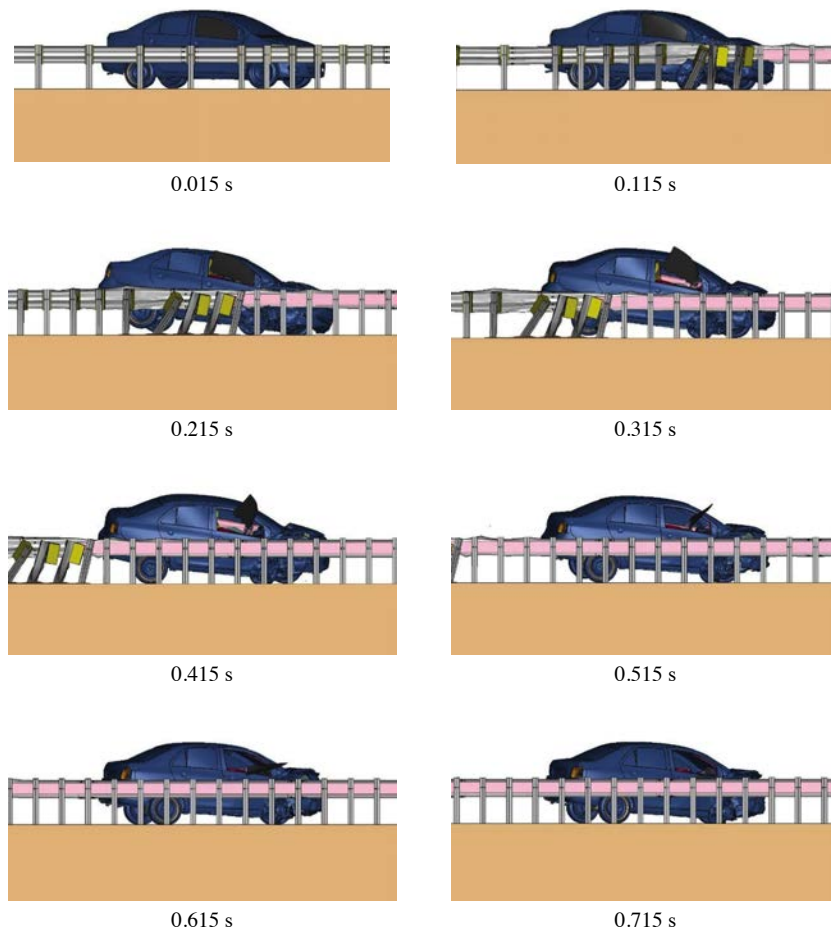


Figure 3.146. Transition to MGS with a combination of quarter-post spacing and HSS8×8×¼ blockout replacement rail – field-side view of MASH Test 3-20.



Figure 3.147. Transition to MGS with a combination of quarter-post spacing and HSS8×8×¼ blockout replacement rail – downstream view of MASH Test 3-20.

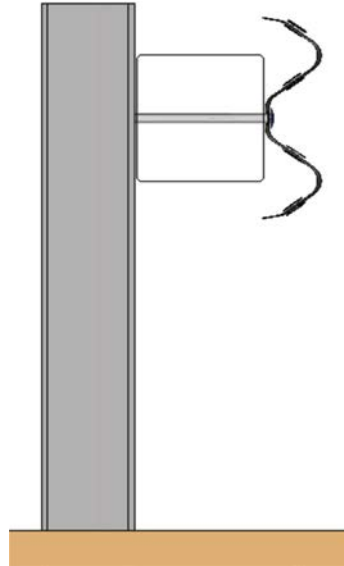


Figure 3.148. Profile view of MGS with a combination of half-post spacing and HSS8×8×³/₁₆ blackout replacement rail.

Combination of Half-Post Spacing and HSS8×8×³/₁₆ Blockout Replacement Rail

The baseline MGS was modified with the inclusion of half-post spacing and an HSS8×8×³/₁₆ blackout replacement rail as shown in Figure 3.148. Full-scale dynamic simulations for MASH Test 3-11 were performed on this system configuration.

MASH Test 3-11 Simulation

Figure 3.149 shows the sequential frames of MASH Test 3-11 on MGS with a combination of half-post spacing and HSS8×8×³/₁₆ blackout replacement rail. In this simulation, the maximum dynamic deflection was 11.1 inches. The OIV was calculated to be 7.8 m/s (preferred limit is 9.1 m/s). The RDA was calculated to be 9.1 g (preferred limit is 15.0 g). This configuration passed MASH Test 3-11 by successfully containing and redirecting the vehicle.

Summary and Conclusions

Based on the stiffening mechanisms chosen after Phase I, the research team performed over 100 computer simulations evaluating the crashworthiness and the deflection-reduction capabilities of a variety of stiffening mechanisms. This effort included computer simulations of MASH Tests 3-11, 3-10, 3-21, and 3-20. Table 3.3 shows a summary of the simulations performed in Phase II. Shaded areas indicate simulations that passed.

Table 3.4 shows a summary of those stiffening mechanisms that were shown to be crashworthy through the computer simulations. The deflection-reducing capability of those crashworthy stiffening mechanisms proved to be wide-ranging. Some of the stiffening mechanisms exhibited limited reductions in deflection for the additional cost beyond a standard MGS. On the other hand, several of the stiffening mechanisms exhibited a high level of deflection reduction, usually accompanied by a larger cost increase. The research team prepared Table 3.5 to show those crashworthy stiffening mechanisms ranked by approximate cost.

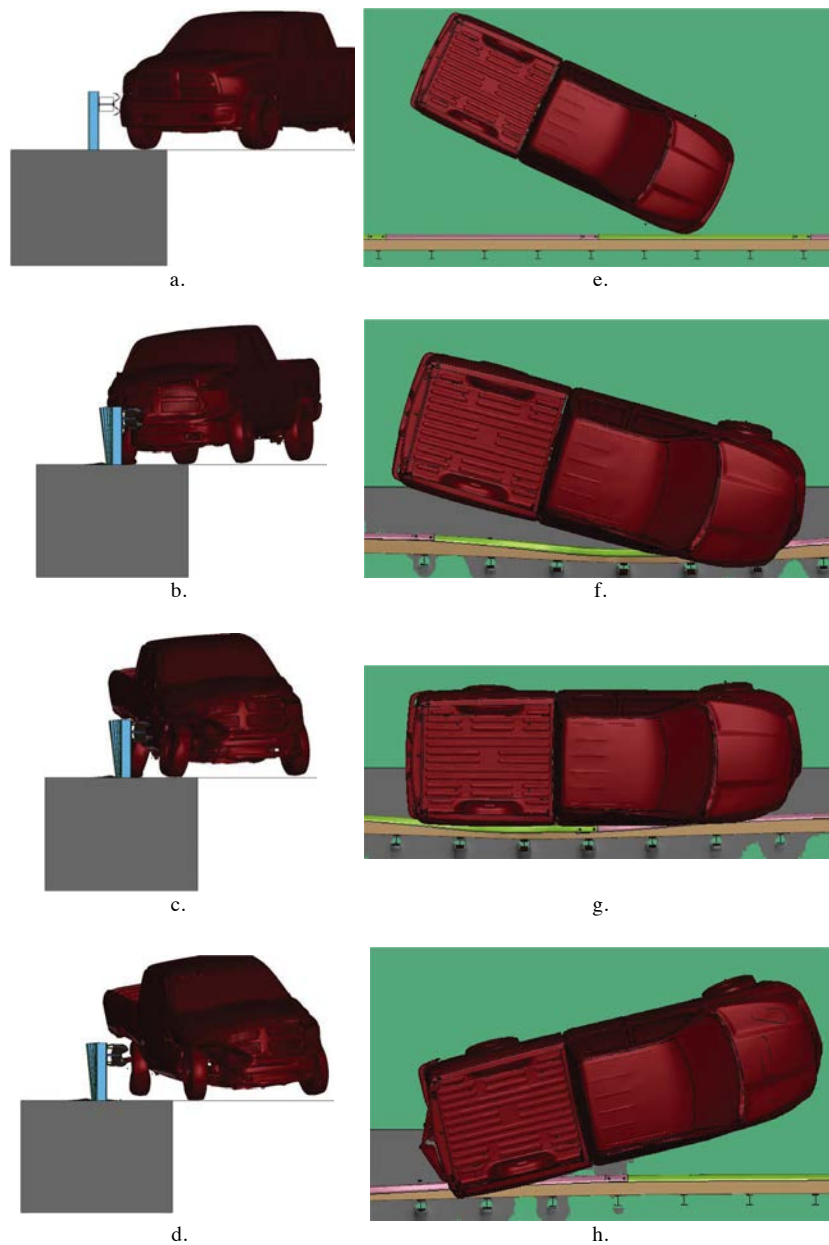


Figure 3.149. MGS with a combination of half-post spacing and HSS8x8x3/16 blockout replacement rail – downstream (left column) and overhead (right column) views of MASH Test 3-11.

Table 3.3. Summary of computer simulations.

Stiffening Mechanism	Stiffening Element	Location	MASH Test 3-11	MASH Test 3-11 Dynamic Deflection (inches)	MASH Test 3-10	MASH Test 3-21	MASH Test 3-20
Baseline	None	N/A	Pass	43.9	—	—	—
Rub Rail	C6x8.2	12 inches above grade	Pass	34.7	DNS	DNS	DNS
	C6x8.2	6 inches above grade	Pass	36.0	DNS	DNS	DNS
	HSS4x4x1/4	12 inches above grade	Fail	NA	NA	NA	NA
	HSS4x4x1/4	6 inches above grade	Fail	NA	NA	NA	NA
	HSS10x10x1/4	12 inches above grade	Fail	NA	NA	NA	NA
	8HU12x135	8 inches above grade	Fail	NA	NA	NA	NA
	10HU5x075	12 inches above grade	Pass	31.5	DNS	DNS	DNS
10-Guage	10-guage rail	NA	Pass	39.2	Pass	Pass	DNS
Backup Rail	C6x8.2	Centerline of W-beam	Pass	36.4	DNS	DNS	DNS
	C6x8.2	17.5 inches above grade	Fail	NA	NA	NA	NA
	C6x8.2	12 inches above grade	Pass	38.8	DNS	DNS	DNS
	HSS4x4x1/4	17.5 inches above grade	Pass	31.1	DNS	DNS	DNS
	HSS4x4x1/4	12 inches above grade	Fail	NA	NA	NA	NA
	HSS4x4x1/4	Centerline Of W-beam	Pass	33.7	Pass	DNS	DNS
	HSS5x5x5/16	Centerline of W-beam	Fail	NA	NA	NA	NA
	HSS6x6x3/8	Centerline of W-beam	Pass	23.5	Fail	NA	NA
	HSS10x10x1/4	Centerline of W-beam	Fail	NA	NA	NA	NA
	10HU5x075	Centerline of W-beam	Fail	NA	NA	NA	NA
	8HU12x135	Centerline of W-beam	Pass	25.4	Pass	DNS	DNS
	HSS8x8x1/4	Blockout replacement	Pass	15.4	Pass	Pass	Pass
	HSS8x8x1/4	Blockout replacement	Pass	15.4	Pass	Pass	Pass
Reduced Post Spacing	Half-post spacing	NA	Pass ^a	25.6 ^a	NC	Pass	NC
	Quarter-post spacing	NA	Pass ^a	19.5 ^a	Pass ^a	Pass ^a	NC
Combination	Half-post spacing and HSS4x4x1/4	Centerline of W-beam	Fail	NA	NA	NA	NA
	Quarter-post spacing and HSS4x4x1/4	Centerline of W-beam	Pass	10.1	Pass	Pass	Pass
	Half-post spacing and HSS8x8x1/4 blockout replacement	Blockout replacement	Pass	10.0	DNS	DNS	DNS
	Quarter-post spacing and HSS8x8x1/4 blockout replacement	Blockout replacement	Pass	7.4	Pass	Pass	Pass
	Half-post spacing and HSS8x8x3/16 blockout replacement	Blockout replacement	Pass	11.1	DNS	DNS	DNS

NOTE: — = not included in this comparison; DNS = Did not simulate; NA = Not applicable; NC = Justified as not critical.

^aDenotes results from physical crash test rather than simulation.

Table 3.4. Summary of successful computer simulations.

Stiffening Mechanism	Stiffening Element	Location	MASH Test 3-11	MASH Test 3-11 Dynamic Deflection (inches)	MASH Test 3-10	MASH Test 3-21	MASH Test 3-20
Baseline	None	NA	Pass	43.9	—	—	—
Rub Rail	C6x8.2	12 inches above grade	Pass	34.7	DNS	DNS	DNS
	C6x8.2	6 inches above grade	Pass	36.0	DNS	DNS	DNS
	10HU5x075	12 inches above grade	Pass	31.5	DNS	DNS	DNS
10-Guage	10-guage rail	NA	Pass	39.2	Pass	Pass	DNS
Backup Rail	C6x8.2	Centerline of W-beam	Pass	36.4	DNS	DNS	DNS
	C6x8.2	12 inches above grade	Pass	38.8	DNS	DNS	DNS
	HSS4x4x1/4	17.5 inches above grade	Pass	31.1	DNS	DNS	DNS
	HSS4x4x1/4	Centerline of W-beam	Pass	33.7	Pass	DNS	DNS
	8HU12x135	Centerline of W-beam	Pass	25.4	Pass	DNS	DNS
	HSS8x8x1/4	Blockout replacement	Pass	15.4	Pass	Pass	Pass
Reduced Post Spacing	Half-post spacing	NA	Pass ^a	25.6 ^a	NC	Pass	NC
	Quarter-post spacing	NA	Pass ^a	19.5 ^a	Pass ^a	Pass ^a	NC
Combination	Half-post spacing and HSS8x8x3/16 blockout replacement	Blockout replacement	Pass	11.1	DNS	DNS	DNS
	Quarter-post spacing and HSS4x4x1/4	Centerline of W-beam	Pass	10.1	Pass	Pass	Pass
	Half-post spacing and HSS8x8x1/4 blockout replacement	Blockout replacement	Pass	10.0	DNS	DNS	DNS
	Quarter-post spacing and HSS8x8x1/4 blockout replacement	Blockout replacement	Pass	7.4	Pass	Pass	Pass

NOTE: — = not included in this comparison; DNS = Did not simulate; NA = Not applicable; NC = Justified as not critical.
^aDenotes results from physical crash test rather than simulation.

The benefits and disadvantages of the numerous stiffening mechanisms were discussed. Much of these discussions centered on the cost efficiency of the stiffening mechanism in relation to its ability to reduce dynamic deflections. While the combination of quarter-post spacing and the HSS8x8x¼ blockout replacement tube provided the largest reduction in dynamic deflection, it was also the most costly to install. Consequently, it was decided to crash test the combination of half-post spacing and an HSS8x8x¾ blockout replacement tube. This combination provided a significant reduction in dynamic deflection while also costing less than the most extensive stiffening mechanism.

When the combination of half-post spacing and an HSS8x8x¾ blockout replacement tube was selected, a transition to this system had not been evaluated through computer simulation. Consequently, the research team recommended utilizing the same transition as was developed with the combination of quarter-post spacing and an HSS8x8x¼ blockout replacement tube. The simulations predicted that the transition from standard MGS to the combination of quarter-post

Table 3.5. Summary of successful computer simulations sorted by approximate cost.

Stiffening Mechanism	Stiffening Element	Location	MASH Test 3-11 Dynamic Deflection (inches)
10-Gauge	10-gauge rail	NA	39.2
Rub Rail	C6x8.2	12 inches above grade	34.7
	C6x8.2	6 inches above grade	36.0
	10HU5x075	12 inches above grade	31.5
Backup Rail	C6x8.2	Centerline of W-beam	36.4
	C6x8.2	12 inches above grade	38.8
	HSS4x4x1/4	17.5 inches above grade	31.1
	HSS4x4x1/4	Centerline of W-beam	33.7
	8HU12x135	Centerline of W-beam	25.4
	HSS8x8x1/4	Blockout replacement	15.4
Reduced Post Spacing	Half-post spacing	NA	25.6 ^a
Combination	Half-post spacing and HSS8x8x3/16 blockout replacement	Blockout replacement	11.1
	Half-post spacing and HSS8x8x1/4 blockout replacement	Blockout replacement	10.0
Reduced Post Spacing	Quarter-post spacing	NA	19.5 ^a
Combination	Quarter-post spacing and HSS4x4x1/4	Centerline of W-beam	10.1
	Quarter-post spacing and HSS8x8x1/4 blockout replacement	Blockout replacement	7.4

NOTE: Table sorted from baseline cost at the top to the largest approximate increase in cost at the bottom. Bold separation lines indicate larger changes in cost. NA = not applicable.
^aDenotes results from physical crash test rather than simulation.

spacing and the HSS8×8×¼ blockout replacement tube was crashworthy. Therefore, the research team concluded that the same transition would also work with the half-post spacing and an HSS8×8×⅜ blockout replacement tube, which was less critical from a difference in stiffness perspective. Consequently, the research team evaluated this transition through full-scale crash testing as presented later in this report.

The research team also discussed several details of the blockout replacement tube installation. First, the termination of the blockout replacement tube, specifically the snagging potential and connections with the posts, was considered. Several variations of terminating the blockout replacement tube were considered through the analysis and computer simulation efforts, including bolting conditions and slope of the end cut. The details shown in Figure 3.197 are the final condition that was evaluated through MASH crash testing and presented later in this report. The referenced Note 2b in Figure 3.150 states the rail is not attached to the post with a bolt.

Splicing the blockout replacement tube was also discussed. The research team chose to not explicitly model splice designs in the computer simulation effort to maximize resources for evaluating as many stiffening mechanisms as possible. Consequently, the research team designed a splice detail that is akin to many bridge-rail designs. The splice detail incorporated an interior steel sleeve that is slid inside the blockout replacement tube. This tube is held in place by

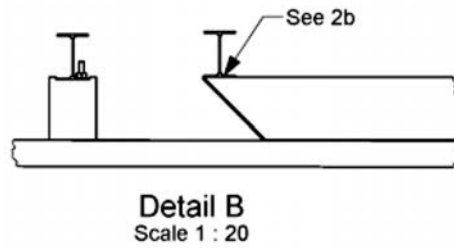


Figure 3.150. End termination of the blackout replacement tube.

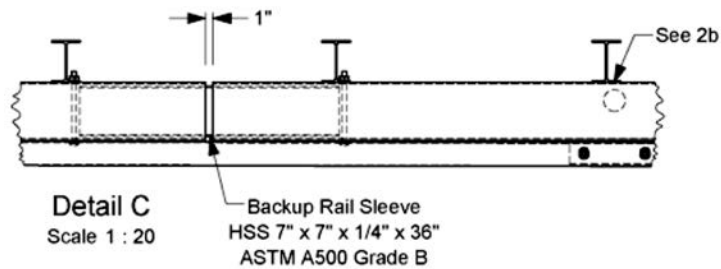


Figure 3.151. End termination of the blackout replacement tube.

the two nearest guardrail bolts and, therefore, no pins or similar elements typically seen on bridge-rail splices are needed. Figure 3.151 shows a detail of the splice design.

Last, the team discussed the crash testing matrix for evaluating this system and chose to evaluate the stiffened MGS and the transition to the full MASH testing matrix. Therefore, four crash tests were chosen: 3-11, 3-10, 3-21, and 3-20. The next chapters discuss the crash testing efforts and results.

System Details

Test Article and Installation Details for Stiffened MGS

The installation consisted of 75 feet of W6×8.5 steel guardrail posts spaced at half-post spacing (37.5 inches) with an HSS8×8× $\frac{3}{16}$ ASTM A500 Grade B blackout replacement tube. The W-beam guardrail was mounted at 31 inches above grade measured to the top of the guardrail. Preceding the half-post spacing section was a 37-foot 6-inch section of W-beam guardrail mounted to timber blockouts on W6×8.5 steel guardrail posts spaced at 75 inches. On the downstream end of the length of need (LON) was a 31-foot 3-inch section of W-beam guardrail mounted to timber blockouts on W6×8.5 steel guardrail posts spaced at 75 inches. Each end of the installation terminated with a steel-post terminal. The total length of the installation was 168 feet 9 inches.

Figure 4.1 presents the overall information on the stiffened MGS for tests 612941-02-1 and 612941-02-2 (MASH Tests 3-11 and 3-10 respectively), and Figure 4.2 through Figure 4.5 provide photographs of the installation. Appendix A.1 provides further details on the stiffened MGS. Drawings were provided by the TTI Proving Ground, and construction was performed by MBC Management and supervised by TTI Proving Ground personnel.

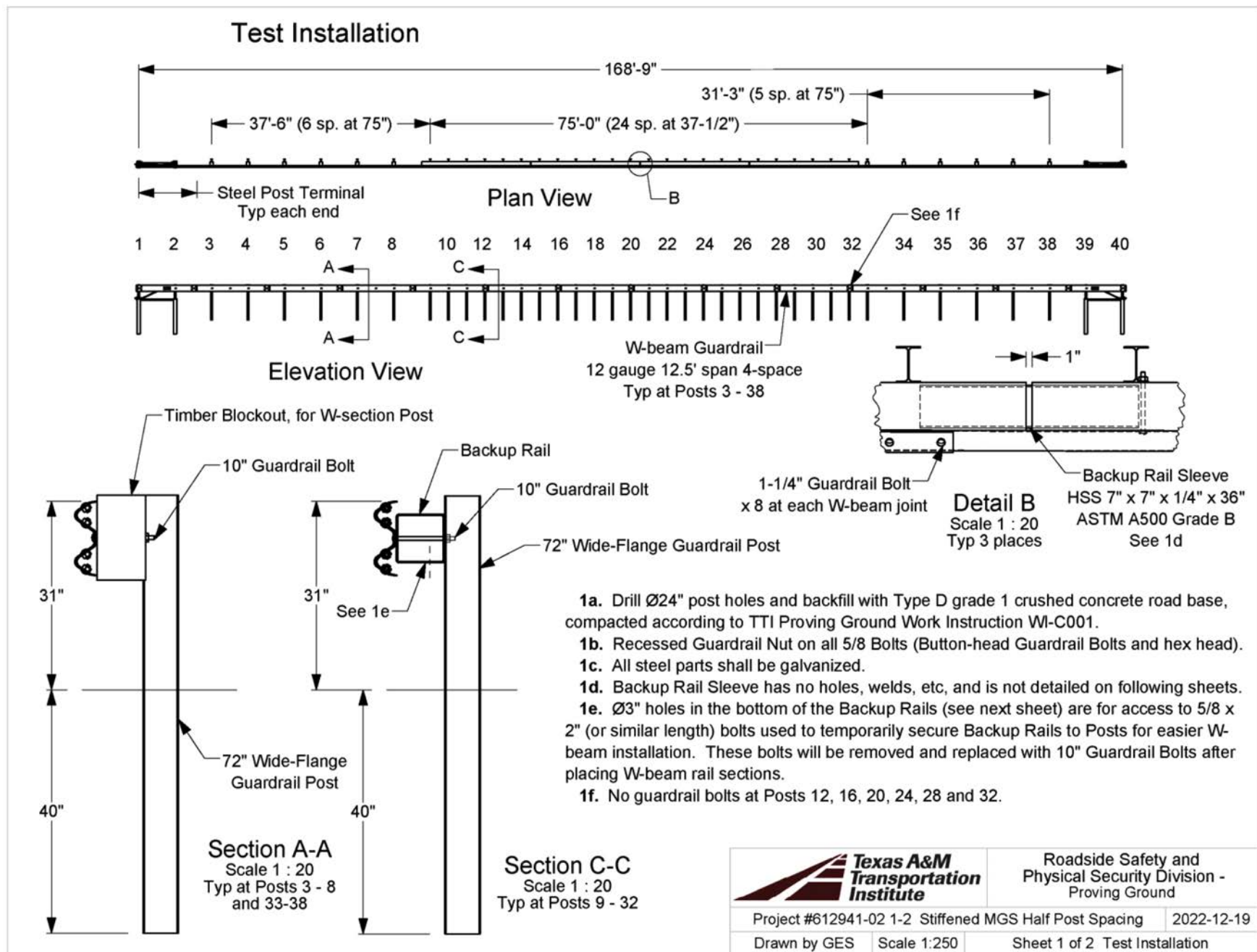
Test Article and Installation Details for Stiffened MGS Transition

For transition tests 612941-02-3 and 612941-02-4 (MASH Tests 3-21 and 3-20, respectively), the overall length was 168 feet 9 inches. The transition incorporated varying post spacing starting with full-post spacing (75 inches) at the upstream end, followed by half- (37.5) and quarter- (18.75 inches) post spacing, and finally, the start of the half-post spacing was combined with the blackout replacement tube. This steel tube incorporated an angular cut to mitigate interaction with the test vehicle.

Figure 4.6 presents the overall information on the stiffened MGS transition, and Figure 4.7 through Figure 4.10 provide photographs of the installation. Appendix A.2 provides further details on the stiffened MGS transition. Drawings were provided by the Texas A&M TTI Proving Ground, and construction was performed by MBC Management and supervised by TTI Proving Ground personnel.

Design Modifications During Tests

No modifications were made to the test installation during testing.



Q:\Accreditation-17025-2017\EIR-000 Project Files\612941-02 - Stiffened MGS - Kovar\612941-02-1 3-11\Drafting, 612941-02 1-2\612941-02 1-2 Drawing

Figure 4.1. Details of stiffened MGS for crash tests 612941-02-1 and 612941-02-2.



Figure 4.2. *Stiffened MGS prior to tests 612941-02-1 and 612941-02-2.*



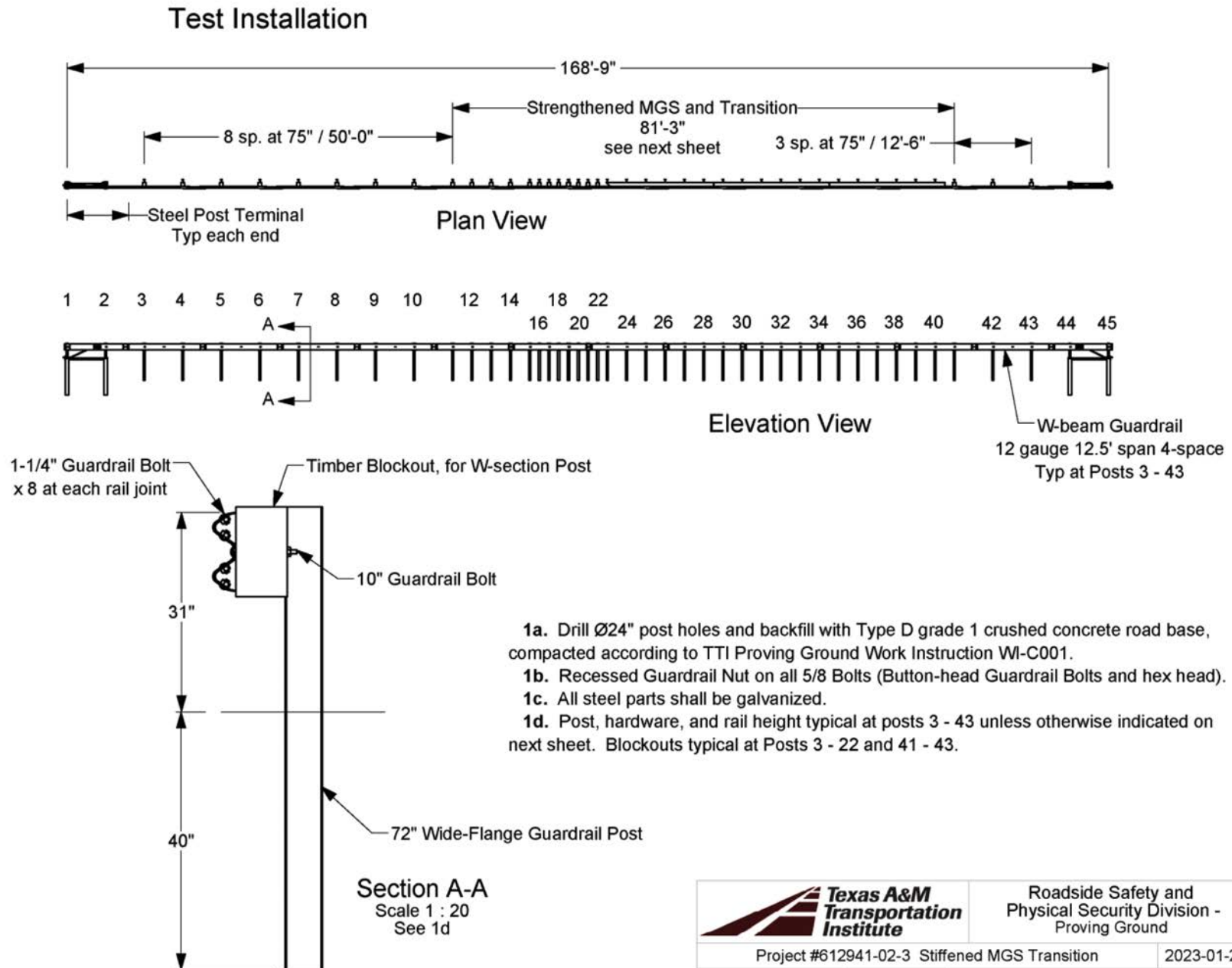
Figure 4.3. *In-line view of the stiffened MGS prior to tests 612941-02-1 and 612941-02-2.*



Figure 4.4. *Field-side view of the stiffened MGS prior to testing.*



Figure 4.5. *Field-side view of the LON on the stiffened MGS prior to tests 612941-02-1 and 612941-02-2.*



S:\Accreditation-17025-2017\EIR-000 Project Files\612941-02 - Stiffened MGS - Kovar\612941-02-3 3-21\Drafting, 612941-02-3\612941-02-3 Drawing

Figure 4.6. Details of stiffened MGS for crash tests 612941-02-3 and 612941-02-4.



Figure 4.7. *Stiffened MGS transition prior to tests 612941-02-3 and 612941-02-4.*



Figure 4.8. *In-line view of the stiffened MGS transition prior to Testing 612941-02-3 and 612941-02-4.*



Figure 4.9. *Field side of the stiffened MGS transition prior to tests 612941-02-3 and 612941-02-4.*



Figure 4.10. *Close-up of the field side of the stiffened MGS transition prior to tests 612941-02-3 and 612941-02-4.*

Material Specifications

Appendix B provides material certification documents for the materials used to install and construct the stiffened MGS and transition.

Soil Conditions

The test installation was installed in standard soil meeting Type D Grade 1 of AASHTO standard specification M147-17, “Materials for Aggregate and Soil Aggregate Subbase, Base, and Surface Courses.”

In accordance with MASH (3), Appendix B, soil strength was measured on the day of the crash test. During the installation of the stiffened MGS for full-scale crash testing, two 6-ft-long W6x16 posts were installed in the immediate vicinity of the stiffened MGS using the same fill materials and installation procedures used in the test installation and the standard dynamic test.

Table 4.1. Soil strength prior to test 612941-02-2.

Displacement (inches)	Minimum Load (lb)	Actual Load (lb)
5	4,420	5,787
10	4,981	7,484
15	5,282	8,363

Table 4.2. Soil strength prior to test 612941-02-1.

Displacement (inches)	Minimum Load (lb)	Actual Load (lb)
5	4,420	5,667
10	4,981	6,212
15	5,282	6,332

Table 4.3. Soil strength prior to test 612941-02-3.

Displacement (inches)	Minimum Load (lb)	Actual Load (lb)
5	4,420	6,303
10	4,981	8,242
15	5,282	10,030

Table 4.4. Soil strength prior to test 612941-02-4.

Displacement (inches)	Minimum Load (lb)	Actual Load (lb)
5	4,420	10,500
10	4,981	11,500
15	5,282	—

MASH Appendix B, Table B.1, presents minimum soil strength properties established through the dynamic testing performed in accordance with MASH Appendix B.

On the day of MASH Test 3-10 (January 6, 2023), the backfill material in which the stiffened MGS was installed, met minimum MASH requirements for soil strength. The minimum and actual post loads are shown in Table 4.1

On the day of MASH Test 3-11 (December 16, 2022), the backfill material in which the stiffened MGS was installed met minimum MASH requirements for soil strength. The minimum and actual post loads are shown in Table 4.2.

On the day of MASH Test 3-21 (January 27, 2023), the backfill material in which the stiffened MGS transition was installed met minimum MASH requirements for soil strength. The minimum and actual post loads are shown in Table 4.3.

On the day of MASH Test 3-20 (March 15, 2023), the backfill material in which the stiffened MGS transition was installed met minimum MASH requirements for soil strength. The minimum and actual post loads are shown in Table 4.4. The actual load at the 15-inch displacement was not measured due to exceeding the high-value safety limits (load cell safety limits) beyond 10 inches.

Test Requirements and Evaluation Criteria

Crash Test Performed/Matrix

Table 5.1 shows the test conditions and evaluation criteria for MASH TL-3 for longitudinal barriers. The target critical impact points (CIPs) for each test were determined using the information provided in MASH Section 2.3.2 (3) and computer simulation. Figure 5.1 shows the target CIP for MASH Tests 3-10 and 3-11 on the stiffened MGS and MASH Tests 3-20 and 3-21 on the stiffened MGS transition.

The crash tests and data analysis procedures were in accordance with guidelines presented in MASH (3). Chapter 6 presents brief descriptions of these procedures.

Evaluation Criteria

The appropriate safety evaluation criteria from Tables 2.2 and 5.1, both of MASH, were used to evaluate the crash tests reported herein. While Table 5.1 herein lists the test conditions and evaluation criteria required for MASH TL-3, Table 5.2 provides detailed information on the evaluation criteria.

Table 5.1. Test conditions and evaluation criteria specified for MASH TL-3 longitudinal barriers.

Test Designation	Test Vehicle	Impact Speed	Impact Angle	Evaluation Criteria ^a
MASH Test 3-10	1100C	62 mi/h	25°	A, D, F, H, I
MASH Test 3-11	2270P	62 mi/h	25°	A, D, F, H, I
MASH Test 3-20	1100C	62 mi/h	25°	A, D, F, H, I
MASH Test 3-21	2270P	62 mi/h	25°	A, D, F, H, I

^aEvaluation criteria are explained in Table 5-2.

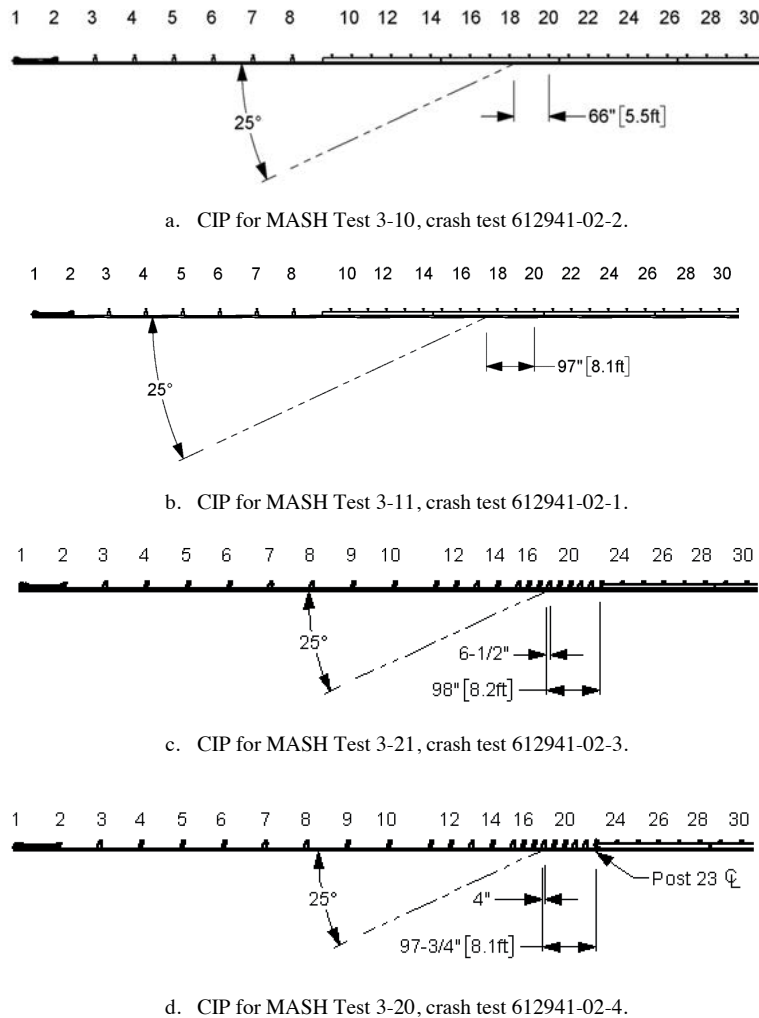


Figure 5.1. Target CIP for MASH TL-3 tests on stiffened MGS and stiffened MGS transition. CL = centerline.

Table 5.2. Evaluation criteria required for MASH testing.

Evaluation Factors	Evaluation Criteria
A.	Test article should contain and redirect the vehicle or bring the vehicle to a controlled stop; the vehicle should not penetrate, underide, or override the installation although controlled lateral deflection of the test article is acceptable.
D.	Detached elements, fragments, or other debris from the test article should not penetrate or show potential for penetrating the occupant compartment, or present undue hazard to other traffic, pedestrians, or personnel in a work zone. Deformations of, or intrusions into, the occupant compartment should not exceed limits set forth in Section 5.2.2 and Appendix E of MASH.
F.	The vehicle should remain upright during and after collision. The maximum roll and pitch angles are not to exceed 75 degrees.
H.	Occupant impact velocities (OIV) should satisfy the following limits: Preferred value of 30 ft/s or maximum allowable value of 40ft/s.
I.	The occupant ridedown accelerations (RDA) should satisfy the following: Preferred value of 15.0 g or maximum allowable value of 20.49 g.

Test Conditions

Test Facility

The full-scale crash tests reported herein were performed at the TTI Proving Ground, an International Standards Organization (ISO)/International Electrotechnical Commission (IEC) 17025-accredited laboratory with American Association for Laboratory Accreditation (A2LA) Mechanical Testing Certificate 2821.01. The full-scale crash tests were performed according to TTI Proving Ground quality procedures as well as MASH guidelines and standards.

The TTI Proving Ground is located on The Texas A&M University System RELLIS Campus, which consists of a 2,000-acre complex of research and training facilities situated 10 miles northwest of the flagship campus of Texas A&M University. The site, formerly a United States Army Air Corps base, has large expanses of concrete runways and parking aprons well suited for experimental research and testing in the areas of vehicle performance and handling, vehicle-roadway interaction, highway pavement durability and efficacy, and roadside safety hardware and perimeter protective device evaluation. The sites selected for construction and testing are along the edge of an out-of-service apron. The apron consists of an unreinforced, jointed-concrete pavement in 12.5-foot by 15-foot blocks nominally 6 inches deep. The aprons were built in 1942, and the joints have some displacement but are otherwise flat and level.

Vehicle Tow and Guidance System

Each test vehicle was towed into the test installation using a steel cable guidance and reverse tow system. A steel cable for guiding the test vehicle was tensioned along the path, anchored at each end, and threaded through an attachment to the front wheel of the test vehicle. An additional steel cable was connected to the test vehicle, passed around a pulley near the impact point and through a pulley on the tow vehicle, and then anchored to the ground such that the tow vehicle moved away from the test site. A 2:1 speed ratio between the test and tow vehicle existed with this system. Just before impact with the installation, the test vehicle was released and ran unrestrained. The vehicle remained freewheeling (i.e., no steering or braking inputs) until it cleared the immediate area of the test site.

Data Acquisition Systems

Vehicle Instrumentation and Data Processing

Each test vehicle was instrumented with a self-contained, onboard data acquisition system (DAS). The signal conditioning and acquisition system is a multichannel DAS produced by Diversified Technical Systems, Inc. The accelerometers, which measure the x, y, and z axes of

vehicle acceleration, are strain gauge type with linear millivolt output proportional to acceleration. Angular rate sensors, measuring vehicle roll, pitch, and yaw rates, are ultra-small, solid-state units designed for crash test service. The data acquisition hardware and software conform to the latest SAE J211 (Instrumentation for Impact Test). Each of the channels is capable of providing precision amplification, scaling, and filtering based on transducer specifications and calibrations. During the test, data are recorded from each channel at a rate of 10,000 samples per second with a resolution of 1 part in 65,536. Once data are recorded, internal batteries back these up inside the unit in case the primary battery cable is severed. Initial contact with the pressure switch on the vehicle bumper provides a time-zero mark and initiates the recording process. After each test, the data are downloaded from the DAS unit into a laptop computer at the test site. The Test Risk Assessment Program (TRAP) software then processes the raw data to produce detailed reports of the test results.

Each DAS is returned to the factory annually for complete recalibration and to ensure that all instrumentation used in the vehicle conforms to the specifications outlined by SAE J211. All accelerometers are calibrated annually using an ENDEVCO 2901 precision primary vibration standard. This standard and its support instruments are checked annually and receive a National Institute of Standards and Technology (NIST) traceable calibration. The rate transducers used in the DAS receive calibration via a Genisco Rate-of-Turn table. The subsystems of each data channel are also evaluated annually, using instruments with current NIST traceability, and the results are factored into the accuracy of the total data channel per SAE J211. Calibrations and evaluations are also made anytime data are suspect. Acceleration data are measured with an expanded uncertainty of $\pm 1.7\%$ at a confidence factor of 95% ($k = 2$).

TRAP uses the DAS-captured data to compute the occupant and compartment impact velocities, time of occupant and compartment impact after vehicle impact, and highest 10-millisecond (ms) average RDA. TRAP calculates the change in vehicle velocity at the end of a given impulse period. In addition, maximum average accelerations over 50-ms intervals in each of the three directions are computed. For reporting purposes, the data from the vehicle-mounted accelerometers are filtered with an SAE Class 180-Hz low-pass digital filter, and acceleration versus time curves for the longitudinal, lateral, and vertical directions are plotted using TRAP.

TRAP uses the data from the yaw, pitch, and roll rate transducers to compute angular displacement in degrees at 0.0001-s intervals and then plots yaw, pitch, and roll versus time. These displacements are in reference to the vehicle-fixed coordinate system with the initial position and orientation being the initial impact. The rate of rotation data are measured with an expanded uncertainty of $\pm 0.7\%$ at a confidence factor of 95% ($k = 2$).

Anthropomorphic Dummy Instrumentation

An Alderson Research Laboratories Hybrid II, 50th percentile male anthropomorphic dummy, restrained with lap and shoulder belts, was placed in the front seat on the impact side of the 1100C vehicles. The dummy was not instrumented.

According to MASH, use of a dummy in the 2270P vehicle is optional; no dummy was used in the tests with the 2270P vehicle.

Photographic Instrumentation Data Processing

Photographic coverage of each test included three digital high-speed cameras:

- One located overhead with a field of view perpendicular to the ground and directly over the impact point.

- A second placed upstream from the installation at an angle to allow a field of view of the interaction of the rear of the vehicle with the installation.
- A third placed with a field of view parallel to and aligned with the installation at the downstream end.

A flashbulb on the impacting vehicle was activated by a pressure-sensitive tape switch to indicate the instant of contact with the test article. The flashbulb was visible from each camera. The video files from these digital high-speed cameras were analyzed to observe phenomena occurring during the collision and to obtain time-event, displacement, and angular data. A digital camera recorded and documented the conditions of each test vehicle and the installation before and after the test.



CHAPTER 7

MASH Test 3-10 (Crash Test No. 612941-02-2)

Test Designation and Actual Impact Conditions

See Table 7.1 for details on MASH impact conditions for this test and Table 7.2 for the exit parameters. Figure 7.1 and Figure 7.2 depict the target impact setup.

Weather Conditions

Table 7.3 provides the weather conditions for test 612941-02-2.

Test Vehicle

Figure 7.3 and Figure 7.4 show the 2017 Nissan Versa used for the crash test. Table 7.4 shows the vehicle measurements. Figure C.1 in Appendix C gives additional dimensions and information on the vehicle.

Table 7.1. Impact conditions for MASH Test 3-10, test 612941-02-2.

Test Parameter	Specification	Tolerance	Measured
Impact Speed (mi/h)	62	± 2.5	63.2
Impact Angle (deg)	25	± 1.5	25.6
Impact Severity (kip-ft)	51	≥ 51.0	60.9
Impact Location	5.5 ft upstream from the centerline of post 20	± 1 ft	5.5 ft upstream from the centerline of post 20

Table 7.2. Exit parameters for MASH Test 3-10, test 612941-02-2.

Exit Parameter	Measured
Speed (mi/h)	44.80
Trajectory (deg)	5.90
Heading (deg)	7.00
Brakes Applied Post-Impact (s)	3.75
Vehicle at Rest Position	<ul style="list-style-type: none">• 229 ft downstream of impact point.• 73 ft to the traffic side.• 20° right.
Comments	<ul style="list-style-type: none">• Vehicle remained upright and stable.• Vehicle crossed the exit box^a 45 ft downstream from loss of contact.

^aNot less than 32.8 ft downstream from loss of contact for cars and pickups is optimal.



Figure 7.1. Stiffened MGS and test vehicle geometrics for test 612941-02-2.



Figure 7.2. Stiffened MGS and test vehicle impact location for 612941-02-2.

Table 7.3. Weather conditions for test 612941-02-2.

Date of Test	January 6, 2023
Wind Speed (mi/h)	8
Wind Direction (deg)	168
Temperature (°F)	66
Relative Humidity (%)	84
Vehicle Traveling (deg)	325



Figure 7.3. Impact side of test vehicle before test 612941-02-2.



Figure 7.4. Opposite impact side of test vehicle before test 612941-02-2.

Table 7.4. Vehicle measurements for test 612941-02-2.

Test Parameter	MASH	Allowed Tolerance	Measured
Dummy (if applicable) ^a (lb)	165	NA	165.0
Inertial Weight (lb)	2,420	±55	2,441.0
Gross Static ^a (lb)	2,585	±25	2,606.0
Wheelbase (inches)	98	±5	102.4
Front Overhang (inches)	35	±4	32.5
Overall Length (inches)	169	±8	175.4
Overall Width (inches)	65	±3	66.7
Hood Height (inches)	28	±4	30.5
Track Width ^b (inches)	59	±2	58.4
CG Aft of Front Axle ^c (inches)	39	±4	41.7
CG Above Ground ^{c,d} (inches)	NA	NA	NA

NOTE: NA = not applicable; CG = center of gravity.

^aIf a dummy is used, the gross static vehicle mass should be increased by the mass of the dummy.

^bAverage of front and rear axles.

^cFor test inertial mass.

^d2270P vehicle must meet minimum CG height requirement.

Table 7.5. Events during test 612941-02-2.

Time (s)	Events
0.0000	Vehicle impacted the installation.
0.0235	Posts 18, 19, and 20 began to move toward the field side.
0.0340	Vehicle began to redirect.
0.0438	Posts 16, 17, 21, and 22 began to move toward the field side.
0.0588	Post 23 began to move toward the field side.
0.0988	Dummy head shattered the side window.
0.2260	Vehicle was parallel with installation.
0.3560	Vehicle exited the installation at 44.8 mi/h with a heading of 7.0 degrees and a trajectory of 5.9 degrees.

Test Description

Table 7.5 lists events that occurred during test 612941-02-2. Figures C.4, C.5, and C.6 in Appendix C present sequential photographs during the test.

Damage to Test Installation

Post 19 was deformed from the tire impact, and the guardrail bolt sheared on post 21. Table 7.6 describes the soil gap and post displacements measured after the test.

Table 7.7 describes the damage to the stiffened MGS. Figure 7.5 and Figure 7.6 show the damage to the stiffened MGS.

Table 7.6. Soil gap and post displacement after test 612941-02-2.

Post	Soil Gap	Post Lean from Vertical
16	0.25 inch t/s and f/s	1.0° f/s
17	0.50 inch t/s and f/s	1.0° f/s
18	0.50 inch t/s, 0.75 inch f/s	0°
19	1.00 inch f/s	0°
20	Not measurable	50.0° d/s
21	Not measurable	50.0° d/s
22	0.75 f/s	1.0° f/s
23	0.25 f/s	1.0° f/s
24	0.25 t/s and f/s	1.0° f/s

NOTE: t/s = traffic side; f/s = field side; d/s = downstream.

Table 7.7. Damage to stiffened MGS during test 612941-02-2.

Test Parameter	Measured
Permanent Deflection/Location	4.75 inches toward the field side on the downstream end of post 19.
Dynamic Deflection	9.4 inches toward the field side at post 20.
Working Width ^a and Height	27.6 inches at a height of 17 inches on the field side of post 20.

^aPer MASH, "The working width is the maximum dynamic lateral position of any major part of the system or vehicle. These measurements are all relative to the pre-impact, traffic face of the test article." In other words, working width is the total barrier width plus the maximum dynamic intrusion of any portion of the barrier or test vehicle past the field-side edge of the barrier.



Figure 7.5. *Stiffened MGS after test at impact location after test 612941-02-2.*



Figure 7.6. *Stiffened MGS after test at posts 20 and 21, test 612941-02-2.*

Damage to Test Vehicle

Figure 7.7 and Figure 7.8 show the damage sustained by the vehicle. Figure 7.9 and Figure 7.10 show the interior of the test vehicle. Table 7.8 and Table 7.9 provide details on the occupant compartment deformation and exterior vehicle damage. Figures C.2 and C.3 in Appendix C provide exterior crush and occupant compartment measurements.

Occupant Risk Factors

Data from the accelerometers were digitized for evaluation of occupant risk, and the results are shown in Table 7.10. In Appendix C, Figure C.7 shows the vehicle angular displacements, and Figures C.8, C.9, and C.10 show acceleration versus time traces.

Test Summary

Figure 7.11 summarizes the results of test 612941-02-2 (MASH Test 3-10).



Figure 7.7. *Impact side of test vehicle after test 612941-02-2.*



Figure 7.8. *Rear impact side of test vehicle after test 612941-02-2.*



Figure 7.9. *Overall interior of test vehicle after test 612941-02-2.*



Figure 7.10. Interior of test vehicle on impact side after test 612941-02-2.

Table 7.8. Occupant compartment deformation, test 612941-02-2.

Test Parameter	Specification	Measured
Roof	≤4.0 inches	0 inches
Windshield	≤3.0 inches	0 inches
A and B Pillars	≤5.0 inches overall, ≤3.0 inches lateral	0 inches
Foot Well/Toe Pan	≤9.0 inches	0 inches
Floor Pan/Transmission Tunnel	≤12.0 inches	0 inches
Side Front Panel	≤12.0 inches	4 inches
Front Door (above seat)	≤9.0 inches	4 inches
Front Door (below seat)	≤12.0 inches	1 inch

Table 7.9. Exterior vehicle damage, test 612941-02-2.

	Damage
Side Windows	The left front side window shattered due to impact from the dummy's head, not due to penetration by the test article.
Maximum Exterior Deformation	10 inches in the front plane at the left front corner at bumper height
VDS	11LFQ5.
CDC	11FLEW5.
Fuel Tank Damage	None.
Overall Description of Damage to Vehicle	
The front bumper, hood, grill, radiator and support, left front strut and tower, left lower control arm, left front tire and rim, left front quarter fender, left front door and glass, left front floor pan, left rear door, left rear tire and rim, and left rear quarter fender were damaged. The left front door had a 5.5-inch gap at the top, and the windshield had some cracking due to the flexing of the body, but there was no deformation and no tearing of the laminate.	

NOTE: VDS = Vehicle Deformation Scale; CDC = Collision Deformation Classification.

Table 7.10. Occupant risk factors for test 612941-02-2.

Test Parameter	MASH ^a	Measured	Time
OIV, Longitudinal (ft/s)	≤ 40.0 <i>30.0</i>	22.8	0.0979 s on left side of interior
OIV, Lateral (ft/s)	≤ 40.0 <i>30.0</i>	27.2	0.0979 s on left side of interior
Ridedown, Longitudinal (g)	≤ 20.49 <i>15.0</i>	7.9	0.0979–0.1079 s
Ridedown, Lateral (g)	≤ 20.49 <i>15.0</i>	10.3	0.1102–0.1202 s
THIV (m/s)	NA	10.6	0.0953 s on left side of interior
ASI	NA	1.9	0.0654–0.1154 s
50-ms MA Longitudinal (g)	NA	–11.5	0.0423–0.0923 s
50-ms MA Lateral (g)	NA	14.5	0.0417–0.0917 s
50-ms MA Vertical (g)	NA	3.5	0.0888–0.1388 s
Roll (deg)	≤ 75.0	12.0	0.4833 s
Pitch (deg)	≤ 75.0	3.0	0.4870 s
Yaw (deg)	NA	56.0	1.9984 s

^aValues in italics are the preferred MASH values.

NOTE: THIV = theoretical head impact velocity; ASI = acceleration severity index; MA = moving average acceleration; NA = not applicable.

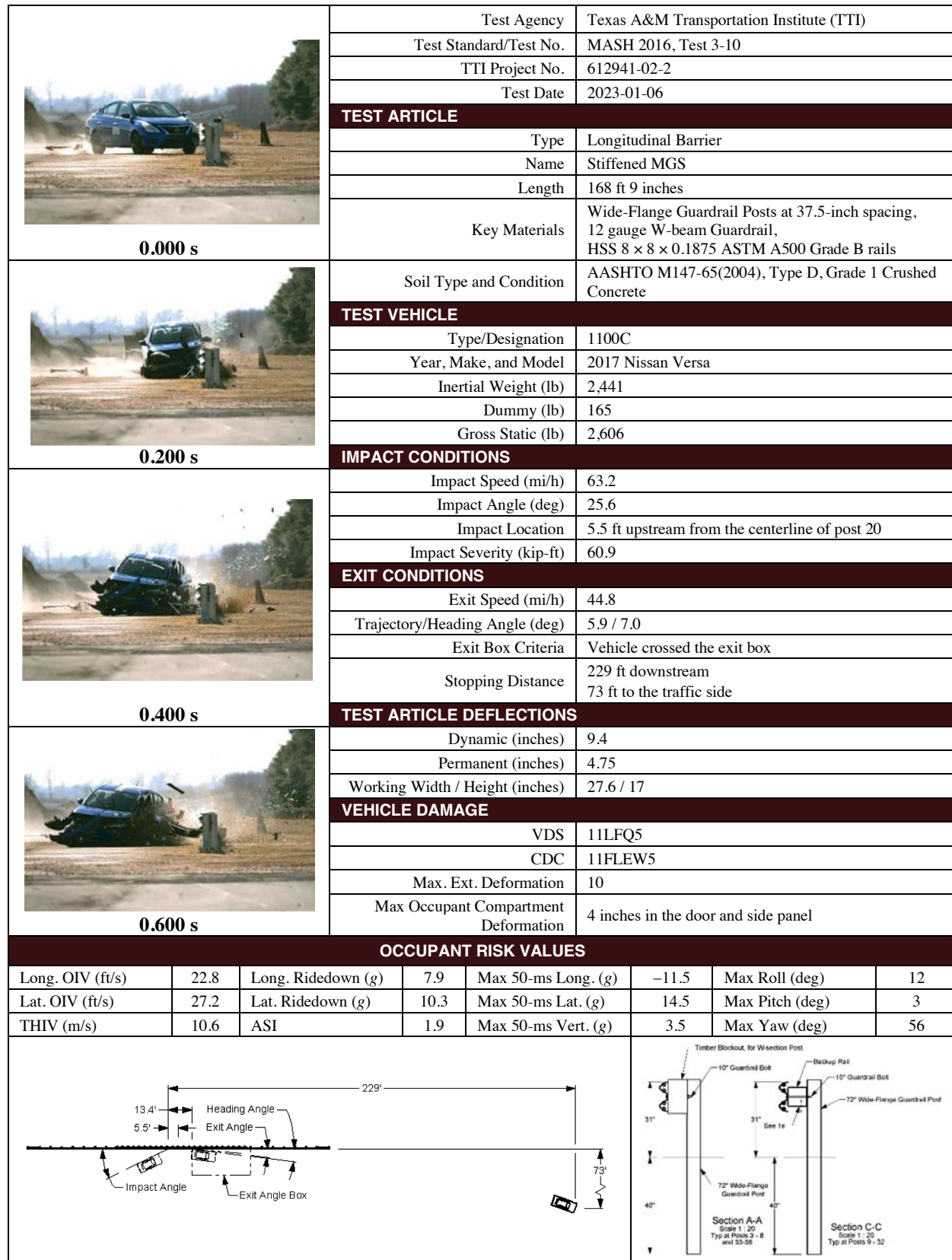


Figure 7.11. Summary of results for MASH Test 3-10 on stiffened MGS.

MASH Test 3-11 (Crash Test No. 612941-02-1)

Test Designation and Actual Impact Conditions

See Table 8.1 for details on MASH impact conditions for this test and Table 8.2 for the exit parameters. Figure 8.1 and Figure 8.2 depict the target impact setup.

Weather Conditions

Table 8.3 provides the weather conditions for test 612941-02-1.

Test Vehicle

Figure 8.3 and Figure 8.4 show the 2018 RAM 1500 used for the crash test. Table 8.4 shows the vehicle measurements. Figure D.1 in Appendix D gives additional dimensions and information on the vehicle.

Table 8.1. Impact conditions for MASH 3-11, test 612941-02-1.

Test Parameter	Specification	Tolerance	Measured
Impact Speed (mi/h)	62	± 2.5	62.7
Impact Angle (deg)	25	± 1.5	25.0
Impact Severity (kip-ft)	106	≥ 106.0	117.7
Impact Location	8.1 ft upstream from the centerline of post 20	± 1 ft	8.3 ft upstream from the centerline of post 20

Table 8.2. Exit parameters for MASH 3-11, test 612941-02-1.

Exit Parameter	Measured
Speed (mi/h)	50.6
Trajectory (deg)	12.3
Heading (deg)	7.5
Brakes Applied Post-Impact (s)	2.2
Vehicle at rest position	<ul style="list-style-type: none"> • 239 ft downstream of impact point. • 2 ft to the field side. • 180°.
Comments	<ul style="list-style-type: none"> • Vehicle remained upright and stable. • Vehicle crossed the exit box^a 62 ft downstream from loss of contact.

^aNot less than 32.8 ft downstream from loss of contact for cars and pickups is optimal.



Figure 8.1. Stiffened MGS and test vehicle geometrics for test 612941-02-1.



Figure 8.2. Stiffened MGS and test vehicle impact location for test 612941-02-1.

Table 8.3. Weather conditions for test 612941-02-1.

Date of Test	December 16, 2022
Wind Speed (mi/h)	10
Wind Direction (deg)	323
Temperature (°F)	52
Relative Humidity (%)	64
Vehicle Traveling (deg)	325



Figure 8.3. Impact side of test vehicle before test 612941-02-1.



Figure 8.4. Opposite impact side of test vehicle before test 612941-02-1.

Table 8.4. Vehicle measurements for test 612941-02-1.

Test Parameter	MASH	Allowed Tolerance	Measured
Dummy (if applicable) ^a (lb)	165	NA	NA
Inertial Weight (lb)	5,000	± 110	5,016.00
Gross Static ^a (lb)	5,000	± 110	5,016.00
Wheelbase (inches)	148	±12	140.50
Front Overhang (inches)	39	±3	40.00
Overall Length (inches)	237	±13	227.50
Overall Width (inches)	78	±2	78.50
Hood Height (inches)	43	±4	46.00
Track Width ^b (inches)	67	±1.5	68.25
CG Aft of Front Axle ^c (inches)	63	±4	61.50
CG Above Ground ^{c,d} (inches)	28	≥28	28.90

NOTE: NA = not applicable; CG = center of gravity.

^aIf a dummy is used, the gross static vehicle mass should be increased by the mass of the dummy.

^bAverage of front and rear axles.

^cFor test inertial mass.

^d2270P vehicle must meet minimum CG height requirement.

Table 8.5. Events during test 612941-02-1.

Time (s)	Events
0.0000	Vehicle impacted the installation.
0.0225	Posts 17, 18, and 19 began to move toward the field side.
0.0287	Posts 16, 20, and 21 began to move toward the field side.
0.0360	Vehicle began to redirect.
0.0750	Post 22 began to move toward the field side.
0.1460	Front passenger side tire lifted off the pavement.
0.1980	Vehicle was parallel with installation.
0.3460	Vehicle exited the installation at 50.7 mi/h with a heading of 7.6 degrees and a trajectory of 12.3 degrees.
0.3790	Front passenger side tire made contact with pavement.

Test Description

Table 8.5 lists events that occurred during test 612941-02-1. Figures D.4, D.5, and D.6 in Appendix D present sequential photographs during the test.

Damage to Test Installation

The rail was scuffed and deformed at impact, and one splice bolt pulled through the rail at post 20. The dirt fell back in the traffic-side soil gaps on posts 18 through 21, making those measurements unobtainable. Table 8.6 describes the soil gap and post displacements measured after the test. Table 8.7 describes the damage to the stiffened MGS. Figure 8.5 and Figure 8.6 show the damage to the stiffened MGS.

Table 8.6. Soil gap and post displacement after test 612941-02-1.

Post	Soil Gap	Post Lean from Vertical
15	0.125 inches t/s and f/s	–0°
16	0.750 inches t/s, 0.250 inches f/s	1.0° f/s
17	0.500 inches t/s, 0.750 inches f/s	1.0° f/s
18	1.25 inches f/s	1.5° f/s
19	1.500 inches f/s	2.0° f/s
20	0.500 inches f/s	7.0° f/s
21	1.250 inches f/s	2.0° f/s
22	0.500 inches f/s	1.5° f/s
23	0.250 inches t/s and f/s	1.0° f/s
24	0.125 inches t/s and f/s	0°

NOTE: t/s = traffic side; f/s = field side.

Table 8.7. Damage to stiffened MGS during test 612941-02-1.

Test Parameter	Measured
Permanent Deflection/Location	5 inches toward the field side at the centerline of post 19.
Dynamic Deflection	10.7 inches toward the field side at post 19.
Working Width ^a and Height	28.8 inches at a height of 64.8 inches at the outer edge of the side mirror.

^aPer MASH, “The working width is the maximum dynamic lateral position of any major part of the system or vehicle. These measurements are all relative to the pre-impact traffic face of the test article.” In other words, working width is the total barrier width plus the maximum dynamic intrusion of any portion of the barrier or test vehicle past the field-side edge of the barrier.



Figure 8.5. Stiffened MGS after test at impact location – test 612941-02-1.



Figure 8.6. Stiffened MGS after test at rail level – test 612941-02-1.

Damage to Test Vehicle

Figure 8.7 and Figure 8.8 show the damage sustained by the vehicle. Figure 8.9 and Figure 8.10 show the interior of the test vehicle. Table 8.8 and Table 8.9 provide details on the occupant compartment deformation and exterior vehicle damage. Figures D.2 and D.3 in Appendix D provide exterior crush and occupant compartment measurements.

Occupant Risk Factors

Data from the accelerometers were digitized for evaluation of occupant risk, and the results are shown in Table 8.10. Figure D.3 in Appendix D.7 shows the vehicle angular displacements, and Figures D.8, D.9, and D.10 in Appendix D show acceleration versus time traces.

Test Summary

Figure 8.11 summarizes the results of test 612941-02-1 (MASH Test 3-11).



Figure 8.7. *Impact side of test vehicle after test 612941-02-1.*



Figure 8.8. *Rear impact side of test vehicle after test 612941-02-1.*



Figure 8.9. *Overall interior of test vehicle after test 612941-02-1.*



Figure 8.10. Interior of test vehicle on impact side after test 612941-02-1.

Table 8.8. Occupant compartment deformation, test 612941-02-1.

Test Parameter	Specification	Measured
Roof	≤4.0 inches	0 inches
Windshield	≤3.0 inches	0 inches
A and B Pillars	≤5.0 inches overall, ≤3.0 inches lateral	0 inches
Foot Well/Toe Pan	≤9.0 inches	1 inch
Floor Pan/Transmission Tunnel	≤12.0 inches	0 inches
Side Front Panel	≤12.0 inches	1 inch
Front Door (above seat)	≤9.0 inches	1 inch
Front Door (below seat)	≤12.0 inches	0 inches

Table 8.9. Exterior vehicle damage, test 612941-02-1.

	Damage
Side Windows	The side windows remained intact.
Maximum Exterior Deformation	14 inches in the front plane at the left front corner at bumper height.
VDS	11LFQ4.
CDC	11FLEW3.
Fuel Tank Damage	None.
Overall Description of Damage to Vehicle	
The front bumper, grill, headlights, radiator and support, left front quarter fender, left front tire and rim, left upper and lower control arms, left front wheel assembly, left front floor pan, left front door, left rear door, left cab corner, left rear quarter fender, left rear rim, and rear bumper and tailgate were all damaged. The left front door had a 6-inch gap at the top.	

NOTE: VDS = Vehicle Deformation Scale; CDC = Collision Deformation Classification.

Table 8.10. Occupant risk factors for test 612941-02-1.

Test Parameter	MASH ^a	Measured	Time
OIV, Longitudinal (ft/s)	≤40.0 <i>30.0</i>	14.9	0.1115 s on left side of interior
OIV, Lateral (ft/s)	≤40.0 <i>30.0</i>	23.7	0.1115 s on left side of interior
Ridedown, Longitudinal (g)	≤20.49 <i>15.0</i>	8.3	0.1260–0.1360 s
Ridedown, Lateral (g)	≤20.49 <i>15.0</i>	10.5	0.2265–0.2365 s
THIV (m/s)	NA	8.5	0.1088 s on left side of interior
ASI	NA	1.4	0.0696–0.1196 s
50-ms MA Longitudinal (g)	NA	–6.3	0.0569–0.1069 s
50-ms MA Lateral (g)	NA	10.9	0.0473–0.0973 s
50-ms MA Vertical (g)	NA	–3.1	0.4410–0.4910 s
Roll (deg)	≤75.0	12.0	1.6000 s
Pitch (deg)	≤75.0	13.0	0.5355 s
Yaw (deg)	NA	35.0	0.5536 s

^aValues in italics are the preferred MASH values.

NOTE: THIV = theoretical head impact velocity; ASI = acceleration severity index; MA = moving average acceleration.

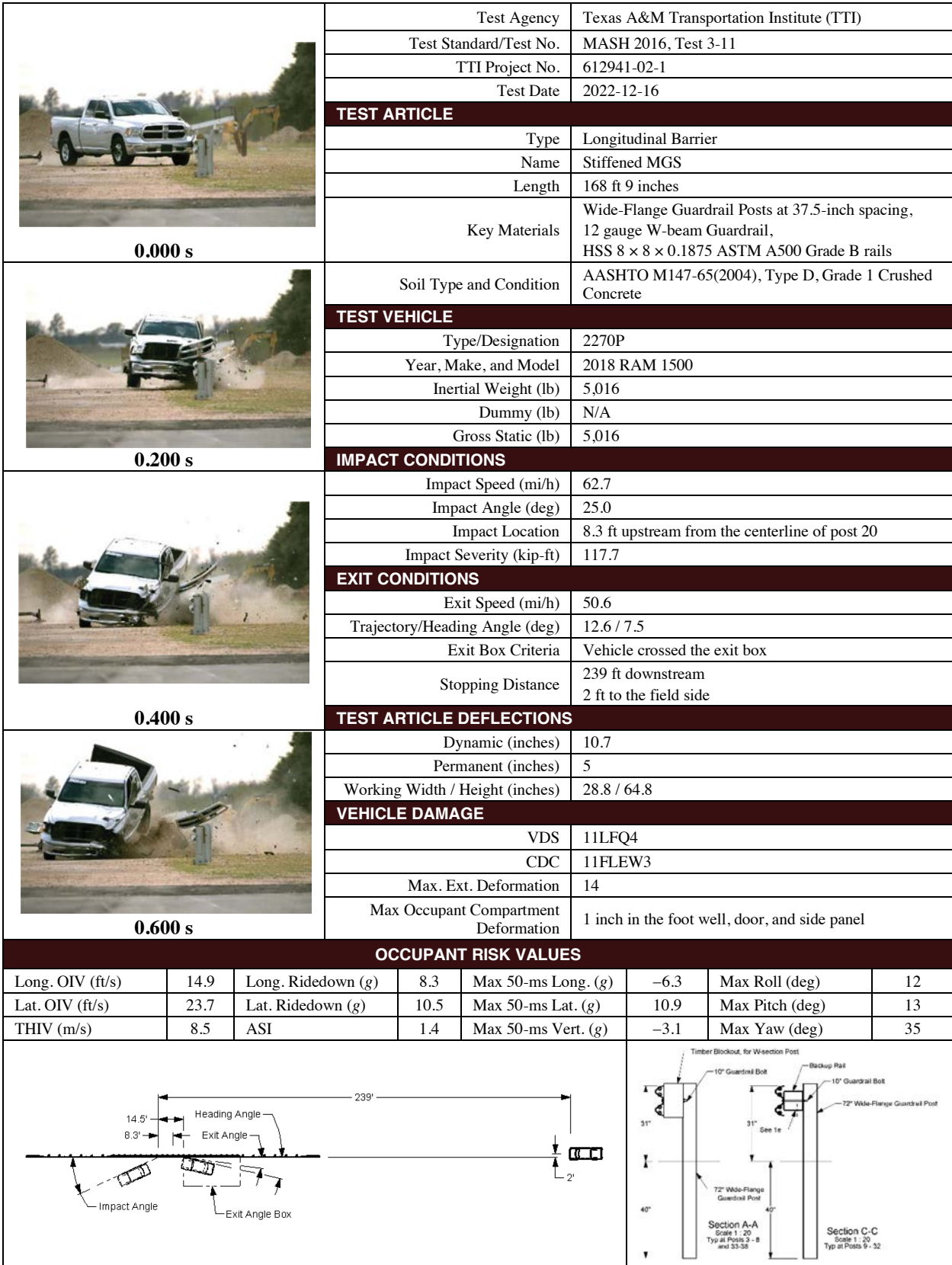


Figure 8.11. Summary of results for MASH Test 3-11 on stiffened MGS.



CHAPTER 9

MASH Test 3-21 (Crash Test No. 612941-02-3)

Test Designation and Actual Impact Conditions

See Table 9.1 for details on MASH impact conditions for this test and Table 9.2 for the exit parameters. Figure 9.1 and Figure 9.2 depict the target impact setup.

Weather Conditions

Table 9.3 provides the weather conditions for test 612941-02-3.

Test Vehicle

Figure 9.3 and Figure 9.4 show the 2017 RAM 1500 used for the crash test. Table 9.4 shows the vehicle measurements. Figure E.1 in Appendix E gives additional dimensions and information on the vehicle.

Table 9.1. Impact conditions for MASH 3-21, test 612941-02-3.

Test Parameter	Specification	Tolerance	Measured
Impact Speed (mi/h)	62	± 2.50	64.0
Impact Angle (deg)	25	± 1.50	25.7
Impact Severity (kip-ft)	106	≥106.00	129.8
Impact Location	6.5 inches upstream from centerline of post 18.	± 12.00 inches	7.3 inches upstream from centerline of post 18.

Table 9.2. Exit parameters for MASH 3-21, test 612941-02-3.

Exit Parameter	Measured
Speed (mi/h)	48.1
Trajectory (deg)	11.2
Heading (deg)	11.8
Brakes Applied Post-Impact (s)	2.6
Vehicle at Rest Position	<ul style="list-style-type: none">• 175 ft downstream of impact point.• 10 ft to the field side.• 45° left.
Comments	<ul style="list-style-type: none">• Vehicle remained upright and stable.• Vehicle crossed the exit box^a 41 ft downstream from loss of contact.

^aNot less than 32.8 ft downstream from loss of contact for cars and pickups is optimal.



Figure 9.1. Stiffened MGS transition and test vehicle geometrics for test 612941-02-3.



Figure 9.2. Stiffened MGS transition and test vehicle impact location for 612941-02-3.

Table 9.3. Weather conditions for test 612941-02-3.

Date of Test	January 27, 2023
Wind Speed (mi/h)	5
Wind Direction (deg)	180
Temperature (°F)	47
Relative Humidity (%)	81
Vehicle Traveling (deg)	325



Figure 9.3. Impact side of test vehicle before test 612941-02-3.



Figure 9.4. Opposite impact side of test vehicle before test 612941-02-3.

Table 9.4. Vehicle measurements for test 612941-02-3.

Test Parameter	MASH	Allowed Tolerance	Measured
Dummy (if applicable) ^a (lb)	165	NA	NA
Inertial Weight (lb)	5,000	± 110.0	5,042.00
Gross Static ^a (lb)	5,000	± 110.0	5,042.00
Wheelbase (inches)	148	±12.0	140.50
Front Overhang (inches)	39	±3.0	40.00
Overall Length (inches)	237	±13.0	227.50
Overall Width (inches)	78	±2.0	78.50
Hood Height (inches)	43	±4.0	46.00
Track Width ^b (inches)	67	±1.5	68.25
CG Aft of Front Axle ^c (inches)	63	±4.0	62.30
CG Above Ground ^{c,d} (inches)	28	≥28.0	28.20

NOTE: NA = not applicable; CG = center of gravity.

^aIf a dummy is used, the gross static vehicle mass should be increased by the mass of the dummy.

^bAverage of front and rear axles.

^cFor test inertial mass.

^d2270P vehicle must meet minimum CG height requirement.

Table 9.5. Events during test 612941-02-3.

Time (s)	Events
0.0000	Vehicle impacted the installation.
0.0310	Vehicle began to redirect.
0.0175	Posts 16, 17, 18, 19, and 20 began to tilt toward the field side.
0.1510	Front passenger side tire lifted off pavement.
0.0287	Posts 20 and 21 began to tilt toward the field side.
0.2220	Vehicle was parallel with installation.
0.3930	Vehicle exited the installation at 48.2 mi/h with a heading of 11.9 degrees and a trajectory of 11.3 degrees.

Test Description

Table 9.5 lists events that occurred during test 612941-02-3. Figures E.4, E.5, and E.6 in Appendix E present sequential photographs during the test.

Damage to Test Installation

The soil was disturbed at post 1. The guardrail bolt broke at post 19, and the rail released from the post. There was scuffing and deformation at impact. The dirt fell back in the soil gaps at posts 20 through 23, making those measurements unobtainable. Table 9.6 describes the soil gap and post displacements measured after the test. Table 9.7 describes the damage to the stiffened MGS transition. Figure 9.5 and Figure 9.6 show the damage to the stiffened MGS transition.

Table 9.6. Soil gap and post displacement after test 612941-02-3

Post	Soil Gap	Post Lean from Vertical
15	0.125 inches t/s	0.2° f/s
16	0.250 inches t/s	1.3° f/s
17	0.500 inches t/s, 0.375 inches f/s	1.0° f/s
18	1.250 inches t/s, 0.250 inches f/s	4.0° f/s
19	2.000 inches t/s, 0.625 inches f/s	8.0° f/s
20	—	30.0° d/s
21	—	11.0° f/s
22	—	14.5° f/s
23	—	12.4° f/s
24	2.750 inches f/s	2.1° f/s
25	2.000 inches f/s	1.5° f/s
26	0.750 inches t/s, 0.500 inches f/s	2.6° f/s
27	0.250 inches f/s	0.4° f/s

NOTE: t/s = traffic side; f/s = field side; d/s = downstream.

Table 9.7. Damage to stiffened MGS during test 612941-02-3.

Test Parameter	Measured
Permanent Deflection/Location	8.5 inches toward the field side, 3.5 inches upstream of post 21.
Dynamic Deflection	16.4 inches toward the field side at post 22.
Working Width ^a and Height	33.9 inches at a height of 22.9 inches at post 20.

^aPer MASH, "The working width is the maximum dynamic lateral position of any major part of the system or vehicle. These measurements are all relative to the pre-impact traffic face of the test article." In other words, working width is the total barrier width plus the maximum dynamic intrusion of any portion of the barrier or test vehicle past the field-side edge of the barrier.



Figure 9.5. *Stiffened MGS transition after the test at the impact location, test 612941-02-3.*



Figure 9.6. *Stiffened MGS transition after the test from the field side, test 612941-02-3.*

Damage to Test Vehicle

Figure 9.7 and Figure 9.8 show the damage sustained by the vehicle. Figure 9.9 and Figure 9.10 show the interior of the test vehicle. Table 9.8 and Table 9.9 provide details on the occupant compartment deformation and exterior vehicle damage. Figures E.2 and E.3 in Appendix E provide exterior crush and occupant compartment measurements.

Occupant Risk Factors

Data from the accelerometers were digitized for evaluation of occupant risk, and the results are shown in Table 9.10. Figure E.7 in Appendix E shows the vehicle angular displacements, and Figures E.8, E.9, and E.10 in Appendix E show acceleration versus time traces.

Test Summary

Figure 9.11 summarizes the results of test 612941-02-3 (MASH Test 3-21).



Figure 9.7. *Impact side of test vehicle after test 612941-02-3.*



Figure 9.8. *Rear impact side of test vehicle after test 612941-02-3.*



Figure 9.9. *Overall interior of test vehicle after test 612941-02-3.*



Figure 9.10. Interior of test vehicle on the impact side after test 612941-02-3.

Table 9.8. Occupant compartment deformation, test 612941-02-3.

Test Parameter	Specification	Measured
Roof	≤4.0 inches	0 inches
Windshield	≤3.0 inches	0 inches
A and B Pillars	≤5.0 inches overall ≤3.0 inches lateral	0 inches
Foot Well/Toe Pan	≤9.0 inches	0 inches
Floor Pan/Transmission Tunnel	≤12.0 inches	0 inches
Side Front Panel	≤12.0 inches	1 inch
Front Door (above seat)	≤9.0 inches	0.5 inches
Front Door (below seat)	≤12.0 inches	0 inches

Table 9.9. Exterior vehicle damage, test 612941-02-3.

	Damage
Side Windows	The side windows remained intact.
Maximum Exterior Deformation	16 inches in the front plane at the left front corner at bumper height.
VDS	11LFQ4.
CDC	11FLEW3.
Fuel Tank Damage	None.
Overall Description of Damage to Vehicle	
The front bumper, hood, grill, radiator and support, left frame rail, left front upper and lower control arms, left front fender, left front door, headlights, left rear door, left cab corner, left rear quarter fender, left rear rim, and rear bumper were damaged. The left front door had a 2.75-inch gap at the top.	

NOTE: VDS = Vehicle Deformation Scale; CDC = Collision Deformation Classification.

Table 9.10. Occupant risk factors for test 612941-02-3.

Test Parameter	MASH ^a	Measured	Time
OIV, Longitudinal (ft/s)	≤ 40.00 <i>30.00</i>	20.0	0.1165 s on left side of interior
OIV, Lateral (ft/s)	≤ 40.00 <i>30.00</i>	22.8	0.1165 s on left side of interior
Ridedown, Longitudinal (g)	≤ 20.49 <i>15.00</i>	6.8	0.1166–0.1266 s
Ridedown, Lateral (g)	≤ 20.49 <i>15.00</i>	8.3	0.1361–0.1461 s
THIV (m/s)	NA	9.0	0.1132 s on left side of interior
ASI	NA	1.1	0.0903–0.1403 s
50-ms MA Longitudinal (g)	NA	–7.8	0.0529–0.1029 s
50-ms MA Lateral (g)	NA	9.1	0.0520–0.1020 s
50-ms MA Vertical (g)	NA	–3.1	0.4877–0.5377 s
Roll (deg)	≤ 75.00	16.0	0.7873 s
Pitch (deg)	≤ 75.00	10.0	0.5230 s
Yaw (deg)	NA	50.0	0.9177 s

^aValues in italics are the preferred MASH values.

NOTE: THIV = theoretical head impact velocity; ASI = acceleration severity index; MA = moving average acceleration.





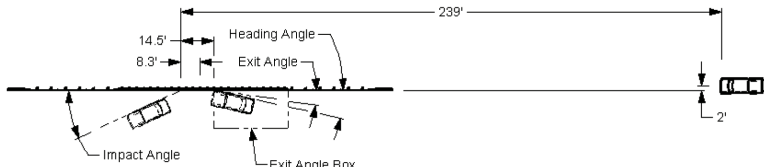
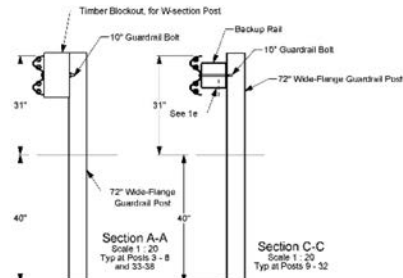
	Test Agency	Texas A&M Transportation Institute (TTI)					
	Test Standard/Test No.	MASH 2016, Test 3-21					
	TTI Project No.	612941-02-3					
	Test Date	2023-01-27					
	TEST ARTICLE						
	Type	Longitudinal Barrier					
	Name	Stiffened MGS Transition					
	Length	168 ft 9 inches					
	Key Materials	Wide-Flange Guardrail Posts, 12 gauge W-beam Guardrail, HSS 8 × 8 × 0.1875 ASTM A500 Grade B rails					
	Soil Type and Condition	AASHTO M147-65(2004), Type D, Grade 1 Crushed Concrete					
	TEST VEHICLE						
	Type/Designation	2270P					
	Year, Make, and Model	2017 RAM 1500					
	Inertial Weight (lb)	5,042					
	Gross (lb)	5,042					
	IMPACT CONDITIONS						
	Impact Speed (mi/h)	64.0					
	Impact Angle (deg)	25.7					
	Impact Location	7.3 inches upstream from centerline of post 18.					
	Impact Severity (kip-ft)	129.8					
	EXIT CONDITIONS						
	Exit Speed (mi/h)	48.1					
	Trajectory/Heading Angle (deg)	11.2 / 11.8					
	Stopping Distance	175 ft downstream 10 ft to the field side					
	TEST ARTICLE DEFLECTIONS						
	Dynamic (inches)	16.4					
	Permanent (inches)	8.5					
	Working Width / Height (inches)	33.9 / 22.9					
	VEHICLE DAMAGE						
	VDS	11LFQ4					
	CDC	11FLEW3					
	Max. Ext. Deformation	16					
	Max Occupant Compartment Deformation	1 inch in the side panel					
	OCCUPANT RISK VALUES						
Long. OIV (ft/s)	20.0	Long. Ridedown (g)	6.8	Max 50-ms Long. (g)	-7.8	Max Roll (deg)	16
Lat. OIV (ft/s)	22.8	Lat. Ridedown (g)	8.3	Max 50-ms Lat. (g)	9.1	Max Pitch (deg)	10
THIV (m/s)	9.0	ASI	1.1	Max 50-ms Vert. (g)	-3.1	Max Yaw (deg)	50
							

Figure 9.11. Summary of results for MASH Test 3-21 on stiffened MGS transition.

MASH Test 3-20 (Crash Test 612941-02-4)

Test Designation and Actual Impact Conditions

See Table 10.1 for details of MASH impact conditions for this test and Table 10.2 for the exit parameters. Figure 10.1 and Figure 10.2 depict the target impact setup.

Weather Conditions

Table 10.3 provides the weather conditions for test 612941-02-4.

Test Vehicle

Figure 10.3 and Figure 10.4 show the 2017 Nissan Versa used for the crash test. Table 10.4 shows the vehicle measurements. Figure F.1 in Appendix F gives additional dimensions and information about the vehicle.

Table 10.1. Impact conditions for MASH Test 3-20, test 612941-02-4.

Test Parameter	Specification	Tolerance	Measured
Impact Speed (mi/h)	62	±2.5	62.6
Impact Angle (deg)	25	±1.5	25.0
Impact Severity (kip-ft)	51	≥51.0	56.9
Impact Location	4 inches upstream from the centerline of post 18.	±12 inches	2 inches upstream from the centerline of post 18

Table 10.2. Exit parameters for MASH Test 3-20, test 612941-02-4.

Exit Parameter	Measured
Speed (mi/h)	39.7
Trajectory (deg)	9.1
Heading (deg)	10.1
Brakes Applied Post-Impact (s)	2.5
Vehicle at Rest Position	<ul style="list-style-type: none"> • 152 ft downstream of impact point. • 78 ft to the traffic side. • 55° right.
Comments	<ul style="list-style-type: none"> • Vehicle remained upright and stable. • Vehicle crossed the exit box^a 41 ft downstream from loss of contact.

^aNot less than 32.8 ft downstream from loss of contact for cars and pickups is optimal.



Figure 10.1. Stiffened MGS transition and the test vehicle geometrics for test 612941-02-4.



Figure 10.2. Stiffened MGS transition and the test vehicle impact location 612941-02-4.

Table 10.3. Weather conditions for test 612941-02-4.

Date of Test	March 15, 2023
Wind Speed (mi/h)	8
Wind Direction (deg)	169
Temperature (°F)	59
Relative Humidity (%)	60
Vehicle Traveling (deg)	325



Figure 10.3. Impact side of test vehicle before test 612941-02-4.



Figure 10.4. Opposite impact side of test vehicle before test 612941-02-4.

Table 10.4. Vehicle measurements for test 612941-02-4.

Test Parameter	MASH	Allowed Tolerance	Measured
Dummy (if applicable) ^a (lb)	165	NA	165.0
Inertial Weight (lb)	2,420	±55	2,432.0
Gross Static ^a (lb)	2,585	±25	2,597.0
Wheelbase (inches)	98	±5	102.4
Front Overhang (inches)	35	±4	32.5
Overall Length (inches)	169	±8	175.4
Overall Width (inches)	65	±3	66.7
Hood Height (inches)	28	±4	30.5
Track Width ^b (inches)	59	±2	58.4
CG aft of Front Axle ^c (inches)	39	±4	42.8
CG above Ground ^{c,d} (inches)	NA	NA	NA

NOTE: NA = not applicable; CG = center of gravity.

^aIf a dummy is used, the gross static vehicle mass should be increased by the mass of the dummy.

^bAverage of front and rear axles.

^cFor test inertial mass.

^d2270P vehicle must meet minimum CG height requirement.

Table 10.5. Events during test 612941-02-4.

Time (s)	Events
0.0000	Vehicle impacted the installation.
0.0390	Vehicle began to redirect.
0.0210	Posts 17, 18, 19, and 20 began to lean toward the field side.
0.0390	Posts 21 and 22 began to lean toward the field side.
0.2100	Vehicle was parallel with installation.
0.3760	Vehicle exited the installation at 39.7mi/h with a heading of 10.2 degrees and a trajectory of 9.1 degrees.

Test Description

Table 10.5 lists events that occurred during test 612941-02-4. Figures F.4, F.5, and F.6 in Appendix F present sequential photographs during the test.

Damage to Test Installation

The blackout at post 20 was shattered, and the flange was deformed on the upstream traffic side of the post. The blackout was rotated at post 21, post 23 was twisted counterclockwise, and the upstream traffic-side flange was deformed. The rail was scuffed and deformed at impact. Table 10.6 describes the soil gap and post lean after impact. Table 10.7 describes the deflection and working width of the stiffened MGS transition. Figure 10.5 and Figure 10.6 show the damage to the stiffened MGS transition.

Table 10.6. Soil gap and post displacement after test 612941-02-4.

Post	Soil Gap	Post Lean from Vertical
16	Soil disturbed	0°
17	0.250 inches t/s	1.1° f/s
18	0.500 inches t/s, 0.125 inches f/s	2.0° f/s
19	0.500 inches f/s, dirt filled in around post t/s	4.1° f/s
20	Dirt filled in around post	32.1° d/s
21	Dirt filled in around post	17.5° d/s
22	0.750 inches f/s, dirt filled in around post t/s	5.0° f/s
23	Dirt filled in around post	15.6° d/s
24	Soil disturbed	0°

NOTE: t/s = traffic side; f/s = field side; d/s = downstream.

Table 10.7. Deflection and working width of the stiffened MGS transition for test 612941-02-4.

Test Parameter	Measured
Permanent Deflection/Location	6.5 inches toward the field side, 11 inches upstream from post 21.
Dynamic Deflection	9.5 inches toward the field side at post 21.
Working Width ^a and Height	32.1 inches at a height of 19.7 inches at the top traffic side of post 21.

^aPer MASH, "The working width is the maximum dynamic lateral position of any major part of the system or vehicle. These measurements are all relative to the pre-impact traffic face of the test article." In other words, working width is the total barrier width plus the maximum dynamic intrusion of any portion of the barrier or test vehicle past the field-side edge of the barrier.



Figure 10.5. *Stiffened MGS transition after test at impact location, test 612941-02-4.*



Figure 10.6. *Stiffened MGS transition after test at the field side of the installation, test 612941-02-4.*

Damage to Test Vehicle

Figure 10.7 and Figure 10.8 show the damage sustained by the vehicle. Figure 10.9 and Figure 10.10 show the interior of the test vehicle. Table 10.8 and Table 10.9 provide details on the occupant compartment deformation and exterior vehicle damage. Figures F.2 and F.3 in Appendix F provide exterior crush and occupant compartment measurements.

Occupant Risk Factors

Data from the accelerometers were digitized for evaluation of occupant risk, and the results are shown in Table 10.10. In Appendix F, Figure F.7 shows the vehicle angular displacements, and Figures F.8, F. 9, and F.10 show acceleration versus time traces.

Test Summary

Figure 10.11 summarizes the results of test 612941-02-4 (MASH Test 3-20).



Figure 10.7. *Impact side of test vehicle after test 612941-02-4.*



Figure 10.8. *Rear impact side of test vehicle after test 612941-02-4.*



Figure 10.9. *Overall interior of test vehicle after test 612941-02-4.*



Figure 10.10. Interior of test vehicle on impact side after test 612941-02-4.

Table 10.8. Occupant compartment deformation, test 612941-02-4.

Test Parameter	Specification	Measured
Roof	≤4.0 inches	0.5 inches
Windshield	≤3.0 inches	0.0 inches
A and B Pillars	≤5.0 inches overall, ≤3.0 inches lateral	0.0 inches
Foot Well/Toe Pan	≤9.0 inches	1.0 inches
Floor Pan/Transmission Tunnel	≤12.0 inches	2.0 inches
Side Front Panel	≤12.0 inches	0.0 inches
Front Door (above seat)	≤9.0 inches	3.0 inches
Front Door (below seat)	≤12.0 inches	0.0 inches

Table 10.9. Exterior vehicle damage, test 612941-02-4.

	Damage
Side Windows	Side windows remained intact.
Maximum Exterior Deformation	9.5 inches in the front plane at the left front corner at bumper height.
VDS	11LFQ4.
CDC	11FLAW3.
Fuel Tank Damage	None.
Overall Description of Damage to Vehicle	
The front bumper, hood, grill, radiator and support, left front tire and rim, left front strut and tower, left front lower control arm, windshield (cracking due to the vehicle flexing), left front door, left front floor pan, left rear door, left rear quarter fender, and rear bumper were damaged. The left front door had a 4.25-inch gap at the top.	

NOTE: VDS = Vehicle Deformation Scale; CDC = Collision Deformation Classification.

Table 10.10. Occupant risk factors for test 612941-02-4.

Test Parameter	MASH ^a	Measured	Time
OIV, Longitudinal (ft/s)	≤ 40.0 <i>30.0</i>	26.0	0.0979 s on left side of interior
OIV, Lateral (ft/s)	≤ 40.0 <i>30.0</i>	25.9	0.0979 s on left side of interior
Ridedown, Longitudinal (g)	≤ 20.49 <i>15.0</i>	11.4	0.1138–0.1238 s
Ridedown, Lateral (g)	≤ 20.49 <i>15.0</i>	11.5	0.1172–0.1272 s
THIV (m/s)	NA	10.9	0.0953 s on left side of interior
ASI	NA	1.8	0.0618–0.1118 s
50-ms MA Longitudinal (g)	NA	–12.5	0.0396–0.0896 s
50-ms MA Lateral (g)	NA	12.5	0.0372–0.0872 s
50-ms MA Vertical (g)	NA	2.5	0.0690–0.1190 s
Roll (deg)	≤ 75.0	6.7	0.4491 s
Pitch (deg)	≤ 75.0	5.5	1.9989 s
Yaw (deg)	NA	55.8	2.0000 s

^aValues in italics are the preferred MASH values.

NOTE: THIV = theoretical head impact velocity; ASI = acceleration severity index; MA = moving average acceleration.





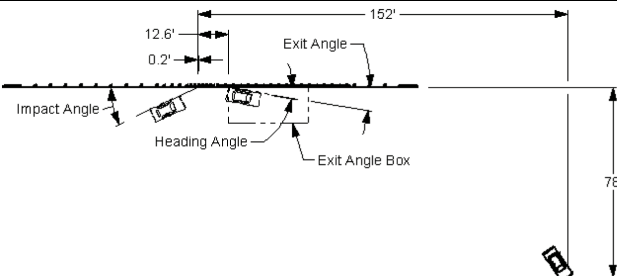
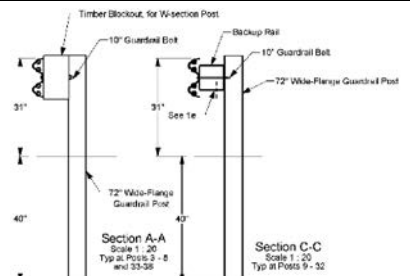
	Test Agency	Texas A&M Transportation Institute (TTI)					
	Test Standard/Test No.	MASH 2016, Test 3-20					
	TTI Project No.	612941-02-4					
	Test Date	2023-03-15					
	TEST ARTICLE						
	Type	Longitudinal Barrier					
	Name	Stiffened MGS Transition					
	[Length Spec]	168 ft 9 inches					
	Key Materials	Wide-Flange Guardrail Posts, 12 gauge W-beam Guardrail, HSS 8 × 8 × 0.1875 ASTM A500 Grade B rails					
	Soil Type and Condition	AASHTO M147-65(2004), Type D, Grade 1 Crushed Concrete					
	TEST VEHICLE						
	Type/Designation	1100C					
	Year, Make, and Model	2017 Nissan Versa					
	Inertial Weight (lb)	2,432					
	Dummy (lb)	165					
	Gross Static (lb)	2,597					
IMPACT CONDITIONS							
Impact Speed (mi/h)		62.6					
Impact Angle (deg)		25.0					
Impact Location		2 inches upstream from the centerline of post 18					
Impact Severity (kip-ft)		56.9					
EXIT CONDITIONS							
Exit Speed (mi/h)		39.7					
Trajectory/Heading Angle (deg)		9.1 / 10.1					
Exit Box Criteria		Vehicle crossed the exit box a 41 ft downstream from loss of contact.					
Stopping Distance		152 ft downstream 78 ft to the traffic side					
TEST ARTICLE DEFLECTIONS							
Dynamic (inches)		9.5					
Permanent (inches)		6.5					
Working Width / Height (inches)		32.1 / 19.7					
VEHICLE DAMAGE							
VDS		11LFQ4					
CDC		11FLAW3					
Max. Ext. Deformation (inches)		9.5					
Max Occupant Compartment Deformation		3 inches in the front door					
OCCUPANT RISK VALUES							
Long. OIV (ft/s)	26.0	Long. Ridedown (g)	11.4	Max 50-ms Long. (g)	-12.5	Max Roll (deg)	6.7
Lat. OIV (ft/s)	25.9	Lat. Ridedown (g)	11.5	Max 50-ms Lat. (g)	12.5	Max Pitch (deg)	5.5
THIV (m/s)	10.9	ASI	1.8	Max 50-ms Vert. (g)	2.5	Max Yaw (deg)	55.8
							

Figure 10.11. Summary of results for MASH Test 3-20 on stiffened MGS.



CHAPTER 11

Conclusions, Findings, and Suggested Research

Assessment of Test Results

The crash tests reported herein were performed in accordance with MASH TL-3, which involves four tests—two on the stiffened MGS and two on the stiffened MGS transition.

Table 11.1 shows that the stiffened MGS and stiffened MGS transition met the performance criteria for MASH TL-3 longitudinal barriers.

Summary of Research Effort

This research project focused on developing guidelines for stiffening the MGS. The research team began by investigating previous research and literature regarding stiffening the MGS. State standards and methods for stiffening guardrail were then combined with the literature review to create a list of stiffening mechanisms suitable for computer simulation evaluation. Prioritized stiffening mechanisms were evaluated through numerous FEAs. Following the computer simulation evaluation, one stiffening mechanism was selected for full-scale MASH crash testing. The combination of half-post spacing and HSS8×8× $\frac{3}{16}$ blockout replacement tube successfully met the MASH criteria for Tests 3-11 and 3-10. The transition from MGS to this stiffened section successfully met the MASH criteria for Tests 3-21 and 3-20. Last, the research team provided a table suitable for implementation into the RDG. The table details dynamic deflections of a variety of hardware systems, including those evaluated under this project through computer simulation or full-scale MASH testing.

Findings and Implementation*

Implementation of Crash-Tested Stiffened MGS and Transition

The stiffened MGS with the half-post spacing and HSS8×8× $\frac{3}{16}$ blockout replacement tube successfully met MASH evaluation criteria for Tests 3-11 and 3-10. The transition from full-post spacing MGS to this stiffened system also successfully met MASH evaluation criteria for tests 3-21 and 3-20. This system is therefore suitable for implementation on the roadside. The research team reviewed installation damage and high-speed video to determine recommended installation lengths of the stiffened MGS. Table 8.6 shows 10 posts were displaced during the impact, which equates to 28 feet 1½ inches of displaced posts. This length was then increased to 34 feet 4½ inches to accommodate the end condition of the HSS8×8× $\frac{3}{16}$ blockout replacement tube.

*The opinions/interpretations identified/expressed in this section of the report are outside the scope of TTI Proving Ground's A2LA Accreditation.

Table 11.1. Assessment summary for MASH TL-3 tests on stiffened MGS and stiffened MGS transition.

Evaluation Criteria ^a	Description	Test No. 612941-02-2	Test No. 612941-02-1	Test No. 612941-02-3	Test No. 612941-02-4
A	Contain, redirect, or controlled stop	S	S	S	S
D	No penetration into occupant compartment	S	S	S	S
F	Roll and pitch limit	S	S	S	S
H	OIV threshold	S	S	S	S
I	RDA threshold	S	S	S	S
Overall		Pass	Pass	Pass	Pass

NOTE: S = Satisfactory.

^aSee Table 5.2 for

Therefore, a minimum of 34 feet 4½ inches of the stiffened MGS with half-post spacing and HSS8×8×¾ blockout replacement tube is recommended to be installed. The maximum dynamic deflection was 10.7 inches measured from the pre-impact traffic face of the rail to the impacted traffic face of the rail. This maximum dynamic deflection was located close to the midspan of the 31¼ ft of damage. The roadside obstacle may therefore be placed near the center of this stiffened section. This placement considers both the primary direction of traffic and conditions where the shielded obstacle is within the clear zone of opposing traffic. The working width was 28.8 inches measured from the pre-impact traffic face of the rail to the furthest extent of the pickup truck's side mirror, and the height of the working width was 64.8 inches above grade.

The as-tested blockout replacement tube included hand access holes (see Figure 11.1) to ease the installation process for contractors and maintenance teams. The research team concluded end users may choose to not incorporate the hand access holes into their installations as they did not significantly contribute to the crashworthiness of the system. Additionally, the research team believes W6x9 posts are an acceptable alternative to the W6x8.5 utilized in this study.

On both the upstream and downstream sides of the stiffened MGS, the research suggests transitioning to standard MGS using the transition evaluated in Chapter 9 and Chapter 10. The research team also proposes terminating the total system with a MASH-compliant terminal or downstream anchor terminal as appropriate.

Comparison of Crash Tests to Simulations

Following the crash tests, the research team compared the physical testing results to the results of the computer simulations. Table 11.2 shows a summary of the quantitative comparison. Figure 11.2 and Figure 11.3 show the sequential frames of the MASH Test 3-11 overlaid with the simulated MASH Test 3-11.

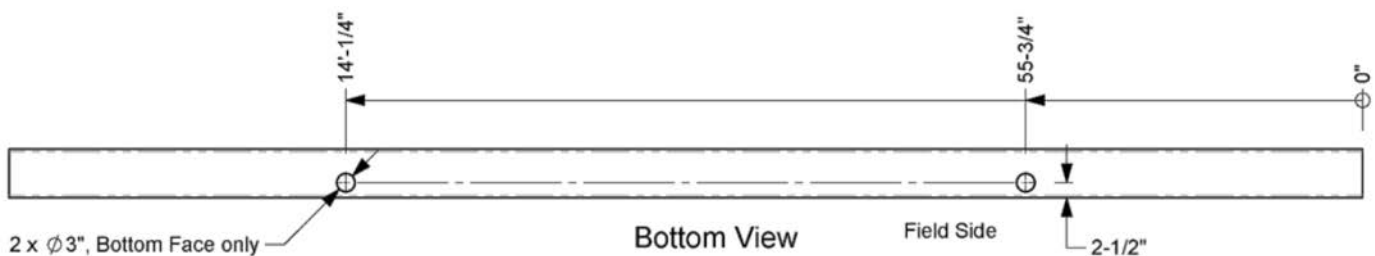
**Figure 11.1. Hand access holes in blockout replacement tube.**

Table 11.2. Crash test and simulation comparison summary.

Data	MASH Test 3-11	
	Crash Test	Simulation
OIV (m/s)	-7.2	-7.8
RDA (g)	10.5	9.1
Working Width (in)	28.8	24.5
Dynamic Deflection (in)	10.7	11.1

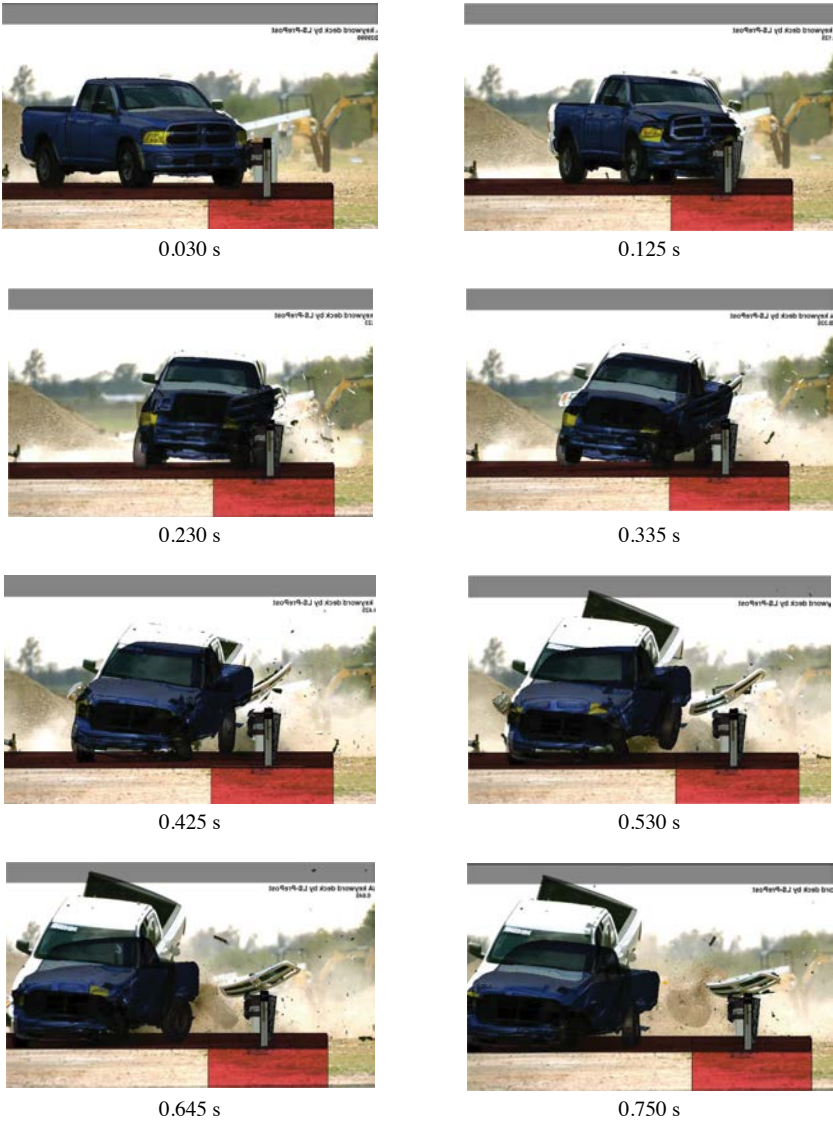


Figure 11.2. Downstream view of MASH Test 3-11 overlaid with the simulated MASH Test 3-11 showing MGS with a combination of half-post spacing and HSS8×8×³/₁₆ blockout replacement rail.

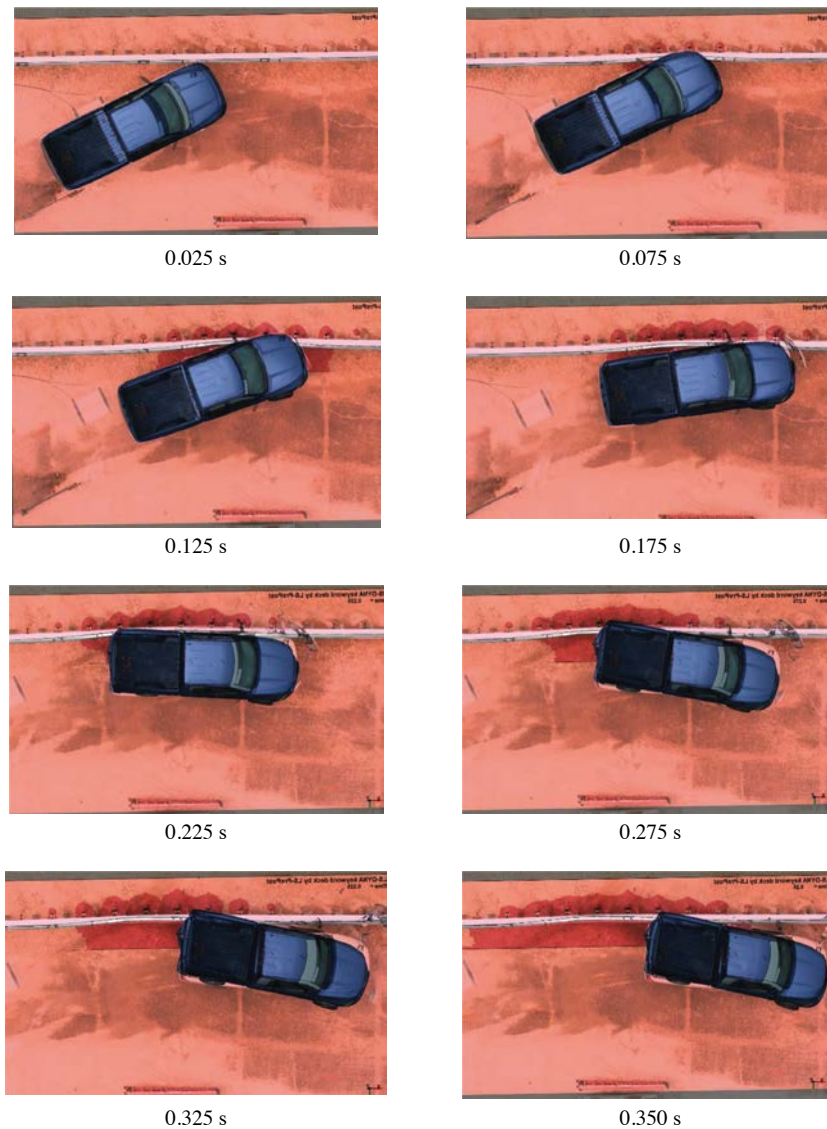


Figure 11.3. Overhead view MASH Test 3-11 overlaid with the simulated MASH Test 3-11 MGS with a combination of half-post spacing and HSS8×8×³/₁₆ blockout replacement rail.

The simulation predicted values for OIV, RDA, working width, and dynamic deflection correlated well with the physical crash-test results. In particular, the difference between the physical crash test and the computer simulation dynamic deflections was 3.7%. Furthermore, the overlay photos included in Figure 11.2 and Figure 11.3 show a positive qualitative comparison between the computer simulation and physical crash testing. These successful quantitative and qualitative comparisons provided the research team with confidence in the predictive capability of the computer simulations. Consequently, the research team believes the computer simulation values are reasonable estimates for the dynamic deflections of the various barrier systems evaluated in this project. Based on this conclusion, the research team included these values in a guardrail deflection table that could be considered for addition to future editions of the RDG, as discussed in the next section. However, the stiffening mechanisms, which were only evaluated through computer simulation, require full-scale testing and/or further analysis before implementation on the roadside.

Updated RDG Deflections

Chapter 2 highlighted the current RDG (1) material regarding deflections of typical guardrail systems. The research team compiled the deflections of previous crash tests and the computer simulations from this project to create Table 11.3, which may be considered for addition to future editions of the RDG.

Table 11.3. Updated guardrail deflection table based on previous crash tests and the computer simulations from this project.

Rail Type	Post Type	Post Spacing (inches)	Unique Feature(s)	Dynamic Deflection (inches)	Working Width (inches)	Working Width Height (inches)	Data Source	Reference
W-Beam	S3x5.7	150	Modified G2 weak post	103.2	108	NA	MASH Test 3-11	<i>NCHRP Web-Only Document 157: Volume I: Evaluation of Existing Roadside Safety Hardware Using Updated Criteria—Technical Report (23)</i>
W-Beam	W6x9	75	Culvert application	92.2	93.4	NA	MASH Test 3-11	<i>Midwest Guardrail System for Long-Span Culvert Applications (24)</i>
W-Beam	W6x9	75	Culvert application	77.5	84	NA	MASH Test 3-11	<i>Midwest Guardrail System for Long-Span Culvert Applications (24)</i>
W-Beam	W6x8.5	75	Rocky terrain	74.8	79	10.9	MASH Test 3-11	<i>MASH Evaluation of TxDOT Roadside Safety Features – Phase II (15)</i>
W-Beam	W6x8.5	75	1V:2H slope	72.9	77.4	NA	MASH Test 3-11	<i>Midwest Guardrail System (MGS) with 6-ft Posts Placed Adjacent to a 1V:2H Fill Slope (14)</i>
W-Beam	Douglas Fir	75	Douglas fir posts	60.2	60.3	NA	MASH Test 3-11	<i>Investigating the Use of Small-Diameter Softwood as Guardrail Posts (Dynamic Test Results) (25)</i>
Box Beam	S3x5.7	72	None	57.7	67.2	NA	MASH Test 3-11	Correspondence from FHWA (26)
W-Beam	W6x9	75	1V:2H slope	57.6	64.2	NA	MASH Test 3-11	<i>Development and Evaluation of the Midwest Guardrail System Placed Adjacent to a 2:1 Fill Slope (13)</i>
Box Beam	S3x5.7	72	G3 weak post	57.6	NA	NA	MASH Test 3-11	<i>Research Results Digest 349: Evaluation of Existing Roadside Safety Hardware Using Manual for Assessing Safety Hardware (MASH) Criteria (27)</i>
W-Beam	W6x9	75	1V:8H slope	57.6	82.8	NA	MASH Test 3-11	<i>Approach Slope for Midwest Guardrail System (28)</i>
W-Beam	Round wood post	75	7.5-inch-diameter posts	57.4	NA	NA	MASH Test 3-11	<i>MASH Evaluation of TxDOT Roadside Safety Features – Phase II (15)</i>
W-Beam	W6x8.5	75	Over underground structure	53.1	62.4	54.3	MASH Test 3-11	Correspondence from FHWA (29)
W-Beam	W6x8.5 (PWE01)	75	Blockouts raised on steel posts	52.6	69.6	53	MASH Test 3-11	<i>MASH Test 3-11 of 28-Inch W-Beam Guardrail System with 8-Inch Composite Blockouts Raised 4 Inches on Steel Post (30)</i>
W-Beam	W6x8.5	75	Face of post 1 foot onto 1V:2H slope	51.6	55.2	NA	MASH Test 3-11	<i>MASH TL-3 Testing and Evaluation of the W-Beam Guardrail on Slope (12)</i>

Table 11.3. (Continued).

Rail Type	Post Type	Post Spacing (inches)	Unique Feature(s)	Dynamic Deflection (inches)	Working Width (inches)	Working Width Height (inches)	Data Source	Reference
W-Beam	W6x8.5	75	Omitted post	49	50.1	NA	MASH Test 3-11	<i>Midwest Guardrail System (MGS) with an Omitted Post (31)</i>
W-Beam	S3x5.7	75	Culvert	48.9	53.2	NA	MASH Test 3-11	<i>Development of a Low-Cost Energy-Absorbing Bridge Rail (32)</i>
W-Beam	W6x9	75	None	47	54.9	NA	MASH Test 3-11	<i>Performance Evaluation of the Modified G4(1S) Guardrail – Update to NCHRP 350 Test No. 3-11 with 28" C.G. Height (2214WB-2) (33)</i>
W-Beam	White pine	75	Slope	46.3	58.4	NA	MASH Test 3-11	<i>Evaluation of the Midwest Guardrail System (MGS) with White Pine Wood Posts (17)</i>
W-Beam	W6x9	75	Concrete box culvert	45.6	49.2	NA	MASH Test 3-11	<i>MASH Test 3-11 of the W-Beam Guardrail on Low-Fill Box Culvert (34)</i>
W-Beam	Round wood post	75	None	44.1	62.2	57.4	MASH Test 3-11	<i>MASH Test 3-11 Evaluation of Modified TxDOT Round Wood Post Guardrail System (16)</i>
W-Beam	W6x8.5	75	Light pole behind system	44.1	47.3	NA	MASH Test 3-11	<i>Placement of Breakaway Light Poles Located Directly Behind Midwest Guardrail System (MGS) (35)</i>
W-Beam	W6x9	75	None	43.9	48.6	NA	MASH Test 3-11	<i>Performance Evaluation of the Midwest Guardrail System – Update to NCHRP 350 Test No. 3-11 with 28" C.G. Height (2214MG-2) (22)</i>
W-Beam	S3x5.7	37.5	Asphalt mow strip	42.3	47.3	NA	MASH Test 3-11	<i>Development and Evaluation of Weak-Post W-Beam Guardrail in Mow Strips (36)</i>
W-Beam	W6x9	75	75-ft installation length	42.2	48.8	NA	MASH Test 3-11	<i>Minimum Effective Guardrail Length for the MGS (37)</i>
Thrie-Beam	W6x8.5	75	None	42.1	55.2	60.4	MASH Test 3-11	<i>Design and Testing of MASH TL-3 Thrie Beam Guardrail System (TGS) for Roadside and Median Application (38)</i>
W-Beam	Southern yellow pine	75	None	40	53.8	NA	MASH Test 3-11	<i>Midwest Guardrail System (MGS) with Southern Yellow Pine Posts (39)</i>
W-Beam	W6x8.5	75	AASHTO Type B curb	39.4	48.5	NA	MASH Test 3-11	<i>Evaluation of the MGS Placed 6 In. Behind a 6-In.-Tall AASHTO Type B Curb to MASH TL-3 (40)</i>
W-Beam	W6x8.5	75	Median rail	39	55	NA	MASH Test 3-11	<i>Development and Evaluation of MASH TL-3 31-Inch W-Beam Median Barrier (41)</i>
W-Beam	W6x8.5	75	AASHTO Type B curb and omitted post	38.6	41.8	NA	MASH Test 3-11	<i>MGS with Curb and Omitted Post: Evaluation to MASH 2016 Test No. 3-11 (42).</i>
W-Beam	Ponderosa pine	75	Ponderosa pine posts	37.6	48.6	NA	MASH Test 3-11	<i>Investigating the Use of Small-Diameter Softwood as Guardrail Posts (Dynamic Test Results) (25)</i>
W-Beam	W6x8.5	75	Non-blocked steel post MGS	35.7	45.2	NA	MASH Test 3-11	<i>Development of an Economical Guardrail System for Use on Wire-Faced, MSE Walls, Draft Report (43)</i>
Thrie-Beam	W6x8.5	75	Modified Thrie-beam system	34.4	49.3	NA	MASH Test 3-11	<i>MASH 2016 Evaluation of the Modified Thrie-Beam System (44)</i>

(continued on next page)

Table 11.3. (Continued).

Rail Type	Post Type	Post Spacing (inches)	Unique Feature(s)	Dynamic Deflection (inches)	Working Width (inches)	Working Width Height (inches)	Data Source	Reference
W-Beam	W6x8.5	75	Non-blocked with backup plates	34.1	43.2	NA	MASH Test 3-11	<i>Safety Performance Evaluation of the Non-Blocked Midwest Guardrail System (MGS) (45)</i>
W-Beam	W6x8.5 and 9	37.5	Culvert	29.6	50.8	NA	MASH Test 3-11	<i>Dynamic Testing and Evaluation of Culvert-Mounted, Strong-Post MGS to TL-3 Guidelines of MASH 2016 (46)</i>
W-Beam	W6x8.5	75	Median barrier	28.1	52.6	31	MASH Test 3-11	<i>MASH TL-3 Evaluation of W-Beam Median Barrier with Rub Rail (47)</i>
W-Beam	W6x8.5	37.5	None	25.6	43.1	10.1	MASH Test 3-11	<i>MASH Crash Testing and Evaluation of the MGS with Reduced Post Spacing (7)</i>
W-Beam	W6x8.5	18.75	None	19.5	37.1	27.9	MASH Test 3-11	<i>MASH Crash Testing and Evaluation of the MGS with Reduced Post Spacing (7)</i>
W-Beam	W6x8.5	37.5	HSS8x8x3/16 blackout replacement	10.7	28.8	64.8	MASH Test 3-11	<i>NCHRP Research Report 1100: MASH TL-3 Deflection Reduction for 31-Inch Guardrail: A Guide (NCHRP Project 22-38)</i>
W-Beam	W6x8.5	75	10-gauge W-beam rail	39.2	52.1	48.1	Simulated MASH Test 3-11	<i>NCHRP Research Report 1100: MASH TL-3 Deflection Reduction for 31-Inch Guardrail: A Guide (NCHRP Project 22-38)</i>
W-Beam	W6x8.5	75	C6x8.2 backup rail 12 inches above grade	38.8	43.7	64.3	Simulated MASH Test 3-11	<i>NCHRP Research Report 1100: MASH TL-3 Deflection Reduction for 31-Inch Guardrail: A Guide (NCHRP Project 22-38)</i>
W-Beam	W6x8.5	75	C6x8.2 backup rail aligned with W-beam	36.4	NA	NA	Simulated MASH Test 3-11	<i>NCHRP Research Report 1100: MASH TL-3 Deflection Reduction for 31-Inch Guardrail: A Guide (NCHRP Project 22-38)</i>
W-Beam	W6x8.5	75	C6x8.2 rub rail 6 inches above grade	36.0	47.0	37.0	Simulated MASH Test 3-11	<i>NCHRP Research Report 1100: MASH TL-3 Deflection Reduction for 31-Inch Guardrail: A Guide (NCHRP Project 22-38)</i>
W-Beam	W6x8.5	75	C6x8.2 rub rail 12 inches above grade	34.7	48.8	19.8	Simulated MASH Test 3-11	<i>NCHRP Research Report 1100: MASH TL-3 Deflection Reduction for 31-Inch Guardrail: A Guide (NCHRP Project 22-38)</i>
W-Beam	W6x8.5	75	HSS4x4x1/4 backup rail aligned with W-beam	33.7	38.9	31.8	Simulated MASH Test 3-11	<i>NCHRP Research Report 1100: MASH TL-3 Deflection Reduction for 31-Inch Guardrail: A Guide (NCHRP Project 22-38)</i>
W-Beam	W6x8.5	75	10HU5x075 rub rail 12 inches above grade	31.5	45.6	22.7	Simulated MASH Test 3-11	<i>NCHRP Research Report 1100: MASH TL-3 Deflection Reduction for 31-Inch Guardrail: A Guide (NCHRP Project 22-38)</i>
W-Beam	W6x8.5	75	HSS4x4x1/4 backup rail 17.5 inches above grade	31.1	36.7	33.4	Simulated MASH Test 3-11	<i>NCHRP Research Report 1100: MASH TL-3 Deflection Reduction for 31-Inch Guardrail: A Guide (NCHRP Project 22-38)</i>

Table 11.3. (Continued).

Rail Type	Post Type	Post Spacing (inches)	Unique Feature(s)	Dynamic Deflection (inches)	Working Width (inches)	Working Width Height (inches)	Data Source	Reference
W-Beam	W6x8.5	75	8HU12x135 backup rail aligned with W-beam	25.4	33.8	38.3	Simulated MASH Test 3-11	<i>NCHRP Research Report 1100: MASH TL-3 Deflection Reduction for 31-Inch Guardrail: A Guide</i> (NCHRP Project 22-38)
W-Beam	W6x8.5	75	HSS8x8x1/4 blackout replacement	15.4	35.4	30.5	Simulated MASH Test 3-11	<i>NCHRP Research Report 1100: MASH TL-3 Deflection Reduction for 31-Inch Guardrail: A Guide</i> (NCHRP Project 22-38)
W-Beam	W6x8.5	18.75	HSS4x4x1/4 backup rail aligned with W-beam	10.1	26.5	26.6	Simulated MASH Test 3-11	<i>NCHRP Research Report 1100: MASH TL-3 Deflection Reduction for 31-Inch Guardrail: A Guide</i> (NCHRP Project 22-38)
W-Beam	W6x8.5	37.5	HSS8x8x1/4 blackout replacement	10.0	23.3	32.5	Simulated MASH Test 3-11	<i>NCHRP Research Report 1100: MASH TL-3 Deflection Reduction for 31-Inch Guardrail: A Guide</i> (NCHRP Project 22-38)
W-Beam	W6x8.5	18.75	HSS8x8x1/4 blackout replacement	7.4	20.9	32.4	Simulated MASH Test 3-11	<i>NCHRP Research Report 1100: MASH TL-3 Deflection Reduction for 31-Inch Guardrail: A Guide</i> (NCHRP Project 22-38)
NA = not available NOTE: Simulated MASH Test 3-11 designs were not evaluated through full-scale crash testing. Further analysis and/or full-scale crash testing may be required before implementation.								

Suggested Research

This project focused on developing deflection estimates for a variety of stiffening mechanisms appropriate for MGS applications. In this project's computer simulation effort, the research team developed 13 different methods for stiffening the typical MGS. These stiffening mechanisms ranged in both cost and deflection-reducing capability. The research team prioritized these mechanisms and selected the previously discussed combination of half-post spacing and HSS8x8x $\frac{3}{16}$ blackout replacement tube for crash testing. While the crash tests showed the computer simulations reasonably predicted the dynamic deflection of the physical testing, state DOTs may desire a physically crash-tested system prior to implementation. Consequently, future research could involve additional testing of those stiffening mechanisms that were not crash tested under this project.

The stiffened system (combination of half-post spacing and HSS8x8x $\frac{3}{16}$ blackout replacement tube) may be desired for installation in conditions outside the scope of this project—for example, connected to approach guardrail transitions (AGTs) or close to the curb. These and other possible conditions not explicitly explored under this project require further evaluation through professional opinions, computer simulation, full-scale crash testing, or a combination of these methodologies.

References

1. AASHTO (American Association for State Highway and Transportation Officials). *Roadside Design Guide*, 4th ed., Washington, DC, 2011.
2. Ross, H.E., D.L. Sicking, R.A. Zimmer, and J.D. Michie. *NCHRP Report 350: Recommended Procedures for the Safety Performance Evaluation of Highway Features*. Transportation Research Board of the National Academies, Washington, DC, 1993.
3. AASHTO (American Association for State Highway Transportation Officials). *Manual for Assessing Safety Hardware [MASH]*. Washington, DC, 2016.
4. Polivka, K.A., R.K. Faller, D.L. Sicking, J.D. Reid, J.R. Rohde, J.C. Holloway, R.W. Bielenberg, and B.D. Kuipers. *Development of the Midwest Guardrail System (MGS) for Standard and Reduced Post Spacing and in Combination with Curbs*. Midwest Roadside Safety Facility, University of Nebraska–Lincoln, 2004.
5. Weiland, N., C. Stolle, J. Reid, R. Faller, R. Bielenberg, and K. Lechtenberg. *MGS Dynamic Deflections and Working Widths at Lower Speeds*. Midwest Roadside Safety Facility, University of Nebraska–Lincoln, 2015.
6. Rosenbaugh, S.K., R.K. Faller, R.W. Bielenberg, K.A. Lechtenberg, D.L. Sicking, and J.D. Reid. *Development of the MGS Approach Guardrail Transition using Standardized Steel Posts*. MwRSF Research Report NO. TRP-03-210-10, Midwest Roadside Safety Facility, University of Nebraska–Lincoln, December 21, 2010.
7. Kovar, J.C., R.P. Bligh, W.L. Menges, G.E. Schroeder, W. Schroeder, S. Wegenast, B.L. Griffith, and D.L. Kuhn. *MASH Crash Testing and Evaluation of the MGS with Reduced Post Spacing*. Report Number 610211-01, Texas A&M Transportation Institute, College Station, TX, 2023. <https://www.roadsidepooledfund.org/wp-content/uploads/2023/06/TRNo610211-01-Final-REV-1-Signed.pdf>.
8. Arrington, D., and R. Rao. *Barrier Deflection Characteristics of 31-inch W-Beam Guardrail Systems*. Texas A&M Transportation Institute Proving Ground, College Station, TX, 2017.
9. Michie, J.D. *NCHRP Report 230: Recommended Procedures for the Safety Performance Evaluation of Highway Appurtenances*. Transportation Research Board of the National Academies, Washington, DC, 1981.
10. Rosson, B.T., M.G. Bierman, and J.R. Rohde. “Assessment of Guardrail-Strengthening Techniques.” *Transportation Research Record*, No.1528, 1996, pp. 69–77.
11. Stout, D., W. Hughes, and H. McGee. *Traffic Barriers on Curves, Curbs, and Slopes*. Report No. FHWA-RD-93-082, submitted to the Office of Safety and Traffic Operations R&D, Federal Highway Administration. Applied Technology and Engineering Division, ENSCO, Inc., Springfield, VA, 1993.
12. Abu-Odeh, A., K. Ha, I. Liu, and W. Menges. *MASH TL-3 Testing and Evaluation of the W-Beam Guardrail on Slope*. Roadside Safety Research Program Pooled Fund, Texas A&M Transportation Institute Proving Ground, College Station, TX, 2013.
13. Wiebelhaus, M.J., K.A. Lechtenberg, R.K. Faller, D.L. Sicking, R.W. Bielenberg, J.D. Reid, J.R. Rohde, and G. Dey. *Development and Evaluation of the Midwest Guardrail System Placed Adjacent to a 2:1 Fill Slope*. Midwest Roadside Safety Facility, University of Nebraska–Lincoln, 2010. http://www.roadsidepooledfund.org/wp-content/uploads/2016/10/MGS221-2_Report.pdf.
14. Haase, A.J., J.E. Kohtz, K.A. Lechtenberg, R.W. Bielenberg, J.D. Reid and R.K. Faller. *Midwest Guardrail System (MGS) with 6-ft Posts Placed Adjacent to a 1V:2H Fill Slope*. Midwest Roadside Safety Facility, University of Nebraska–Lincoln, 2016. <https://mwrsf.unl.edu/researchhub/files/Report325/TRP-03-320-16.pdf>.
15. Bligh, R.P., W.L. Menges, B.L. Griffith, G.E. Schroeder, and D.L. Kuhn. *MASH Evaluation of TxDOT Roadside Safety Features – Phase II*. Texas A&M Transportation Institute, College Station, TX, 2019. <https://static.tti.tamu.edu/tti.tamu.edu/documents/0-6946-R2.pdf>.
16. Kovar, J.C., R.P. Bligh, B.L. Griffith, D.L. Kuhn, and G.E. Schroeder. *MASH Test 3-11 Evaluation of Modified TxDOT Round Wood Post Guardrail System*. Report Number 0-6968-R4, Texas A&M Transportation Institute, College Station, TX, 2019.

17. Stolle C., K.A. Lechtenberg, R.K. Faller, S. Rosenbaugh, D.L. Sicking, and J.D. Reid. *Evaluation of the Midwest Guardrail System (MGS) with White Pine Wood Posts*. Midwest Roadside Safety Facility, University of Nebraska–Lincoln, 2011. https://www.roadsidepooledfund.org/wp-content/uploads/2016/10/MGSPW-1_Report.pdf.
18. Dobrovolsky, C.S., K.M. White, and R.P. Bligh. *Synthesis of System/Vehicle Interaction Similarities/Dissimilarities with 12-Inch vs. 8-Inch Blockouts with 31-Inch Mounting Height, Mid-Span Slices*. Texas Transportation Institute, College Station, TX, 2014.
19. Reid, J.D., R.W. Bielenberg, R.K. Faller, and K.A. Lechtenberg. “Midwest Guardrail System Without Blockouts.” *Transportation Research Record: Journal of the Transportation Research Board*, No. 2377, 2011, pp. 1–13.
20. Plaxico, C.A., J.C. Kennedy, Jr., and C.R. Miele. *Evaluation and Design of ODOT’s Type 5 Guardrail with Tubular Backup*. Battelle, Columbus, OH, 2005.
21. AASHTO (American Association for State Highway and Transportation Officials). *Roadside Design Guide*, 3rd ed. Washington, DC, 2006.
22. Polivka K.A., R.K. Faller, D.L. Sicking, J.R. Rohde, R.W. Bielenberg, and J.D. Reid. *Performance Evaluation of the Midwest Guardrail System – Update to NCHRP 350 Test No. 3-11 with 28” C.G. Height (2214MG-2)*. Midwest Roadside Safety Facility, University of Nebraska–Lincoln, 2006. <https://mwrsf.unl.edu/researchhub/files/Report149/TRP-03-171-06.pdf>.
23. Bullard, Jr., D.L., R.P. Bligh, W.L. Menges, and R.R. Haug. *NCHRP Web-Only Document 157: Volume I: Evaluation of Existing Roadside Safety Hardware Using Updated Criteria—Technical Report*. Transportation Research Board, Washington, DC, 2010. <https://www.trb.org/Publications/Blurbs/163969.aspx>.
24. Bielenberg, R.W., R.K. Faller, J.R. Rohde, J.D. Reid, D.L. Sicking, J.C. Holloway, E.M. Allison, and K.A. Polivka. *Midwest Guardrail System for Long-Span Culvert Applications*. Midwest States’ Regional Pooled Fund Research Program, Midwest Roadside Safety Facility, University of Nebraska–Lincoln, 2007. <https://mwrsf.unl.edu/researchhub/files/Report109/TRP-03-187-07.pdf>.
25. Hascall, J.A., R.K. Faller, J.D. Reid, D.L. Sicking, and D.E. Kretschmann. *Investigating the Use of Small-Diameter Softwood as Guardrail Posts (Dynamic Test Results)*. Midwest Roadside Safety Facility, University of Nebraska–Lincoln, 2007. <https://mwrsf.unl.edu/researchhub/files/Report125/TRP-03-179-07.pdf>.
26. Griffith, M.S. Correspondence to S.G. Carlson, Wyoming Department of Transportation from FHWA, 2020. <https://www.roadsidepooledfund.org/wp-content/uploads/2020/07/B-334.pdf>.
27. Bullard, D.L., R.P. Bligh, W.L. Menges, and R.R. Haug. *Research Results Digest 349: Evaluation of Existing Roadside Safety Hardware using Manual for Assessing Safety Hardware (MASH) Criteria*. Transportation Research Board of the National Academies, Washington, DC, 2010. <https://doi.org/10.17226/14409>.
28. Johnson, E.A. K.A. Lechtenberg, J.D. Reid, D.L. Sicking, R.K. Faller, R.W. Bielenberg, and J.R. Rohde. *Approach Slope for Midwest Guardrail System*. Midwest States’ Regional Pool Fund Research Program, Midwest Roadside Safety Facility, University of Nebraska–Lincoln, 2008. <https://mwrsf.unl.edu/researchhub/files/Report81/TRP-03-188-08.pdf>.
29. Griffith, M.S. Correspondence to H. Raza, Pennsylvania Department of Transportation from FHWA, 2020. <https://www.roadsidepooledfund.org/wp-content/uploads/2020/05/b332.pdf>.
30. Dobrovolsky, C.S., W.L. Mengs, and D.L. Kuhn. *MASH Test 3-11 of 28-Inch W-Beam Guardrail System with 8-Inch Composite Blockouts Raised 4 Inches on Steel Post*. Roadside Safety Pooled Fund, Texas Transportation Institute Proving Ground, Texas A&M University System, Bryan, TX, 2017. <https://www.roadsidepooledfund.org/wp-content/uploads/2017/11/TRNo-608421-1-Finalv2.pdf>.
31. Lingenfelter, J.L., S. Rosenbaugh, R.W. Bielenberg, K.A. Lechtenberg, R.K. Faller, and J.D. Reid. *Midwest Guardrail System (MGS) with an Omitted Post*. Midwest States’ Pooled Fund Research Program, Midwest Roadside Safety Facility, University of Nebraska–Lincoln, 2016. <https://mwrsf.unl.edu/researchhub/files/Report317/TRP-03-326-16.pdf>.
32. Thiel, J.C., D.L. Sicking, R.K. Faller, R.W. Bielenberg, K.A. Lechtenberg, J.D. Reid, and S.K. Rosenbaugh. *Development of a Low-Cost Energy-Absorbing Bridge Rail*. Midwest States Regional Pooled Fund Research Program, Midwest Roadside Safety Facility, University of Nebraska–Lincoln, 2010. <https://mwrsf.unl.edu/researchhub/files/Report53/TRP-03-226-10.pdf>.
33. Polivka K.A., R.K. Faller, D.L. Sicking, J.R. Rohde, R.W. Bielenberg, and J.D. Reid. *Performance Evaluation of the Modified G4(1S) Guardrail – Update to NCHRP 350 Test No. 3-11 with 28” C.G. Height (2214WB-2)*. Midwest Roadside Safety Facility, University of Nebraska–Lincoln, 2006. <https://www.roadsidepooledfund.org/wp-content/uploads/2017/05/TRP-03-169-06.pdf>.
34. Williams, W.F., and W.L. Menges. *MASH Test 3-11 of the W-Beam Guardrail on Low-Fill Box Culvert*. Texas A&M Transportation Institute Proving Ground, Texas A&M University System, Bryan, TX, 2011. https://www.roadsidepooledfund.org/wp-content/uploads/2016/10/405160-23-2_Report.pdf.
35. Pajoub, M.A., R.W. Bielenberg, J. Schmidt, J. Lingenfelter, R.K. Faller, and J.D. Reid. *Placement of Breakaway Light Poles Located Directly Behind Midwest Guardrail System (MGS)*. Midwest Roadside Safety Facility, University of Nebraska–Lincoln, 2017. <https://www.roadsidepooledfund.org/wp-content/uploads/2017/09/TRP-03-361-17.pdf>.

36. Rosenbaugh, S.K., R.K. Faller, K.A. Lechtenberg, and J.C. Holloway. *Development and Evaluation of Weak-Post W-Beam Guardrail in Mow Strips*. Mid-American Transportation Center, Midwest States Regional Pooled Fund Program, Midwest Roadside Safety Facility, University of Nebraska–Lincoln, 2015. <https://mwrsf.unl.edu/researchhub/files/Report315/TRP-03-322-15.pdf>.
37. Weiland, N.A., J.D. Reid, R.K. Faller, D.L. Sicking, R.W. Bielenberg, and K.A. Lechtenberg. *Minimum Effective Guardrail Length for the MGS*. Midwest Roadside Safety Facility, University of Nebraska–Lincoln, 2013. <https://mwrsf.unl.edu/researchhub/files/Report281/TRP-03-276-13.pdf>.
38. Kiani, M., J. Kovar, W.L. Menges, W. Schroeder, B.L. Griffith, S. Wegenast, and D.L. Kuhn. *Design and Testing of MASH TL-3 Thrie Beam Guardrail System (TGS) for Roadside and Median Application*. Texas A&M Transportation Institute Proving Ground, Texas A&M University System, Bryan, TX, 2021. https://www.roadsidepooledfund.org/wp-content/uploads/2023/04/TRNo614341-01-Final_V2.pdf.
39. Gutierrez, D.A., K.A. Lechtenberg, R.W. Bielenberg, R.K. Faller, J.D. Reid, and D.L. Sicking. *Midwest Guardrail System (MGS) with Southern Yellow Pine Posts*. Midwest Roadside Safety Facility, University of Nebraska–Lincoln, 2013. <https://mwrsf.unl.edu/researchhub/files/Report282/TRP-03-272-13.pdf>.
40. Ronspies, K., S. Rosenbaugh, R.W. Bielenberg, R.K. Faller, and C. Stolle. *Evaluation of the MGS Placed 6 In. Behind a 6-In.-Tall AASHTO Type B Curb to MASH TL-3*. Midwest Pooled Fund Program, Midwest Roadside Safety Facility, University of Nebraska–Lincoln, 2020. <https://mwrsf.unl.edu/researchhub/files/Report389/TRP-03-390-20.pdf>.
41. Abu-Odeh, A.Y., R.P. Bligh, M.L. Mason, and W.L. Menges. *Development and Evaluation of MASH TL-3 31-Inch W-Beam Median Barrier*. Texas A&M Transportation Institute, College Station, TX, 2013. <https://www.roadsidepooledfund.org/wp-content/uploads/2016/10/9-1002-12-8draftsubmit-1.pdf>.
42. Rosenbaugh, S.K., and S.J. Corey. *MGS with Curb and Omitted Post: Evaluation to MASH 2016 Test No. 3-11*. Midwest Roadside Safety Facility, University of Nebraska–Lincoln, 2021. <https://mwrsf.unl.edu/researchhub/files/Report395/TRP-03-433-21.pdf>.
43. McGhee, M.D., R.K. Faller, J.R. Rohde, K.A. Lechtenberg, D.L. Sicking, and J.D. Reid. *Development of an Economical Guardrail System for Use on Wire-Faced, MSE Walls*, Draft Report. Midwest Roadside Safety Facility, University of Nebraska–Lincoln, 2012. [https://mwrsf.unl.edu/researchhub/files/Report26/TRP-03-235-11_\(draft_final_to_FHWA-CFL\).pdf](https://mwrsf.unl.edu/researchhub/files/Report26/TRP-03-235-11_(draft_final_to_FHWA-CFL).pdf).
44. Bielenberg, R.W., R.K. Faller, J. Jiang, and J.C. Holloway. *MASH 2016 Evaluation of the Modified Thrie-Beam System*. Midwest Roadside Safety Facility, University of Nebraska–Lincoln, 2020. <https://www.roadsidepooledfund.org/wp-content/uploads/2020/07/TRP-03-417-20.pdf>.
45. Schrum, K.D., K.A. Lechtenberg, R.W. Bielenberg, S.K. Rosenbaugh, R.K. Faller, and J.D. Reid. *Safety Performance Evaluation of the Non-Blocked Midwest Guardrail System (MGS)*. Midwest Roadside Safety Facility, University of Nebraska–Lincoln, 2013. <https://www.roadsidepooledfund.org/wp-content/uploads/2016/10/TRP-03-262-12.pdf>.
46. Pajoub, M.A., R.W. Bielenberg, J.D. Rasmussen, F. Bai, R.K. Faller, and J.C. Holloway. *Dynamic Testing and Evaluation of Culvert-Mounted, Strong-Post MGS to TL-3 Guidelines of MASH 2016*. Midwest Roadside Safety Facility, University of Nebraska–Lincoln, 2020. <https://www.roadsidepooledfund.org/wp-content/uploads/2021/01/TRP-03-383-20-R1.pdf>.
47. Sheikh, N.M., J.C. Kovar, W.L. Menges, G.E. Schroeder, and D.L. Kuhn. *MASH TL-3 Evaluation of W-Beam Median Barrier with Rub Rail*. Texas A&M Transportation Institute Proving Ground, Texas A&M University System, Bryan, TX, 2020. <https://www.roadsidepooledfund.org/wp-content/uploads/2021/05/TRNo611971-3-Final.pdf>.



Acronyms

A2LA	American Association for Laboratory Accreditation
AASHTO	American Association of State Highway and Transportation Officials
CG	Center of gravity
CIP	Critical Impact Point
DAS	Data Acquisition System
FE	Finite Element
FEA	Finite Element Analysis
HPRC	High-Performance Research Computing
IEC	International Electrotechnical Commission
ISO	International Standards Organization
KDOT	Kansas Department of Transportation
LON	Length of Need
MA	Moving Average Accelerations
MASH	Manual for Assessing Safety Hardware, Second Edition
MGS	Midwest Guardrail System
MwRSF	Midwest Roadside Safety Facility
NIST	National Institute of Standards Technology
OIV	Occupant Impact Velocity
RDA	Ridedown Acceleration
RDG	Roadside Design Guide
RSVVP	Roadside Safety Verification and Validation Program
TGS	Thrie-Beam Guardrail System
THIV	Theoretical Head Impact Velocity
TL	Test Level
TRAP	Test Risk Assessment Program
TTI	Texas A&M Transportation Institute
WP	White pine



APPENDIX A

Details for the Stiffened MGS and Transition



APPENDIX A - 1

Details for 612941-02-1 and 2

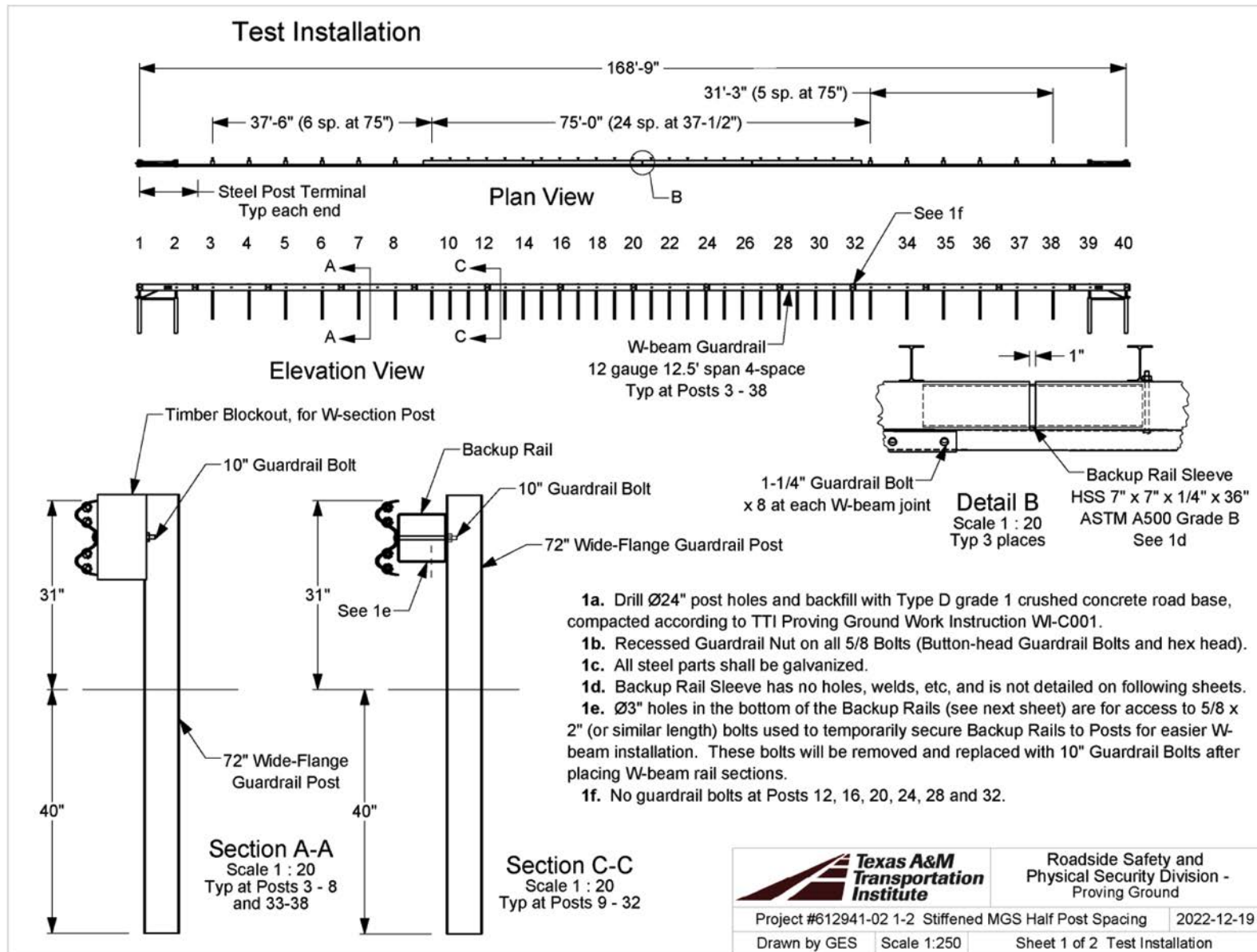


Figure A-1.1. Tests 612941-02-1 and -2 installation details.

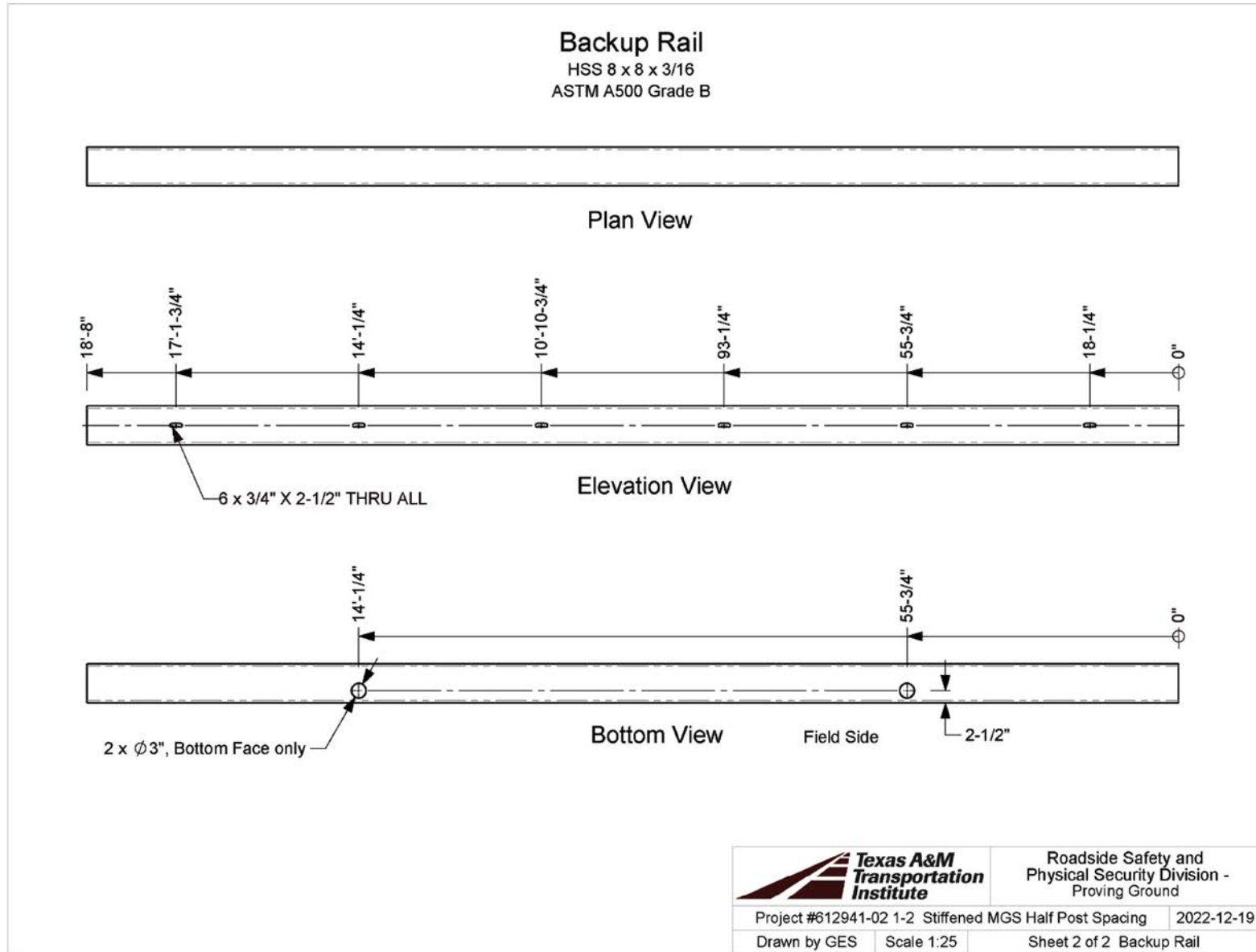
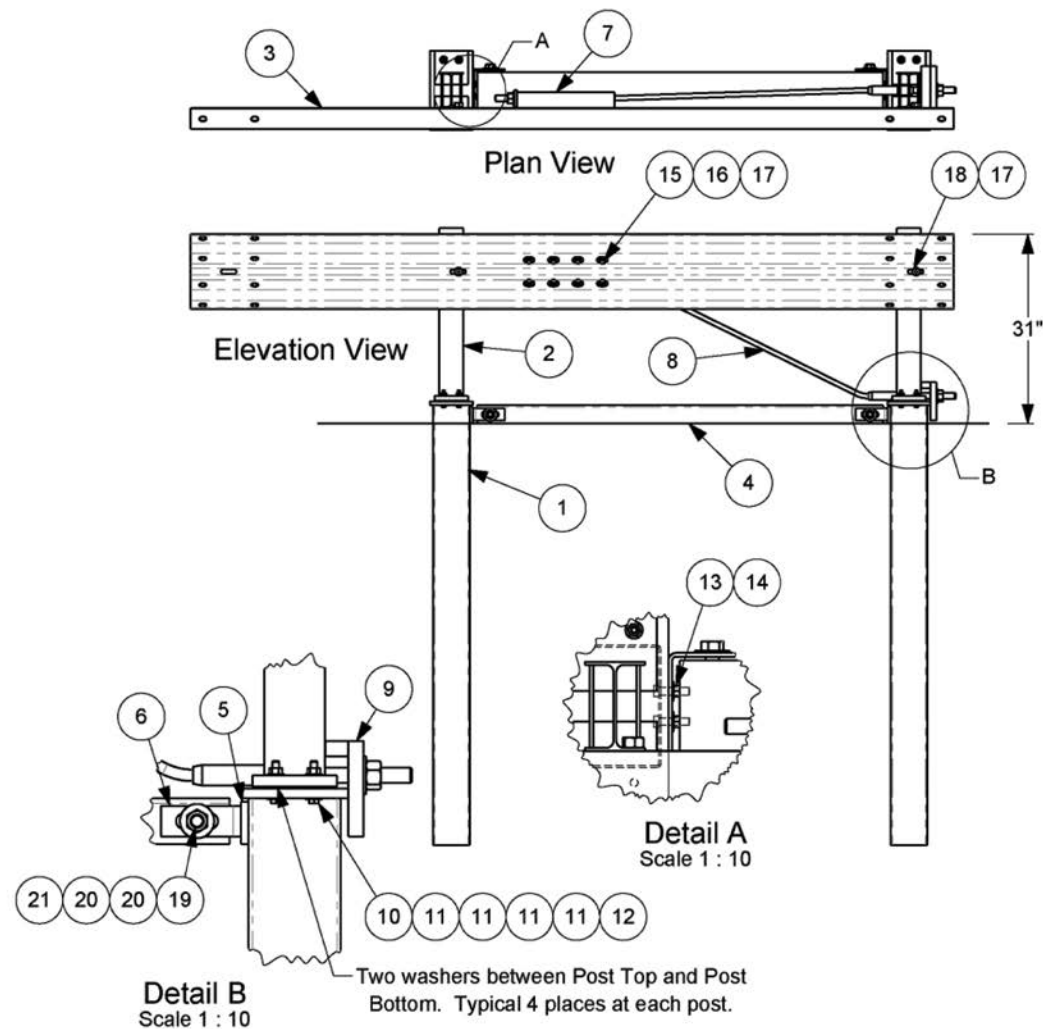


Figure A-1.2. Tests 612941-02-1 and -2 backup rail.

Terminal Details

#	Part Name	QTY.
1	Post Bottom	2
2	Post Top	2
3	9'-4-1/2" span Terminal Rail	1
4	Strut	1
5	Strut Spacer	2
6	Strut Bracket	2
7	Guardrail Anchor Bracket	1
8	Anchor Cable Assembly	1
9	Bearing Plate	1
10	Bolt, 7/16 x 2 1/2" hex	8
11	Washer, 7/16 F844	32
12	Nut, 7/16 heavy hex	8
13	Nut, 1/2 hex	4
14	Washer, 1/2 F844	4
15	Bolt, 5/8 x 1 1/2" hex	8
16	Washer, 5/8 F844	8
17	Recessed Guardrail Nut	10
18	1-1/4" Guardrail Bolt	2
19	Bolt, 7/8 x 8 1/2" hex	2
20	Washer, 7/8 F844	4
21	Nut, 7/8 hex	2



1a. 7/16" x 2-1/2" Bolts are ASTM A449. All other Bolts are ASTM A307. All Nuts (except Recessed Guardrail Nuts) are ASTM A563A unless otherwise indicated.

1c. All steel parts shall be galvanized.



Roadside Safety and
Physical Security Division -
Proving Ground

Project # Terminal

2022-11-10

Drawn by GES

Scale 1:25

Sheet 1 of 6 Terminal Details

T:\Drafting Department\Solidworks\Standard Parts\Guardrail Parts and Subs\Guardrail Drawings\Midwest Terminal

Figure A-1.3. Tests 612941-02-1 and -2 terminal details.

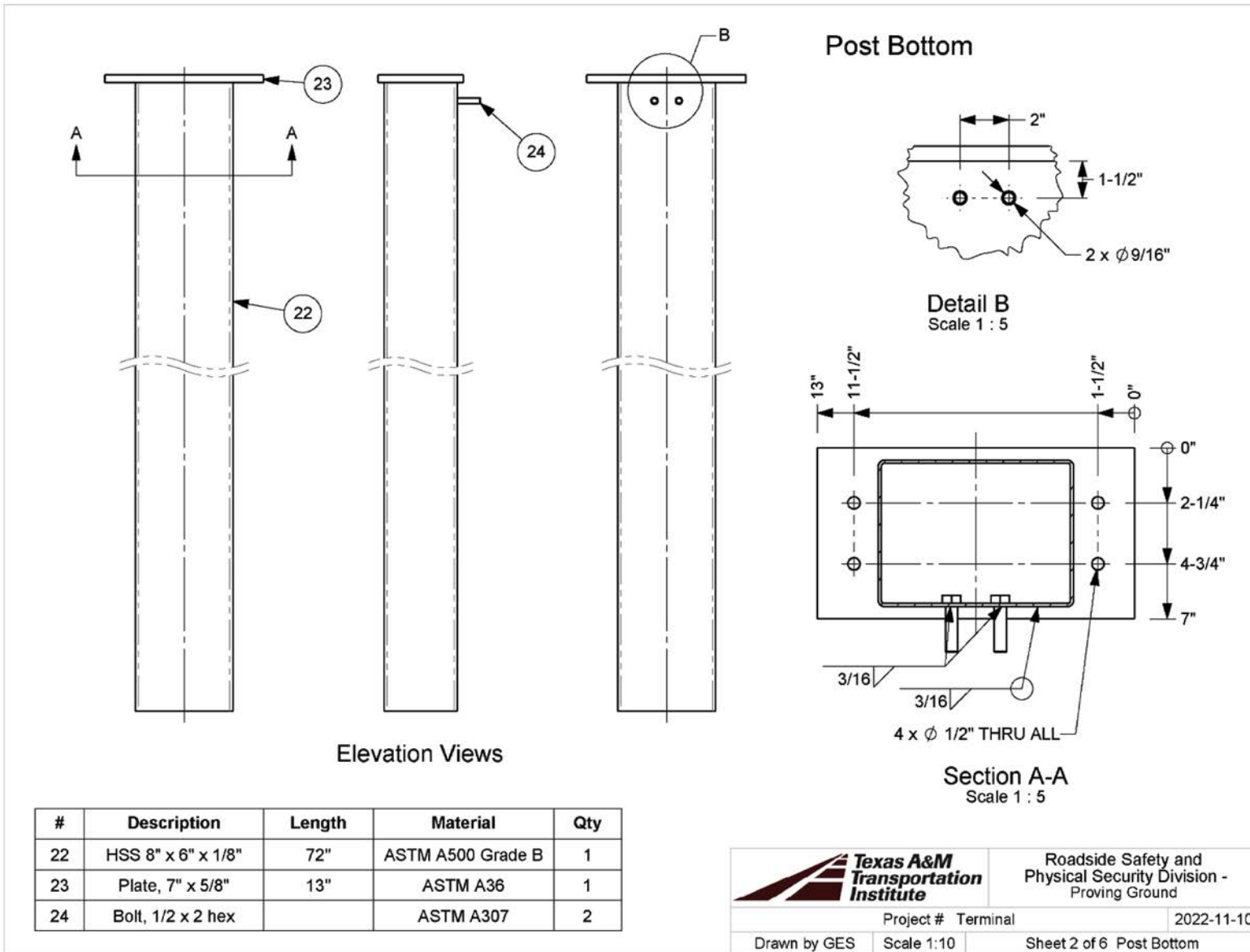
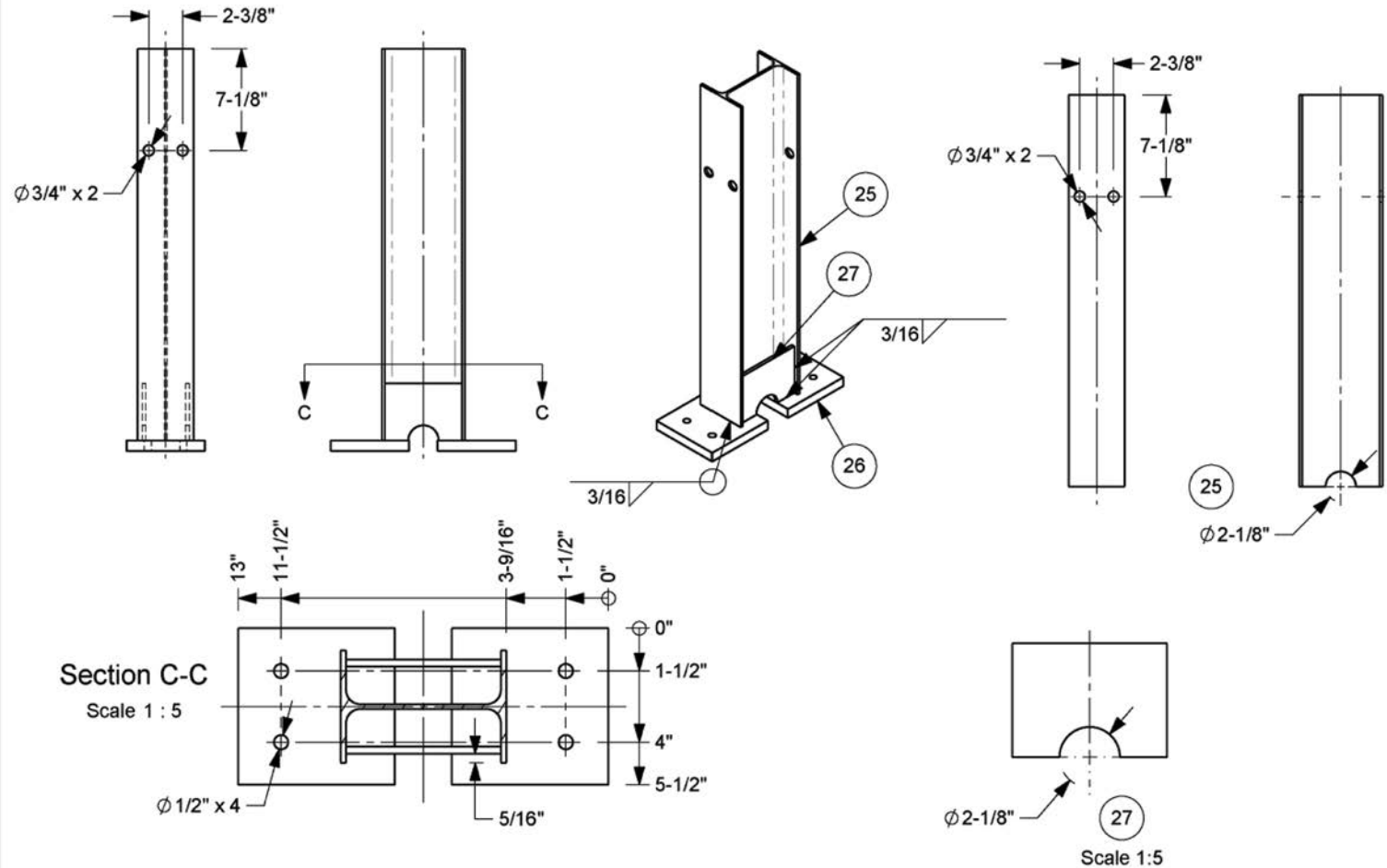


Figure A-1.4. Tests 612941-02-1 and -2 additional terminal details.



#	Description	Length	Material	Qty
25	W6x8.5	27 1/2"	ASTM A992	1
26	Plate, 5 1/2" x 3/4"	5 1/2"	ASTM A36	2
27	Plate, 5 7/16" x 1/4"	4"	ASTM A36	2



Roadside Safety and
Physical Security Division -
Proving Ground

Project # Terminal

2022-11-10

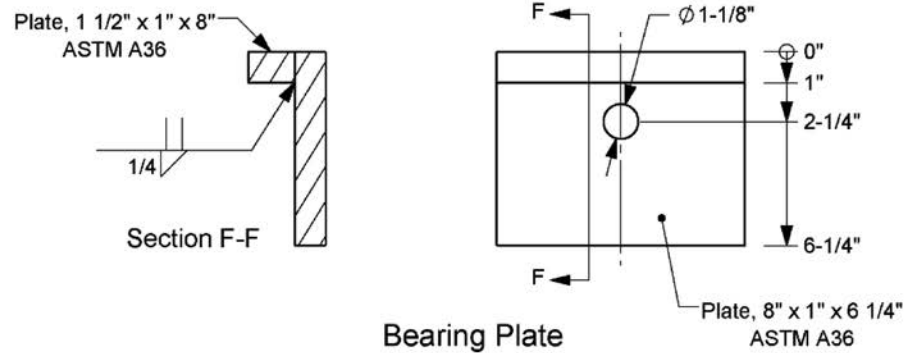
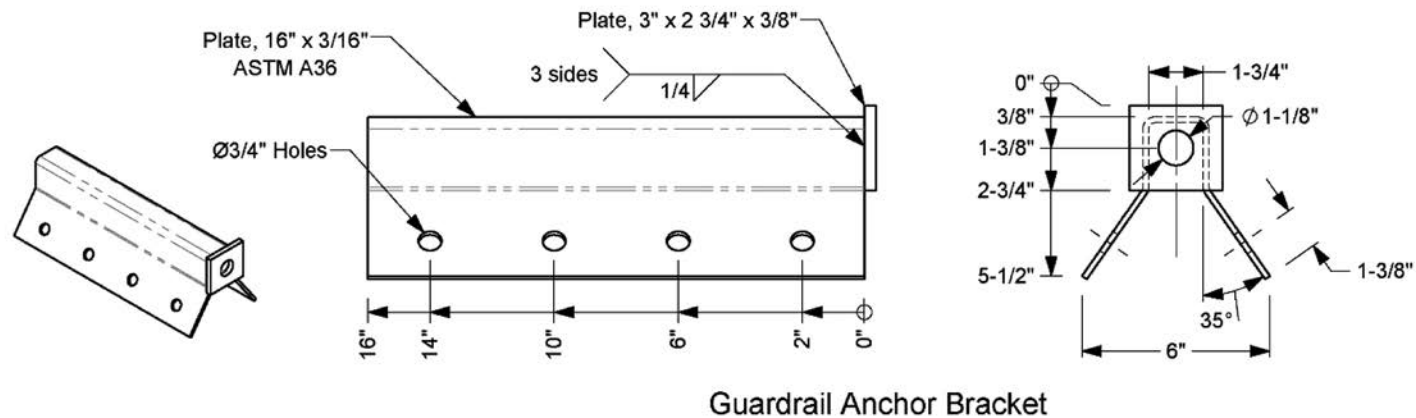
Drawn by GES


Scale 1:10

Sheet 3 of 6 Post Top

T:\Drafting Department\Solidworks\Standard Parts\Guardrail Parts and Subs\Guardrail Drawings\Midwest Terminal

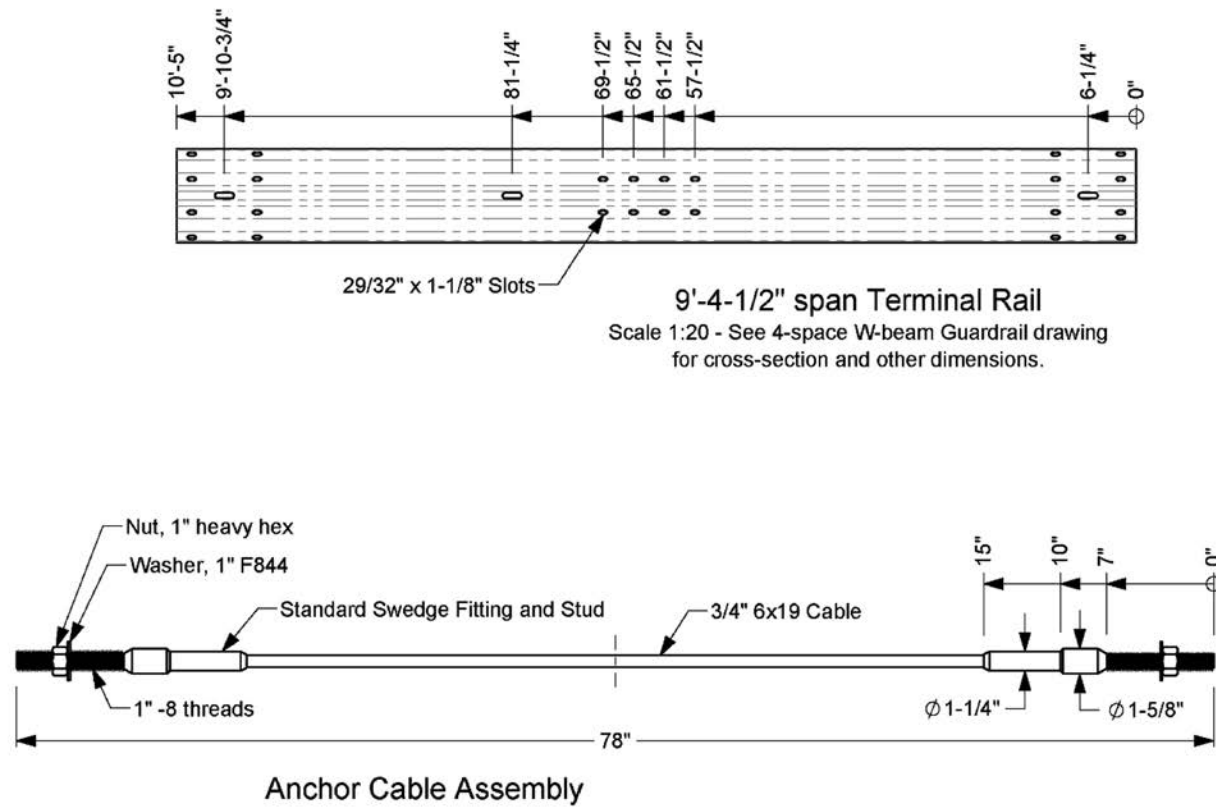
Figure A-1.5. Tests 612941-02-1 and -2 additional terminal details.



		Roadside Safety and Physical Security Division - Proving Ground
Project #	Terminal	2022-11-10
Drawn by GES	Scale 1:5	Sheet 5 of 6 Assorted Parts A

T:\Drafting Department\Solidworks\Standard Parts\Guardrail Parts and Subs\Guardrail Drawings\Midwest Terminal

Figure A-1.7. Tests 612941-02-1 and -2 additional terminal details.



Roadside Safety and
Physical Security Division -
Proving Ground

Project # Terminal

2022-11-10

Drawn by GES

Scale 1:5

Sheet 6 of 6 Assorted Parts B

T:\Drafting Department\Solidworks\Standard Parts\Guardrail Parts and Subs\Guardrail Drawings\Midwest Terminal

Figure A-1.8. Tests 612941-02-1 and -2 additional terminal details.

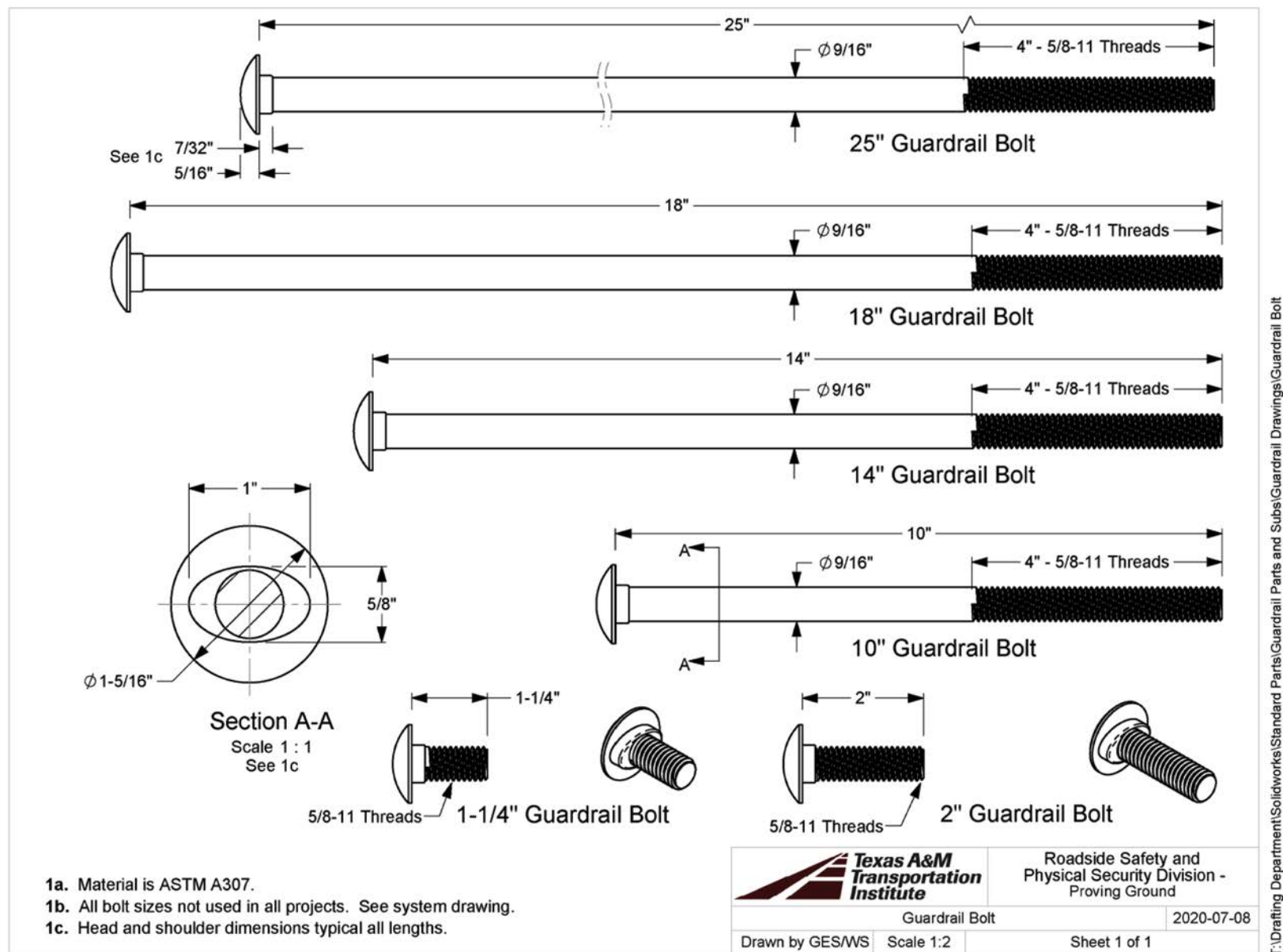
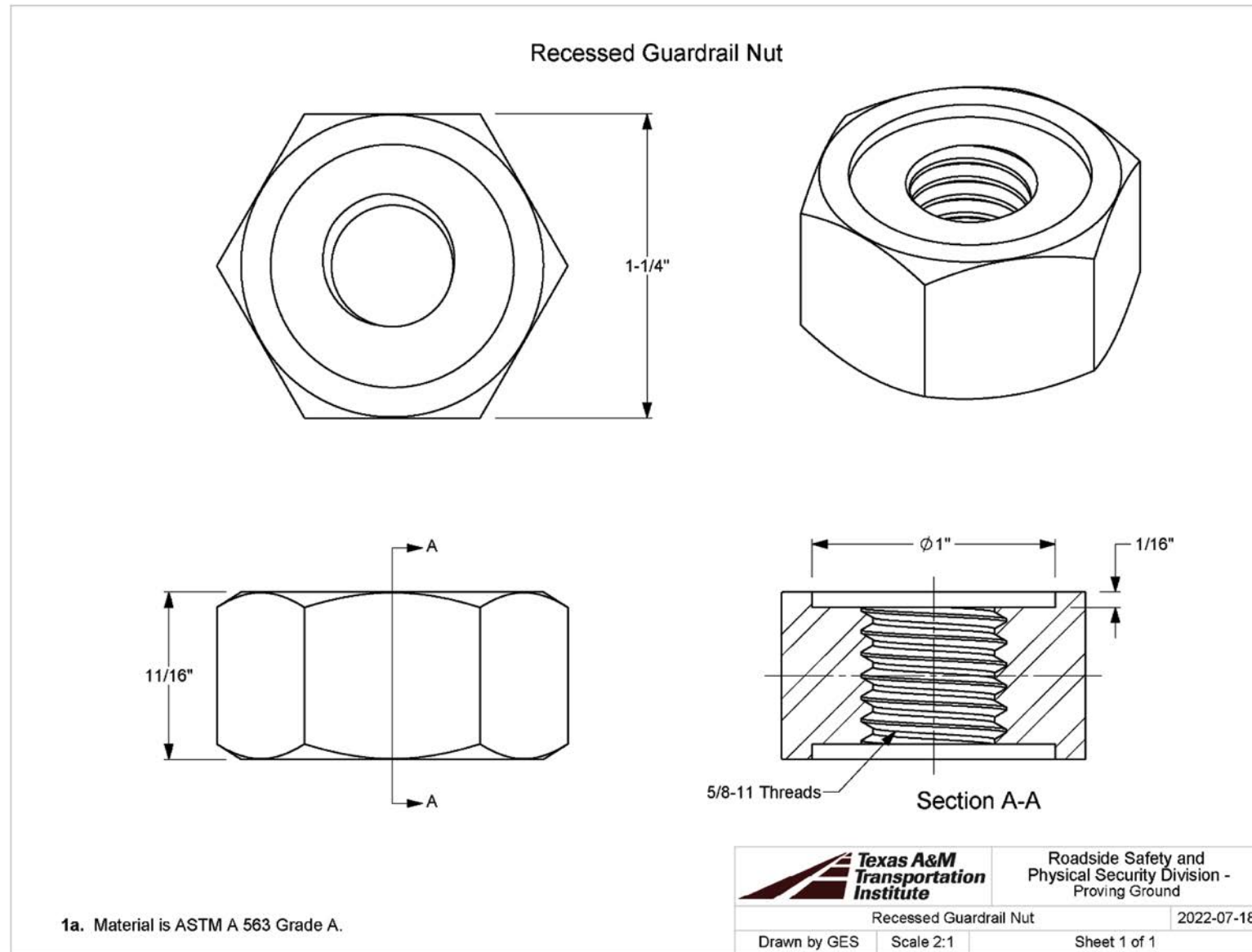


Figure A-1.9. Tests 612941-02-1 and -2 guardrail bolts.



T:\Drafting Department\Solidworks\Standard Parts\Guardrail Parts and Subs\Guardrail Drawings\Nut, Recessed Guardrail

Figure A-1.10. Tests 612941-02-1 and -2 guardrail nut.

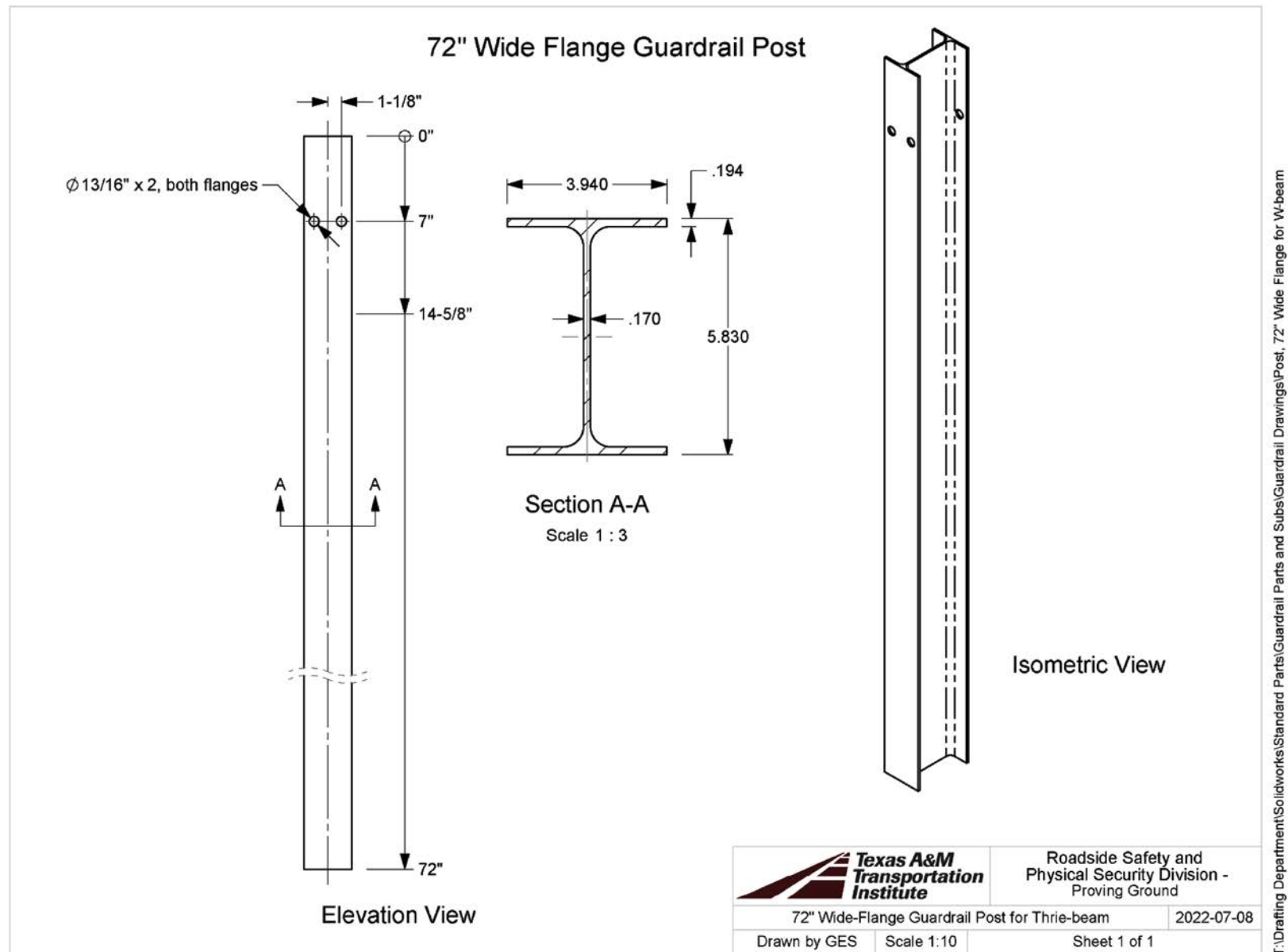
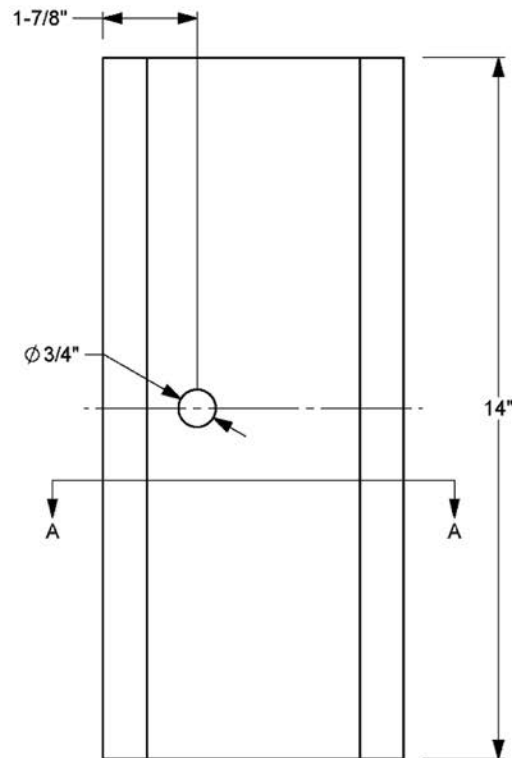


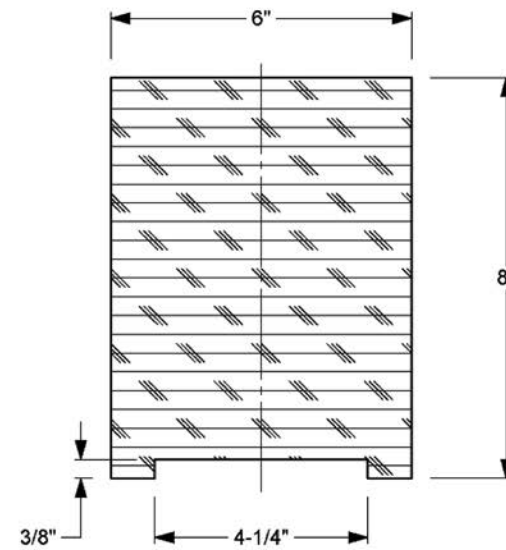
Figure A-1.11. Tests 612941-02-1 and -2 guardrail post.

Timber Blockout for W-section Post

All dimensions except hole diameter are nominal



Elevation View



Section A-A

1a. Timber blockouts are treated with a preservative in accordance with AASHTO M 133 after all cutting and drilling.



Roadside Safety and
Physical Security Division -
Proving Ground

Timber Blockout, for W-section Post

2022-12-16

Drawn by GES

Scale 1:3

Sheet 1 of 1

T:\Drafting Department\Solidworks\Standard Parts\Guardrail Parts and Subs\Guardrail Drawings\Timber Blockout for W-section Post

Figure A-1.12. Tests 612941-02-1 and -2 timber blockout.

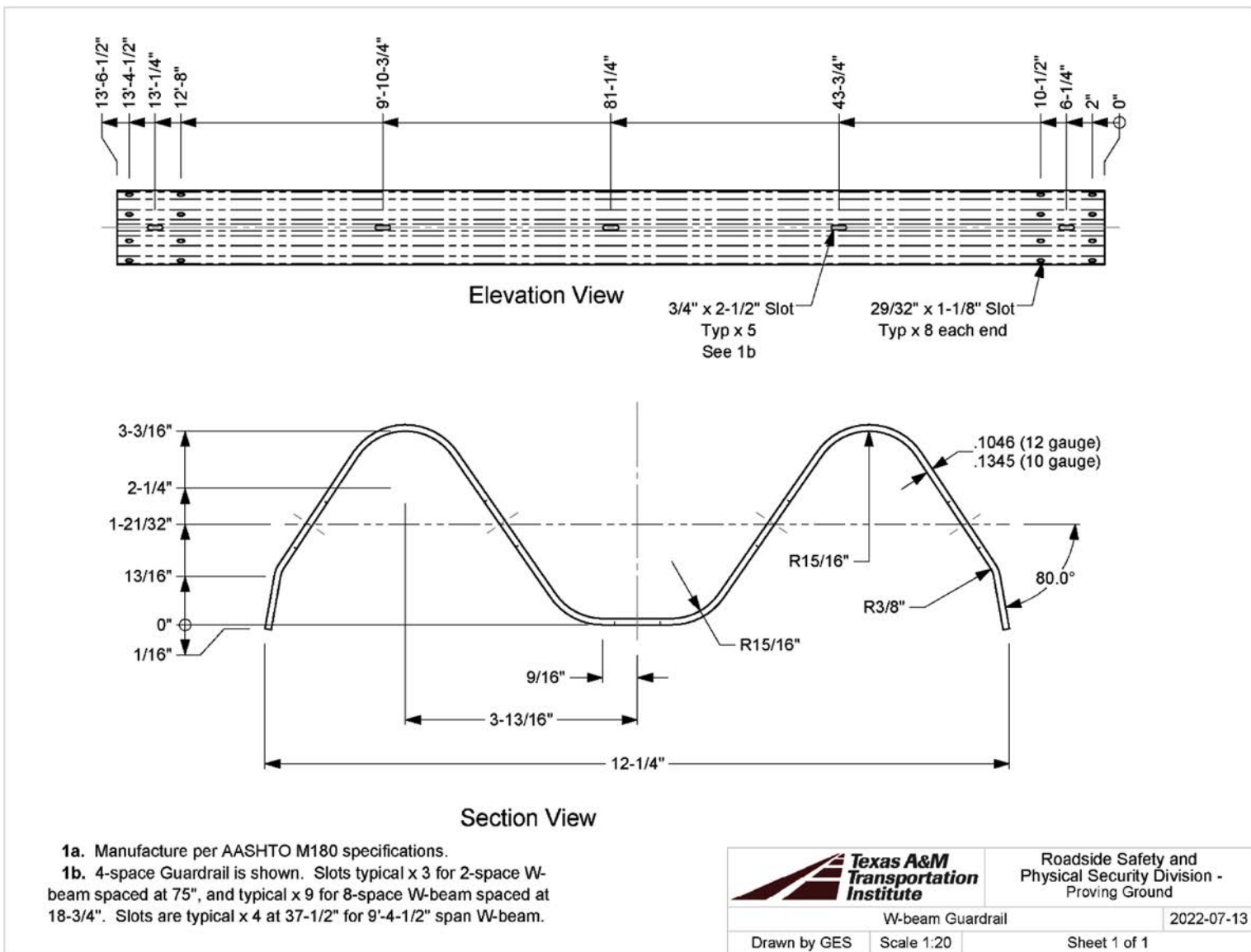
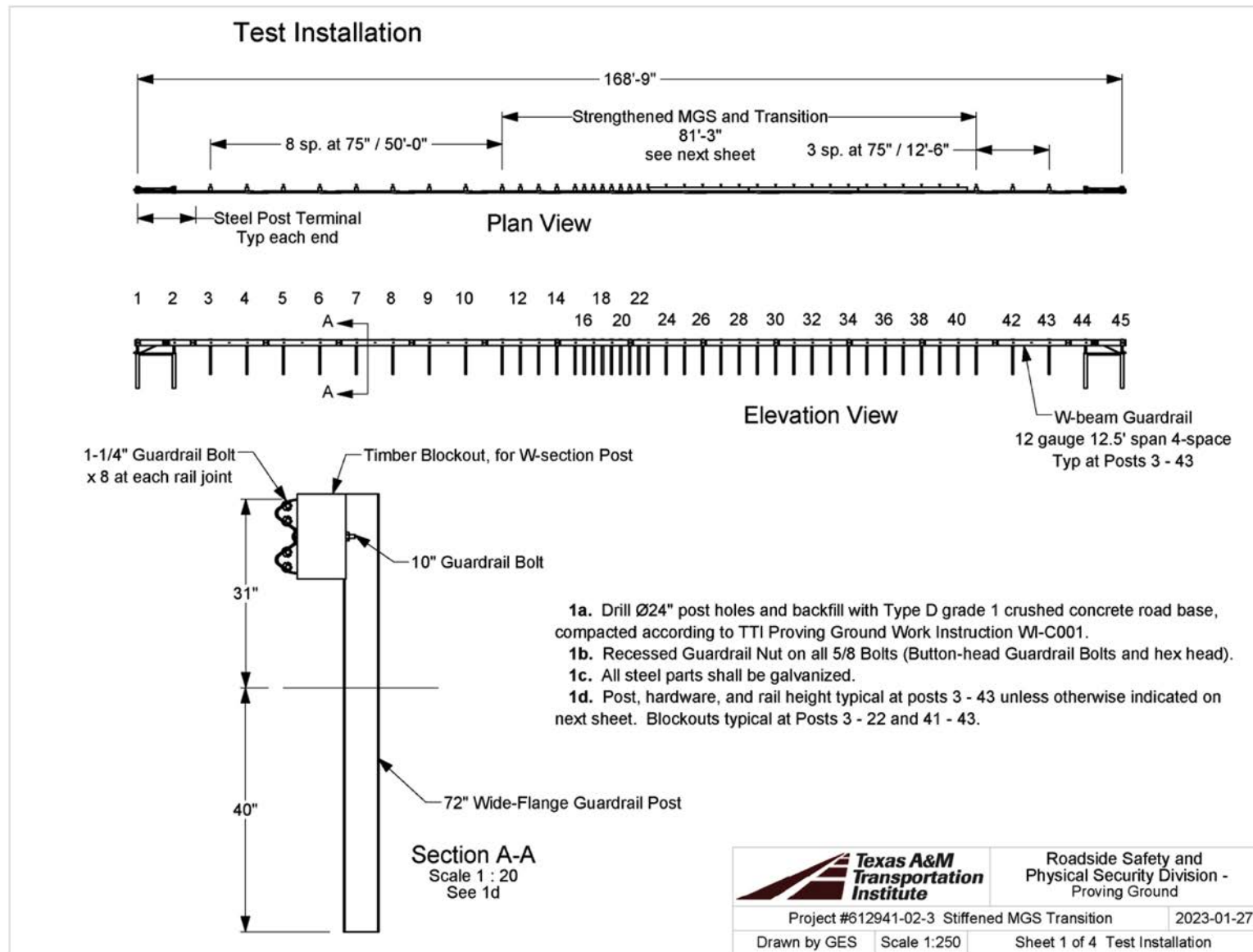


Figure A-1.13. Tests 612941-02-1 and -2 W-beam guardrail.



APPENDIX A - 2

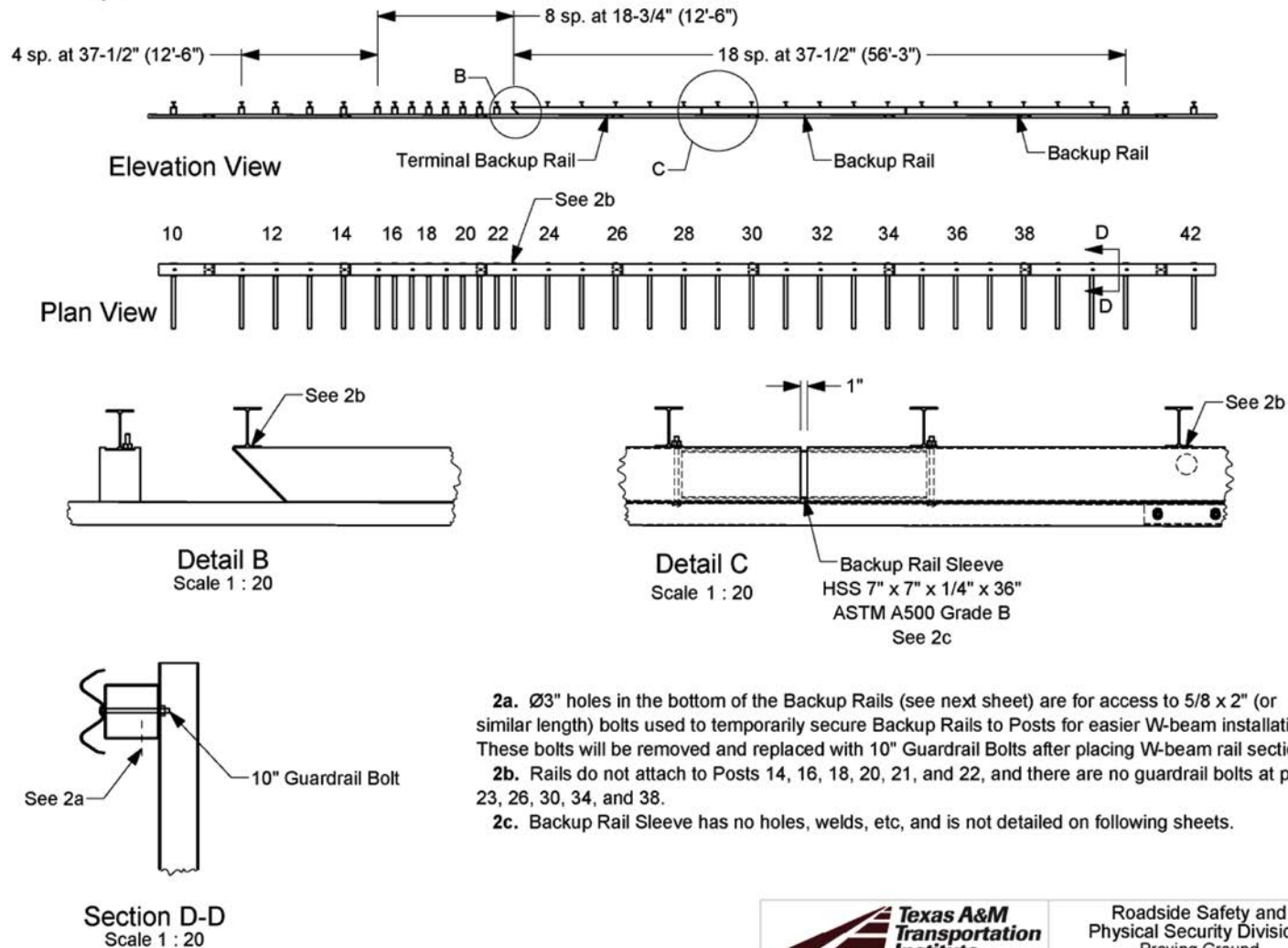
Details for 612941-02-3 and 612941-02-4



S:\Accreditation-17025-2017\EIR-000 Project Files\612941-02 - Stiffened MGS - Kovar\612941-02-3 3-21\Drafting, 612941-02-3\612941-02-3 Drawing

Figure A-2.1. Tests 612941-02-3 and -4 installation details.

At Backup Rails



Roadside Safety and
Physical Security Division -
Proving Ground

Project #612941-02-3 Stiffened MGS Transition

2023-01-27

Drawn by GES

Scale 1:150

Sheet 2 of 4 At Backup Rails

S:\Accreditation-17025-2017\EIR-000 Project Files\612941-02 - Stiffened MGS - Kovar\612941-02-3 3-21\Drafting, 612941-02-3\612941-02-3 Drawing

Figure A-2.2. Tests 612941-02-3 and -4 additional installation details.

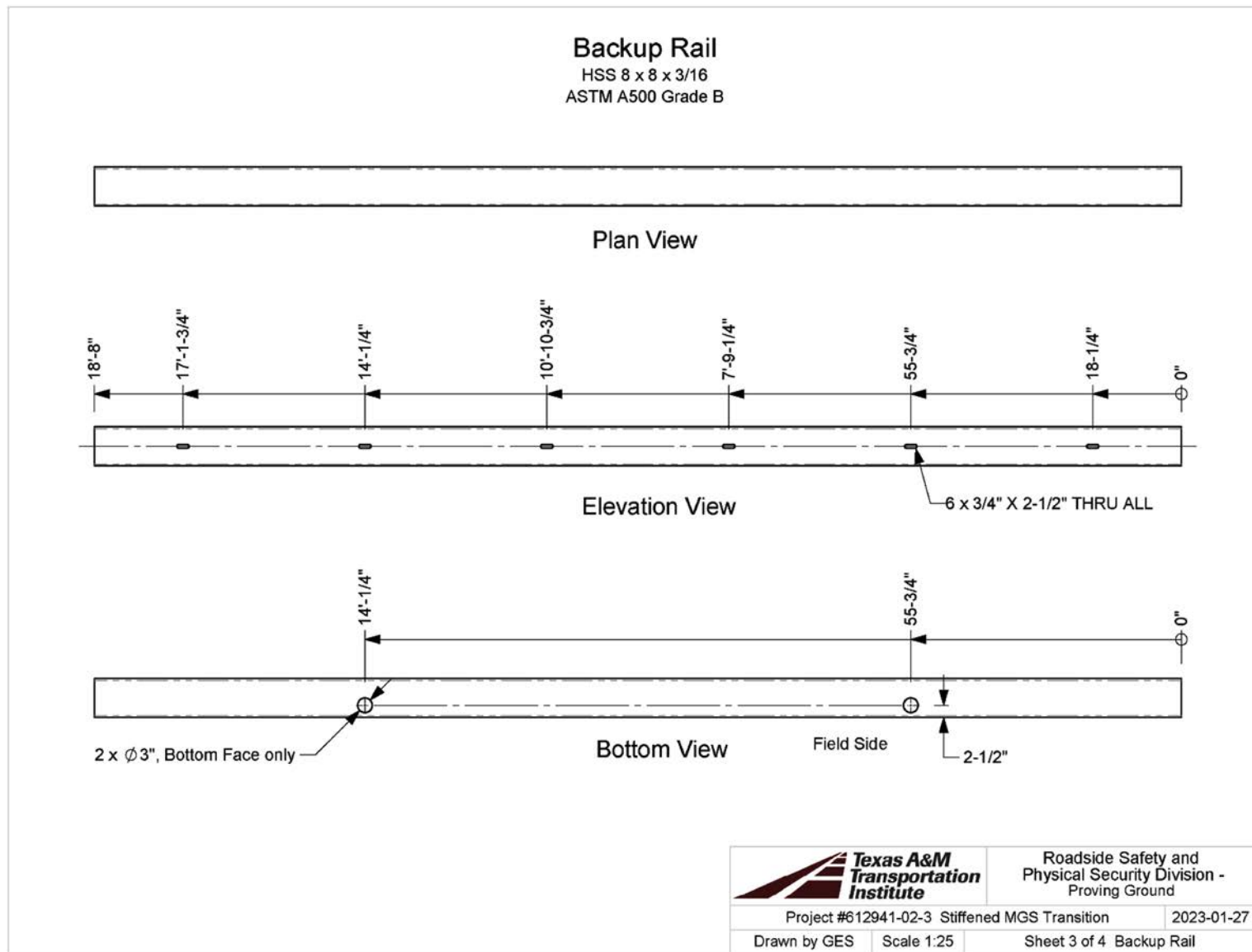


Figure A-2.3. Tests 612941-02-3 and -4 backup rail.

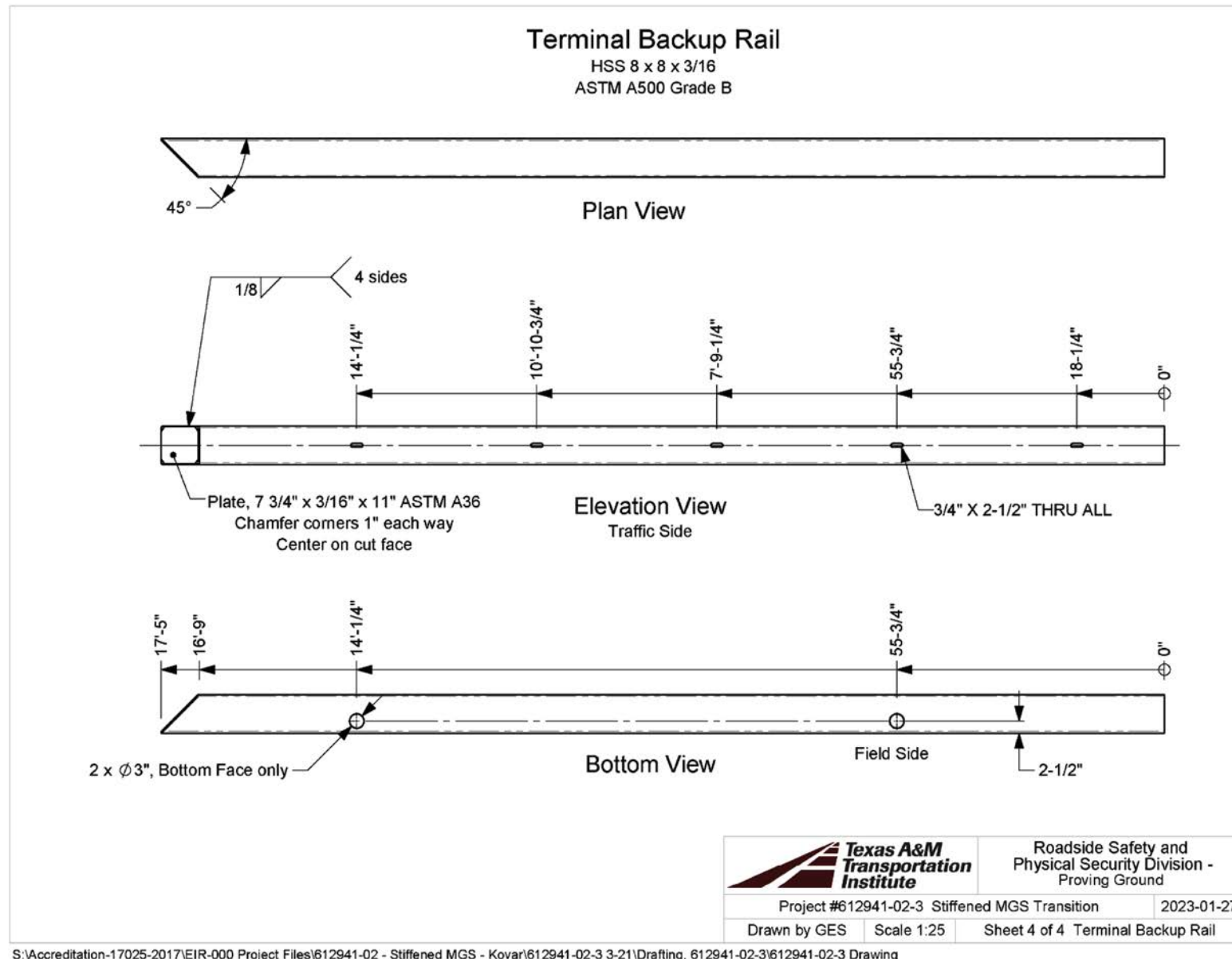
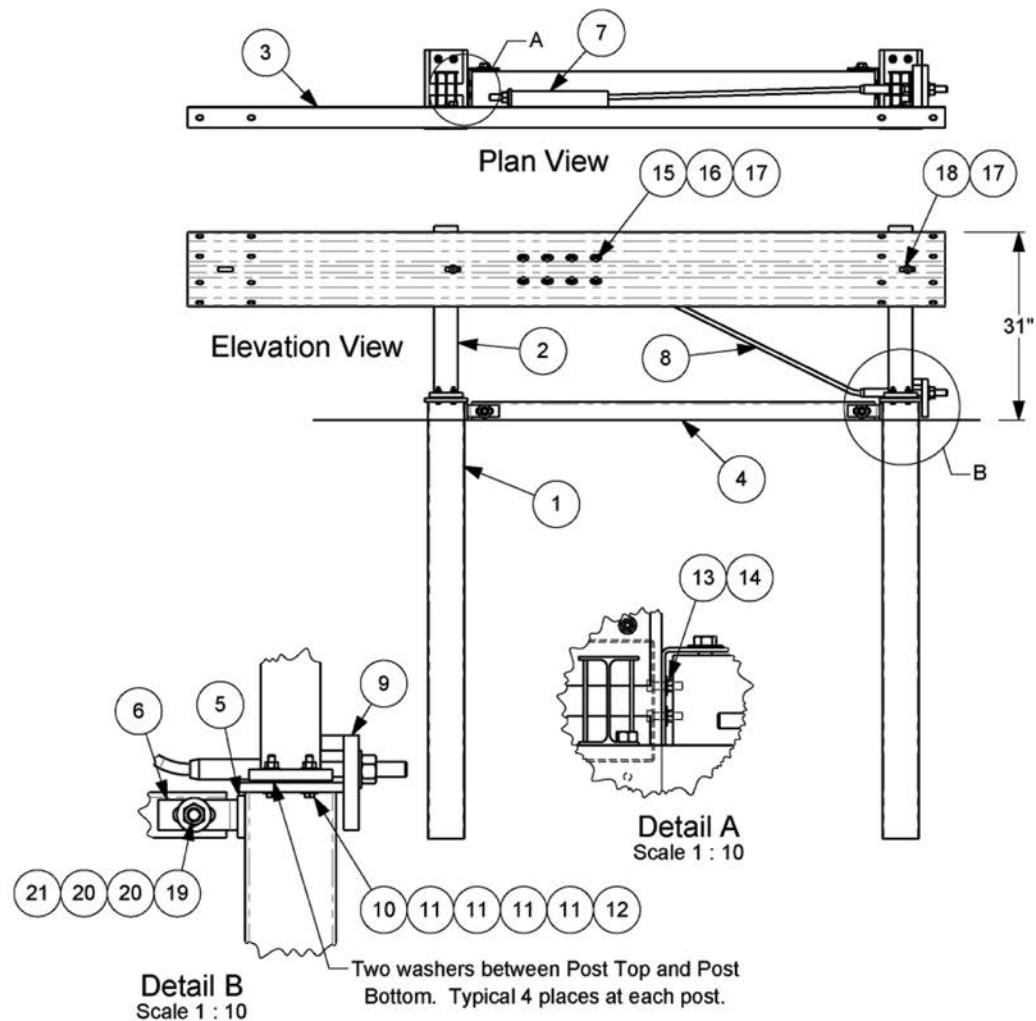


Figure A-2.4. Tests 612941-02-3 and -4 terminal backup rail.

Terminal Details

#	Part Name	QTY.
1	Post Bottom	2
2	Post Top	2
3	9'-4-1/2" span Terminal Rail	1
4	Strut	1
5	Strut Spacer	2
6	Strut Bracket	2
7	Guardrail Anchor Bracket	1
8	Anchor Cable Assembly	1
9	Bearing Plate	1
10	Bolt, 7/16 x 2 1/2" hex	8
11	Washer, 7/16 F844	32
12	Nut, 7/16 heavy hex	8
13	Nut, 1/2 hex	4
14	Washer, 1/2 F844	4
15	Bolt, 5/8 x 1 1/2" hex	8
16	Washer, 5/8 F844	8
17	Recessed Guardrail Nut	10
18	1-1/4" Guardrail Bolt	2
19	Bolt, 7/8 x 8 1/2" hex	2
20	Washer, 7/8 F844	4
21	Nut, 7/8 hex	2



1a. 7/16" x 2-1/2" Bolts are ASTM A449. All other Bolts are ASTM A307. All Nuts (except Recessed Guardrail Nuts) are ASTM A563A unless otherwise indicated.

1c. All steel parts shall be galvanized.



Roadside Safety and
Physical Security Division -
Proving Ground

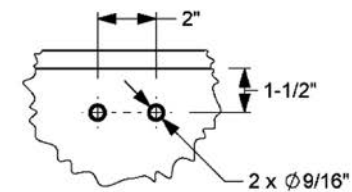
Project #	Terminal	2022-11-10
Drawn by GES	Scale 1:25	Sheet 1 of 6 Terminal Details

T:\Drafting Department\Solidworks\Standard Parts\Guardrail Parts and Subs\Guardrail Drawings\Midwest Terminal

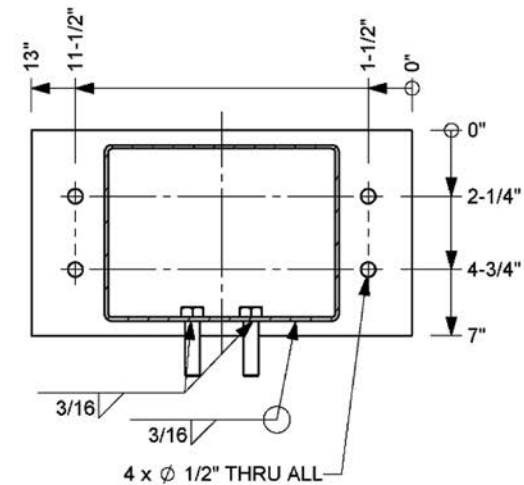
Figure A-2.5. Tests 612941-02-3 and -4 terminal details.



#	Description	Length	Material	Qty
22	HSS 8" x 6" x 1/8"	72"	ASTM A500 Grade B	1
23	Plate, 7" x 5/8"	13"	ASTM A36	1
24	Bolt, 1/2 x 2 hex		ASTM A307	2



Detail B
Scale 1 : 5



Section A-A
Scale 1 : 5



Roadside Safety and
Physical Security Division -
Proving Ground

Project #	Terminal
1	1
2	2
3	3
4	4
5	5
6	6
7	7
8	8
9	9
10	10
11	11
12	12
13	13
14	14
15	15
16	16
17	17
18	18
19	19
20	20
21	21
22	22
23	23
24	24
25	25
26	26
27	27
28	28
29	29
30	30
31	31
32	32
33	33
34	34
35	35
36	36
37	37
38	38
39	39
40	40
41	41
42	42
43	43
44	44
45	45
46	46
47	47
48	48
49	49
50	50
51	51
52	52
53	53
54	54
55	55
56	56
57	57
58	58
59	59
60	60
61	61
62	62
63	63
64	64
65	65
66	66
67	67
68	68
69	69
70	70
71	71
72	72
73	73
74	74
75	75
76	76
77	77
78	78
79	79
80	80
81	81
82	82
83	83
84	84
85	85
86	86
87	87
88	88
89	89
90	90
91	91
92	92
93	93
94	94
95	95
96	96
97	97
98	98
99	99
100	100

2022-11-10

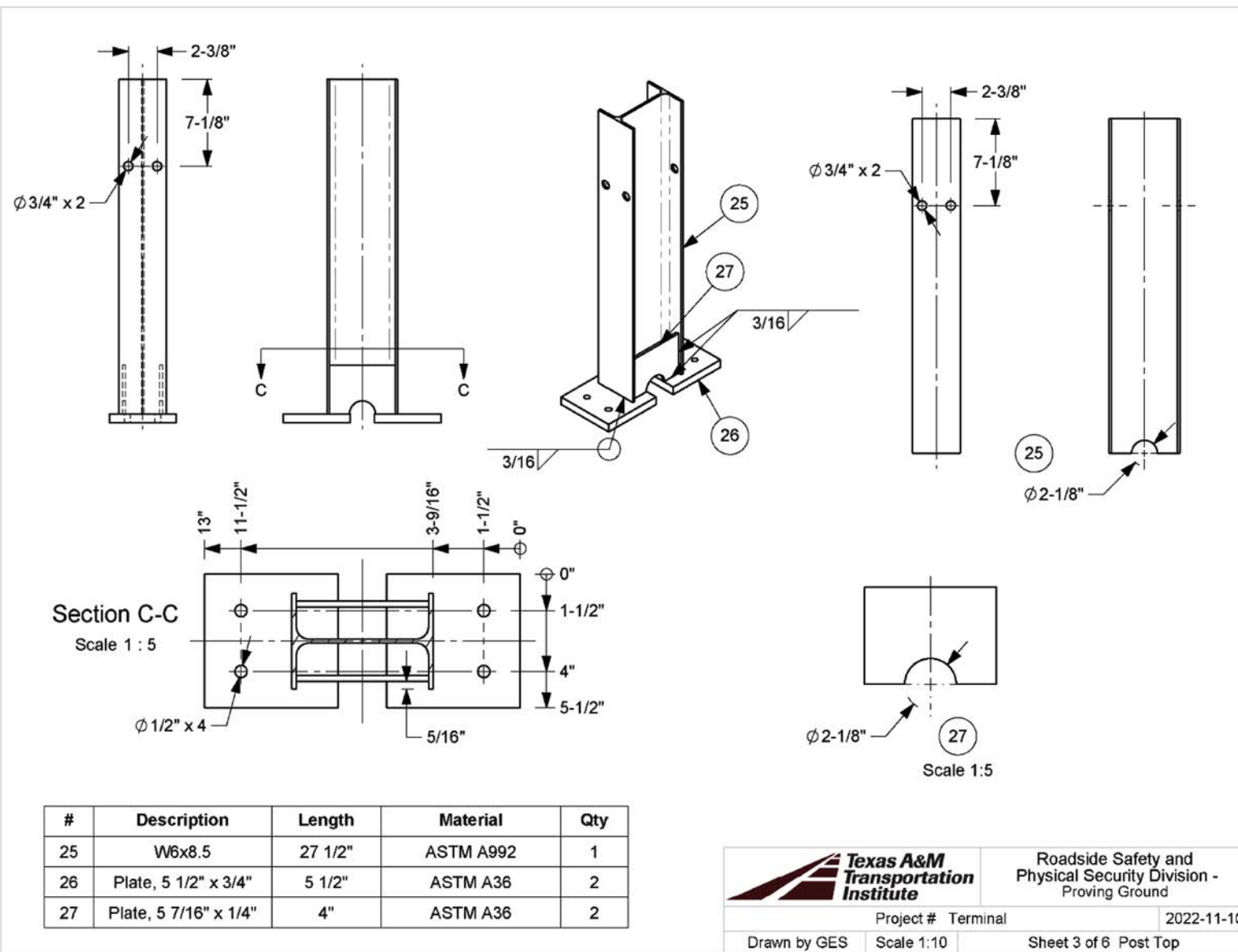
Drawn by GES

Scale 1:10

Sheet 2 of 6 Post Bottom

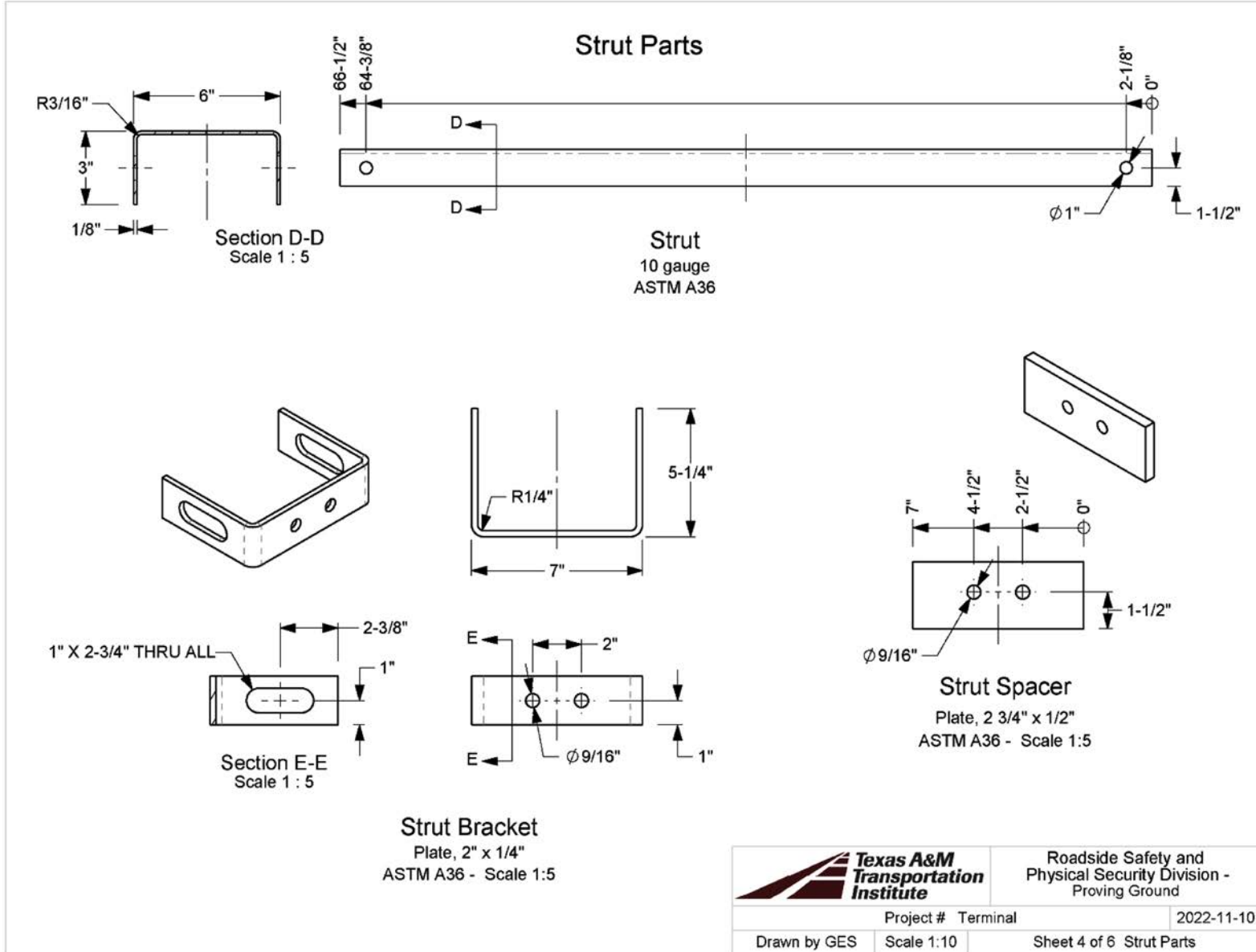
T:\Drafting Department\Solidworks\Standard Parts\Guardrail Parts and Subs\Guardrail Drawings\Midwest Terminal

Figure A-2.6. Tests 612941-02-3 and -4 additional terminal details.



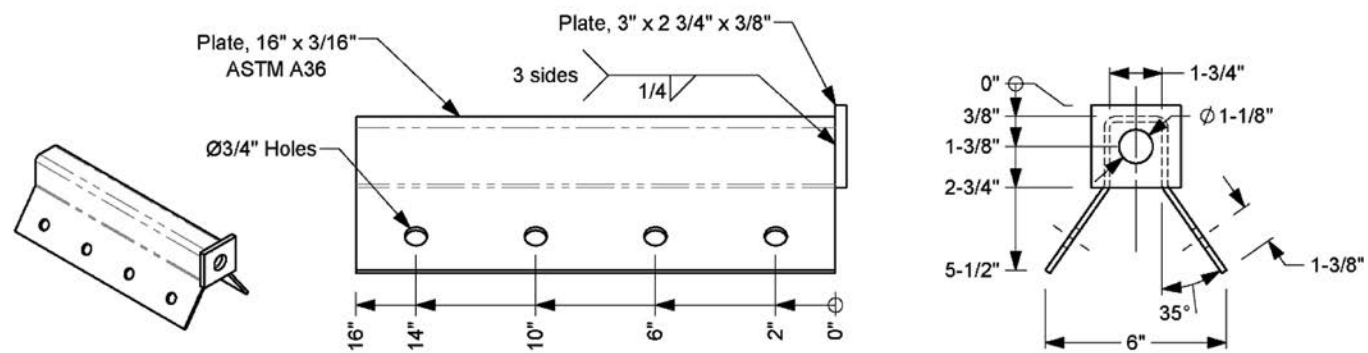
T:\Drafting Department\Solidworks\Standard Parts\Guardrail Parts and Subs\Guardrail Drawings\Midwest Terminal

Figure A-2.7. Tests 612941-02-3 and -4 additional terminal details.

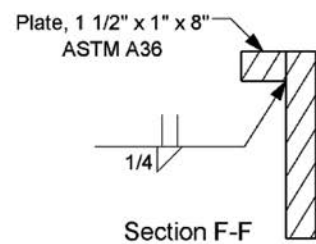


T:\Drafting Department\Solidworks\Standard Parts\Guardrail Parts and Subs\Guardrail Drawings\Midwest Terminal

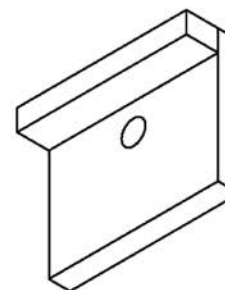
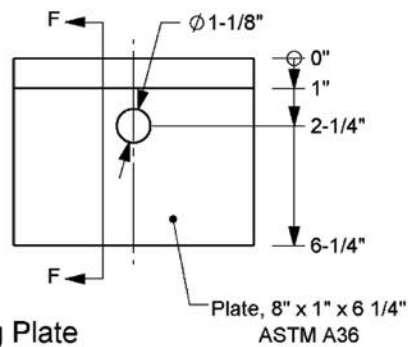
Figure A-2.8. Tests 612941-02-3 and -4 additional terminal details.



Guardrail Anchor Bracket



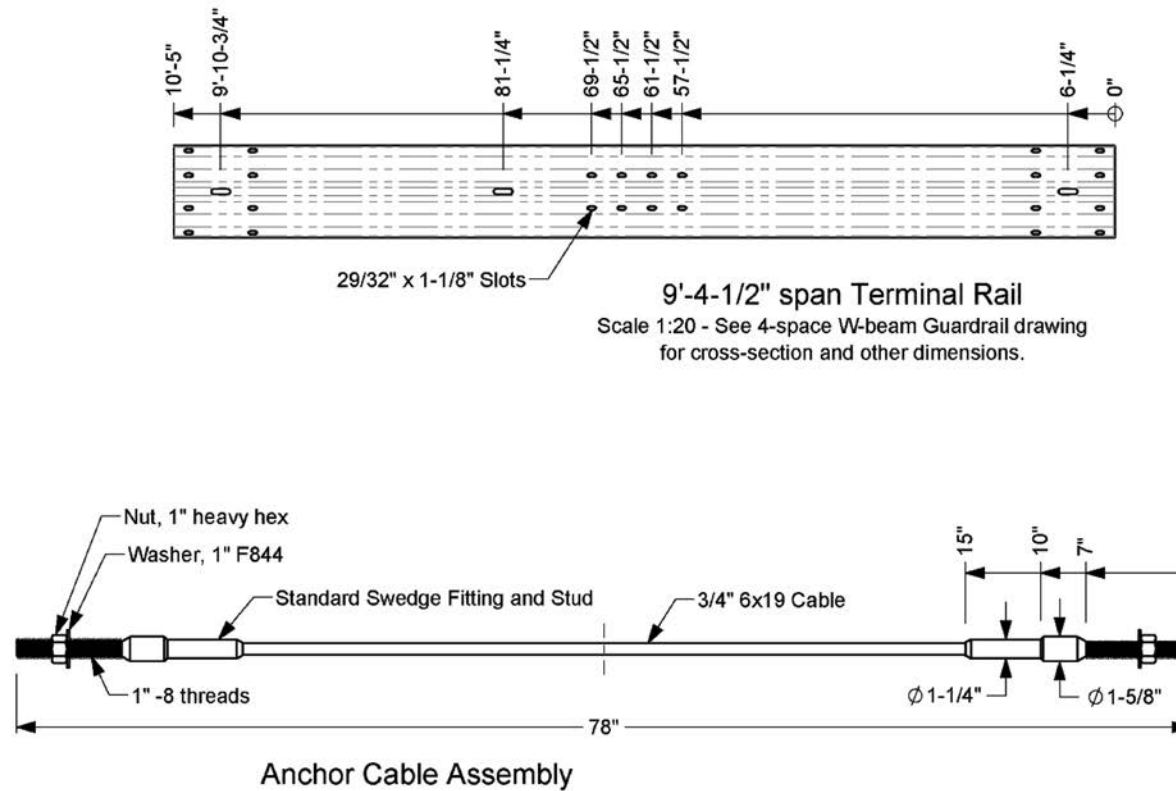
Bearing Plate




		Roadside Safety and Physical Security Division - Proving Ground
Project #	Terminal	2022-11-10
Drawn by GES	Scale 1:5	Sheet 5 of 6 Assorted Parts A

T:\Drafting Department\Solidworks\Standard Parts\Guardrail Parts and Subs\Guardrail Drawings\Midwest Terminal

Figure A-2.9. Tests 612941-02-3 and -4 additional terminal details.



		Roadside Safety and Physical Security Division - Proving Ground	
Project #		Terminal	2022-11-10
Drawn by GES	Scale 1:5	Sheet 6 of 6 Assorted Parts B	

T:\Drafting Department\Solidworks\Standard Parts\Guardrail Parts and Subs\Guardrail Drawings\Midwest Terminal

Figure A-2.10. Tests 612941-02-3 and -4 additional terminal details.

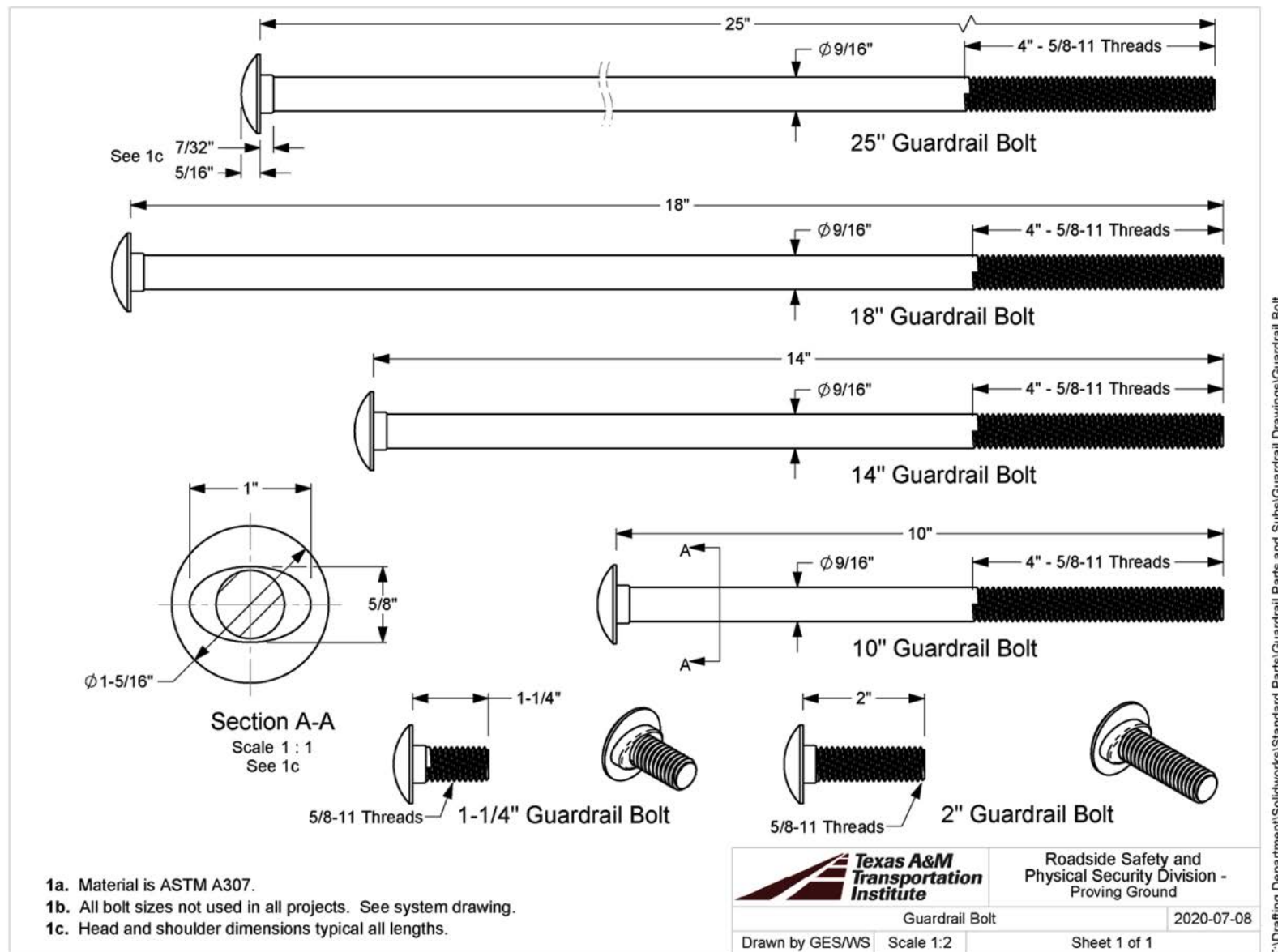


Figure A-2.11. Tests 612941-02-3 and -4 guardrail bolts.

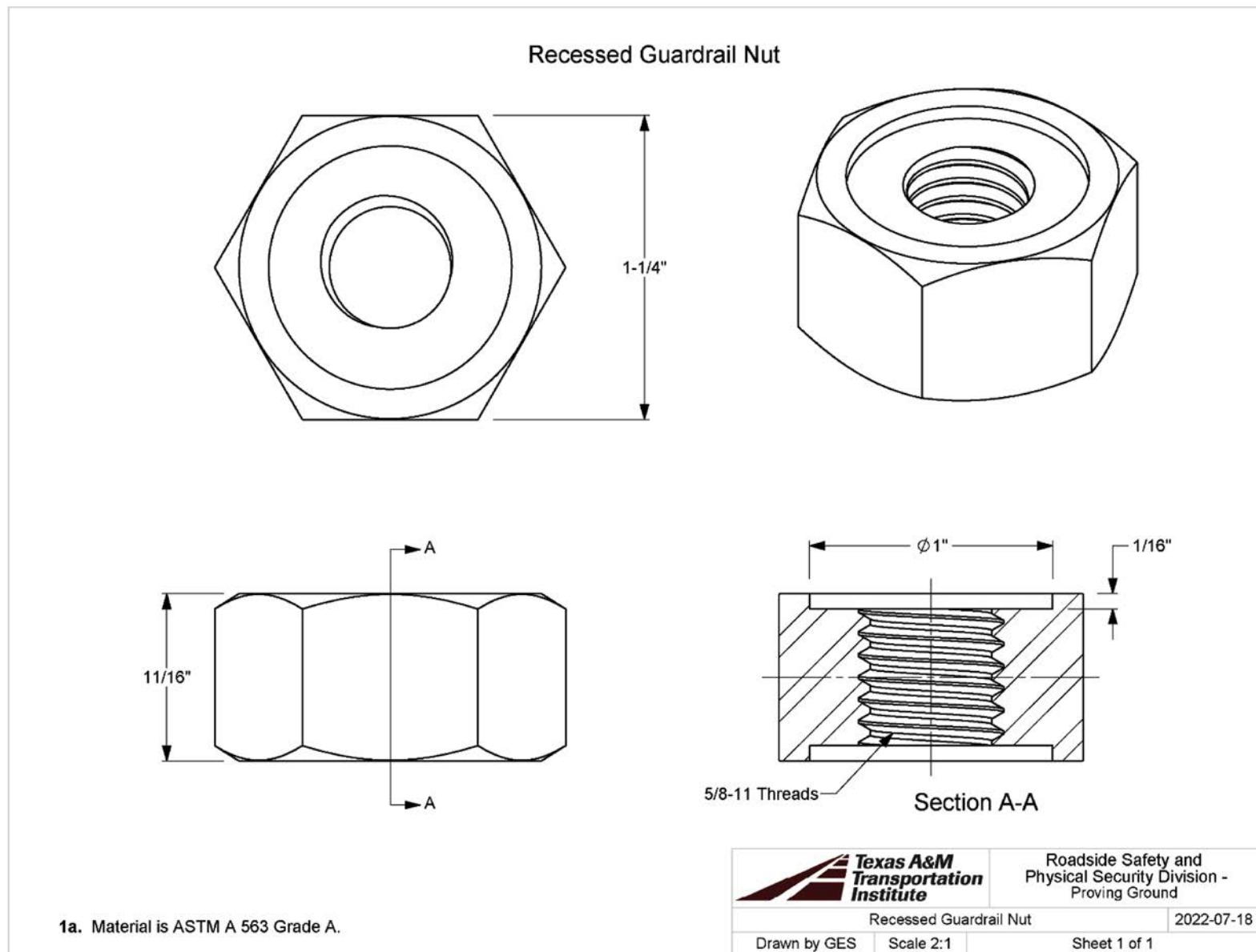


Figure A-2.12. Tests 612941-02-3 and -4 guardrail nuts.

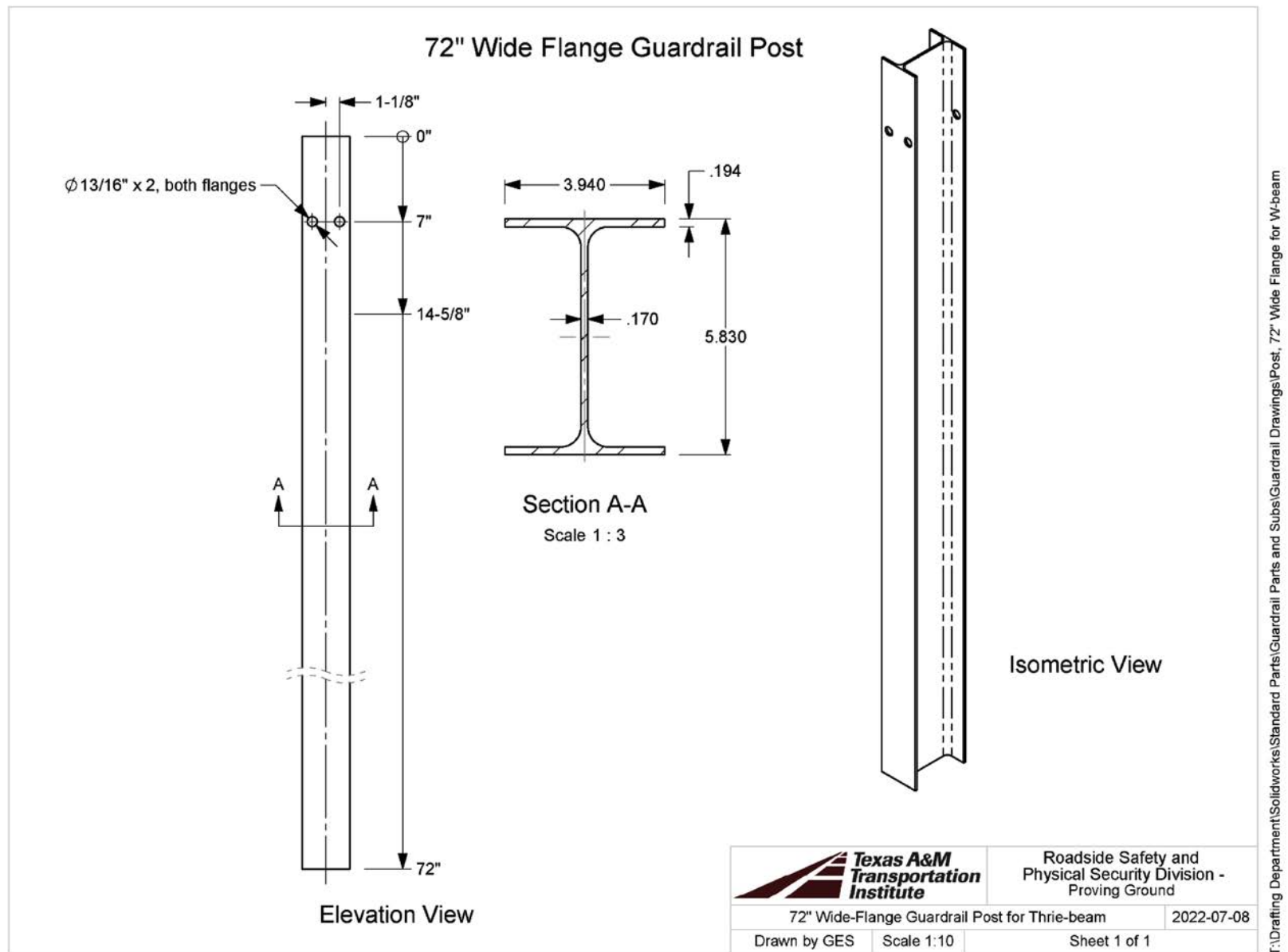
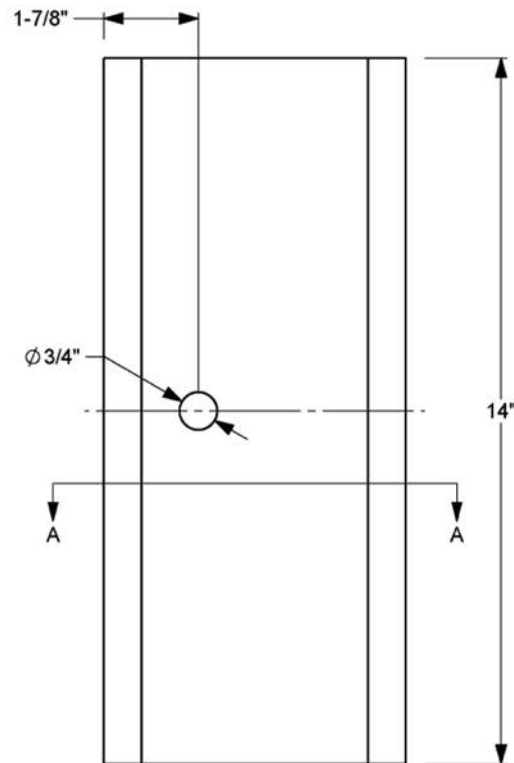


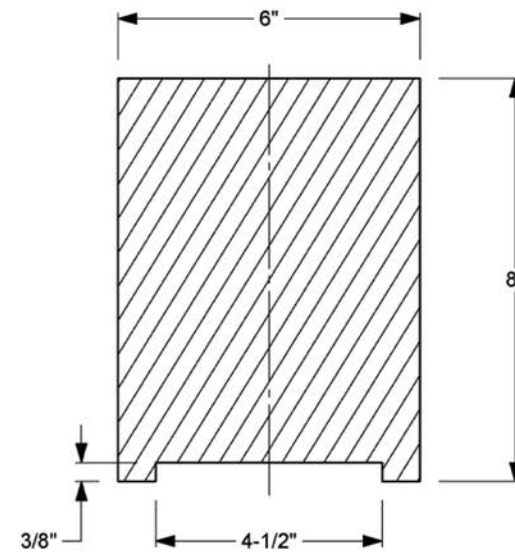
Figure A-2.13. Tests 612941-02-3 and -4 guardrail post.

Timber Blockout for W-section Post

All dimensions except hole diameter are nominal



Elevation View



Section A-A

1a. Timber blockouts are treated with a preservative in accordance with AASHTO M 133 after all cutting and drilling.



Roadside Safety and
Physical Security Division -
Proving Ground

Timber Blockout, for W-section Post

2022-10-25

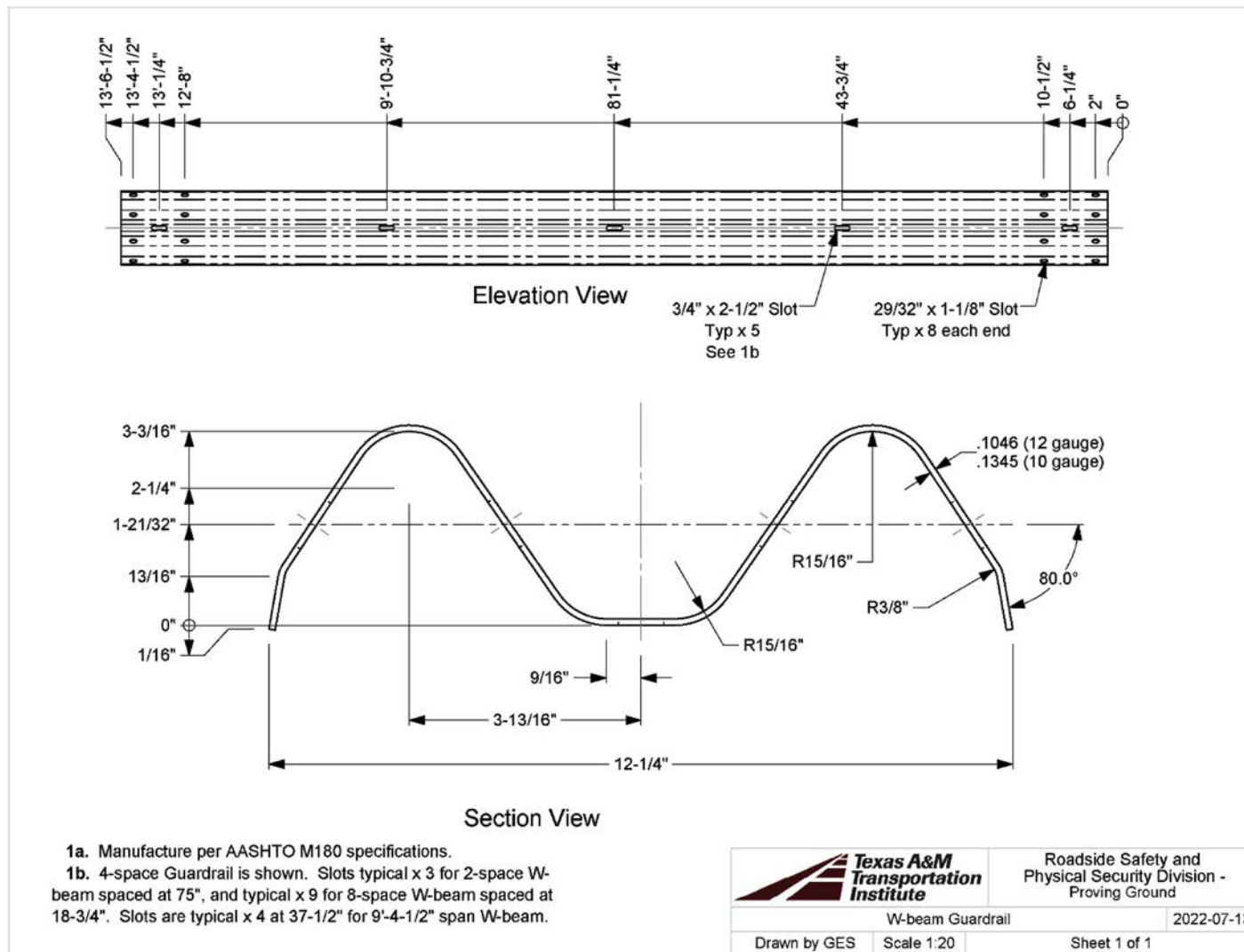
Drawn by GES

Scale 1:3

Sheet 1 of 1

T:\Drafting Department\Solidworks\Standard Parts\Guardrail Parts and Subs\Guardrail Drawings\Timber Blockout for W-section Post

Figure A-2.14. Tests 612941-02-3 and -4 timber blockout.



T:\Drafting\Department\Solidworks\Standard Parts\Guardrail Parts and Subs\Guardrail Drawings\W-Beam Guardrail

Figure A-2.15. Tests 612941-02-3 and -4 W-beam guardrail.



APPENDIX B

Supporting Certification Documents



MATERIAL TEST REPORT

8/25/22

Page 3

Submitted Hanna Steel Corporation
 By: Tuscaloosa Division
 1701 Boone Blvd
 P O Box 428
 Northport AL 35476

Load
 Tally: 5-23730
 Date
 Shipped: 8/26/2022

Send Triple S Steel Supply Co.
 To: P O Box 21119
 Houston TX 77026

Ship Intsel Steel Distributors
 To: 11310 W. Little York
 PO Box 41041
 Houston TX 77041

Material: 7 X 7 .250 A500 GR B 40.000FT Sales Order: 135245-03 PO#: WLY-28797
 Hot rolled carbon steel cold formed ERW square tubing

Heat#: 230390 ASTM A500 2021 Grade B/C Type 1															
C	Mn	P	S	Si	Al	Cb	Cr	Cu	Mo	Ni	V	N	Nb	Ti	B
.201	.873	.004	.002	.013	.045	.000	.019	.026	.002	.015	.001	.0075	.0010	.0010	.0001
Yield(psi)		Tensile(psi)		%E		Rock		CEV							
63,329		72,401		28.4		B85		.354							

Melted and manufactured in the USA

Heat# 230390 contains more than 0.020% Aluminum and is therefore considered to be fully killed and fine grained.

LEED Information

Year 2021 Recycled Content 20.0% Scrap 80.0% Post consumer 20.0% Pre consumer
 Exact scrap% per heat is unknown; LEED data is an average for that mill/production year.

Products manufactured to this specification may not be suitable for those applications such as dynamically loaded elements in welded structures, etc., where low-temperature notch-toughness properties (Charpy impact testing) may be important.

Repair welding of ASTM A500-21 tubing is allowed under certain conditions as described in Section 16.2.1. However, Hanna Steel does not currently perform any repair welding on our tubing.

Bundle#	Heat#	Pieces	Feet	Weight
4996449	230390	6	240	5,381


Sales order total: 6 5,381

The above results are a true and correct copy of physical tests performed to the ASTM A370 standard by Hanna Steel Corporation and contained in the records of Hanna Steel Corporation. Chemical tests are from records maintained by Hanna Steel Corporation as supplied by our mill sources.

Hanna Steel Corporation

William Blade
 Tuscaloosa Quality Assurance Technician

Figure B.1. Material test report for tubing.



MATERIAL TEST REPORT - QUALITY MANAGEMENT SYSTEM
 CONSTANCIA DE INSPECCION
 INSPECTION CONSTANCY
 (EN 10204 3.1 B- ISO10474 3.1B)
 FORZA STEEL - PRODUCTION FACILITY:

Packing List	2928	Cod (Code):	FPD-PR-01-08
		Edition (Edición):	Rev: 0
		Date of Rev (Fecha Rev):	20-01-2021
		Page (Hoja):	1/1

Carretera Salinas Victoria K.m. 2 s/n Salinas Victoria, Nuevo León, México C.P. 65500 Tel: +52 (51) 1958-3780

CUSTOMER (Cliente)	PURCHASE ORDER (Orden de Compra)	DELIVERY (Remisión)	DATE (Fecha)	REFERENCE NUMBER (No. Referencia)
INTSEL/TRIPLE-S Houston WLY	WLY-27904	5058324	03/31/2022	30032022-24195

PIPE TYPE PRODUCT	FORZA WORK ORDER	SIZE	WALL THICKNESS	HEAT	SPECIFICATION	GRADE	LENGTH	INCHES (Length)	MASS (Peso Unitario)	MASS PER METER	HYDROSTATIC TEST	SPECIAL REQUIREMENTS	TUBE NUMBER	
Tipo de producto	Orden Interna de Fab.	Diámetro	Cédula/Espeor	No. Colada	Especificación Norma	Grado	Metros	Pulg.	Lbs	Kg	Peso Unal kg x metros	Prueba Hidrostática (psi)	Requerimientos especiales	No. Piezas
HSS	OIF 1966	8x8	0.188	SP96977	ASTM A500	B/C	12.20	40.03	796.42	361.25	29.63	N/A	N/A	7
HSS	OIF 1966	8x8	0.188	SU71673	ASTM A500	B/C	12.20	40.03	796.42	361.25	29.63	N/A	N/A	51
HSS	OIF 5022	8x8	0.188	129630	ASTM A500	B/C	12.20	40.03	796.42	361.25	29.63	N/A	N/A	1

Tube (Lotes) 1966-30-8, 1966-30-6, 1966-31-37, 1966-29-28, 1966-29-25, 1966-32-13, 1966-32-12, 1966-32-4, 1966-32-10, 1966-32-15, 1966-31-36, 1966-29-29, 1966-32-7, 1966-29-26, 5022-1-45, 1966-35-28, 1966-30-7, 1966-32-9, 1966-30-10, 1966-29-27, 1966-32-17, 1966-32-8, 1966-32-14, 1966-32-11, 1966-32-16, 1966-30-2, 1966-35-28, 1966-37-16, 1966-35-27, 1966-29-31, 1966-32-3, 1966-34-11, 1966-29-30, 1966-30-8, 1966-30-4, 1966-29-35, 1966-32-5, 1966-31-34, 1966-32-30, 1966-35-31, 1966-32-33, 1966-29-32, 1966-32-34, 1966-30-5, 1966-32-32, 1966-34-10, 1966-29-33, 1966-32-29, 1966-35-29, 1966-30-3, 1966-32-31, 1966-32-35, 1966-35-30, 1966-39-8, 1966-32-8, 1966-32-28, 1966-32-2, 1966-31-35

Chemical Analyses (Análisis Químico)												Mechanical Test (Pruebas mecánicas)		
Heat (Colada)	Tube/Lote	C	Si	Mn	P	S	V	Cr	Cu	Ni	Mo	Yield Strength (KSI) (Límite elástico)	Tensile Strength (KSI) (Última tensión)	Elongation (%) (Elongación)
123630	5022-1-45	0.178	0.013	0.506	0.013	0.010	0.001	0.018	0.016	0.002	0.001	57.68	69.42	36
SP96977	1966-35-26	0.139	0.150	0.887	0.012	0.002	0.002	0.024	0.023	0.014	0.003	58.43	74.47	33
SP96977	1966-35-27	0.139	0.150	0.887	0.012	0.002	0.002	0.024	0.023	0.014	0.003	58.43	74.47	33
SP96977	1966-35-28	0.139	0.150	0.887	0.012	0.002	0.002	0.024	0.023	0.014	0.003	58.43	74.47	33
SP96977	1966-35-29	0.139	0.150	0.887	0.012	0.002	0.002	0.024	0.023	0.014	0.003	58.43	74.47	33
SP96977	1966-35-30	0.139	0.150	0.887	0.012	0.002	0.002	0.024	0.023	0.014	0.003	58.43	74.47	33
SP96977	1966-35-31	0.139	0.150	0.887	0.012	0.002	0.002	0.024	0.023	0.014	0.003	58.43	74.47	33
SP96977	1966-37-16	0.139	0.150	0.887	0.012	0.002	0.002	0.024	0.023	0.014	0.003	58.43	74.47	33
SU71673	1966-39-9	0.138	0.149	0.910	0.012	0.002	0.001	0.032	0.036	0.013	0.002	65.46	78.22	34
SU71673	1966-29-25	0.138	0.149	0.910	0.012	0.002	0.001	0.032	0.036	0.013	0.002	65.46	78.22	34
SU71673	1966-29-26	0.138	0.149	0.910	0.012	0.002	0.001	0.032	0.036	0.013	0.002	65.46	78.22	34
SU71673	1966-29-27	0.138	0.149	0.910	0.012	0.002	0.001	0.032	0.036	0.013	0.002	65.46	78.22	34
SU71673	1966-29-28	0.138	0.149	0.910	0.012	0.002	0.001	0.032	0.036	0.013	0.002	65.46	78.22	34
SU71673	1966-29-29	0.138	0.149	0.910	0.012	0.002	0.001	0.032	0.036	0.013	0.002	65.46	78.22	34
SU71673	1966-29-30	0.138	0.149	0.910	0.012	0.002	0.001	0.032	0.036	0.013	0.002	65.46	78.22	34
SU71673	1966-29-31	0.138	0.149	0.910	0.012	0.002	0.001	0.032	0.036	0.013	0.002	65.46	78.22	34
SU71673	1966-29-32	0.138	0.149	0.910	0.012	0.002	0.001	0.032	0.036	0.013	0.002	65.46	78.22	34
SU71673	1966-29-33	0.138	0.149	0.910	0.012	0.002	0.001	0.032	0.036	0.013	0.002	65.46	78.22	34
SU71673	1966-29-35	0.138	0.149	0.910	0.012	0.002	0.001	0.032	0.036	0.013	0.002	65.46	78.22	34
SU71673	1966-30-10	0.138	0.149	0.910	0.012	0.002	0.001	0.032	0.036	0.013	0.002	65.46	78.22	34
SU71673	1966-30-11	0.138	0.149	0.910	0.012	0.002	0.001	0.032	0.036	0.013	0.002	65.46	78.22	34
SU71673	1966-30-2	0.138	0.149	0.910	0.012	0.002	0.001	0.032	0.036	0.013	0.002	65.46	78.22	34
SU71673	1966-30-3	0.138	0.149	0.910	0.012	0.002	0.001	0.032	0.036	0.013	0.002	65.46	78.22	34
SU71673	1966-30-4	0.138	0.149	0.910	0.012	0.002	0.001	0.032	0.036	0.013	0.002	65.46	78.22	34
SU71673	1966-30-5	0.138	0.149	0.910	0.012	0.002	0.001	0.032	0.036	0.013	0.002	65.46	78.22	34
SU71673	1966-30-6	0.138	0.149	0.910	0.012	0.002	0.001	0.032	0.036	0.013	0.002	65.46	78.22	34
SU71673	1966-30-7	0.138	0.149	0.910	0.012	0.002	0.001	0.032	0.036	0.013	0.002	65.46	78.22	34
SU71673	1966-30-8	0.138	0.149	0.910	0.012	0.002	0.001	0.032	0.036	0.013	0.002	65.46	78.22	34
SU71673	1966-30-9	0.138	0.149	0.910	0.012	0.002	0.001	0.032	0.036	0.013	0.002	65.46	78.22	34

Figure B.2. Material test report.
(continued on next page)

Chemical Analyses (Análisis Químico)												Mechanical Test (Pruebas mecánicas)		
Heat (Cotada)	Tube/Lote	C	Si	Mn	P	S	V	Cr	Cu	Ni	Mo	Yield Strength (KSI) (Límite elástico)	Tensile Strength (KSI) (Última tensión)	Elongation (%) (Elongación)
SU71673	1966-31-34	0.138	0.149	0.910	0.012	0.002	0.001	0.032	0.036	0.013	0.002	65.46	78.22	34
SU71673	1966-31-35	0.138	0.149	0.910	0.012	0.002	0.001	0.032	0.036	0.013	0.002	65.46	78.22	34
SU71673	1966-31-36	0.138	0.149	0.910	0.012	0.002	0.001	0.032	0.036	0.013	0.002	65.46	78.22	34
SU71673	1966-31-37	0.138	0.149	0.910	0.012	0.002	0.001	0.032	0.036	0.013	0.002	65.46	78.22	34
SU71673	1966-32-10	0.138	0.149	0.910	0.012	0.002	0.001	0.032	0.036	0.013	0.002	65.46	78.22	34
SU71673	1966-32-11	0.138	0.149	0.910	0.012	0.002	0.001	0.032	0.036	0.013	0.002	65.46	78.22	34
SU71673	1966-32-12	0.138	0.149	0.910	0.012	0.002	0.001	0.032	0.036	0.013	0.002	65.46	78.22	34
SU71673	1966-32-13	0.138	0.149	0.910	0.012	0.002	0.001	0.032	0.036	0.013	0.002	65.46	78.22	34
SU71673	1966-32-14	0.138	0.149	0.910	0.012	0.002	0.001	0.032	0.036	0.013	0.002	65.46	78.22	34
SU71673	1966-32-15	0.138	0.149	0.910	0.012	0.002	0.001	0.032	0.036	0.013	0.002	65.46	78.22	34
SU71673	1966-32-16	0.138	0.149	0.910	0.012	0.002	0.001	0.032	0.036	0.013	0.002	65.46	78.22	34
SU71673	1966-32-17	0.138	0.149	0.910	0.012	0.002	0.001	0.032	0.036	0.013	0.002	65.46	78.22	34
SU71673	1966-32-2	0.138	0.149	0.910	0.012	0.002	0.001	0.032	0.036	0.013	0.002	65.46	78.22	34
SU71673	1966-32-28	0.138	0.149	0.910	0.012	0.002	0.001	0.032	0.036	0.013	0.002	65.46	78.22	34
SU71673	1966-32-29	0.138	0.149	0.910	0.012	0.002	0.001	0.032	0.036	0.013	0.002	65.46	78.22	34
SU71673	1966-32-3	0.138	0.149	0.910	0.012	0.002	0.001	0.032	0.036	0.013	0.002	65.46	78.22	34
SU71673	1966-32-30	0.138	0.149	0.910	0.012	0.002	0.001	0.032	0.036	0.013	0.002	65.46	78.22	34
SU71673	1966-32-31	0.138	0.149	0.910	0.012	0.002	0.001	0.032	0.036	0.013	0.002	65.46	78.22	34
SU71673	1966-32-32	0.138	0.149	0.910	0.012	0.002	0.001	0.032	0.036	0.013	0.002	65.46	78.22	34
SU71673	1966-32-33	0.138	0.149	0.910	0.012	0.002	0.001	0.032	0.036	0.013	0.002	65.46	78.22	34
SU71673	1966-32-34	0.138	0.149	0.910	0.012	0.002	0.001	0.032	0.036	0.013	0.002	65.46	78.22	34
SU71673	1966-32-35	0.138	0.149	0.910	0.012	0.002	0.001	0.032	0.036	0.013	0.002	65.46	78.22	34
SU71673	1966-32-4	0.138	0.149	0.910	0.012	0.002	0.001	0.032	0.036	0.013	0.002	65.46	78.22	34
SU71673	1966-32-5	0.138	0.149	0.910	0.012	0.002	0.001	0.032	0.036	0.013	0.002	65.46	78.22	34
SU71673	1966-32-6	0.138	0.149	0.910	0.012	0.002	0.001	0.032	0.036	0.013	0.002	65.46	78.22	34
SU71673	1966-32-7	0.138	0.149	0.910	0.012	0.002	0.001	0.032	0.036	0.013	0.002	65.46	78.22	34
SU71673	1966-32-8	0.138	0.149	0.910	0.012	0.002	0.001	0.032	0.036	0.013	0.002	65.46	78.22	34
SU71673	1966-32-9	0.138	0.149	0.910	0.012	0.002	0.001	0.032	0.036	0.013	0.002	65.46	78.22	34
SU71673	1966-34-10	0.138	0.149	0.910	0.012	0.002	0.001	0.032	0.036	0.013	0.002	65.46	78.22	34
SU71673	1966-34-11	0.138	0.149	0.910	0.012	0.002	0.001	0.032	0.036	0.013	0.002	65.46	78.22	34

Forza Steel certifica que los productos descritos en este documento fueron fabricados en cumplimiento con los requerimientos de la especificación descrita, obteniendo resultados satisfactorios en todas sus pruebas e inspecciones incluidas en los planes de calidad de forza steel para cumplir con los requerimientos del pedido en referencia.

Forza steel certifies that the products described in this document were manufactured in compliance with the requirements of the specification described, obtaining satisfactory results in all tests and inspections included in the quality plans of Forza Steel to meet the requirements of the order in reference.

Comentarios/Certificado

Certify By (Autorizo)

Edg. Ollive

Ing. Edgar Eduardo Ollive Hernández

QUALITY ASSURANCE MANAGER

Figure B.2. (Continued).



APPENDIX C

MASH Test 3-10 (Crash Test No. 612941-02-2)

VEHICLE PROPERTIES AND INFORMATION

Date: 2023-01-06 Test No.: 612941-02-2 VIN No.: 3N1CN7AP4HL839914

Year: 2017 Make: Nissan Model: Versa

Tire Inflation Pressure: 36 PSI Odometer: 134152 Tire Size: P185/65R15

Describe any damage to the vehicle prior to test: None

- Denotes accelerometer location.

NOTES: None

Engine Type: 4 CYL

Engine CID: 1.6 L

Transmission Type:

☒ Auto or ☐ Manual

☒ FWD ☐ RWD ☐ 4WD

Optional Equipment:

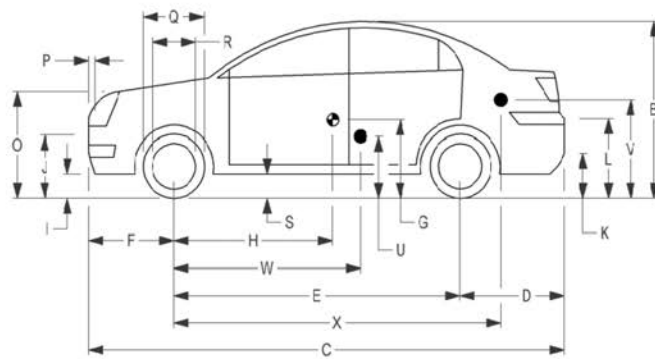
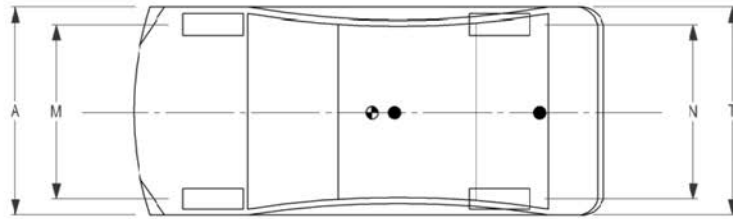
None

Dummy Data:

Type: 50th Percentile Male

Mass: 165 lb

Seat Position: IMPACT SIDE



Geometry: inches

A <u>66.70</u>	F <u>32.50</u>	K <u>12.50</u>	P <u>4.50</u>	U <u>15.50</u>
B <u>59.60</u>	G <u> </u>	L <u>26.00</u>	Q <u>24.00</u>	V <u>21.25</u>
C <u>175.40</u>	H <u>41.65</u>	M <u>58.30</u>	R <u>16.25</u>	W <u>41.50</u>
D <u>40.50</u>	I <u>7.00</u>	N <u>58.50</u>	S <u>7.50</u>	X <u>79.75</u>
E <u>102.40</u>	J <u>22.50</u>	O <u>30.50</u>	T <u>64.50</u>	
Wheel Center Ht Front <u>11.50</u>		Wheel Center Ht Rear <u>11.50</u>		W-H <u>-0.15</u>

RANGE LIMIT: A = 65 ±3 inches; C = 169 ±8 inches; E = 98 ±5 inches; F = 35 ±4 inches; H = 39 ±4 inches; O (Top of Radiator Support) = 28 ±4 inches
(M+N)/2 = 59 ±2 inches; W-H < 2 inches or use MASH Paragraph A4.3.2

GVWR Ratings:	Mass: lb	Curb	Test Inertial	Gross Static
Front <u>1750</u>	M _{front}	<u>1440</u>	<u>1448</u>	<u>1533</u>
Back <u>1687</u>	M _{rear}	<u>904</u>	<u>993</u>	<u>1073</u>
Total <u>3389</u>	M _{Total}	<u>2344</u>	<u>2441</u>	<u>2606</u>

Allowable TIM = 2420 lb ±55 lb | Allowable GSM = 2585 lb ± 55 lb

Mass Distribution:

lb LF: 749 RF: 699 LR: 476 RR: 517

Figure C.1. Vehicle properties for test no. 612941-02-2.

Date: 2023-01-06 Test No.: 612941-02-2 VIN No.: 3N1CN7AP4HL839914
 Year: 2017 Make: Nissan Model: Versa

VEHICLE CRUSH MEASUREMENT SHEET¹

Complete When Applicable	
<p style="text-align: center;">End Damage</p> <p>Undeformed end width _____</p> <p>Corner shift: A1 _____</p> <p style="padding-left: 100px;">A2 _____</p> <p>End shift at frame (CDC)</p> <p style="padding-left: 40px;">(check one)</p> <p style="padding-left: 40px;">< 4 inches _____</p> <p style="padding-left: 40px;">≥ 4 inches _____</p>	<p style="text-align: center;">Side Damage</p> <p>Bowing: B1 _____ X1 _____</p> <p style="padding-left: 100px;">B2 _____ X2 _____</p> <p>Bowing constant</p> <p style="text-align: center;">$\frac{X1 + X2}{2} = \underline{\hspace{2cm}}$</p>

Note: Measure C₁ to C₆ from Driver to Passenger Side in Front or Rear Impacts – Rear to Front in Side Impacts.

Specific Impact Number	Plane* of C-Measurements	Direct Damage		Field L**	C ₁	C ₂	C ₃	C ₄	C ₅	C ₆	±D
		Width*** (CDC)	Max**** Crush								
1	AT FT BUMPER	14	6	28							-14
2	SAME	14	10	57							54
	Measurements recorded										
	<input checked="" type="checkbox"/> inches or <input type="checkbox"/> mm										

¹Table taken from National Accident Sampling System (NASS).

*Identify the plane at which the C-measurements are taken (e.g., at bumper, above bumper, at sill, above sill, at beltline, etc.) or label adjustments (e.g., free space).

Free space value is defined as the distance between the baseline and the original body contour taken at the individual C locations. This may include the following: bumper lead, bumper taper, side protrusion, side taper, etc. Record the value for each C-measurement and maximum crush.

**Measure and document on the vehicle diagram the beginning or end of the direct damage width and field L (e.g., side damage with respect to undamaged axle).

***Measure and document on the vehicle diagram the location of the maximum crush.

Note: Use as many lines/columns as necessary to describe each damage profile.

Figure C.2. Exterior crush measurements for test 612941-02-2.

Date:2023-01-06

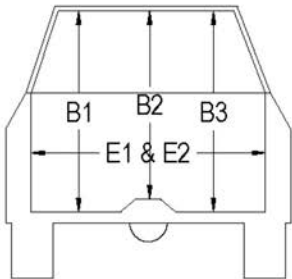
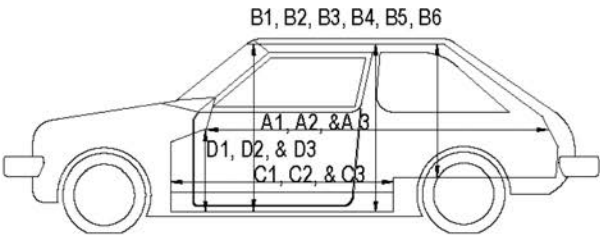
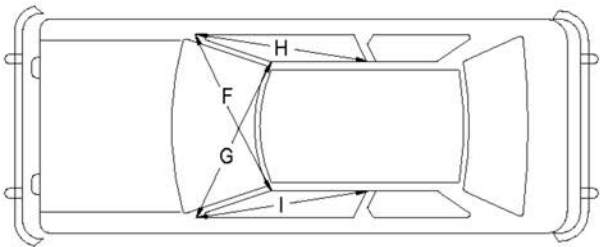
Test No.:612941-02-2

VIN No.:3N1CN7AP4HL839914

Year:2017

Make:Nissan

Model:Versa



OCCUPANT COMPARTMENT DEFORMATION MEASUREMENT

	Before	After (inches)	Differ.
A1	67.50	67.50	0.00
A2	67.25	67.25	0.00
A3	67.75	67.75	0.00
B1	40.50	40.50	0.00
B2	39.00	39.00	0.00
B3	40.50	40.50	0.00
B4	36.25	36.25	0.00
B5	36.00	36.00	0.00
B6	36.25	36.25	0.00
C1	26.00	26.00	0.00
C2	0.00	0.00	0.00
C3	26.00	26.00	0.00
D1	9.50	9.50	0.00
D2	0.00	0.00	0.00
D3	9.50	9.50	0.00
E1	50.00	46.00	-4.00
E2	51.00	50.00	-1.00
F	51.00	51.00	0.00
G	51.00	51.00	0.00
H	37.50	37.50	0.00
I	37.50	37.50	0.00
J*	49.00	45.00	-4.00

*Lateral area across the cab from driver's side kick panel to passenger's side kick panel.

Figure C.3. Occupant compartment measurements for test 612941-02-2.

SEQUENTIAL PHOTOGRAPHS



(a) 0.000 s



(b) 0.100 s



(c) 0.200 s



(d) 0.300 s



(e) 0.400 s



(f) 0.500 s



(g) 0.600 s



(h) 0.700 s

Figure C.4. Sequential photographs for test 612941-02-2 (overhead views).



(a) 0.000 s



(b) 0.100 s



(c) 0.200 s



(d) 0.300 s



(e) 0.400 s



(f) 0.500 s



(g) 0.600 s



(h) 0.700 s

Figure C.5. Sequential photographs for test 612941-02-2 (frontal views).

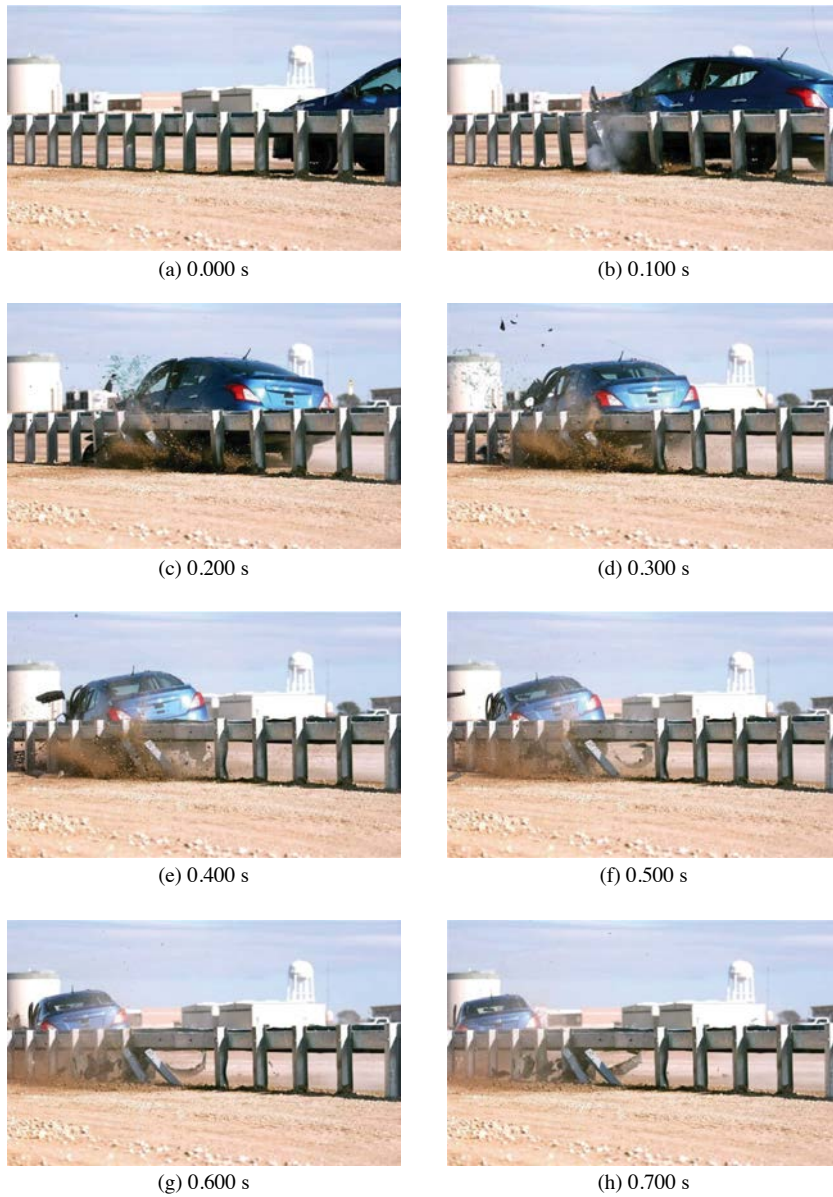


Figure C.6. Sequential photographs for test 612941-02-2 (field-side views).

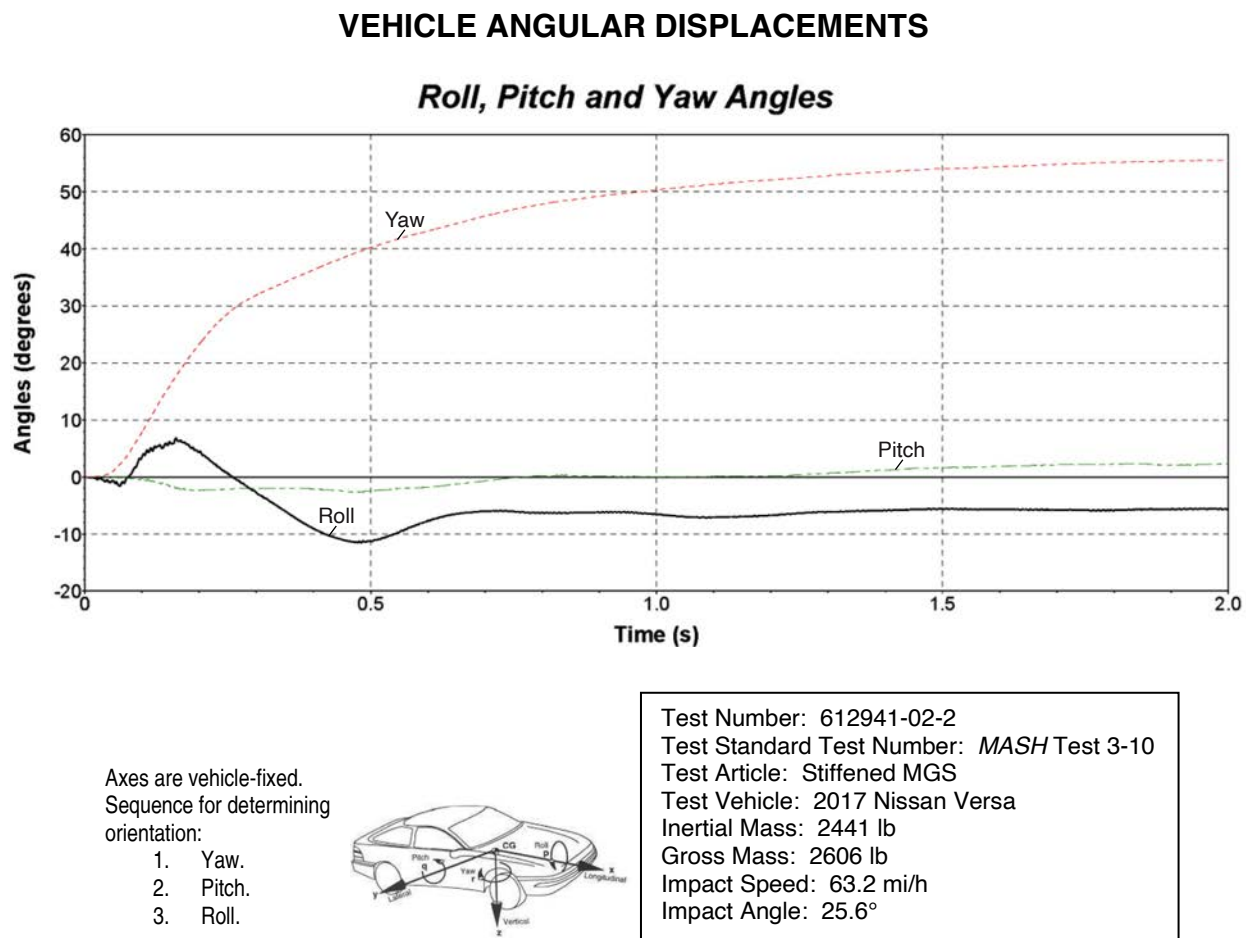


Figure C.7. Vehicle angular displacements for test 612941-02-2.

VEHICLE ACCELERATIONS

X Acceleration at CG

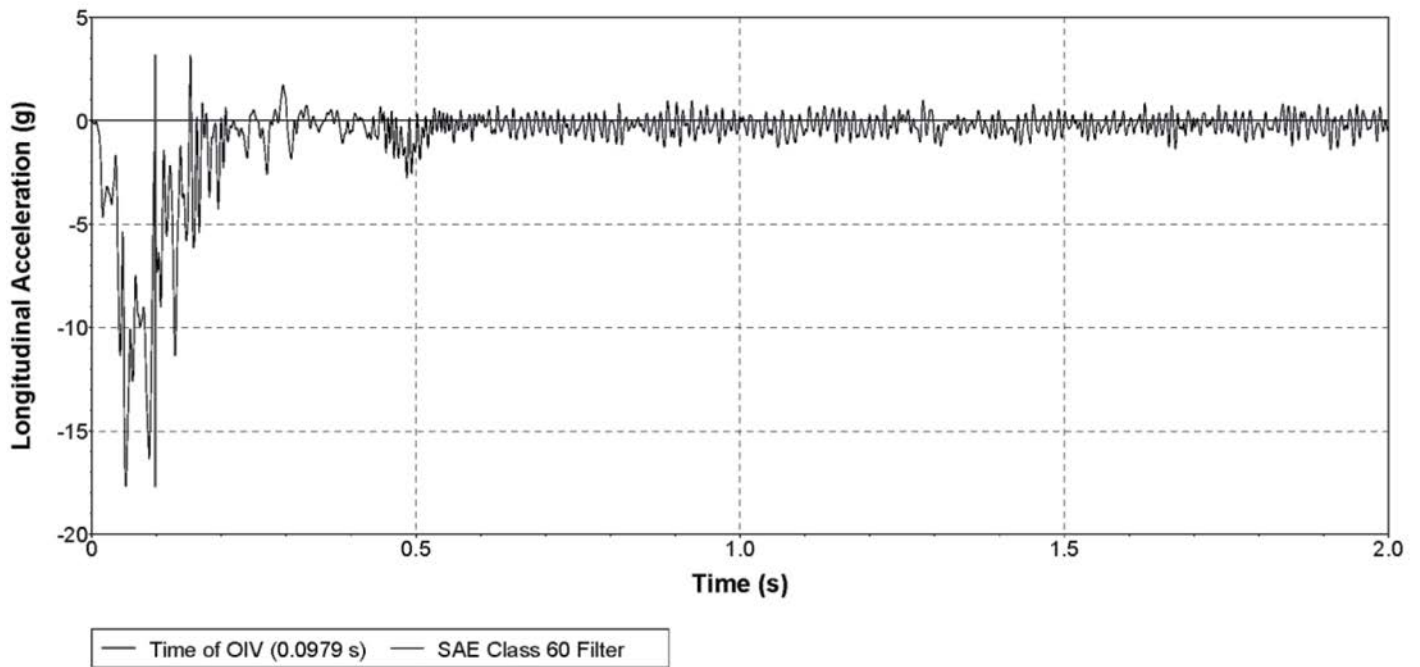


Figure C.8. Vehicle longitudinal accelerometer trace for test 612941-02-2 (accelerometer located at center of gravity, CG).

Y Acceleration at CG

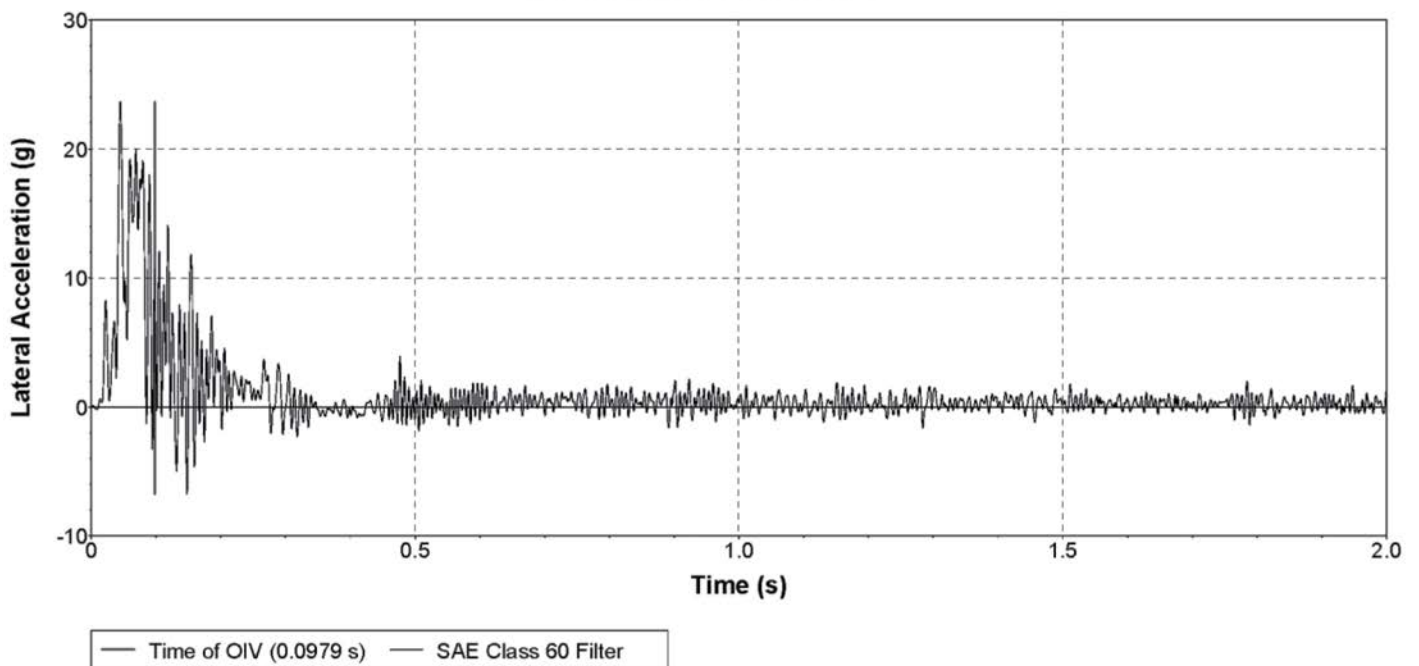


Figure C.9. Vehicle lateral accelerometer trace for test 612941-02-2 (accelerometer located at center of gravity, CG).

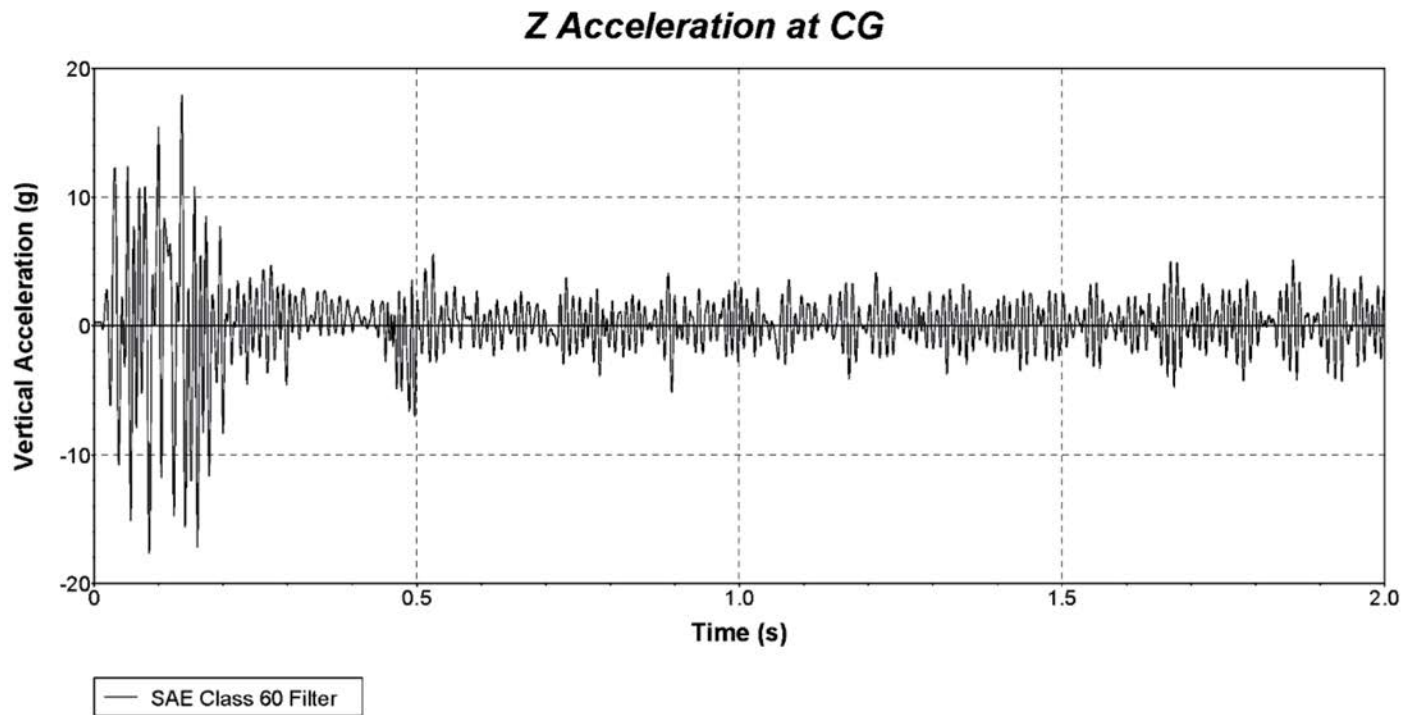


Figure C.10. Vehicle vertical accelerometer trace for test 612941-02-2 (accelerometer located at center of gravity, CG).



APPENDIX D

MASH Test 3-11 (Crash Test No. 612941-02-1)

VEHICLE PROPERTIES AND INFORMATION

Date: 2022-12-16 Test No.: 612941-02-1 VIN No.: 1C6RR6GT0JS131328
 Year: 2018 Make: RAM Model: 1500
 Tire Size: 265/70 R 17 Tire Inflation Pressure: 35 psi
 Tread Type: Highway Odometer: 100154
 Note any damage to the vehicle prior to test: None

• Denotes accelerometer location.

NOTES: None

Engine Type: V-8

Engine CID: 5.7 liter

Transmission Type:

☒ Auto or ☐ Manual
☐ FWD ☒ RWD ☐ 4WD

Optional Equipment:

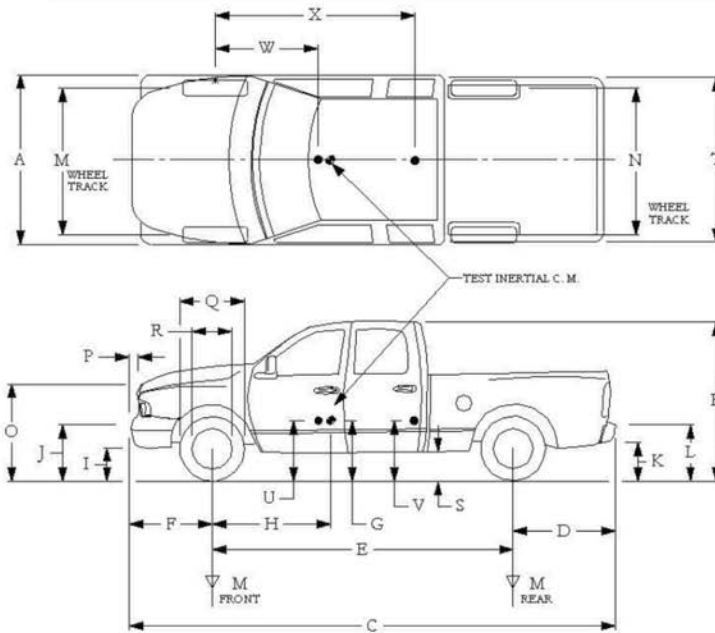
None

Dummy Data:

Type: NONE

Mass:

Seat Position:



Geometry: inches

A	78.50	F	40.00	K	20.00	P	3.00	U	26.75
B	74.00	G	28.87	L	30.00	Q	30.50	V	30.25
C	227.50	H	61.53	M	68.50	R	18.00	W	61.50
D	44.00	I	11.75	N	68.00	S	13.00	X	79.00
E	140.50	J	27.00	O	46.00	T	77.00		
Wheel Center Height Front	14.75	Wheel Well Clearance (Front)	6.00	Bottom Frame Height - Front	12.50				
Wheel Center Height Rear	14.75	Wheel Well Clearance (Rear)	9.25	Bottom Frame Height - Rear	22.50				

RANGE LIMIT: A=78 ±2 inches; C=237 ±13 inches; E=148 ±12 inches; F=39 ±3 inches; G = > 28 inches; H = 63 ±4 inches; O=43 ±4 inches; (M+N)/2=67 ±1.5 inches

GVWR Ratings:

Front	3700
Back	3900
Total	6700

Mass: lb

M _{front}	2905
M _{rear}	1916
M _{Total}	4821

Curb

2905
1916
4821

Test Inertial

2819
2197
5016

Gross Static

2819
2197
5016

(Allowable Range for TIM and GSM = 5000 lb ±110 lb)

Mass Distribution:

lb

LF: 1422

RF: 1397

LR: 1112

RR: 1085

Figure D.1. Vehicle properties for test 612941-02-1.

Date:	2022-12-16	Test No.:	612941-02-1	VIN No.:	1C6RR6GT0JS131328
Year:	2018	Make:	RAM	Model:	1500

VEHICLE CRUSH MEASUREMENT SHEET¹

Complete When Applicable	
End Damage	Side Damage
Undeformed end width _____	Bowing: B1 _____ X1 _____
Corner shift: A1 _____	B2 _____ X2 _____
A2 _____	
End shift at frame (CDC)	Bowing constant
(check one)	$\frac{X1 + X2}{2} = \underline{\hspace{2cm}}$
< 4 inches _____	
≥ 4 inches _____	

Note: Measure C₁ to C₆ from Driver to Passenger Side in Front or Rear Impacts – Rear to Front in Side Impacts.

[illegible]

¹Table taken from National Accident Sampling System (NASS).

*Identify the plane at which the C-measurements are taken (e.g., at bumper, above bumper, at sill, above sill, at beltline, etc.) or label adjustments (e.g., free space).

Free space value is defined as the distance between the baseline and the original body contour taken at the individual C locations. This may include the following: bumper lead, bumper taper, side protrusion, side taper, etc. Record the value for each C-measurement and maximum crush.

**Measure and document on the vehicle diagram the beginning or end of the direct damage width and field L (e.g., side damage with respect to undamaged axle).

***Measure and document on the vehicle diagram the location of the maximum crush.

Note: Use as many lines/columns as necessary to describe each damage profile.

Figure D.2. Exterior crush measurements for test 612941-02-1.

Date: 2022-12-16 Test No.: 612941-02-1 VIN No.: 1C6RR6GT0JS131328
 Year: 2018 Make: RAM Model: 1500

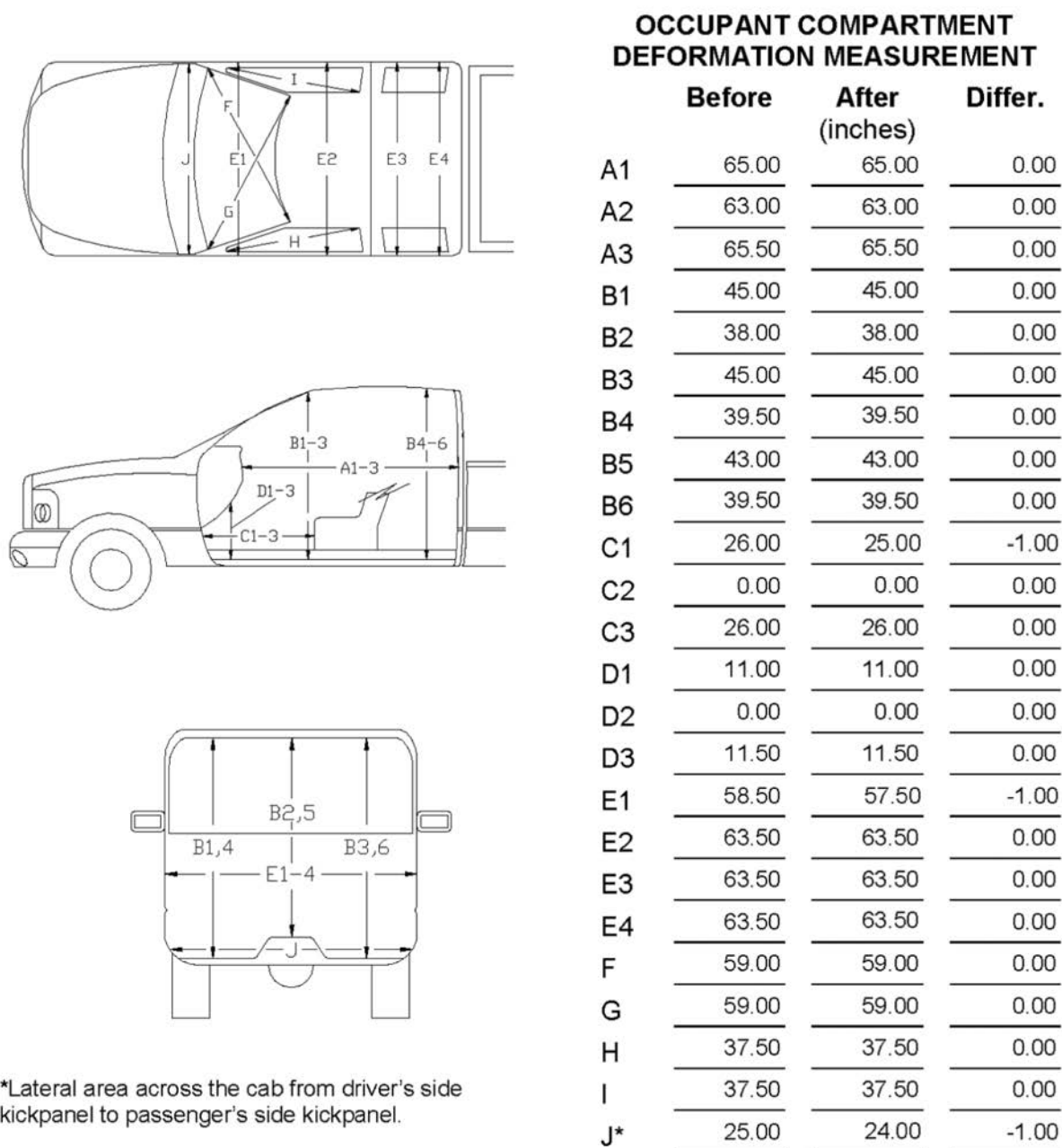


Figure D.3. Occupant compartment measurements for test 612941-02-1.

SEQUENTIAL PHOTOGRAPHS



Figure D.4. Sequential photographs for test 612941-02-1 (overhead views).



Figure D.5. Sequential photographs for test 612941-02-1 (frontal views).



(a) 0.000 s



(b) 0.100 s



(c) 0.200 s



(d) 0.300 s



(e) 0.400 s



(f) 0.500 s



(g) 0.600 s

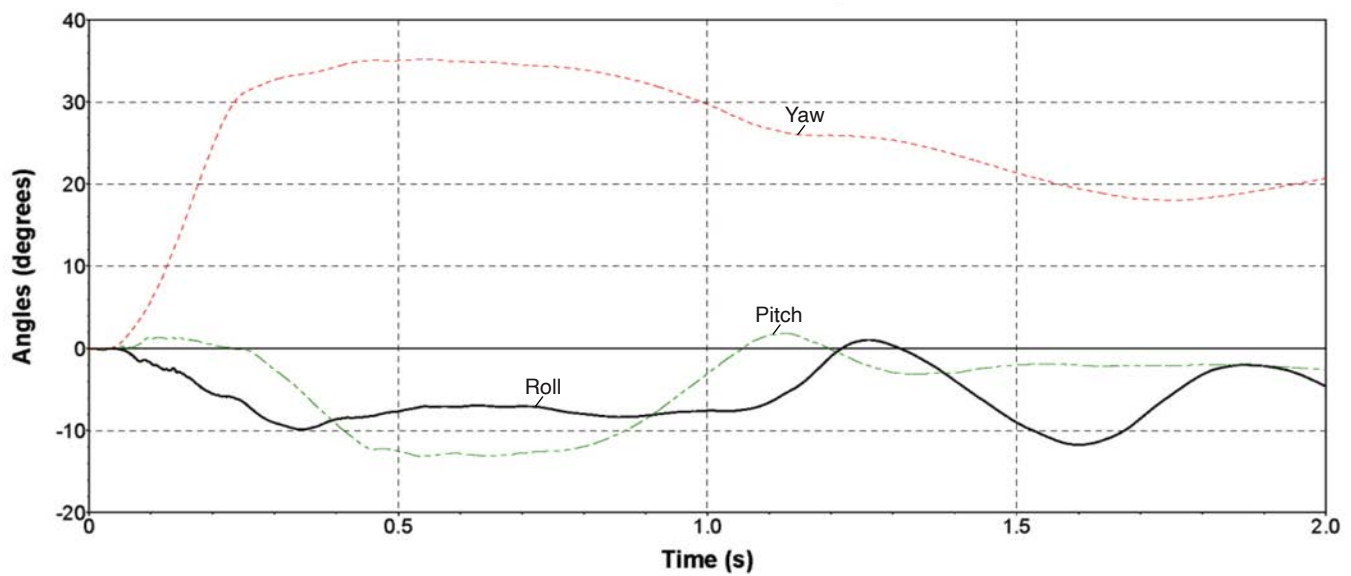


(h) 0.700 s

Figure D.6. Sequential photographs for test 612941-02-1 (field-side views).

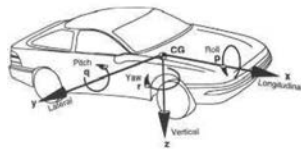
VEHICLE ANGULAR DISPLACEMENTS

Roll, Pitch and Yaw Angles



Axes are vehicle-fixed.
Sequence for determining
orientation:

4. Yaw.
5. Pitch.
6. Roll.



Test Number: 612941-02-1
Test Standard Test Number: *MASH* Test 3-11
Test Article: Stiffened MGS
Test Vehicle: 2018 RAM 1500
Inertial Mass: 5016 lb
Gross Mass: 5016 lb
Impact Speed: 62.7 mi/h
Impact Angle: 25.0°

Figure D.7. Vehicle angular displacements for test 612941-02-1.

VEHICLE ACCELERATIONS

X Acceleration at CG

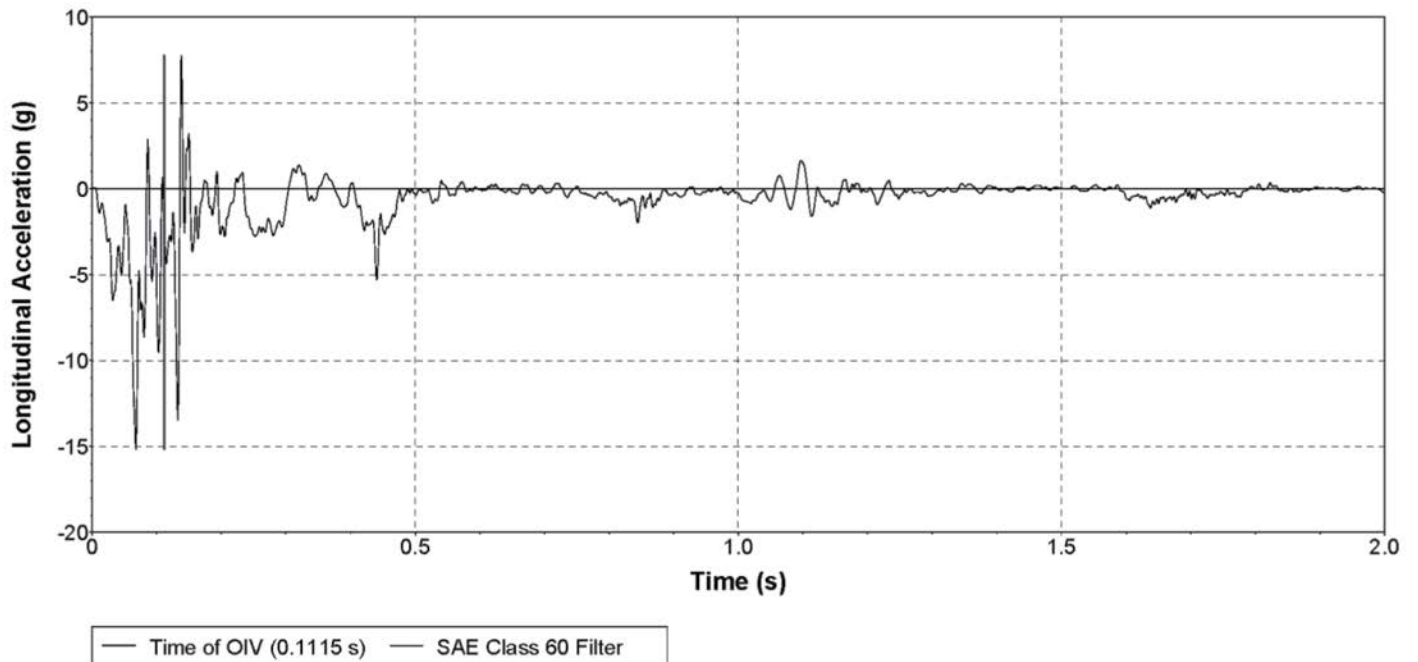


Figure D.8. Vehicle longitudinal accelerometer trace for test 612941-02-1 (accelerometer located at center of gravity, CG).

Y Acceleration at CG

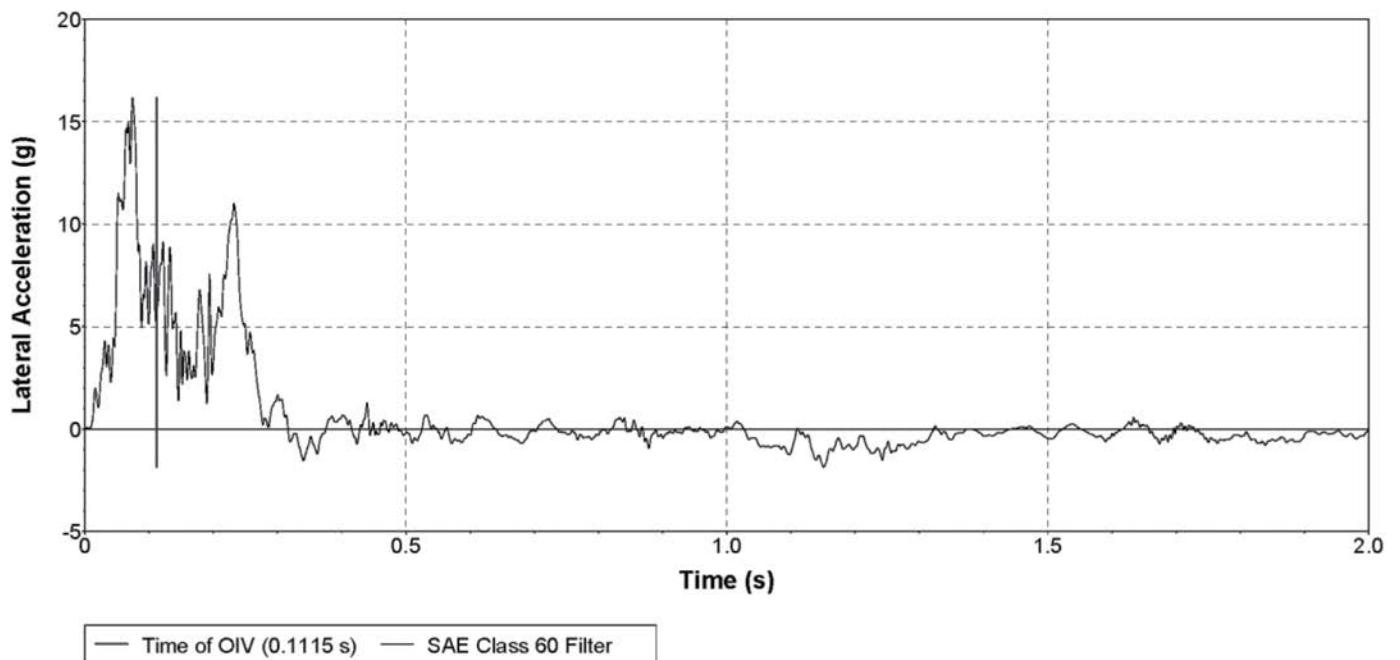


Figure D.9. Vehicle lateral accelerometer trace for test 612941-02-1 (accelerometer located at center of gravity, CG).

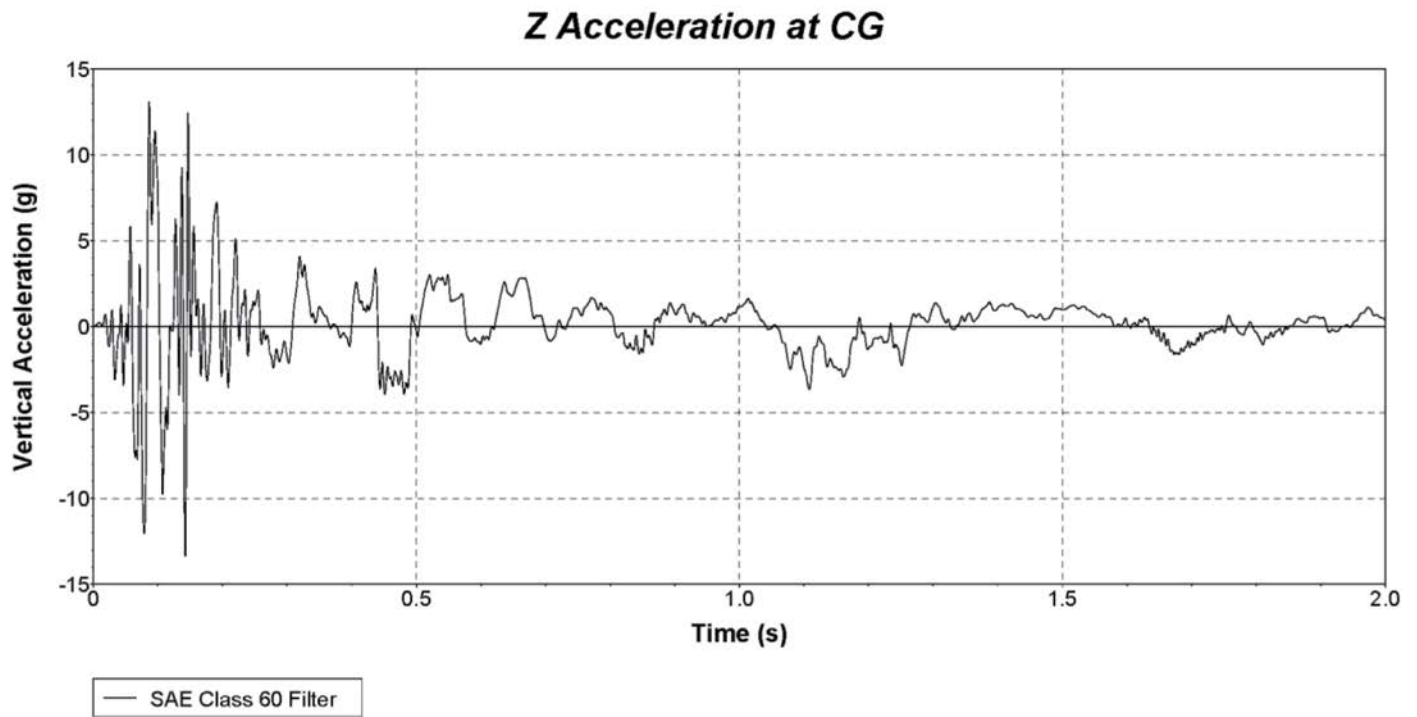


Figure D.10. Vehicle vertical accelerometer trace for test 612941-02-1 (accelerometer located at center of gravity, CG).



APPENDIX E

MASH Test 3-21 (Crash Test No. 612941-02-3)

VEHICLE PROPERTIES AND INFORMATION

Date: 2023-01-27 Test No.: 612941-02-3 VIN No.: 1C6RR6FT8HS524876
 Year: 2017 Make: RAM Model: 1500
 Tire Size: 265/70 R 17 Tire Inflation Pressure: 35 psi
 Tread Type: Highway Odometer: 186241
 Note any damage to the vehicle prior to test: None

- Denotes accelerometer location.

NOTES: None

Engine Type: V-8
 Engine CID: 5.7 liter

Transmission Type:

☒ Auto or ☐ Manual
☐ FWD ☒ RWD ☐ 4WD

Optional Equipment:

None

Dummy Data:

Type: NONE

Mass: lb

Seat Position:

Geometry: inches

A	78.50	F	40.00	K	20.00	P	3.00	U	26.75
B	74.00	G	28.20	L	30.00	Q	30.50	V	30.25
C	227.50	H	62.30	M	68.50	R	18.00	W	62.25
D	44.00	I	11.75	N	68.00	S	13.00	X	79.00
E	140.50	J	27.00	O	46.00	T	77.00		
Wheel Center Height Front		14.75	Wheel Well Clearance (Front)		6.00	Bottom Frame Height - Front		12.50	
Wheel Center Height Rear		14.75	Wheel Well Clearance (Rear)		9.25	Bottom Frame Height - Rear		22.50	

RANGE LIMIT: A=78 ±2 inches; C=237 ±13 inches; E=148 ±12 inches; F=39 ±3 inches; G = > 28 inches; H = 63 ±4 inches; O=43 ±4 inches; (M+N)/2=67 ±1.5 inches

GVWR Ratings:

Front	3700
Back	3900
Total	6700

Mass: lb

M _{front}	2911
M _{rear}	2025
M _{Total}	4936

Curb

2911
2025
4936

Test Inertial

2806
2236
5042

Gross Static

2806
2236
5042

(Allowable Range for TIM and GSM = 5000 lb ±110 lb)

Mass Distribution:

lb

LF: 1399

RF: 1407

LR: 1145

RR: 1091

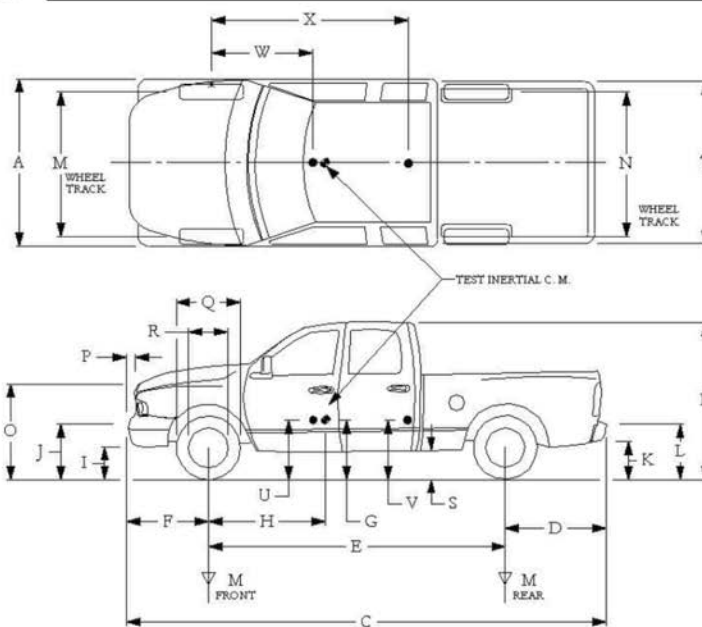


Figure E.1. Vehicle properties for test 612941-02-3.

Date:	2023-01-27	Test No.:	612941-02-3	VIN No.:	1C6RR6FT8HS524876
Year:	2017	Make:	RAM	Model:	1500

VEHICLE CRUSH MEASUREMENT SHEET¹

Complete When Applicable	
End Damage	Side Damage
Undeformed end width _____	Bowing: B1 _____ X1 _____
Corner shift: A1 _____	B2 _____ X2 _____
A2 _____	
End shift at frame (CDC)	Bowing constant
(check one)	$\frac{X1 + X2}{2} = \underline{\hspace{2cm}}$
< 4 inches _____	
≥ 4 inches _____	

Note: Measure C₁ to C₆ from Driver to Passenger Side in Front or Rear Impacts – Rear to Front in Side Impacts.

[illegible]

¹Table taken from National Accident Sampling System (NASS).

*Identify the plane at which the C-measurements are taken (e.g., at bumper, above bumper, at sill, above sill, at beltline, etc.) or label adjustments (e.g., free space).

Free space value is defined as the distance between the baseline and the original body contour taken at the individual C locations. This may include the following: bumper lead, bumper taper, side protrusion, side taper, etc. Record the value for each C-measurement and maximum crush.

***Measure and document on the vehicle diagram the beginning or end of the direct damage width and field L (e.g., side damage with respect to undamaged axle).

***Measure and document on the vehicle diagram the location of the maximum crush.

Note: Use as many lines/columns as necessary to describe each damage profile.

Figure E.2. Exterior crush measurements for test 612941-02-3.

Date:2023-01-27

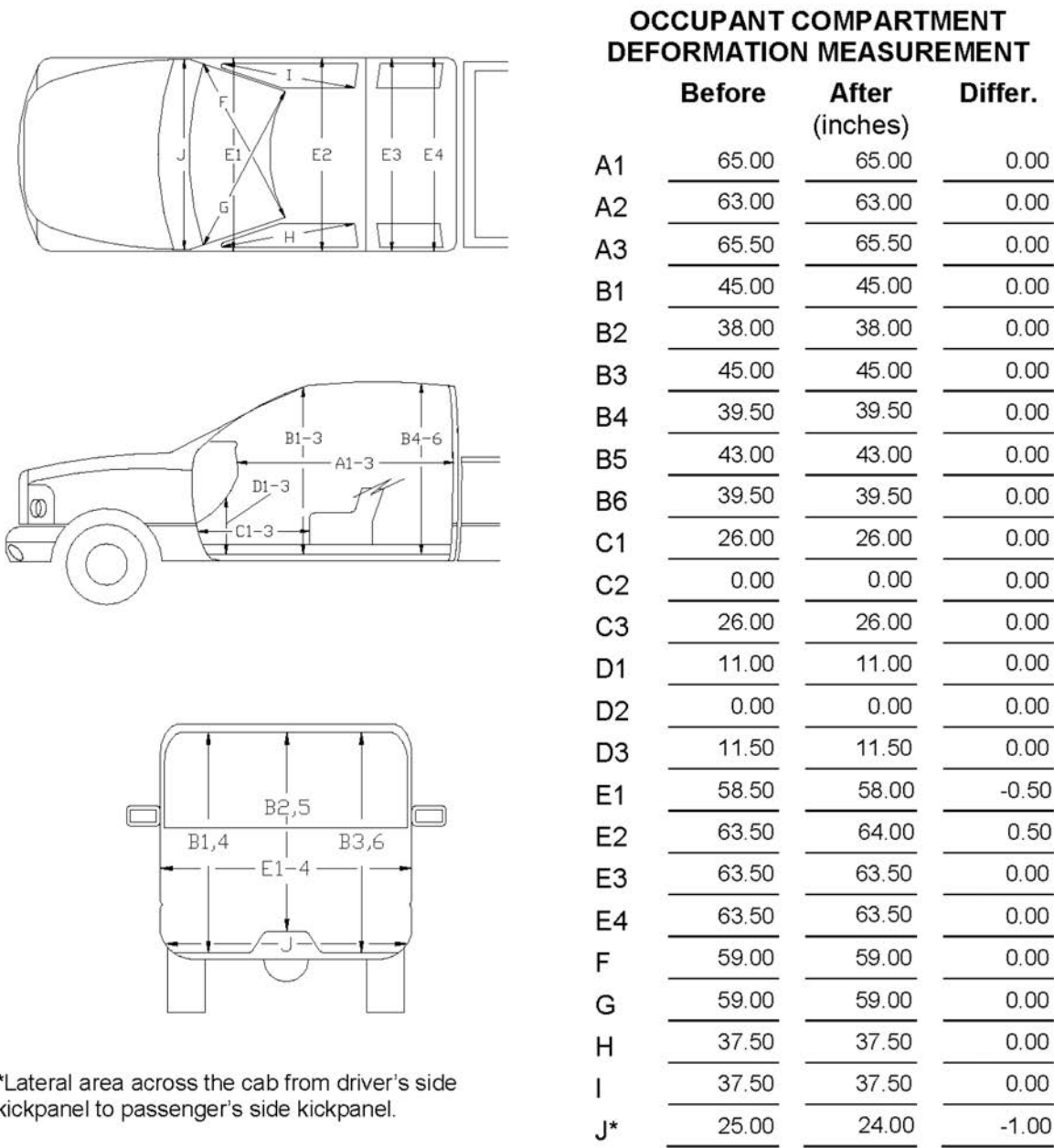
Test No.:612941-02-3

VIN No.:1C6RR6FT8HS524876

Year:2017

Make:RAM

Model:1500



*Lateral area across the cab from driver's side kickpanel to passenger's side kickpanel.

Figure E.3. Occupant compartment measurements for test 612941-02-3.

SEQUENTIAL PHOTOGRAPHS

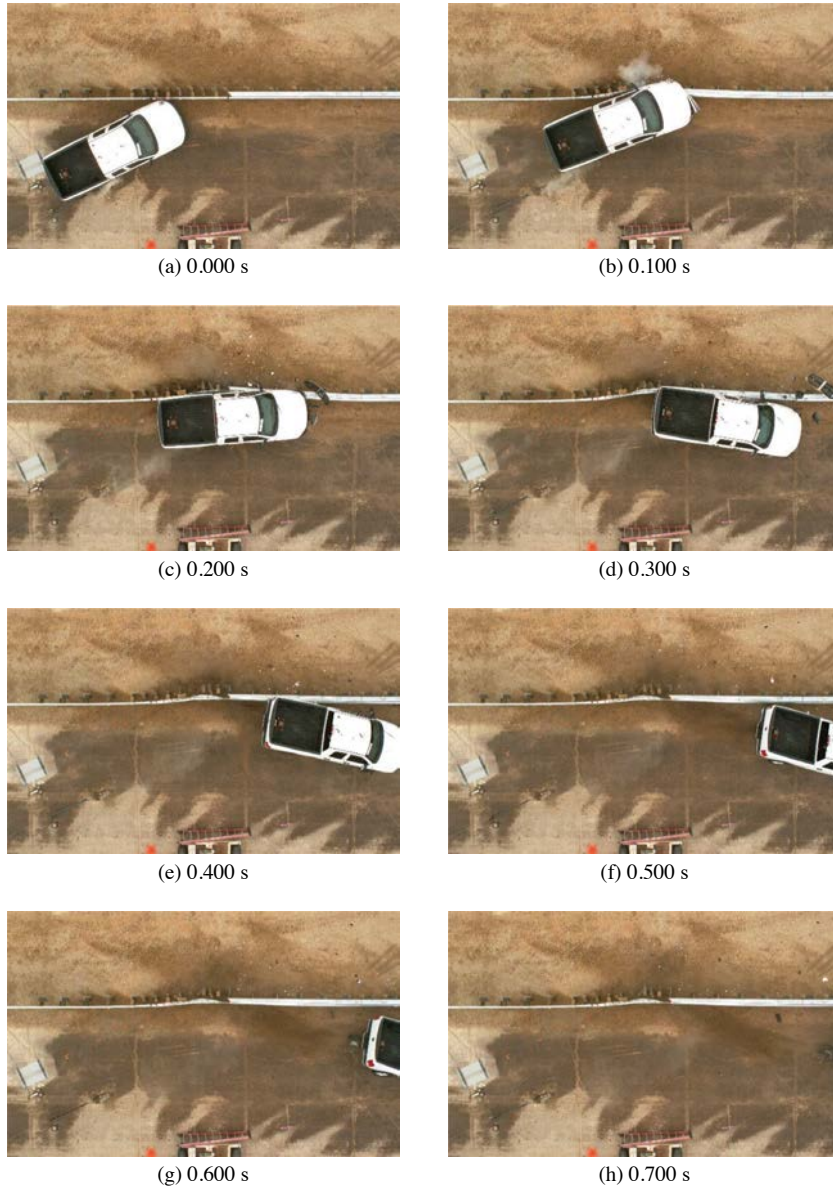


Figure E.4. Sequential photographs for test 612941-02-3 (overhead views).



(a) 0.000 s



(b) 0.100 s



(c) 0.200 s



(d) 0.300 s



(e) 0.400 s



(f) 0.500 s



(g) 0.600 s



(h) 0.700 s

Figure E.5. Sequential photographs for test 612941-02-3 (frontal views).



(a) 0.000 s



(b) 0.100 s



(c) 0.200 s



(d) 0.300 s



(e) 0.400 s



(f) 0.500 s



(g) 0.600 s

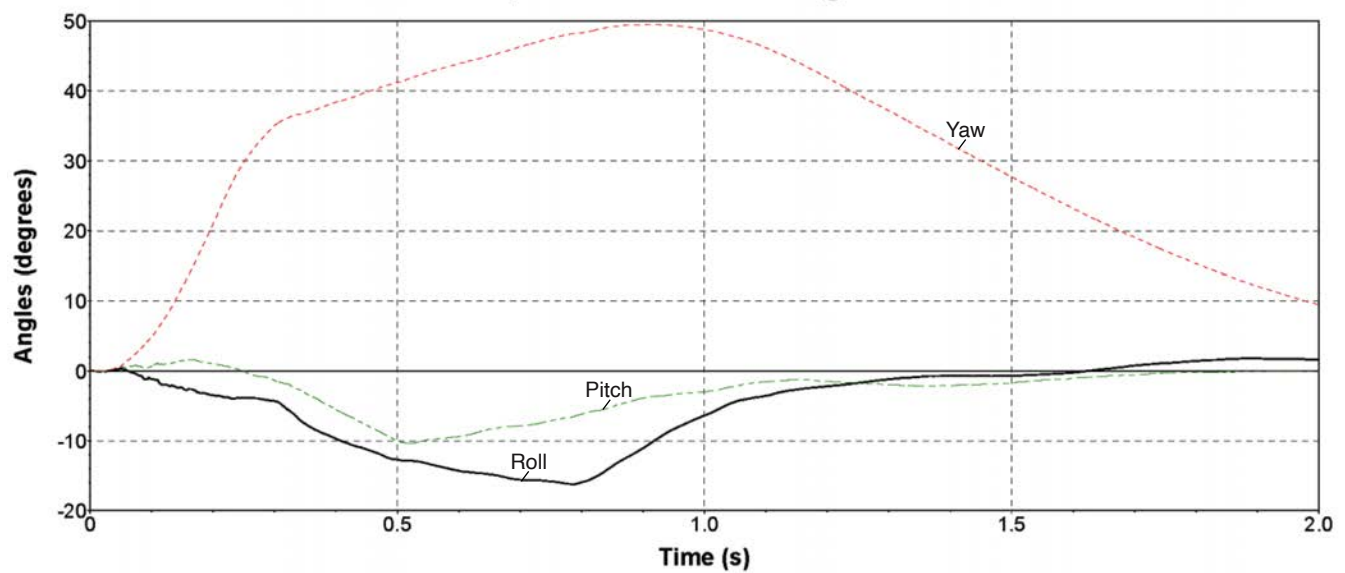


(h) 0.700 s

Figure E.6. Sequential photographs for test 612941-02-3 (field-side views).

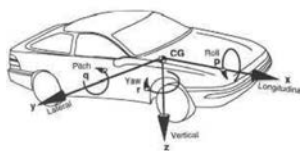
VEHICLE ANGULAR DISPLACEMENTS

Roll, Pitch and Yaw Angles



Axes are vehicle-fixed.
Sequence for determining
orientation:

7. Yaw.
8. Pitch.
9. Roll.



Test Number: 612941-02-3
Test Standard Test Number: *MASH* Test 3-21
Test Article: Stiffened MGS Transition
Test Vehicle: 2017 RAM 1500
Inertial Mass: 5042 lb
Gross Mass: 5042 lb
Impact Speed: 64.0 mi/h
Impact Angle: 25.7°

Figure E.7. Vehicle angular displacements for test 612941-02-3.

VEHICLE ACCELERATIONS

X Acceleration at CG

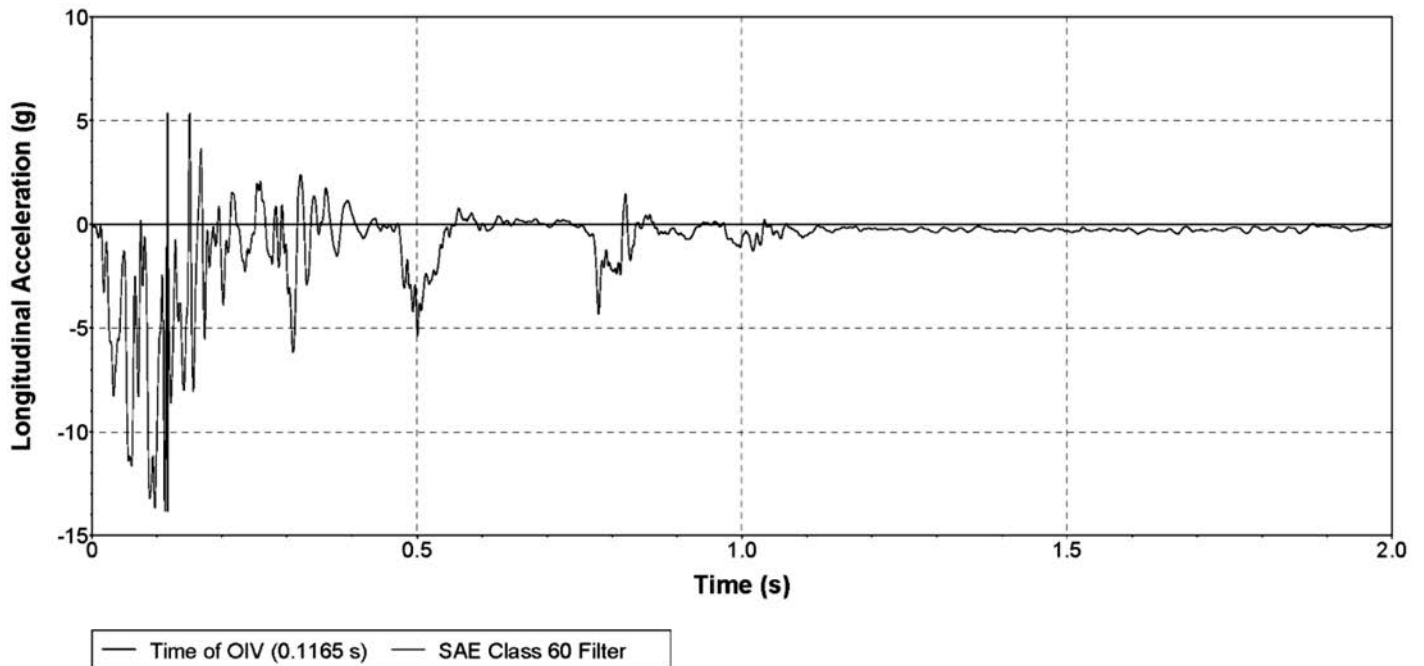


Figure E.8. Vehicle longitudinal accelerometer trace for test 612941-02-3 (accelerometer located at center of gravity, CG).

Y Acceleration at CG

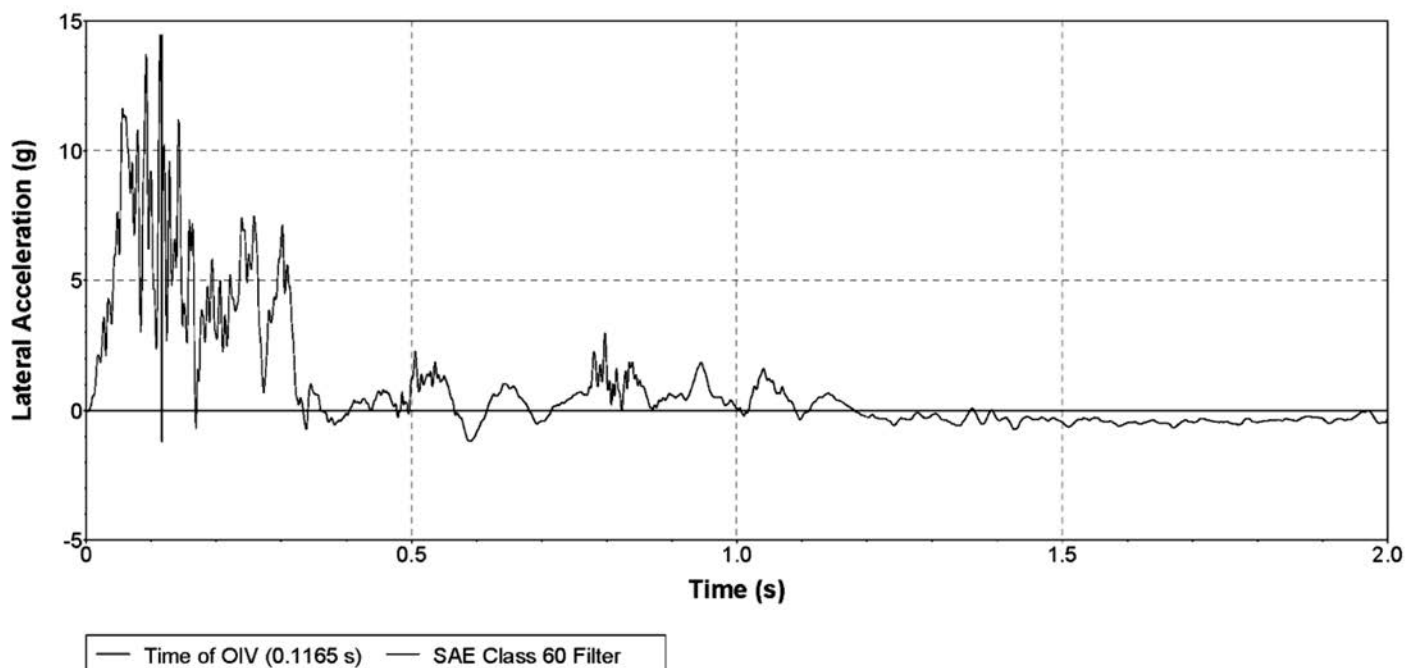


Figure E.9. Vehicle lateral accelerometer trace for test 612941-02-3 (accelerometer located at center of gravity, CG).

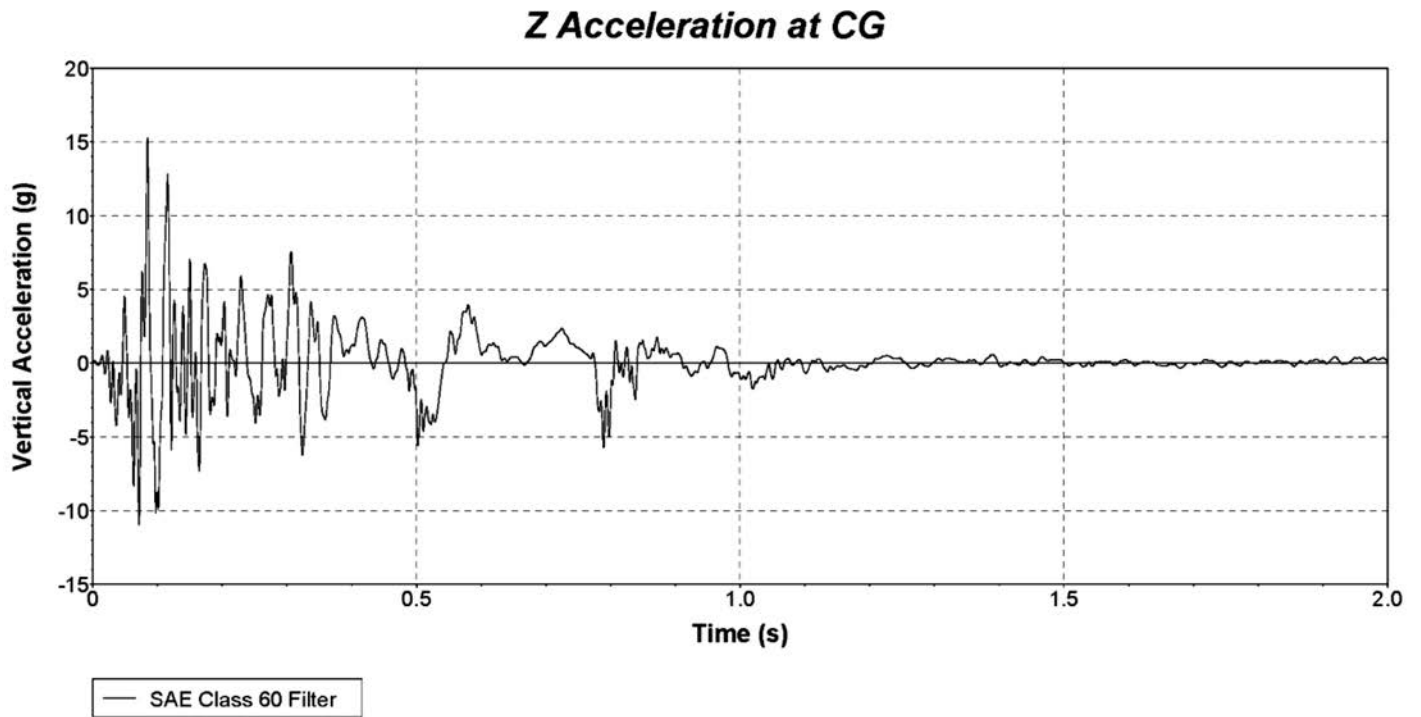


Figure E.10. Vehicle vertical accelerometer trace for test 612941-02-3 (accelerometer located at center of gravity, CG).



APPENDIX F

MASH Test 3-20 (Crash Test No. 612941-02-4)

VEHICLE PROPERTIES AND INFORMATION

Date: 2023-03-15 Test No.: 612941-02-4 VIN No.: 3N1CN7AP0HL879715

Year: 2017 Make: Nissan Model: Versa

Tire Inflation Pressure: 36 PSI Odometer: 59678 Tire Size: P185/65R15

Describe any damage to the vehicle prior to test: None

- Denotes accelerometer location.

NOTES: None

Engine Type: 4 CYL

Engine CID: 1.6 L

Transmission Type:

☐ Auto or ☒ Manual

☒ FWD ☐ RWD ☐ 4WD

Optional Equipment:

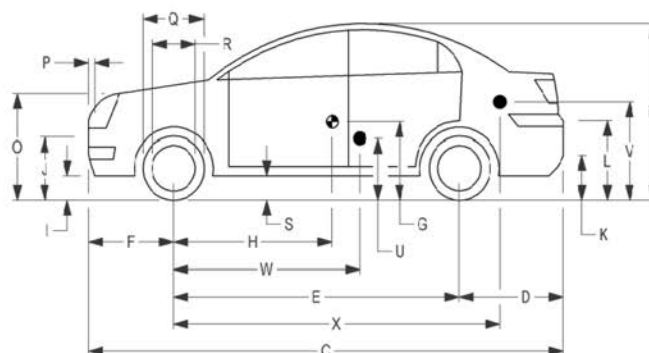
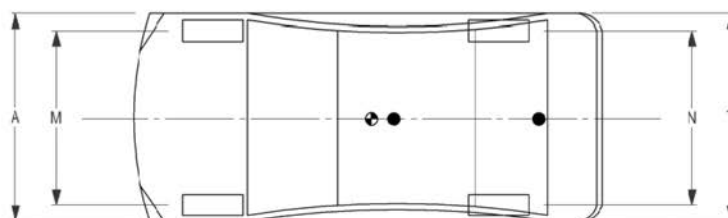
None

Dummy Data:

Type: 50th Percentile Male

Mass: 165 lb

Seat Position: IMPACT SIDE



Geometry: inches

A <u>66.70</u>	F <u>32.50</u>	K <u>12.50</u>	P <u>4.50</u>	U <u>15.50</u>
B <u>59.60</u>	G <u> </u>	L <u>26.00</u>	Q <u>24.00</u>	V <u>21.25</u>
C <u>175.40</u>	H <u>42.82</u>	M <u>58.30</u>	R <u>16.25</u>	W <u>42.80</u>
D <u>40.50</u>	I <u>7.00</u>	N <u>58.50</u>	S <u>7.50</u>	X <u>79.75</u>
E <u>102.40</u>	J <u>22.50</u>	O <u>30.50</u>	T <u>64.50</u>	
Wheel Center Ht Front <u>11.50</u>		Wheel Center Ht Rear <u>11.50</u>		W-H <u>-0.02</u>

RANGE LIMIT: A = 65 ±3 inches; C = 169 ±8 inches; E = 98 ±5 inches; F = 35 ±4 inches; H = 39 ±4 inches; O (Top of Radiator Support) = 28 ±4 inches
(M+N)/2 = 59 ±2 inches; W-H < 2 inches or use MASH Paragraph A4.3.2

GVWR Ratings:

	Mass: lb	Curb	Test Inertial	Gross Static
Front	<u>1750</u>	<u>M_{front} 1375</u>	<u>1415</u>	<u>1500</u>
Back	<u>1687</u>	<u>M_{rear} 962</u>	<u>1017</u>	<u>1097</u>
Total	<u>3389</u>	<u>M_{Total} 2337</u>	<u>2432</u>	<u>2597</u>

Allowable TIM = 2420 lb ±55 lb | Allowable GSM = 2585 lb ± 55 lb

Mass Distribution:

lb LF: 676 RF: 739 LR: 536 RR: 481

Figure F.1. Vehicle properties for test 612941-02-4.

Date:	2023-03-15	Test No.:	612941-02-4	VIN No.:	3NICN7AP0HL879715
Year:	2017	Make:	Nissan	Model:	Versa

VEHICLE CRUSH MEASUREMENT SHEET¹

Complete When Applicable	
End Damage	Side Damage
Undeformed end width _____	Bowing: B1 _____ X1 _____
Corner shift: A1 _____	B2 _____ X2 _____
A2 _____	
End shift at frame (CDC)	Bowing constant
(check one)	$\frac{X1 + X2}{2} = \underline{\hspace{2cm}}$
< 4 inches _____	
≥ 4 inches _____	

Note: Measure C₁ to C₆ from Driver to Passenger Side in Front or Rear Impacts – Rear to Front in Side Impacts.

[illegible]

¹Table taken from National Accident Sampling System (NASS).

*Identify the plane at which the C-measurements are taken (e.g., at bumper, above bumper, at sill, above sill, at beltline, etc.) or label adjustments (e.g., free space).

Free space value is defined as the distance between the baseline and the original body contour taken at the individual C locations. This may include the following: bumper lead, bumper taper, side protrusion, side taper, etc.

Record the value for each C-measurement and maximum crush.

*Measure and document on the vehicle diagram the beginning or end of the direct damage width and field L (e.g., side damage with respect to undamaged axle).

***Measure and document on the vehicle diagram the location of the maximum crush.

Note: Use as many lines/columns as necessary to describe each damage profile.

Figure F.2. Exterior crush measurements for test 612941-02-4.

Date:2023-03-15

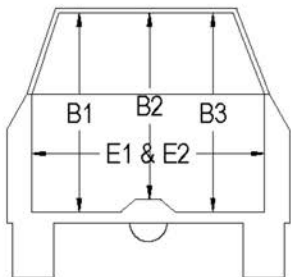
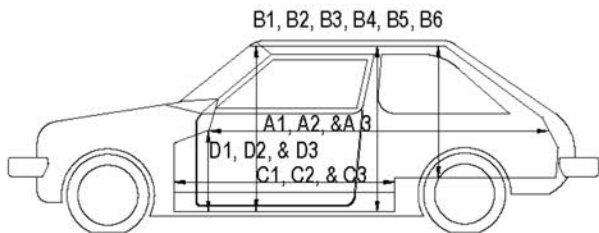
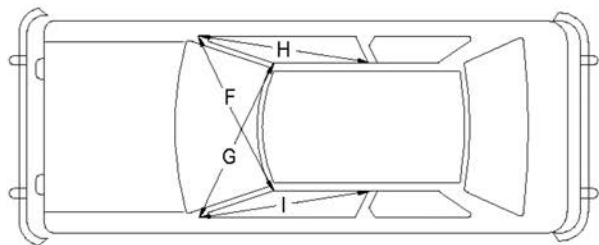
Test No.:612941-02-4

VIN No.:3NICN7AP0HL879715

Year:2017

Make:Nissan

Model:Versa



*Lateral area across the cab from driver's side kick panel to passenger's side kick panel.

OCCUPANT COMPARTMENT DEFORMATION MEASUREMENT

	Before	After (inches)	Differ.
A1	67.50	67.50	0.00
A2	67.25	67.25	0.00
A3	67.75	67.75	0.00
B1	40.50	40.00	-0.50
B2	39.00	39.00	0.00
B3	40.50	40.50	0.00
B4	36.25	36.25	0.00
B5	36.00	36.00	0.00
B6	36.25	36.25	0.00
C1	26.00	25.00	-1.00
C2	0.00	0.00	0.00
C3	26.00	26.00	0.00
D1	9.50	7.50	-2.00
D2	0.00	0.00	0.00
D3	9.50	9.50	0.00
E1	51.50	48.50	-3.00
E2	51.00	53.00	2.00
F	51.00	51.00	0.00
G	51.00	51.00	0.00
H	37.50	37.50	0.00
I	37.50	37.50	0.00
J*	51.00	51.00	0.00

Figure F.3. Occupant compartment measurements for test 612941-02-4.

SEQUENTIAL PHOTOGRAPHS

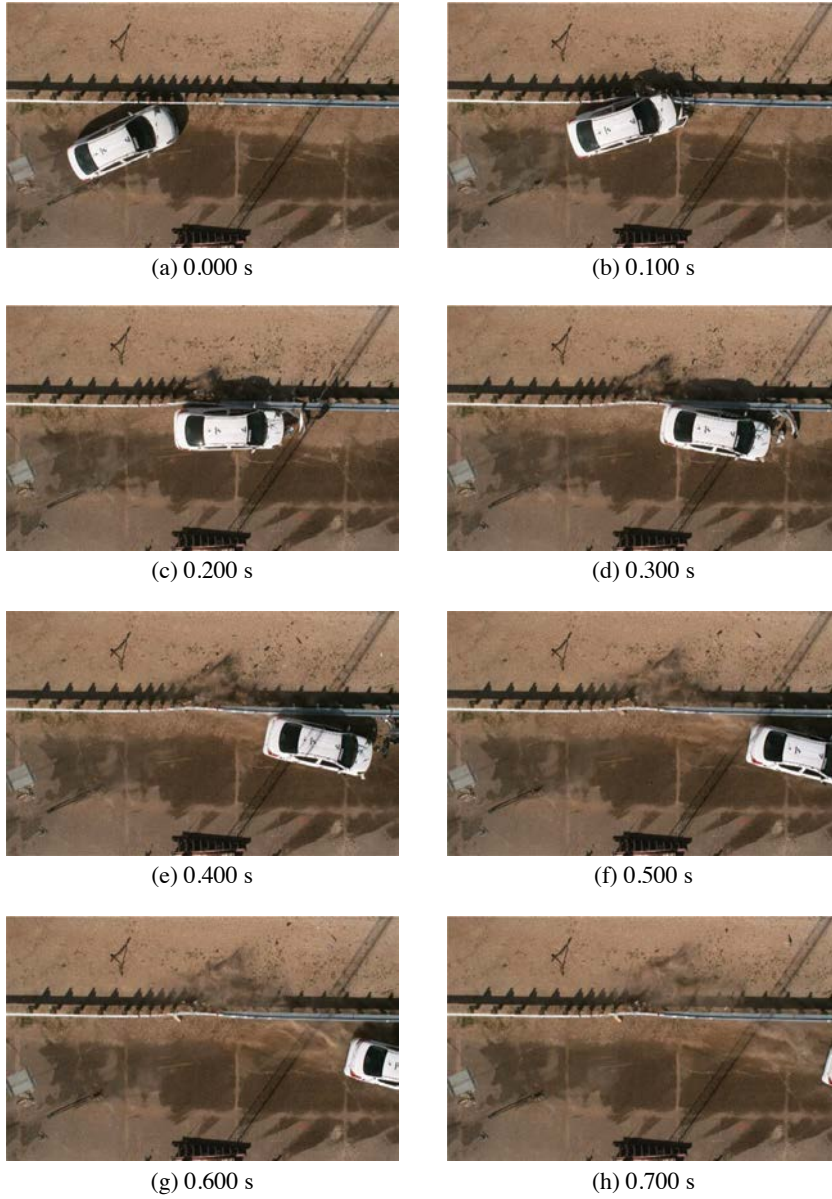


Figure F.4. Sequential photographs for test 612941-02-4 (overhead views).

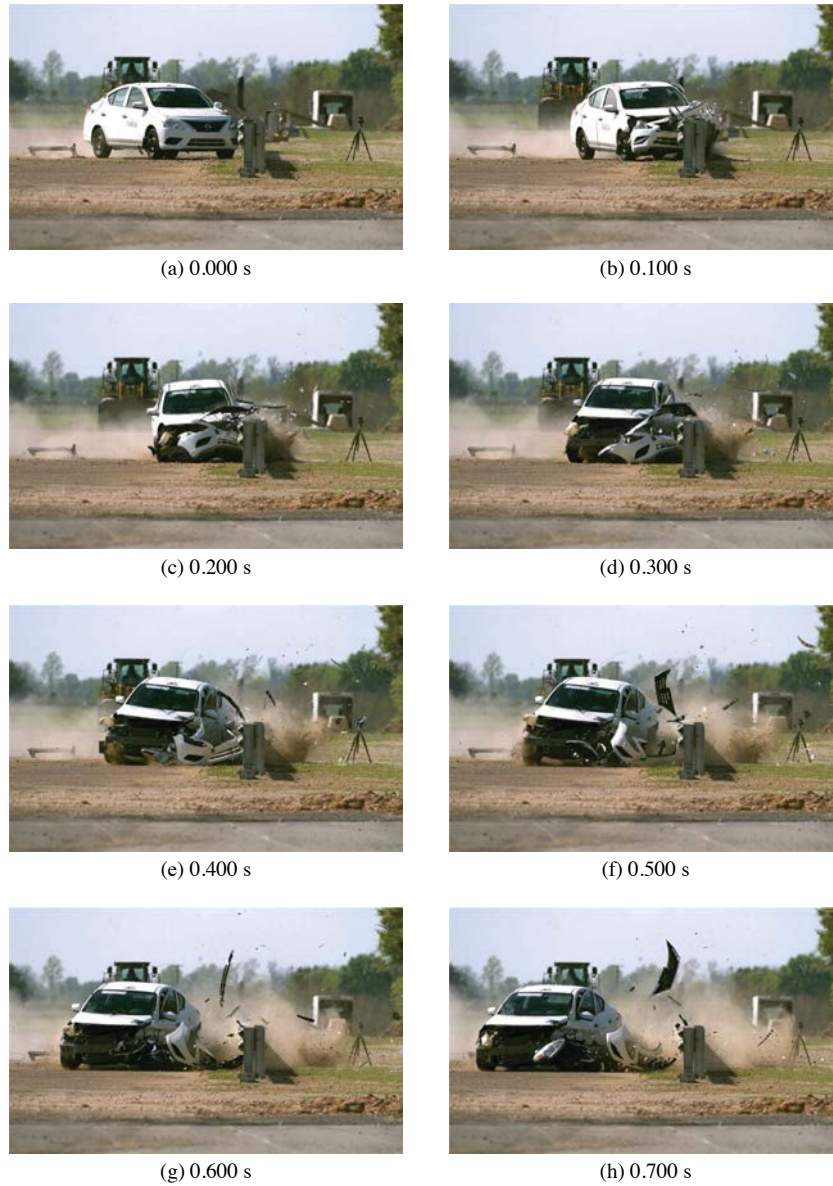


Figure F.5. Sequential photographs for test 612941-02-4 (frontal views).

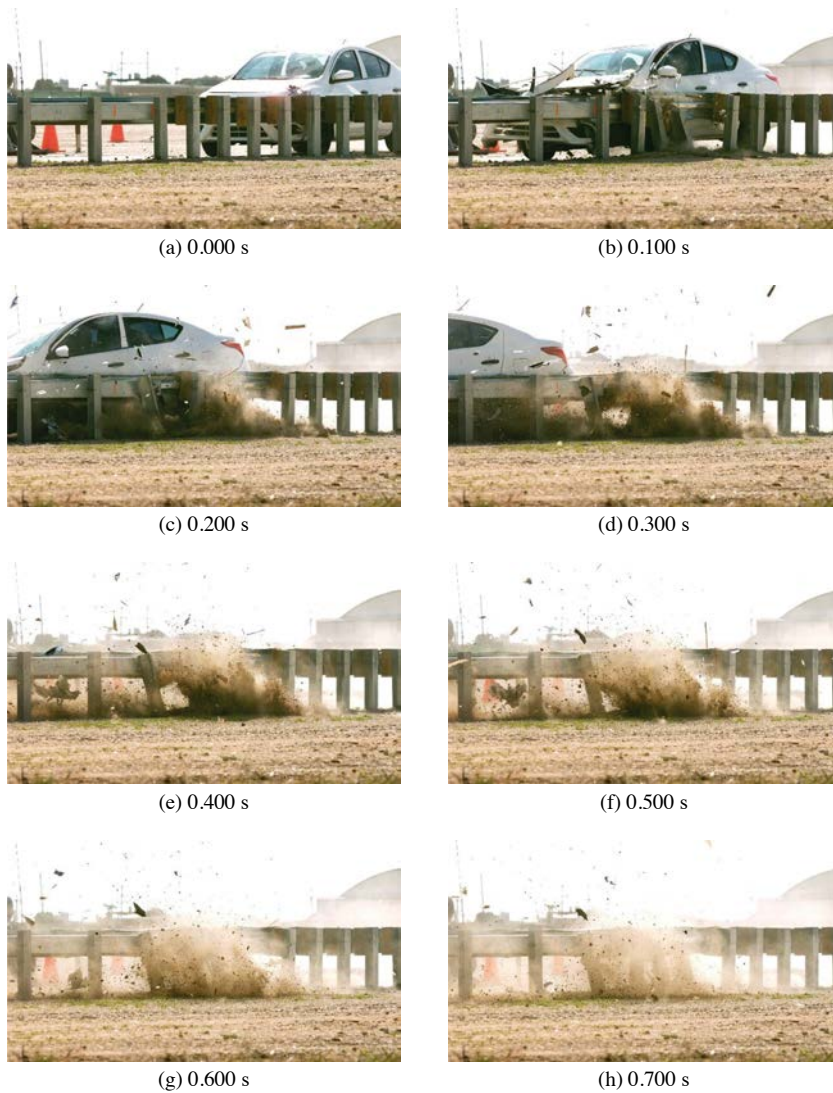
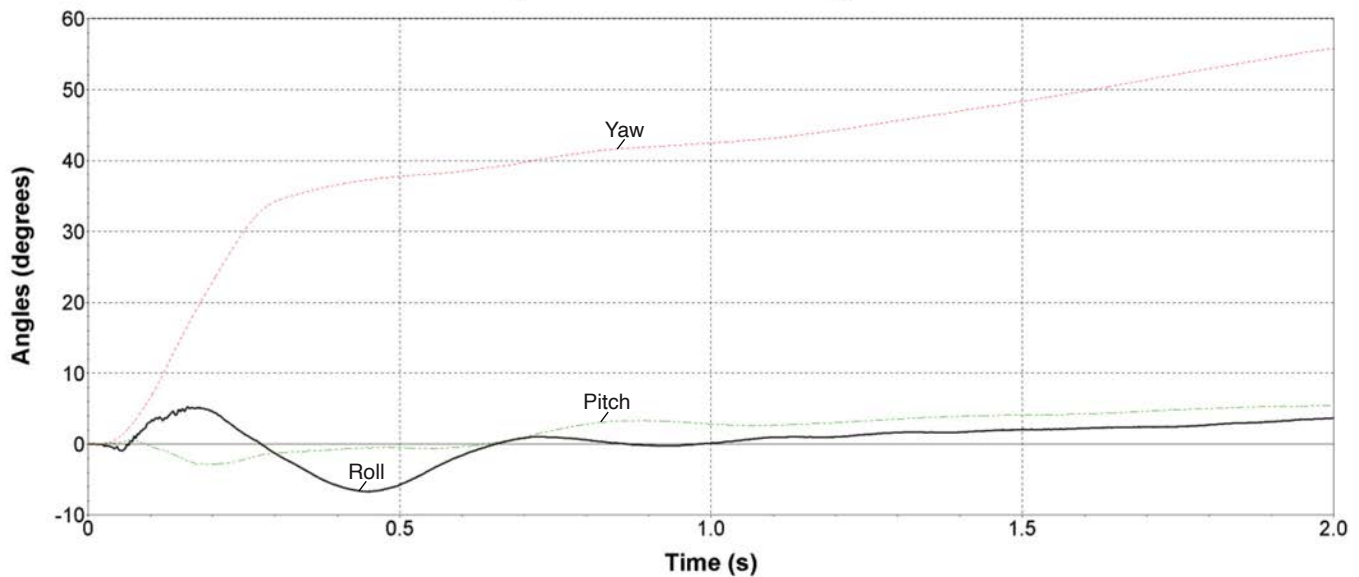


Figure F.6. Sequential photographs for test 612941-02-4 (field-side views).

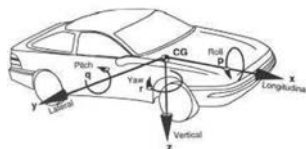
VEHICLE ANGULAR DISPLACEMENTS

Roll, Pitch and Yaw Angles



Axes are vehicle-fixed.
Sequence for determining
orientation:

10. Yaw.
11. Pitch.
12. Roll.



Test Number: 612941-02-4
Test Standard Test Number: *MASH* Test 3-20
Test Article: Stiffened MGS Transition
Test Vehicle: 2017 Nissan Versa
Inertial Mass: 2432 lbs
Gross Mass: 2597 lbs
Impact Speed: 62.6 mi/h
Impact Angle: 25.0 °

Figure F.7. Vehicle angular displacements for test 612941-02-4.

VEHICLE ACCELERATIONS

X Acceleration at CG

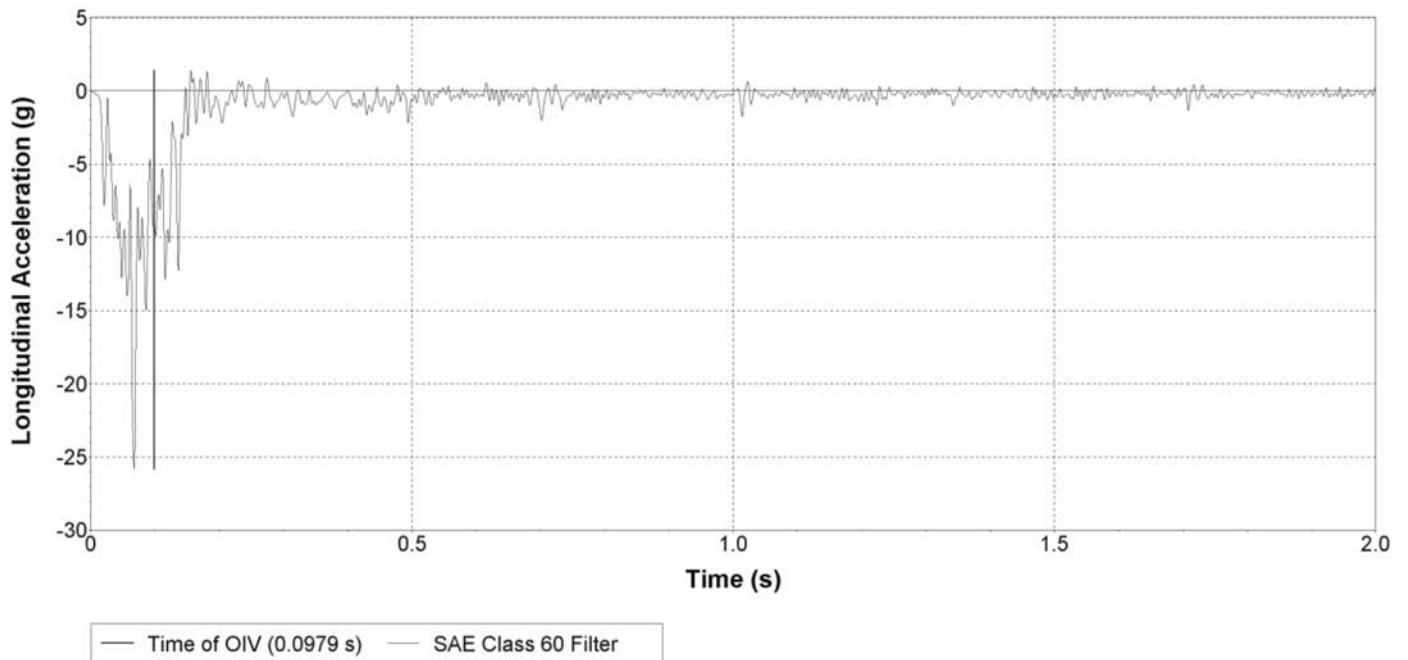


Figure F.8. Vehicle longitudinal accelerometer trace for test 612941-02-4 (accelerometer located at center of gravity, CG).

Y Acceleration at CG

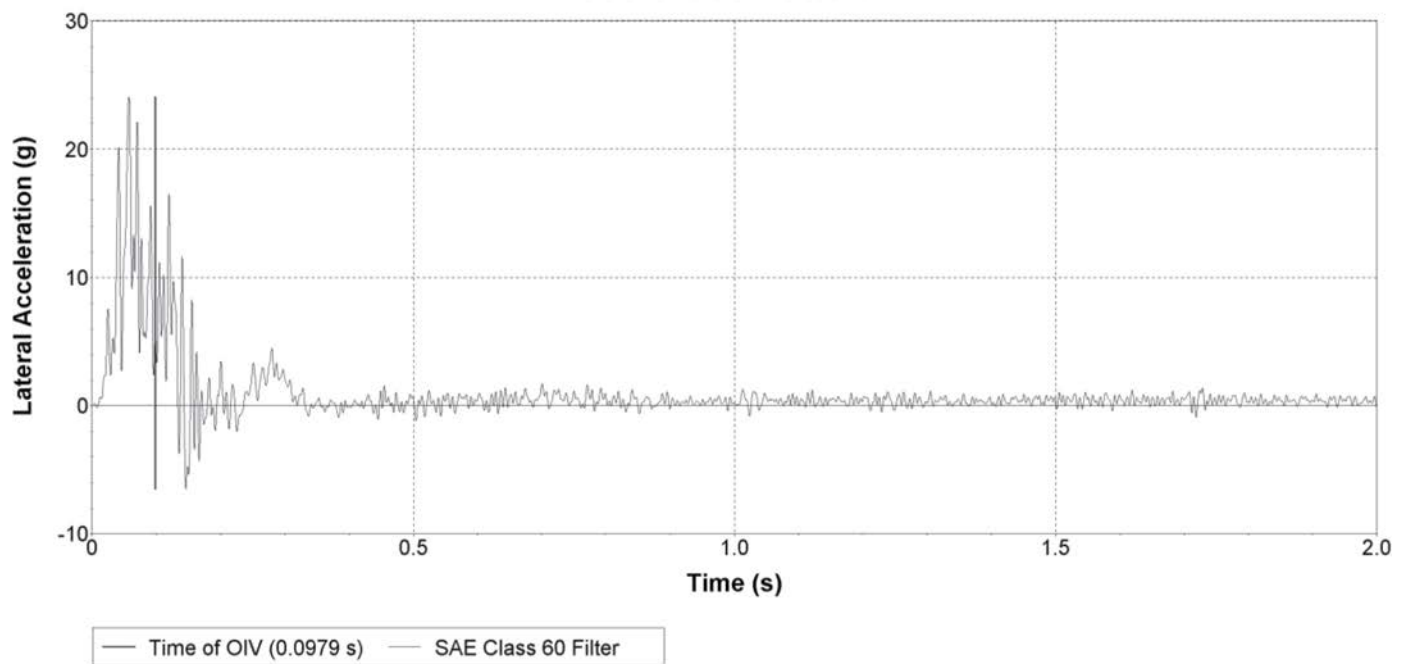


Figure F.9. Vehicle lateral accelerometer trace for test 612941-02-4 (accelerometer located at center of gravity, CG).

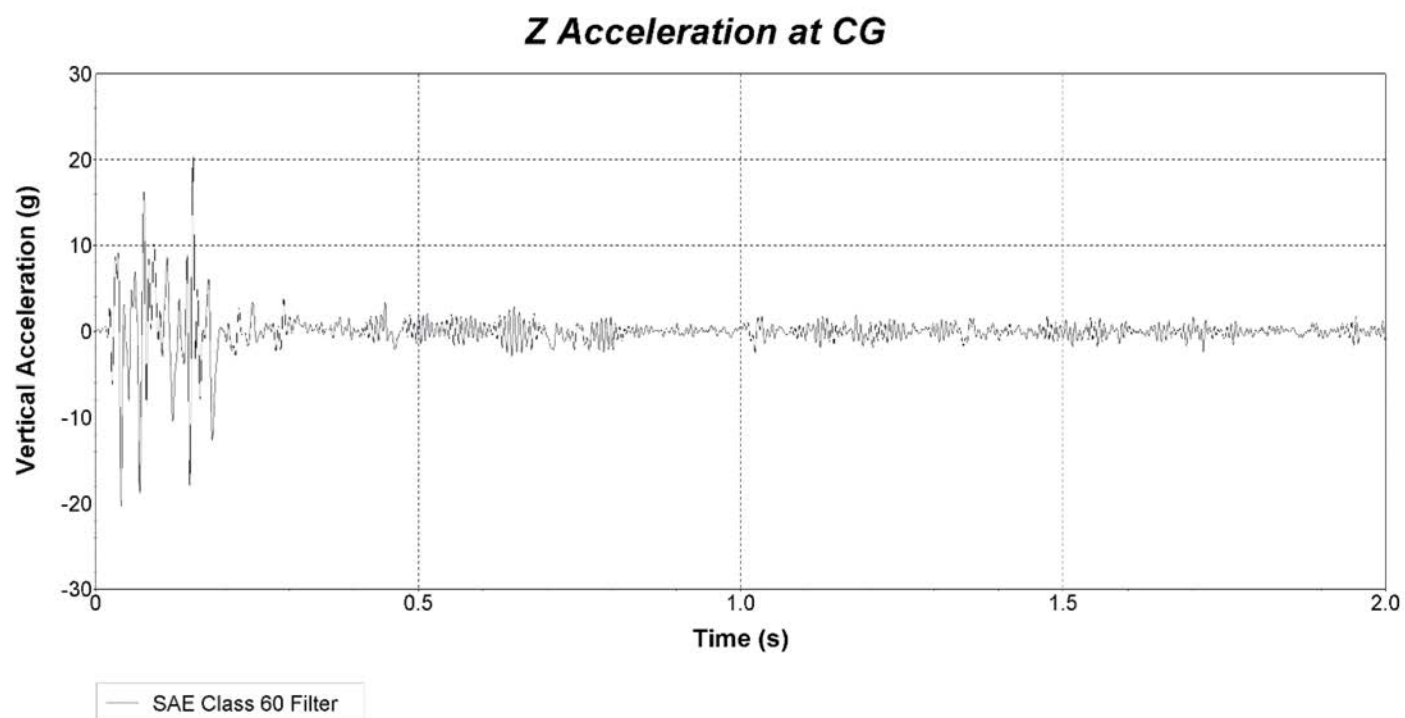


Figure F.10. Vehicle vertical accelerometer trace for test 612941-02-4 (accelerometer located at center of gravity, CG).

Abbreviations and acronyms used without definitions in TRB publications:

A4A	Airlines for America
AAAE	American Association of Airport Executives
AASHO	American Association of State Highway Officials
AASHTO	American Association of State Highway and Transportation Officials
ACI-NA	Airports Council International-North America
ACRP	Airport Cooperative Research Program
ADA	Americans with Disabilities Act
APTA	American Public Transportation Association
ASCE	American Society of Civil Engineers
ASME	American Society of Mechanical Engineers
ASTM	American Society for Testing and Materials
ATA	American Trucking Associations
CTAA	Community Transportation Association of America
CTBSSP	Commercial Truck and Bus Safety Synthesis Program
DHS	Department of Homeland Security
DOE	Department of Energy
EPA	Environmental Protection Agency
FAA	Federal Aviation Administration
FAST	Fixing America's Surface Transportation Act (2015)
FHWA	Federal Highway Administration
FMCSA	Federal Motor Carrier Safety Administration
FRA	Federal Railroad Administration
FTA	Federal Transit Administration
GHSA	Governors Highway Safety Association
HMCRP	Hazardous Materials Cooperative Research Program
IEEE	Institute of Electrical and Electronics Engineers
ISTEA	Intermodal Surface Transportation Efficiency Act of 1991
ITE	Institute of Transportation Engineers
MAP-21	Moving Ahead for Progress in the 21st Century Act (2012)
NASA	National Aeronautics and Space Administration
NASAO	National Association of State Aviation Officials
NCFRP	National Cooperative Freight Research Program
NCHRP	National Cooperative Highway Research Program
NHTSA	National Highway Traffic Safety Administration
NTSB	National Transportation Safety Board
PHMSA	Pipeline and Hazardous Materials Safety Administration
RITA	Research and Innovative Technology Administration
SAE	Society of Automotive Engineers
SAFETEA-LU	Safe, Accountable, Flexible, Efficient Transportation Equity Act: A Legacy for Users (2005)
TCRP	Transit Cooperative Research Program
TEA-21	Transportation Equity Act for the 21st Century (1998)
TRB	Transportation Research Board
TSA	Transportation Security Administration
U.S. DOT	United States Department of Transportation

Transportation Research Board
500 Fifth Street, NW
Washington, DC 20001

ADDRESS SERVICE REQUESTED

**NATIONAL
ACADEMIES** *Sciences
Engineering
Medicine*

The National Academies provide
independent, trustworthy advice
that advances solutions to society's
most complex challenges.

www.nationalacademies.org

ISBN: 978-0-309-70953-8

